Regulatory T Cells Shape the CD4 T Cell Response to *Salmonella*

Slater Lowe Clay
BSc, MSc

Submitted in fulfilment of the requirements
for the degree of Doctor of Philosophy

Institute of Infection, Immunity and Inflammation
College of Medical Veterinary and Life Sciences
University of Glasgow

April 2019

Abstract

FoxP3$^+$ regulatory T cells (Tregs) play an important role in controlling inflammation and maintaining homeostasis at mucosal sites. Tregs may also limit immunopathology during infection but their role in this context remains poorly understood. CD4 T helper (Th) cells are important drivers of immune responses and can express master transcription factors (TFs) including T-bet, GATA3 and RORγT, which identify Th1, Th2 and Th17 cells, respectively. Tregs can also express these TFs, and recent research suggests that Tregs expressing master TFs may be able to selectively suppress their corresponding Th subsets. T-bet$^+$ Tregs have been shown to selectively target Th1 cells in some contexts, but it is unclear whether the same dynamic occurs with Tregs expressing other TFs. It is also unclear whether selective suppression can influence the overall CD4 T cell bias during infection. To address these questions, an infection model using *Salmonella enterica* serotype Typhimurium (STM) was developed to induce non-lethal colitis. This allowed STM-specific and polyclonal CD4 T cells to be tracked in multiple tissues.

Using this model, a dynamic and site-specific CD4 T cell response was revealed. An early and transient colonic Th17 response was followed by a sustained Th1 bias. This Th response develops in parallel with an early increase in the proportion of T-bet$^+$ Tregs and a later increase in the proportion of RORγT$^+$ Tregs. This reciprocal dynamic between Th subsets and Tregs expressing the same TF is consistent with the hypothesis that specific populations of Tregs selectively suppress Th subsets. To determine if Tregs are required for the dynamic Th bias, Treg depletion experiments were carried out at different timepoints. Results show that Tregs are essential for both the early Th17 response and the later Th1 response. Together, these results support the hypothesis that Tregs shape the dynamic Th bias by selective suppression. Further research is needed to address what mechanism might drive this targeted regulation. This research shows the potential for Tregs to not just inhibit the overall T cell response, but to actively shape Th bias. This highlights the potential for Tregs expressing specific TFs to be used in targeted therapeutic approaches. Further work is warranted to improve our basic understanding of how Tregs shape immunity and to develop appropriate clinical applications.

Acknowledgements

First, I would like to thank my supervisors Simon and Megan. They have always been there to offer guidance when needed but have also given me independence to develop this project and make it my own. I've been lucky to have supervisors who are excellent scientists with very different approaches. Between the two, I never lost sight of the fine details or the big picture- at least not for long. I learned a lot from each of them, whether they agreed with each other or not. Especially perhaps when they didn't! I would also like to say thanks for putting in so much time these last few months reading this thesis and giving such helpful feedback.

I would like to thank Allan for all the interesting science discussions and for sharing his vast immunology knowledge and passion for research. I feel lucky to have been part of the last generation of Mowlings who had a chance to hear his vaguely unimpressed voice at lab meetings asking: “but why??’ I’m also grateful for all the chat, stories from constant travels and sage advice about science and beyond.

To all the Millings, thanks for making the last few years unforgettable. Thanks to all the Millings who made the last few years unforgettable. Alberto, thanks for being a voice of reason and stability in an often unstable world. Thanks for taking time to teach me the techniques and skills I needed, and for putting up with endless questions in the beginning. Thanks to Verena for advice about surviving the PhD and for making sure I will never forget the PCR song. Thanks to Kgray for being an excellent bff, to Kbae for being such a nice boss, to Anna for letting your crow guide us, to Hannah for the smiles and M&Ms, and to Reshmi for keeping it real.

Thanks to everyone else who’s shared laughs, drinks or long days and nights in the lab. Thanks to Josh and Shaima for help with experiments and sharing drinks in the Hill. A big thank you is in order for Diane, Alana and Liz who go above and beyond to make sure the flow facility keeps running, against all the odds. Thanks to Dónal for providing microbiology expertise and facilities. And thanks to everyone at the CRF, especially Tony and Sandra. I couldn’t have done this without your help.

I would like to thank friends and family who kept me sane over the last few years and pulled me away from work once in a while. Thanks to my parents who have always believed in me and are always interested in what I’m working on. Finally, Claire deserves much more than a thank you. Thanks for pushing me when I needed it, for picking me up and taking me to A&E when I was broken. Thanks for always looking out for me despite your own stresses, and thanks for putting up with me through it all.

Author's Declaration

I declare that, except where reference is made to the contribution of others, this thesis is the result of my own work and has not been submitted for any other degree at the University of Glasgow or any other institution.

Signature:  Name: Slater L. Clay

Table of Contents

Table of Figures

Abbreviations

Abbreviation	Meaning
ACK	Ammonium-Chloride-Potassium
AF	Alexa Fluor
AhR	Aryl hydrocarbon receptor
AMP	Adenosine monophosphate
ANOVA	Analysis of variance
APC	Antigen presenting cell
ATP	Adenosine Triphosphate
BCR	B cell receptor
BSA	Bovine serum albumin
BUV	Brilliant ultra-violet
BV	Brilliant violet
cAMP	Cyclic adenosine monophosphate
CCL	C-C motif chemokine ligand
CCR	C-C motif chemokine receptor
cDC	Conventional dendritic cell
CFU	Colony forming unit
CLR	C-type lectin receptors
cMLN	Colon/caecum draining lymph nodes
CP	Caecal patch
CTL	Cytotoxic T lymphocyte
CTLA-4	Cytotoxic T-lymphocyte-associated protein 4
CTV	Cell trace violet
CXCL	C-X-C motif chemokine ligand
CXCR	C-X-C motif chemokine receptor
DAMP	damage-associated molecular pattern
DC	Dendritic cell
DEREG	Depletion of regulatory T cell
DSS	Dextran sodium sulfate
DT	Diphtheria toxin
EAE	Experimental autoimmune encephalomyelitis
EDTA	Ethylenediaminetetraacetic acid
FACS	Fluorescence activated cell sorting
FAE	Follicle-associated epithelium
Fas-L	Fas ligand
FCF	Follicular dendritic cell
FCS	Foetal calf serum
FoxP3	Forkhead box P3
FoxROR	$FoxP3^{RFP}xROR\gamma T^{GFP}$
FRC	Fibroblastic reticular cells
GALT	Gut-associated lymphoid tissue
GATA3	GATA binding protein 3
GF	Germ-free
GFP	Green fluorescent protein

GPR	G-protein-coupled receptor
GvHD	Graft-versus-host disease
HBSS	Hanks' Balanced Salt Solution
HEV	High endothelial venules
IBD	Inflammatory bowel disease
ICER	Inducible cAMP early repressor
ICOS	Inducible T cell co-stimulator
IDO	Indoleamine 2,3-dioxygenase
IEL	Intra-epithelial cell
IF	Immunofluorescence
IFNγ	Interferon gamma
IgA	Immunoglobulin A
IL	Interleukin
ILC	Innate lymphoid cell
ILF	Isolated lymphoid follicles
IP	Intraperitoneal
IPEX	Immunodysregulation polyendocrinopathy enteropathy X-linked
IV	Intravenous
LAG3	Lymphocyte activation gene 3
LB	Luria-Bertani
LCMV	Lymphocytic choriomeningitis virus
LP	Lamina propria
LPS	Lipopolysaccharide
LTi	Lymphoid tissue inducers
MADCAM-1	Mucosal vascular addressin cell adhesion molecule 1
MAIT cell	Mucosal associated invariant T cell
MALT	Mucosa-associated lymphoid tissue
MHC	Major histocompatibility complex
MLN	Mesenteric lymph nodes
MNP	mononuclear phagocytes
ND	Not detected
NFAT	Nuclear factor of activated T cells
NK cell	Natural killer cell
NLR	NOD-like receptors
NS	Not significant
NTS	Non-typhoid *Salmonella*
O/N	Overnight
OCT	Optimal cutting temperature
OD	Optical density
OVA	Ovalbumin
p.i.	Post-infection
PAMP	pathogen-associated molecular pattern
PB	Permeabilization buffer
PBMC	Peripheral blood mononuclear cell
PBS	Phosphate buffered saline
PBST	Phosphate buffered saline with 0.1% tween
PD-1	Programmed death-1
PE	Phycoerythrin
PMA	phorbol 12-myristate 13-acetate

PP	Peyer's patch
PRR	pattern recognition receptor
RBC	Red blood cell
RLR	RIG-1 like receptors
RNA-Seq	RNA sequencing
RORγT	Retinoic acid receptor-related orphan nuclear receptor *gamma*
RT	Room temperature
SCFA	Short chain fatty acid
SCID	Severe combined immunodeficiency
scRNA-Seq	Single cell RNA sequencing
SCS	Sub-capsular sinus
SD	Standard deviation
SED	Sub-epithelial dome
SEM	Standard error of the mean
SI	Small intestine
SILT	Solitary intestinal lymphoid tissues
sMLN	Small intestine draining lymph nodes
SPF	Specific pathogen-free
STAT	Signal transducer and activator of transcription
STM	*Salmonella enterica* serotype Typhimurium
T3SS	Type three secretory system
Tconv	Conventional T cell
TCR	T cell receptor
TGFβ	Transforming growth factor β
Th	T helper
Tim-3	T-cell immunoglobulin and mucin-domain containing-3
TLR	Toll-like receptor
TNF	Tumour necrosis factor
Treg	Regulatory T cell
Tresp	Responder T cell
TRM	Tissue-resident memory
t-SNE	t-Distributed Stochastic Neighbour Embedding
UC	Ulcerative colitis
WT	Wild type

Chapter 1 General Introduction

1.1 The intestinal immune system

The intestines are essential for nutrient absorption and host a vast microbial ecosystem that shapes our health and behaviour. Close contact with a complex and dynamic microbiome and exposure to dietary antigens and potential pathogens make the intestines a critical barrier site. The intestinal immune system is required to perform a delicate balancing act between tolerance to dietary antigens and commensal microbiota, and prevention of infection by microbial pathogens. If the balance between immune tolerance and activation is skewed towards inflammation, immunopathology including food intolerance and chronic inflammation can result. On the other hand, excessive tolerance can lead to increased susceptibility to infection or cancer. The intestinal immune system must therefore be tightly regulated to facilitate both tolerogenic and inflammatory responses and to restore balance quickly following physical damage or infection.

1.1.1 Gross anatomy of the intestines

Although the intestinal tract is a contiguous tube-like structure, the intestines comprises multiple organs with distinct characteristics, structural morphology, cellular components and microbial symbionts (Agace and McCoy, 2017; Mowat and Agace, 2014). The small intestine (SI) includes the duodenum, which begins at the pyloric sphincter, the jejunum, and the ileum, which terminates at the caecum. The inner wall of the small intestine is covered in finger-like villi, which maximise surface area exposed to the luminal contents to facilitate nutrient absorption. Peyer's patches (PPs) are visible through the outer layer of the SI and are important components of the gut-associated lymphoid tissue (GALT).

The large intestine begins at the ileocaecal valve that separates the terminal ileum from the caecum. The large intestine includes the caecum and colon, which terminates at the anal canal. The luminal side of the large intestine does not contain villi but is covered with embedded crypts. The lack of villi underlies a functional difference between the SI and colon; instead of nutrient absorption, the colon primarily reabsorbs water from luminal

contents. Two layers of mucus line the colon, which provides the first defence against infection by potentially pathogenic microbes (Hansson, 2012; Swidsinski et al., 2007). The large intestinal lumen is less acidic than the SI, and there is high abundance and diversity of commensal bacteria (Gu et al., 2013; Quigley, 2013). The microbiome plays an import role breaking down complex carbohydrates into readily absorbed metabolites such as short-chain fatty acids (SCFA) (Cho et al., 2012; Fleming and Floch, 1986; Morrison and Preston, 2016). There are no PPs in the large intestine although a caecal patch is present in the caecum; in humans this is located in the appendix. Throughout the SI and large intestine, there are thousands of microscopic lymphoid aggregates known as solitary intestinal lymphoid tissues (SILT).

Despite differences between the large and small intestines, there are structural similarities. The inner layer of the intestines is mucous-covered epithelium, which is a barrier between the luminal contents and the underlying lamina propria (LP). The LP contains a wide range of immune cells and contains SILTs. Together, the epithelium and LP comprise the intestinal mucosa. Beneath the mucosa is the highly vascularised sub-mucosa, which also contains lymphoid tissue such as PPs. Below the sub-mucosa is the lamina muscularis, which contains highly innervated musculature, and the serosa, which is the outermost layer of the intestines. Intestinal lymphatic vessels drain to mesenteric lymph nodes (MLN), which drain distinct intestinal regions (Fig 1.1). MLNs play an important role in initiating immune responses to antigen encountered in the intestines (Huang et al., 2000; Macpherson and Smith, 2006). The structure and cellular components of the MLN and intestinal mucosa including GALT are shown in Figs 1.2 and 1.3, respectively.

1.1.2 Intestinal epithelium

The intestinal epithelium lines the luminal side of the intestines and contains enterocytes with microvilli. These enterocytes differentiate from stem cells within microscopic depressions or crypts (Barker et al., 2008; Bjerknes and Cheng, 1999; Clevers, 2013). As new epithelial cells are generated, older cells move out of the crypts and towards SI villi

or colonic apical surfaces, where they are eventually shed into the lumen. In this way, aging or damaged epithelial cells are constantly replaced every 2-5 days (van der Flier and Clevers, 2009; Garrett et al., 2010). In addition to enterocytes, the intestinal epithelium contains microfold cells (M cells), intra-epithelial lymphocytes (IELs) and secretory cells, such as goblet cells, Paneth cells and tuft cells.

Goblet cells are mucus-secreting cells located throughout the intestines, but are enriched in the large intestine, where there is a thicker mucous lining comprising two layers (Ermund et al., 2013; McGuckin and Hasnain, 2017). Mucus facilitates passage of luminal contents and provides a crucial physical barrier between the host and the microbiota. Mucus contains mucins including Muc2 and salts, suspended in water, which form a dense glycoprotein gel (Lievin-Le Moal and Servin, 2006; Rodríguez-Piñeiro et al., 2013; Schroeder, 2019). The intestinal mucus layers are not only a barrier for pathogens, but provide a niche for commensal microbiota. Intestinal mucus can be broken down and consumed by specific species of bacteria, so mucus composition can selectively regulate the microbes that colonises the lumen (Marcobal et al., 2013; Martens et al., 2018; Sonnenburg, 2005). The importance of mucus for intestinal health is demonstrated by the finding that mucus thickness is reduced during intestinal inflammation and increases susceptibility to infection (Desai et al., 2016; Johansson et al., 2014; Swidsinski et al., 2007). Indeed, reduced mucus production is associated with inflammatory bowel disease (IBD) and is a fundamental aspect of Dextran Sodium Sulfate (DSS)-induced colitis (Gersemann et al., 2009; Johansson, 2014; Schultsz et al., 1999).

In addition to their role as mucous secretors, goblet cells facilitate the passage of luminal antigen to LP antigen presenting cells (APCs) through goblet cell-associated passages (GAPS). GAP-mediated antigen transport plays a role in maintaining tolerance to food- and microbial-derived antigen (McDole et al., 2012). GAPS have been identified in the SI and colon and have been shown to be blocked during intestinal infection (Knoop et al., 2017; Kulkarni et al., 2018).

While goblet cells are enriched in the large intestinal epithelium, Paneth cells are primarily located in the SI epithelium. Paneth cells can detect inflammation through interleukin (IL)-22 signalling or directly detect bacteria through toll-like receptors (TLRs) and Myd88 signalling (Vaishnava et al., 2008). Following activation, they can produce antimicrobial and inflammatory proteins including defensins, lysozyme and tumour necrosis factor (TNF)α (Elphick, 2005; Vaishnava et al., 2008; Wilson, 1999).

Tuft cells are chemosensory cells that differentiate from intestinal stem cells They are upregulated during helminth infection, produce the alarmin IL-25 and play an important role in anti-parasite responses (Gerbe et al., 2016; Harris, 2016; Howitt et al., 2016).

Microfold cells (M cells) are specialised epithelial cells that differentiate in the follicle-associate epithelium (FAE) above GALT. M cells transport microbes and microbial antigens from the intestinal lumen into the sub-epithelial dome (SED) of PPs/CPs, or into the LP. M cells deliver antigen to antigen presenting cells (APC) such as dendritic cells (DCs), and play an important role in initiating immune response (Kraehenbuhl and Neutra, 2000; Mabbott et al., 2013).

In addition to cells derived from intestinal stem cells, the epithelium also contains a population of intra-epithelial lymphocytes (IELs) that act as an early defence against pathogens. These lymphocytes are mostly $CD3^+$ T cells, including those with αβ and γδ T cell receptors (TCRs). In humans, IELs are predominantly αα or αβ $CD8^+$ T cells, although the frequency of γδ T cells is increased in inflammatory conditions such as coeliac disease (Meresse et al., 2012; Sollid, 2004). IELs are antigen-experienced cells and are primed to initiate rapid responses against pathogens (Mayassi and Jabri, 2018; Sheridan and Lefrançois, 2010).

1.1.3 Intestinal lamina propria

Separated from the intestinal lumen by the epithelium, the LP contains abundant immune cells including lymphocytes, granulocytes and mononuclear phagocytes (MNPs). MNPs include monocytes, macrophages and dendritic cells (DCs) that are important immune

sentinels. LP macrophages are resident phagocytic cells that clear apoptotic debris and detect microbial antigens, metabolites and other danger signals with pattern recognition receptors (PRRs). PRRs include surface-bound C-type lectin receptors (CLRs), cell membrane-bound TLRs and cytoplasmic NOD-like receptors (NLRs) and RIG-1 like receptors (RLRs). PRRs recognise structural motifs specific to bacteria, viruses, parasites or other pathogens, referred to as pathogen-associated molecular patterns (PAMPs). Once PAMPS are detected, macrophages may become activated, phagocytose microbes for lysosomal degradation, and produce cytokines or growth factors to recruit and regulate other immune cells (Bain and Mowat, 2014; Geissmann et al., 2010).

In addition to similar phagocytic activity, DCs are specialised antigen presenting cells (APCs) that play a crucial role in driving adaptive, antigen-specific immune response. DCs are migratory cells and following activation, they upregulate C-C chemokine receptor (CCR)7, which facilitates migration to lymphoid tissues such as mesenteric lymph nodes (MLN) (Cerovic et al., 2014). Activated DCs upregulate major histocompatibility complex class II (MHC II), co-stimulatory molecules and cytokines that control the activation and differentiation of T cells (Jenkins et al., 2001; Langenkamp et al., 2000; Mondino et al., 1996).

Lymphocytes comprise an abundant and heterogenous group of cells in the LP that play fundamental roles in both innate and adaptive immunity. The role of T cells and B cells in the intestines are well characterised but innate lymphoid cells (ILCs) have recently been shown to play important roles in intestinal immune responses (Hepworth et al., 2013; Sonnenberg and Artis, 2012). ILCs lack both T cell receptors (TCRs) and B cell receptors (BCRs), and therefore respond to non-antigen-specific cues. Natural killer (NK) cells, are well-described ILCs that recognise host cells that are missing MHC class I proteins (Vivier et al., 2011). NK cells can be considered a population of ILC1 cells; ILC2 cells play an important role in early response to helminth infection; and ILC3 cells produce cytokines such as IL-22 and IL-17 early after infection and are a major source of IL-2 in the LP (Spits et al., 2013; Takatori et al., 2009; Zhou et al., 2019). Lymphoid tissue inducer (LTi) cells

are a specialised ILC3 type that is required for the genesis of lymphoid follicles such as cryptopatches and intestinal lymphoid follicles (ILFs) (Sonnenberg et al., 2011) (Fig 1.3).

T cells differentiate from thymic precursors and include cells that require classical antigen presentation and innate cells that can respond quickly to non-specific stimuli, before adaptive responses can develop. Intestinal innate-like T cells include γδ T cells, which express TCRs with γ and δ chains and are typically IELs (Di Marco Barros et al., 2016; Holtmeier and Kabelitz, 2005).

In contrast to innate-like T cells that can respond rapidly to infection, conventional $CD3^+$ T cells express a single TCR clone that binds a specific peptide presented within MHC molecules. Conventional T cells can be broadly characterised by co-receptors CD8 or CD4. $CD8^+$ T cells are cytotoxic cells that can target cells infected by intracellular pathogens, which they recognise by antigen presented by MHC I molecules. Following antigen recognition, CD8 T cells can respond by releasing inflammatory cytokines such as TNFα and IFNγ, by releasing granzyme and perforin to kill infected cells, or by inducing apoptosis through FasL-Fas interactions (Kägi et al., 1994; Rouvier et al., 1993). $CD4^+$ T helper (Th) cells are classically activated by recognising cognate antigen presented in MHC II molecules in addition to co-stimulatory signals. Once activated, CD4 T cells can differentiate into different Th subsets and orchestrate a wide range of immune responses, including tolerogenic or inflammatory responses directed against a wide range of pathogens. The activation and differentiation of CD4 T cells will be discussed further below.

B cells are another group of lymphocytes crucial to intestinal immunity and are both APCs and producers of Immunoglobulin (Ig) antibodies, that bind specific molecular epitopes on pathogens. B cells are produced in the bone marrow and express B cell receptors (BCRs) that are transmembrane Ig molecules that can bind cognate antigen independently of MHC molecules. Following activation, B cells can differentiate into antibody-producing plasmablasts, long-lived plasma cells or memory B cells, that can rapidly become activated during re-infection. In the intestine, B cells primarily produce IgA antibodies,

which are secreted by B cells in follicles of the MLN and locally in PPs or ILFs (Bouskra et al., 2008; Craig and Cebra, 1971; Reboldi and Cyster, 2016).

The adaptive immune response requires multiple cell types to converge and communicate through antigen presentation, co-stimulation or cytokine production. The convergence of different cells to drive adaptive immunity in the intestines occurs in lymphoid tissue including MLNs and GALT.

1.1.4 Mesenteric lymph nodes

The MLNs are draining lymph nodes for the intestines and are important induction sites for adaptive immune responses to intestinal pathogens or other antigens. A chain of colon- and SI- draining MLNs (sMLN and cMLN respectively) each drain a distinct portion of the intestines (Houston et al., 2015), and this regionalised drainage is depicted in Fig 1.1.

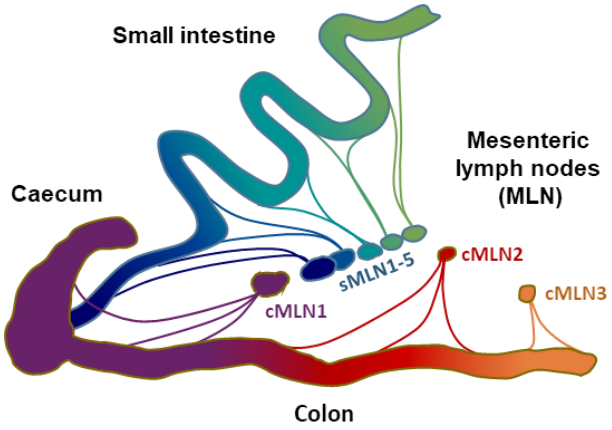

Figure 1.1 Mesenteric lymph nodes drain distinct regions of the intestines.
Schematic representation of regionalised drainage of lymph from different areas or the murine SI (blue-green) or large intestine (purple-orange) into specific MLNs. cMLN1 and the sMLNs form a single chain in a layer of mesenteric adipose tissue, while cMLN2 and cMLN3 are located separately along the distal colon and rectum.

MLNs, like other LNs are encapsulated tissues with distinct regions, populated with resident and migratory cells, facilitating the presentation of antigen to both T cells and B cells (Fig 1.2). Lymphatic fluid, containing migratory cells including T cells, B cells and DCs, flows from the intestines through afferent vessels into the MLN subcapsular sinus (SCS), which contains $CD169^{+}$ SCS macrophages that can bind and phagocytose lymph-borne pathogens (Junt et al., 2007; Kuka and Iannacone, 2014). Migratory cells in afferent lymph transit into the cortex, containing B cell follicles with B cells and follicular DCs

(FDCs), and interfollicular regions. The interfollicular regions and neighbouring paracortex contain T cell zones populated with DCs, naïve T and FoxP3+ regulatory T cells (Liu et al., 2015; Mondino et al., 1996). The paracortex is vascularised with HEVs that are entry points for naïve lymphocytes arriving from the peripheral blood.

MLN fibroblastic reticular cells (FRCs) express C-C motif chemokine ligand (CCL)19 and CCL21, ligands for CCR7. CCR7 is expressed by migratory DCs, activated B cells, naïve T cells, regulatory T cells (Tregs), and a sub population of memory T cells (Kain and Owens, 2013). CCR7 expression by migratory cells and CCR7 ligand expression by FRCs are required for optimal induction of adaptive immunity (Luther et al., 2000). The medullary sinus, containing medullary macrophages and plasma cells, provides a conduit for migrating cells to pass from the cortex into the efferent lymphatic vessels. Once efferent lymph exits the MLN, it travels through the lymphatics into the thoracic duct, from where it drains into the subclavian veins.

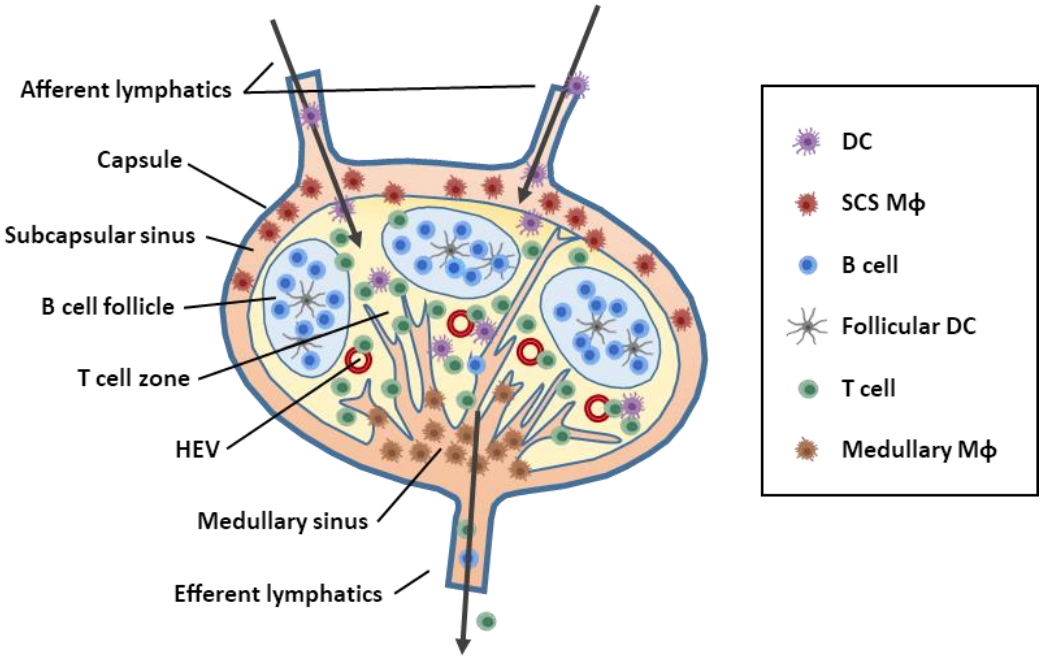

Figure 1.2 Structure and cells of a mesenteric lymph node.

Cartoon depiction of a lymph node, which is capsulated and divided into distinct regions. Afferent lymphatic vessels carry lymph into the subcapsular sinus (SCS), which surrounds cortex encompassing B cell follicles and interfollicular regions. The sub-cortex includes T cell zones and high endothelial venules (HEV) that deliver lymphocytes from circulating peripheral blood. The medullary sinus feeds from the cortex into efferent lymphatic vessels that carry lymph out of the nodes. Mφ, macrophage; DC, dendritic cell. Adapted from Girard et al. (2012).

In summary, MLNs facilitate a convergence of lymph-borne cells migrating from the intestines with lymphocytes circulating in peripheral blood. This convergence is essential for the development of antigen-specific immune responses to pathogens or tumours and the maintenance of tolerance to microbial and food antigen. In addition to being important sites for the induction of adaptive immunity, MLNs have been shown to play an important role in limiting dissemination of intestinal pathogens, including *Salmonella* (Griffin et al., 2011; Voedisch et al., 2009). Together, these functions make the MLNs crucial tissues for the intestinal immune system.

1.1.5 Gut-associated lymphoid tissue

The GALT are a network of lymphoid tissue containing aggregates of immune cells in the intestines. While MLNs are sometimes characterised as part of the GALT, here the term is used to specify tissue within the intestines. The GALT include a series of Peyer's patches (PP), which are multi-follicle lymphoid aggregates located along the SI; the caecal patch (CP), which is a similar tissue in the mouse caecum or human appendix; and solitary intestinal lymphoid tissues (SILT). The intestines contain thousands of SILT including a developmental continuum of aggregates from microscopic cryptopatches to ILFs. The structure and cellular components of the GALT are shown in Fig 1.3.

Peyer's patches and caecal patches

PPs and CPs develop embryonically and occupy areas in the intestinal wall that extend from the intestinal submucosa to the sub-epithelial dome (SED) beneath follicle-associated epithelium (FAE) (Jung et al., 2010). The structure of PPs is similar to MLNs, with multiple B cell follicles surrounded by areas containing T cells and DCs. SED-associated $CCR6^+$ DCs populate an area beneath the FAE, which itself is enriched with M cells (Iwasaki and Kelsall, 2000). These DCs are poised to phagocytose microbiota and food antigen that transit through M cells and have also been shown to acquire antigen by extending dendrites through the FAE (Allen et al., 2016; Lelouard et al., 2012; Niess, 2005). Once antigen is acquired by PP DCs, they can present this to CD4 T cells that are recruited to the PPs by B cells expressing CXCL9 (Iwasaki and Kelsall, 1999; Wang et

al., 2018). Unlike MLNs, there are no afferent lymphatics for PPS or CPs, although they contain HEVS, where naïve lymphocytes can enter from the peripheral blood.

PPs/CPs have several important roles in the intestinal immune system. Like MLNs, they are induction sites for adaptive immunity, including priming and activation of T cells and maturation of B cells. Their position adjacent to the M cell-enriched FAE, means that SED DCs have access to antigen as it passes through M cells, and can present this antigen to T cells *in situ* without requiring lymphatic migration. PPs are therefore important tissues for rapid responses against pathogens or to maintain tolerance to dietary antigen. The location of the CP suggests that it may play a role in maintaining tolerance to microbial antigens, including the high abundance of aerobic microbiota in the caecum (Marteau et al., 2001). PPs have been shown to be major sources of intestinal IgA (Craig and Cebra, 1971; Reboldi and Cyster, 2016) and their position below the FAE means that immunoglobulin A (IgA) produced by follicle plasma cells can be released in close proximity to luminal pathogens.

Solitary intestinal lymphoid tissues

SILTs include a developmental continuum from microscopic cryptopatches to mature ILFs, which can be found throughout the SI and large intestine (Pabst et al., 2005). Unlike PPs/CPs, mouse ILFs do not develop embryonically but do so after birth. SI ILF formation is dependent on the microbiota and do not form in germ-free (GF) mice, although they quickly develop following microbial colonisation in a TLR-dependent manner (Bouskra et al., 2008; Herbrand et al., 2008). On the other hand, colonic ILFs have been shown to develop independently of microbiota and develop in GF mice (Donaldson et al., 2015). In contrast to mice, human ILFs develop *in utero* and play an important role in priming early intestinal responses and IgA production (Gustafson et al., 2014).

ILF development begins with microscopic cryptopatches, which are small clusters of LTi cells and follicular DCs (FDCs) (Pabst et al., 2005). Cryptopatches develop into immature ILFs as B cells join the cluster of cells, and immature ILFs may then develop into mature ILFs. Intestinal ILFs can develop in the LP or the submucosa; as they mature, B cells and

FDCs develop into a follicle-like structure that can become vascularised by high endothelial vessels (HEVs) and lymphatics (Buettner and Lochner, 2016; Wang et al., 2018). Mature ILFs contain DCs and CD4 T cells, including both conventional T cells (Tconv) and FoxP3$^+$ Tregs. Following maturation, ILFs can regress to immature stages or disappear altogether (Bouskra et al., 2008; Pabst et al., 2005). The development of ILFs and cellular components of the intestinal mucosa are shown in Fig 1.3.

The similarities between ILF and PP/CP structure, cellular components and location suggest that GALTs may have similar functions. Like PPs/CPs, ILFs are important sources of IgA (Knoop and Newberry, 2012; Lorenz and Newberry, 2004), and the accumulation of CD4 Tconvs and Tregs suggests that ILFs are localised induction sites for adaptive immunity (Hamada et al., 2002). The specialised role of ILFs compared to PPs/CPs is likely related to the large number and dispersal of ILFs throughout the intestines. Murine SI contain 50-60 ILFs/cm^2, which is a similar density to the human SI (Pabst et al., 2005; Senda et al., 2019). In the colon, there are ~150 ILFs/cm^2, which comprises 2.5-5.0% of the colonic surface area (Senda et al., 2019). This dense network of ILFs allows a rapid and highly localised response to be initiated to throughout the intestines. Further research is warranted to clarify how lymphocytes activated in ILFs, and the GALT in general, can disseminate to carry out more regional immune responses.

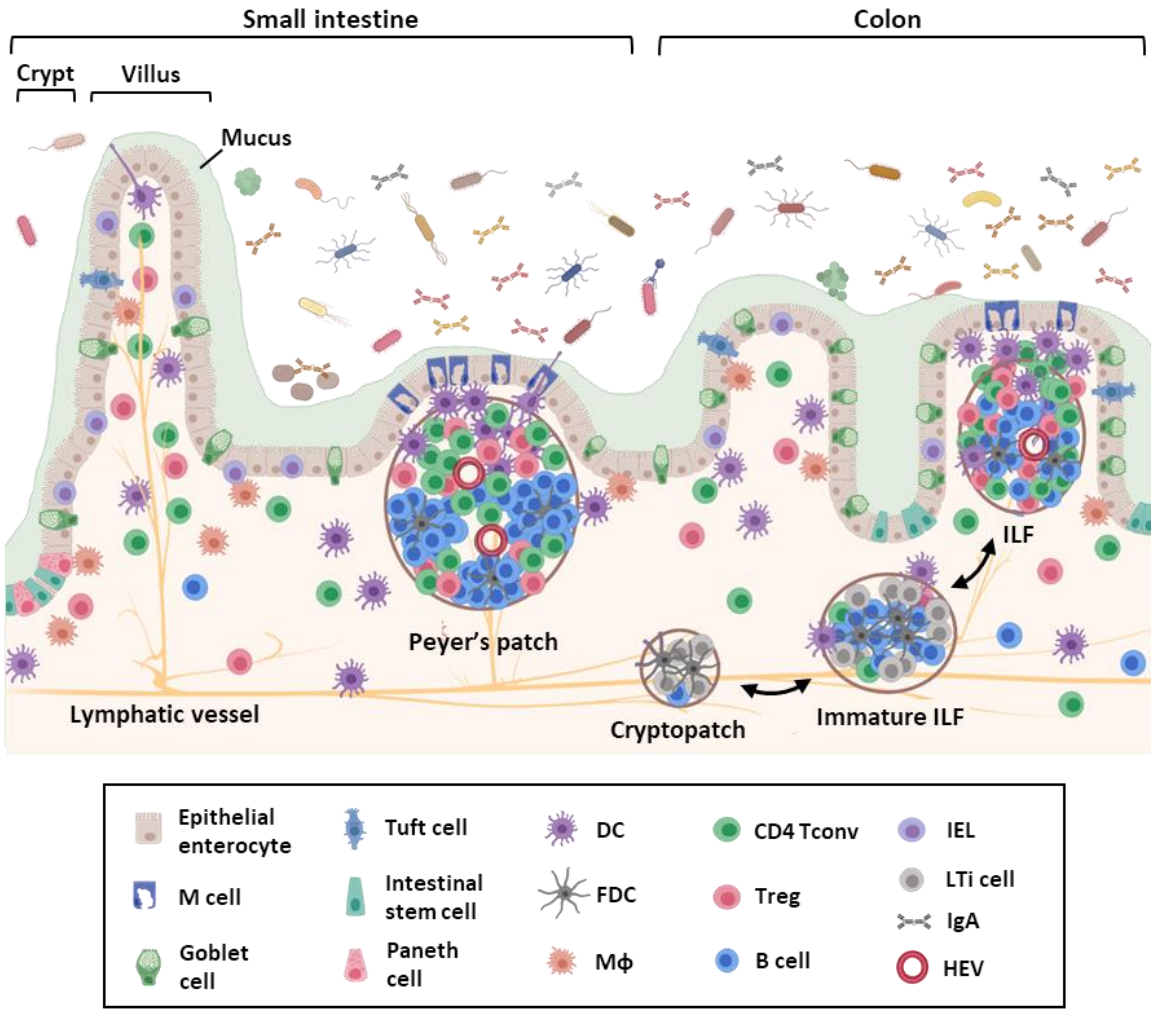

Figure 1.3 Cellular components of the intestinal mucosa with gut-associated lymphoid tissue.

Cells of the SI (left) and colonic epithelium and LP (right) are diagrammed with luminal microbes and IgA. GALT follicles are shown, including a PP in the SI and an ILF in the colon. The development of a mature ILF from an immature follicle, which itself develops from a colonic cryptopatch, is indicated by arrows. Mature ILFs can become vascularised, with efferent lymphatics and HEV present. Bidirectional arrows represent the potential for mature ILFs to regress to immature stages or cryptopatches. DC, dendritic cell; FDC, follicular dendritic cells, IEL, intra-epithelial cell; HEV, high endothelial venule; ILF, isolated lymphoid follicle; LTi cell, lymphoid tissue inducers cells; M cell, microfold cell; Mφ, macrophage; Tconv, conventional T cell; Treg, regulatory T cell. Adapted from Buettner and Lochner (2016).

1.2 Intestinal CD4 T helper cells

CD4 T cells are also known as T helper (Th) cells to discriminate them from $CD8^+$ cytotoxic T lymphocytes (CTLs). Here, CD4 T cells may be referred to as Th cells in reference to different Th subsets, or conventional T cells (Tconvs) to distinguish them from Tregs, discussed below. CD4 T cells play a major role in the intestinal immune system: orchestrating responses against pathogens; tolerance to microbes, food and self-antigens; and maintaining immunological memory. They produce cytokines that modulate the function of cells including other lymphocytes, MNPs and stromal cells. The capability

of CD4 T cells to protect the host against pathogens and limit immune pathology requires a fine-tuned balance. The diversity and plasticity of CD4 T cells underlies their potential to coordinate complex, dynamic and highly regulated immune responses in the gut.

CD4 T cells develop from haemopoietic progenitors in the thymus. Initially, positive selection leads to survival of T cells that recognise self-MHC and subsequent negative selection leads to the deletion of T cells that strongly recognise self-peptides. Following selection for survival, CD4 T cells emerge as naïve T cells expressing αβTCR clones specific for a peptide-MHCII complex (Hedrick et al., 1984; Yanagi et al., 1984). Naïve CD4 T cells express CCR7 and CD62L, which facilitates migration between secondary lymphoid tissues, where they may encounter cognate antigen, presented by DCs (Langenkamp et al., 2000; Sallusto and Lanzavecchia, 2000).

1.2.1 CD4 T cell activation

As previously mentioned, activation of naïve CD4 T cells occurs in secondary lymphoid organs following TCR and CD4 engagement with cognate antigen presented on the surface of APCs with MHC II molecules (Grakoui, 1999; Jenkins et al., 2001). In addition to TCR/CD4 engagement, T cell activation requires co-stimulation by APC surface molecules. These included CD80/CD86, which interact with T cell CD28, CD40 which interacts with T cell CD40L, and inducible T cell co-stimulator (ICOS), which interacts with T cell ICOS-L (Clark and Ledbetter, 1994; Dong et al., 2001; Mueller et al., 1989). If TCR-MHC II engagement is accompanied with sufficient co-stimulation, TCR signalling can activate transcriptional programmes, leading to proliferation and upregulation of a wide range of proteins including chemokine receptors (Linsley, 1991; Sallusto et al., 1998). Depending on the cytokines present during activation, CD4 T cells can be induced to proliferate and differentiate into T helper (Th) subsets that can carry out various effector functions (Ivanov et al., 2006; Mosmann and Sad, 1996). On the other hand, if TCRs engage their cognate antigen without sufficient co-stimulation, they can become anergic, apoptotic or tolerised (Gimmi et al., 1993; Schwartz, 1990; Van Parijs et al., 1996).

1.2.2 Differentiation of T helper subsets

Following activation, CD4 T cells can differentiate into T helper (Th) subsets including Th1, Th2 or Th17 cells (Fig 1.4) (Harrington et al., 2006; Langenkamp et al., 2000). Each of these subsets express a 'master' transcription factor (TF), that controls a transcriptional programme for protein expression and effector functions to target specific types of pathogens (Ivanov et al., 2006; Szabo et al., 2000; Zheng and Flavell, 1997). The differentiation of Th subsets is at least partially controlled by cytokines produced by cells including APCs, other T cells and innate lymphocytes (Hsieh et al., 1993; O'Garra, 1998).

Th1 cells play an important role in host defence against intracellular pathogens including viruses and bacteria (Hsieh et al., 1993; Zhu and Paul, 2008). Cytokines IL-12 and interferon γ (IFNγ), produced by cells including ILCs and DCs, instruct Th1 differentiation. Th1 cells express the TF T-bet, which can drive expression of chemokine receptor CXCR3 and cytokines including IFNγ and tumour necrosis factor (TNF) (Hsieh et al., 1993; Romagnani, 1997). Th1 cytokines can activate MNPs to enhance anti-bacterial and anti-viral responses, and increase the activation of other Th1 cells and other type I lymphocytes including ILC1s (Macatonia et al., 1995; Szabo et al., 2000).

Th2 cells are important for protection against helminths or other parasites and they also play a role in allergic responses (Pearce, 1991; Prescott et al., 1998). Th2 differentiation is instructed by IL-4, which is produced by cells including T cells, basophils and mast cells (Ballesteros-Tato et al., 2016; Coquet et al., 2015; Piehler et al., 2011), although IL-4 is not required for Th2 differentiation (Brewer et al., 1999). Th2 cells express the GATA binding protein 3 (GATA3), which can drive expression of chemokine receptors CXCR4, CCR8, and cytokines IL-4, IL-5 and IL-13 (Yamashita et al., 2004; Zheng and Flavell, 1997).

Th17 cells were first identified in 2005 and play an important role in defence against extracellular pathogens including bacteria and fungi (Harrington et al., 2005; Ivanov et al., 2006; Park et al., 2005). Th17 cells are enriched at mucosal sites and have been shown to play a role in inflammatory diseases and autoimmunity (Fina et al., 2008; Wang et al.,

2009a). Th17 differentiation is induced by IL-6, IL-23 and TGFβ via STAT3 signalling (Bettelli et al., 2006; Mangan et al., 2006). Conversely, the differentiation of Th17 cells is inhibited by Th1- and Th2-associated cytokines such as IL-12, IFNγ and IL-4 (Damsker et al., 2010; Olsen et al., 2011; Sallusto et al., 1998). Th17 cells express the TF Retinoic acid receptor-related orphan nuclear receptor gamma (RORγT), which can upregulate expression of the chemokine receptor CCR6 and cytokines including IL-17A, IL17F, IL-21 and IL-22 (Liang et al., 2006; Mangan et al., 2006; Zhou et al., 2009). A simplified overview of Th subset differentiation pathways is outlined in Fig 1.4.

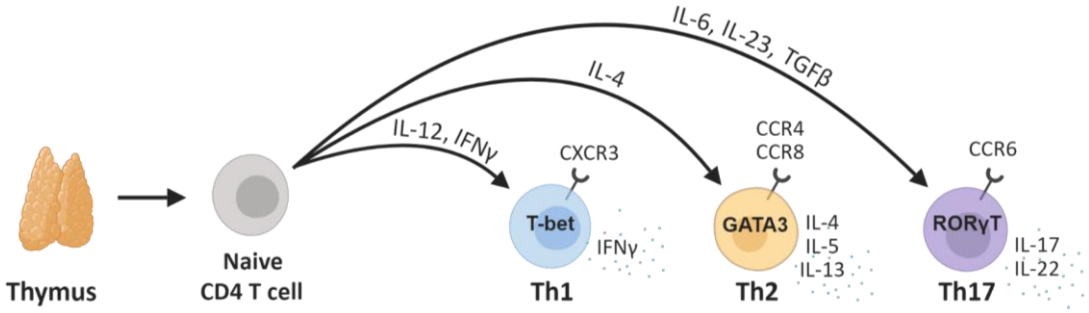

Figure 1.4 Differentiation pathways of CD4 T helper subsets.
The differentiation pathways of Th1, Th2 and Th17 subsets are shown from naïve CD4 T cells. 'Master' TF expression is noted within cell symbols. Cytokines that instruct differentiation are shown above arrows and cytokines produced by each population are listed to the right of cell symbols. Important chemokine receptors are noted.

1.2.3 Conventional T cell trafficking to the intestines

During intestinal infection or inflammation, Th cells migrate from lymphoid tissues where they are activated to locations where they can carry out effector functions and promote host defence against infection.

Expression of Th subset 'signature' chemokine receptors (Fig 1.4) are important for directing Th cells to specific regions of inflamed sites throughout the body. CXCR3 expression by Th1 cells directs migration to its ligands CXCL9 and CXCL10, expressed by multiple cell types including DCs and endothelial cells, and can be upregulated during inflammation (Hardison et al., 2006; Romagnani et al., 2004). $CXCR3^{+}$ Th1 cells may therefore be preferentially recruited to sites of inflammation through chemokine gradients.

In the intestines, CXCR3 ligands are upregulated in mouse models of colitis and IBD, and anti-CXCL10 therapy has been promoted as a possible therapeutic for ulcerative colitis (UC) patients (Mayer et al., 2014b; Sasaki et al., 2002; Schroepf et al., 2010; Singh et al., 2016). CCR6 expression by Th17 cells also plays an important role in migration to inflamed sites. CCR6 ligand CCL20 is upregulated by inflamed intestinal epithelium and is also expressed by FAE adjacent to GALT (Wang et al., 2009a). Mice with induced colitis and IBD patients have increased CCL20 expression, indicating an important role for CCR6-dependent migration in intestinal inflammation (Kaser et al., 2004; Teramoto et al., 2005). CCR4 and CCR8 expression by Th2 cells facilitates migration to chemokines CCL17, CCL22, CCL1 and CCL18. As with CXCR3 and CCR6 ligands, Th2-associated chemokines have been shown to be upregulated during inflammation (Islam et al., 2011; Yoshie and Matsushima, 2015)

While Th-associated chemokine receptors are important for recruiting T cell subsets to sites of inflammation, further homing instruction is required to specifically direct Th cells to the intestines. Site-specific homing can be imprinted during T cell priming and induces expression of various receptors and integrins that direct Th cells out of the MLN or GALT towards receptor ligands in intestinal vasculature, epithelium and LP.

One well characterised receptor important for gut homing is the integrin α4β7, which binds mucosal vascular addressin cell adhesion molecule 1 (MADCAM-1), expressed by stromal cells in intestinal LP venules (Agace, 2010; Berlin et al., 1993; Campbell et al., 2001). CCR9 is another homing receptor shown to direct T cells to the SI, where its ligand CCL25 is expressed by epithelial cells (Briskin et al., 1997; Kunkel et al., 2000). Receptors that instruct colon-specific trafficking has been more elusive, although the G-protein-coupled receptor 15 (GPR15) has been shown to play an important role in homing of Tconvs and Tregs to the colon (Kim et al., 2013; Nguyen et al., 2015). GPR15 expression by Tconvs was required for a transfer model of colitis (Nguyen et al., 2015; Picarella et al., 1997) and is highly expressed on human colonic Tconvs, especially Th2 cells (Fischer et al., 2016; Kim et al., 2013). GPR15 is not expressed by T cells in the cMLNs, and are

upregulated in the colon, suggesting this receptor may play a role in colonic T cell retention rather than homing (Houston et al., 2015). GPR15 is not exclusively expressed in the colon however, and GPR15^{+} T cells have been identified in tissues including the skin and liver (Fischer et al., 2016; Lahl et al., 2014).

A combination of GPR15 and α4β7 expression has been suggested to instruct colon-specific homing or retention, but further research is required to clarify this. Difficulty identifying GPR15 ligands has added to uncertainty about its role as a homing receptor. One ligand, GPR15L, has recently been identified that is expressed in tissues including colonic epithelium, skin and the cervix; and another ligand, C10orf99, has been identified that is expressed by vascular endothelial cells (Pan et al., 2017; Suply et al., 2017).

In summary, Th populations can be programmed to express subset-associated chemokine receptors that direct cells to sites of inflammation, and site-specific receptors that direct them to specific sites in the intestines. Together, these receptors can direct cell migration and retention to specific regions to carry out effector functions. This is a crucial aspect for Th cells to quickly and efficiently accumulate in areas where a response is required. A rapid and specific CD4 T cell response is crucial for host defence of the intestines. Once an inflammatory response is initiated, CD4 T cells orchestrate multiple cell processes, including affinity maturation and antibody production by B cells, and the development of a long lasting memory population. However, the immune response must be tightly regulated to prevent acute immunopathology and facilitate resolution of inflammation following infection or other injury. Tregs are a population of CD4 T cells that play a critical role in modulating immune responses and protecting the host from immunopathology.

1.3 Intestinal regulatory T cells

FoxP3^{+} Tregs play an integral part in intestinal immune responses: maintaining tolerance to dietary antigen, the microbiota and self-antigen; controlling immune response to limit immunopathology and restoring homeostasis following inflammation. The importance of Tregs is evident in Treg-deficient scurfy mice and in humans with IPEX syndrome, who

succumb to systemic immunopathology and autoimmunity (Barzaghi et al., 2012; Bennett et al., 2001; Clark et al., 1999). The essential role of Tregs in maintaining intestinal homeostasis is further validated by Treg depletion models that induce severe and potentially fatal colitis (Boehm et al., 2012; Coombes et al., 2005; Mottet et al., 2003). Intestinal Tregs are a heterogenous family of cells with diverse development pathways and functional roles.

1.3.1 Regulatory T cell differentiation

Thymically derived Tregs (tTregs) are self-reactive and are selected in the thymus. Their role in preventing autoimmunity is well described (Kim et al., 2007; Sakaguchi et al., 1995, 2001). Peripherally induced (pTregs) can differentiate from naïve CD4 T cells and also play a crucial role in immune regulation (Bluestone and Abbas, 2003; Shevach and Thornton, 2014). pTregs can differentiate in environments where cognate antigen is presented in low doses, when induced by tolerogenic DCs, and in the presence of immunoregulatory cytokines including IL-10, TGFβ and IL-2 (Bluestone and Abbas, 2003; Chen et al., 2003; Earle et al., 2005). pTregs and tTregs both constitutively express the TF FoxP3, which is crucial for suppression and functional stability (Fontenot et al., 2003; Wing and Sakaguchi, 2012). FoxP3 can drive the expression of a wide range of surface receptors including high levels of IL-2R, several co-inhibitory molecules (discussed below) and cytokines including IL-10, TGFβ and IL-35 (Annacker et al., 2003; Collison et al., 2007; Fahlén et al., 2005). Reliable markers that differentiate these two developmental pathways have been elusive. The TF Helios and the membrane protein neuropillin-1 (Nrp-1) have been used to identify tTregs, but both markers can be expressed, at least at low levels, by *in vitro* induced Tregs and pTregs *in vivo* (Szurek et al., 2015; Weiss et al., 2012; Yadav et al., 2012).

In addition to FoxP3, Tregs can express Th 'master' TFs T-bet, RORγT or GATA3, which can upregulate the same 'signature' chemokine receptors as Th1, Th2 and Th17 subsets (Duhen et al., 2012; Halim et al., 2017; Levine et al., 2017; Sefik et al., 2015) *(Fig 1.5).* There is evidence that these 'Th-like' Treg populations differentiate in response to similar

cytokines but it is unclear if they differentiate from pTregs, tTregs or both (Chaudhry et al., 2009; Wing and Sakaguchi, 2012).

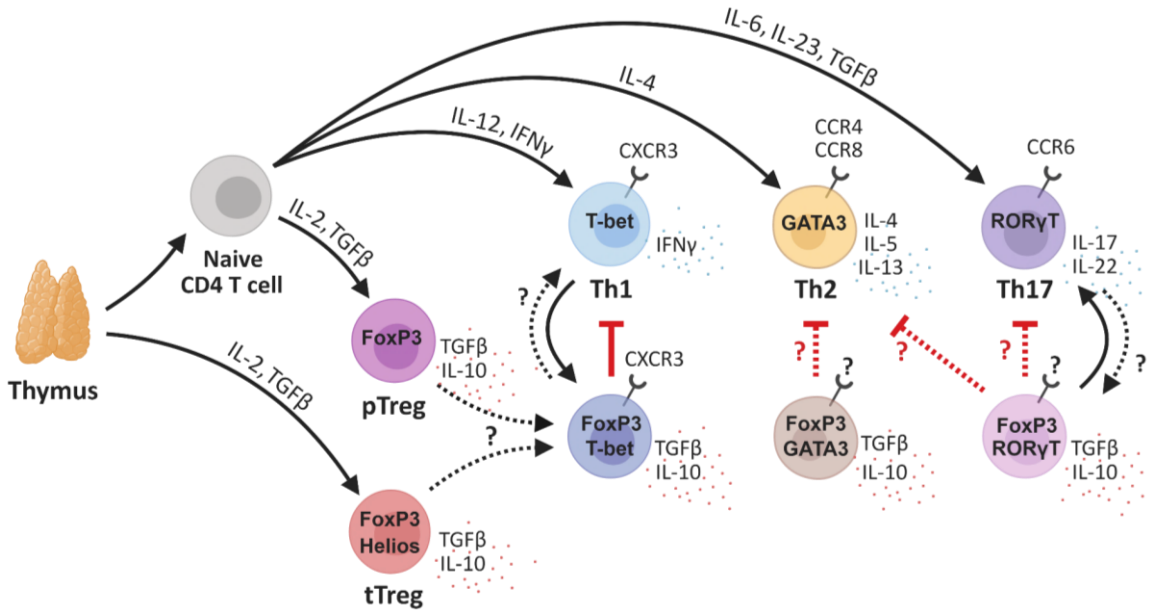

Figure 1.5 Differentiation pathways of conventional and regulatory CD4 T cells.

The differentiation pathways of FoxP3⁻ Tconvs and FoxP3⁺ Tregs is shown from thymic precursors. 'Master' TF expression is noted within cell symbols. Cytokines that instruct differentiation are shown above arrows and cytokines produced by each population are listed to the right of cell symbols. Important chemokine receptors are noted and selective inhibition is represented by red T arrows. Where pathways of differentiation or inhibition are unknown or unclear, dashed lines are used. pTreg, peripherally induced Treg; tTreg, thymic derived Treg.

The functional role of distinct Th-like Treg populations is the subject of ongoing research and there is evidence that Tregs expressing Th TFs may be able to selectively supress their respective Th subsets in some contexts (Chaudhry et al., 2009; Koch et al., 2009; Levine et al., 2017).

1.3.2 Selective suppression of T helper subsets

Selective suppression of Th subsets by Tregs expressing the same TFs has been hypothesised to be a natural consequence of Tregs and Tconvs being activated in the same setting and cytokine milieu. If this is true, then by sharing aspects of Tconv transcriptional programmes, Tregs have the potential to suppress inflammation in a targeted and fine-tuned manner (Wing and Sakaguchi, 2012). There is increasing evidence that this type of selective suppression occurs *in vivo*. For instance, Tregs have been shown to upregulate T-bet in response to type 1 inflammation and T-bet⁺ Tregs are

required for optimal control of Th1-mediated inflammation (Koch et al., 2009). It has also been demonstrated that Tregs express T-bet during *Listeria* infection, selectively suppress Th1 cells, and comprise a stable population that proliferates rapidly during reinfection (Levine et al., 2017). Furthermore, specific components of the microbiota induce RORγT^{+} Tregs that inhibit Th17-mediated colitis, and ablation of Treg-specific STAT3 (co-expressed with RORγT) induces Th17 inflammation (Chaudhry et al., 2009; Sefik et al., 2015).

These findings support the model of selective suppression, but the extent of selective suppression in other contexts or its importance for the overall immune response is unclear. It is also unclear whether Tregs expressing TFs GATA3 can selectively suppress Th2 or if these TFs facilitate broader suppressive functions (Cretney et al., 2011; Wang et al., 2011; Zheng et al., 2009). Questions remain about mechanisms that facilitate selective suppression, although chemokine receptor-mediated colocalization is a potential mechanism supported by immunofluorescent imaging (Levine et al., 2017). Further research is warranted to address the question of whether colocalization of Tregs and Tconvs expressing the same TFs can drive selective suppression in other settings.

1.3.3 Regulatory T cell intestinal trafficking

Treg suppression can be carried out by contact-dependent and independent mechanisms to target Tconvs and DCs (discussed below). Furthermore, Tregs can exert suppressive functions in both lymphoid sites such as the MLNs and GALT, or in mucosal sites of intestinal inflammation. In both cases, homing to specific sites is essential for Treg function. Like other lymphocytes, Tregs can express CCR7, which recruits them via CCL19 and CCL21 to lymphoid tissue. Both tTregs and pTregs include populations of CCR7^{+} and CCR7^{-} cells which have been referred to as central Tregs (cTregs) and effector Tregs (eTregs), respectively (Campbell, 2015; Hayatsu et al., 2017; Smigiel et al., 2014). This classification system mirrors that of central and effector memory T cells, where ‘central’ populations migrate between lymphoid tissues and ‘effector’ populations have a

more activated phenotype in peripheral effector sites such as the intestinal mucosa (Sallusto and Lanzavecchia, 2000; Sallusto et al., 1999).

Like CD4 Tconvs, the integrin α4β7 has been shown to be important for Treg intestinal homing. Using a CD45RB^{hi} transfer colitis model, researchers found that although β7$^{-/-}$ Tregs were able to rescue colitis, they were unable to accumulate in the colon as seen with WT Tregs (Denning et al., 2005). This suggests that although β7 integrins were required for Treg homing to the colon, suppression was not required in the intestines. CCR9 also plays an important role in Treg migration to the SI, as its expression has been shown to be required for Treg-mediated resolution of ileitis and for induction of oral tolerance (Cassani et al., 2011; Wermers et al., 2011).

As with Tconvs, GPR15 expression by Tregs has been shown to be important for colonic homing. GPR15-deficient mice succumb to severe colitis during *Citrobacter rodentium* infection, which can be rescued by transfer of GPR15 sufficient Tregs (Kim et al., 2013). GPR15 is also expressed by human Tregs and IBD patients have an increased proportion of Tregs expressing GPR15 and α4β7 in PBMCs compared to healthy controls (Adamczyk et al., 2017; Fischer et al., 2016). In addition to gut-tropic receptors, Tregs can express the same chemokine receptors as Th subsets (Fig 1.5). As with Tconvs, these receptors may play a role directing Tregs to sites of inflammation and furthermore, may allow co-localisation of Tregs with sites of Th-specific immune responses, potentially facilitating selective suppression.

1.3.4 Antigen specificity of regulatory T cells

Unlike Tconvs, which are classically activated in a well characterised antigen-specific process, the role of antigen specificity in Treg activation and differentiation is less well understood. Although tTregs are thymically selected for TCRs that recognise self-antigen, both tTregs and pTregs have been shown to recognise foreign antigen and play a role in maintaining tolerance and modulating immune response during infection (Lee et al., 2012a; Pacholczyk et al., 2007; Shevach and Thornton, 2014; Taylor et al., 2009). The identification of pathogen-specific Tregs in the context of infection has been challenging,

although the use of peptide-MHC tetramers has facilitated their detection. Pathogen-specific Tregs have been isolated from PBMCs with specificity for influenza, HIV and lymphocytic choriomeningitis virus (LCMV) antigens (Brincks et al., 2013; Su et al., 2016). While pathogen-specific Tregs have been identified, it is unclear whether immune regulation by Tregs requires pathogen-specificity. Once activated by cognate antigen, Tregs can supress nearby T cells regardless of their TCR specificity. More research is required to delineate the importance of Treg antigen specificity in regulating immune responses.

1.3.5 Mechanisms of Treg suppression

Tregs can suppress Tconvs in multiple ways. These include production of immunomodulatory cytokines, cytolysis, metabolic disruption, and inhibition of DC-mediated Tconv activation (Fig 1.6).

Immunomodulatory cytokines

The production of cytokines IL-10, TGFβ and IL-35 have been well characterised as important aspects of Treg suppression (Asseman et al., 1999; Collison et al., 2007; Hawrylowicz and O'Garra, 2005). Despite being known as a 'signature' Treg cytokine, IL-10 is not always necessary for Treg suppression of inflammation (Joetham et al., 2007; Kearley et al., 2005). The requirement for TGFβ signalling is also context-dependent but has been shown to play important roles in controlling intestinal inflammation (Fahlén et al., 2005; Li et al., 2006). In addition to the secreted form, membrane-bound TGFβ has been shown to mediate contact-mediated suppression (Green et al., 2003; Nakamura et al., 2001). Finally, IL-35, which is in the IL-12 cytokine family, has been shown to be necessary for optimum Treg suppression and sufficient to inhibit intestinal inflammation *in vivo* (Collison et al., 2007; Gavin et al., 2007). Although the necessity for each of these cytokines for Treg suppressive potency is context dependent, immunomodulatory cytokines are an important aspect of Treg suppression.

Cytotoxicity

Although cytotoxic functions are best characterised in CTLs and NK cells, human and mouse FoxP3+ Tregs have been shown to be capable of targeting Tconvs and B cells for cytolysis in a granzyme-dependent manner (Grossman et al., 2004; Herman et al., 2004; Zhao, 2006). This cytolytic activity has been reported to be enhanced in tumour sites, where this mechanism is perforin-dependent (Cao et al., 2007). In addition to granzyme-induced cytolysis, there have also been reports of Treg-induced apoptosis by contact-dependent interactions of Treg Galactin-9 with Tconv Tim-3. This mechanism has been disputed however, and the *in vivo* relevance of this interaction is unclear (Leitner et al., 2013; Wang et al., 2009b). It has also been reported that human Tregs can target Tconvs through FasL binding of Fas on Tconvs, although this has not been well described in mice (Baatar et al., 2007).

Metabolic disruption

Tregs have been shown to disrupt Tconv metabolic pathways in three ways. First, there is evidence that high expression of IL-2 receptors by Tregs can lead to IL-2 deprivation in Tconvs, which can lead to increased levels of intracellular cyclic adenosine monophosphate (cAMP) and apoptosis (Duthoit et al., 2005; de la Rosa et al., 2004). While this mechanism may play a role in Treg suppression in some contexts, acting as an IL-2 'sink' is not required for *in vivo* suppression in some models (Duthoit et al., 2005; Fontenot et al., 2005). A second mechanism of Treg disruption of Tconv metabolism is the co-expression of CD39 and CD73, which converts adenosine triphosphate (ATP) to adenosine monophosphate (AMP) and releases adenosine (Deaglio et al., 2007; Kobie et al., 2006). Adenosine can then engage Tconv adenosine receptor 2A ($A_{2A}R$), leading to accumulation of intracellular cAMP (Borsellino et al., 2007; Deaglio et al., 2007). Finally, cAMP can be transferred directly from Tregs to Tconvs through membrane gap junctions (Bopp et al., 2007). In all three cases, increased levels of intracellular cAMP dysregulate Tconv metabolism and can induce apoptosis.

Targeting dendritic cells

In addition to directly targeting Tconvs, Tregs can suppress immune responses by targeting DCs (Houot et al., 2006; Lewkowich et al., 2005; Misra et al., 2004). A well characterised mechanism of DC targeting is suppression of co-stimulatory molecules CD80/CD86 (Linsley et al., 1991; Wing et al., 2008a). Cytotoxic T-lymphocyte antigen 4 (CTLA-4) is constitutively expressed by Tregs and binds CD80/86 with higher avidity than CD28. Once bound by CTLA-4, CD80/CD86 cannot bind CD28 and CTLA-4 can effectively capture CD80/86 molecules from DC surfaces, leading to their uptake and degradation by Tregs (Qureshi et al., 2011; Tadokoro et al., 2006). Although Tconvs can also express CTLA-4, the importance of CTLA-4 on Treg suppression has been shown *in vivo*, where selective depletion of CTLA-4 on Tregs led to severe autoimmunity (Wing et al., 2008b). Besides blocking Tconv co-stimulation, CTLA-4 engagement with CD80/86 has been shown to drive a regulatory phenotype in DCs through induction of indoleamine 2,3-dioxygenase (IDO) (Fallarino et al., 2003; Mellor and Munn, 2004). IDO expression induces expression of kynurenine metabolites which can bind intracellular aryl hydrocarbon receptors (AhR) to promote suppression (Cherayil, 2009; Nguyen et al., 2010). Another mechanism of DC targeting by Tregs is through lymphocyte-activation gene 3 (LAG3). LAG3 is a CD4 homologue that can bind MHCII with high affinity to inhibit antigen presentation and suppresses DC maturation and activation (Baecher-Allan and Hafler, 2004; Huang et al., 2004; Workman and Vignali, 2005).

In summary, Tregs have a wide range of potential mechanisms to regulate Tconv activation: whether through secreted cytokines, contact-dependent mechanisms or targeting DCs (Fig 1.6). The wide range of mechanisms highlight questions about which are sufficient and which are necessary to regulate Tconv responses *in vivo*, and which mechanisms are important for suppression during infection.

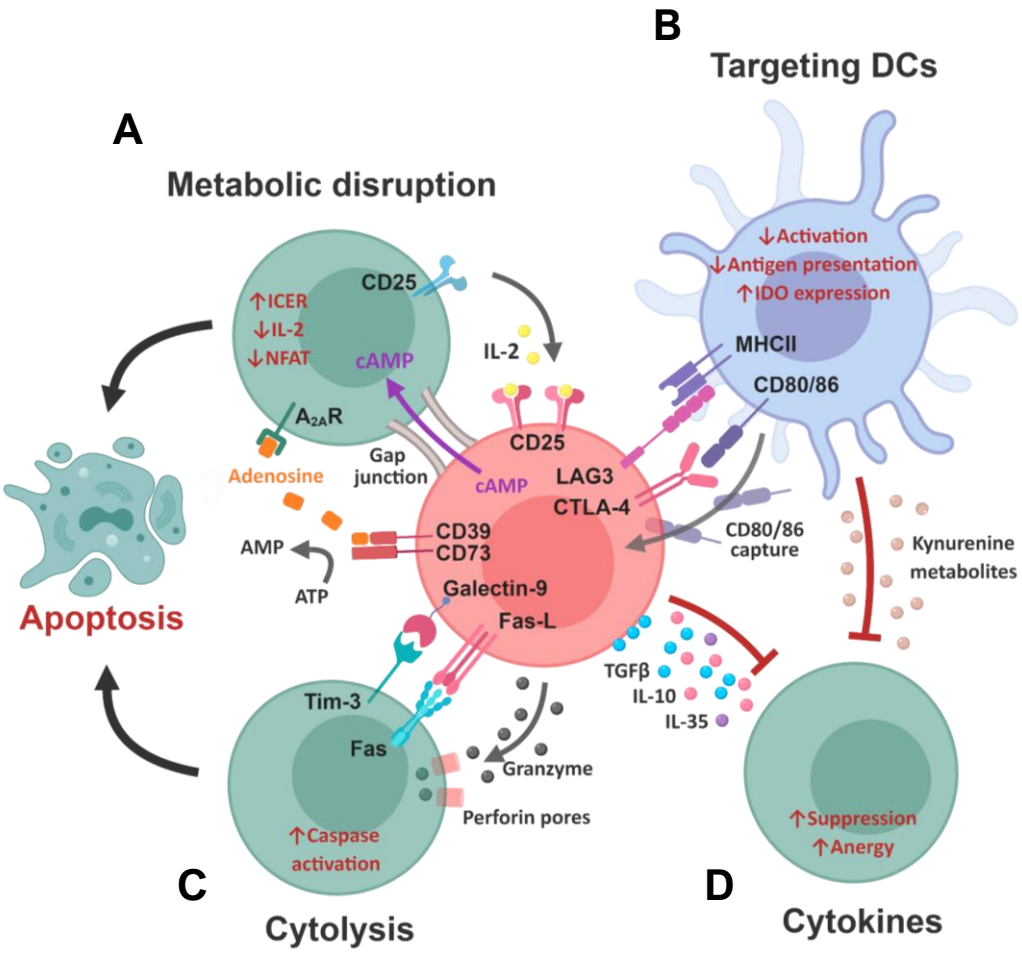

Figure 1.6 Proposed pathways of regulatory T cell suppression.

(A) Metabolic disruption of Tconvs can be induced by expression of CD39 and CD73, which metabolise ATP into AMP and produce adenosine that binds Tconv $A_{2A}R$, leading to accumulation of intracellular cAMP. cAMP can also be passed from Tregs to Tconvs directly through membrane gap junctions. High CD25 expression by Tregs may also act to deprive Tconvs of IL-2. Together, these processes induce upregulation of ICER, inhibit IL-2 and NFAT expression and drives apoptosis. **(B)** Tregs can target DCs by binding MHC II with LAG3, which inhibits antigen presentation. Tregs can inhibit DC activation by sequestering CD80 and CD86 with CTLA-4, which inhibits co-stimulation of T cells, and upregulates DC expression of IDO and metabolism of Kynurenine, which can suppress Tconvs by binding intracellular (AhR). **(C)** Tregs may induce Tconv lysis by secreting granzyme and perforin, and might be able to induce apoptosis by binding Fas or Tim-3 with Fas-L and Galectin-9, respectively. **(D)** Tregs can also inhibit Tconvs by producing inhibitory cytokines TGFβ, IL-10 and IL-35. Abbreviations: ATP, Adenosine Triphosphate; AMP, Adenosine monophosphate; $A_{2A}R$, A_{2a} receptor, cAMP, Cyclic adenosine monophosphate; ICER, Inducible cAMP early repressor; NFAT, Nuclear factor of activated T cells; LAG3, Lymphocyte activation gene 3; CTLA-4, Cytotoxic T-lymphocyte-associated protein 4; IDO, Indoleamine 2,3-dioxygenase; AhR, Aryl hydrocarbon receptor; TGFβ, Transforming growth factor β. Adapted from Safinia et al., 2015; Shevach, 2018; Vignali et al., 2008.

1.4 *Salmonella enterica* serotype Typhimurium

1.4.1 Overview of *Salmonella* infection

Salmonella species are Gram negative, facultative intracellular bacteria that comprise over 2,600 serotypes, including important pathogens of humans and other animals. *Salmonella enterica* species present a serious public health burden, causing

gastroenteritis or systemic infection in humans and domestic animals. *S. enterica* serovars Typhi and Paratyphi cause systemic typhoid fever in humans; with over 14 million cases and 130,000 deaths annually (Radhakrishnan et al., 2018; Stanaway et al., 2019). *Salmonella enterica* serovar Typhimurium (STM) infects a wide range of animals and is one of the most common non-typhoidal Salmonella (NTS) serotypes in humans. NTS strains are a common cause of localized gastroenteritis, but virulent STM strains have recently emerged in sub-Saharan Africa with 20-25% mortality (Feasey et al., 2012). While there are two vaccines available for typhoid-causing Salmonella strains, there are no vaccines in use for NTS strains (Guzman et al., 2006; Tennant et al., 2016). While the development of STM vaccines remain elusive, many STM strains have been generated to study *Salmonella* infection and the immune response to it (Dougan et al., 1987; Mastroeni et al., 2001; Strugnell et al., 1992).

1.4.2 Murine models of *Salmonella* infection

STM can be used in mice to induce typhoid-like systemic disease or intestinal infection and inflammation (Barthel et al., 2003; Santos et al., 2001; Tsolis et al., 2011). Wild mice are inherently resistant to STM but laboratory strains including C57BL/6 and BALB/c carry a mutation in the *Slc11a1* (*Nramp1*) gene, which encodes a phagolysosome trans-membrane protein. *Slc11a1*$^{-/-}$ species have increased susceptibility to STM infection and increased bacterial replication and systemic disease, even following oral administration (Caron et al., 2002; Vidal et al., 1996). As such, this model has similarities with human typhoid fever and has been widely used to study systemic STM infection and immunity (Fritsche et al., 2012; Griffin and McSorley, 2011; Tsolis et al., 2011). To study STM intestinal infection and inflammation, as seen in human *Salmonella*-induced enter-colitis, a streptomycin pre-treatment model has been developed.

It has been known for over 60 years that streptomycin treatment increases susceptibility to *Salmonella* entero-colitis, although the reasons were not known (Bohnhoff et al., 1954). Almost 50 years later, Wolf Dietrich Hardt and others developed a now well-characterised streptomycin model of Salmonella-induced colitis (Barthel et al., 2003; Hapfelmeier and

Hardt, 2005; Kaiser et al., 2012). In this model, streptomycin treatment 24 hours before oral infection clears >90% of the intestinal microbiome, reducing bacterial abundance and diversity, creating a niche for STM to colonise (Hapfelmeier and Hardt, 2005; Kaiser et al., 2012; Stecher et al., 2007). As such, this model not only facilitates intestinal colonisation, it also improves the reliability and reproducibility of infections across facilities. This has been a long-term disadvantage of some other models. Recent work has shown that high variability in STM susceptibility is caused by variations in the microbiota of mice in different facilities. In particular, the colonisation with Enterobacteriaceae was shown to reduce susceptibility to STM infection (Velazquez et al., 2019).

Streptomycin pre-treatment induces consistent intestinal infection and colitis in both resistant and susceptible mouse strains, with pathology including oedema, mucosal ulcerations, colonic shortening, transmural inflammation and fibrosis (Grassl et al., 2008; Stecher et al., 2006). However, the use of virulent STM strains in susceptible mice causes high mortality. Using attenuated STM strains is one approach to maintain consistent intestinal infection while reducing pathology and mortality. Infection with attenuated strains can induce colitis and provide an opportunity to study longer processes including the development of adaptive immune responses, the resolution of infection and protective immunity (Kaiser et al., 2012).

Attenuated STM strains used in infection models include auxotrophic vaccine strains, which have deficient biosynthesis pathways for essential metabolites (Hoiseth and Stocker, 1981; Poirier, 1988; Ward et al., 1999). *AroA* mutants are strains auxotrophic for aromatic amino acids that have limited availability in mammalian hosts (Dougan et al., 1987; Hoiseth and Stocker, 1981). These strains have been widely used to study adaptive immune responses to STM infection (Griffin and McSorley, 2011; Hess et al., 1996; Lee et al., 2012b; Tsolis et al., 2011). While most of this work has focused on the adaptive response to systemic Typhoid-like STM infection, the adaptive immune response to STM-induced colitis has been less well-characterised. Further work with this model has

potential to improve our understanding of the adaptive immune response to intestinal pathogens and gut inflammation in general.

1.4.3 Innate immune response and bacterial dissemination

Following oral ingestion, STM passes into the intestinal lumen where bacteria upregulate virulence factors (Lawley et al., 2008; Tsolis et al., 1999; Yoon et al., 2009). STM may then pass through the mucous layer, especially where it is thinner over GALT, and contact the intestinal epithelium. STM has been shown to cross the epithelium via M cells, by trans-epithelial sampling by mononuclear phagocytes or by transcytosis of epithelial enterocytes (Griffin and McSorley, 2011; Jones, 1994; Müller et al., 2012; Sansonetti, 2004). STM employ a type 3 secretion system (T3SS) to target M cells, which disrupts tight junctions, increases epithelial permeability and enhances further bacterial invasion (Jepson and Clark, 2001; Martinez-Argudo and Jepson, 2008). This process can lead to penetration of the FAE over PPs in under 1 hr post-infection (p.i.) and has also been shown to occur in colonic GALT, including ILFs (Halle et al., 2007). The importance of M cells at the frontline in STM infection is highlighted by research showing STM can induce differentiation of M cells to promote infection and recent work showing that host nociceptors can sense STM and suppress M cell differentiation as a host defence mechanism (Lai et al., 2019; Tahoun et al., 2012).

Once STM breaches the epithelium, there is an influx of host cells including neutrophils, monocytes, DCs, and ILCs. There is a concurrent release of inflammatory cytokines in the LP, including IL-1β, IL-12 and IL-18 produced by MNPs and epithelial cells; and IFNγ and IL-17A, produced by innate cells including neutrophils, ILCs and γδ T cells (Broz et al., 2010; Kupz et al., 2013; Miao et al., 2006; Rydstrom and Wick, 2007; Spees et al., 2014; Tam et al., 2008). Additionally, CD4 T cells have been shown to respond to STM infection in an innate, non-cognate capacity. This ‘bystander’ T cell response includes IFNγ production and has been shown to depend on IL-18R expression by T cells and Myd88 signalling (McSorley, 2014; Pham et al., 2017). In this complex inflammatory setting, STM can be rapidly phagocytosed by MNPs such as DCs and macrophages, that detect

PAMPs with PRRs including TLRs and NLRs and sequester bacteria in phagolysosomes and inflammasomes (Barton, 2003; Man et al., 2014). Despite cellular defences, STM can survive and replicate intracellularly by employing a T3SS and other virulence factors to evade lysosomal killing (Arpaia et al., 2011; Bueno et al., 2008).

Following phagocytosis of STM, DCs can become activated and upregulate expression of MHC II, CD40, CD80, CD86 and CCR7, which facilitates migration to MLNs (Reis e Sousa, 2006; Yrlid et al., 2001). Migration of infected DCs and other cells to MLNs is important to establish adaptive immunity but can also be a route of bacterial dissemination. (Bravo-Blas et al., 2018; Tam et al., 2008). Indeed, the MLNs are known to be an important firewall against systemic STM dissemination (Griffin et al., 2011; Voedisch et al., 2009; Wick, 2011). Antigen presentation by DCs is a crucial aspect for driving STM-specific CD4 T cells and adaptive immunity, and STM employs multiple strategies to block this process (Cheminay et al., 2005; Lapaque et al., 2009; Rydstrom and Wick, 2010; Tobar et al., 2006). Despite multiple evasion strategies, antigen presentation by DCs can occur rapidly in MLNs or the GALT, where transferred STM-specific T cells can be activated just 3 hrs p.i., (McSorley et al., 2002; Salazar-Gonzalez et al., 2006).

1.4.4 Adaptive immune responses to *Salmonella*

CD4 T cells have been well established as critical for both clearance of STM infection and protection from re-infection (Hess et al., 1996; Nauciel, 1990). While CD8 T cells contribute to the anti-STM response, CD8 T cell depletion has been shown to have no impact on the outcome of infection (Kupz et al., 2014). B cell depletion has also been shown to have little impact on STM clearance, although B cell deficient mice fail to develop protective immunity (Kupz et al., 2014; Mastroeni et al., 2000; Mittrücker et al., 2000). While B cells are essential for protection from re-infection, this protective immunity is not dependent on antibody (Nanton et al., 2012).

Th1 cells and IFNγ have been well characterised as requirements for STM clearance and protective immunity in systemic infection (Hess et al., 1996; Kupz et al., 2014; Pie et al.,

1997; Ravindran and McSorley, 2005; Srinivasan et al., 2004). As with antibodies, transfer of circulating lymphocytes fails to confer protective immunity, masking the cellular correlate of STM immunity. However, recent work has identified tissue-resident memory (TRM) Th1 cells as an essential component of protective immunity (Benoun et al., 2018). These cells were isolated from livers of mice infected using a Typhoid model; it would be interesting to investigate if intestinal TRMs were also protective in colitis-models of STM infection.

In addition to Th1 cells, an early Th17 response has been reported in the intestines (Lee et al., 2012b). Targeting Th17 cells by genetic mutation, HIV infection, or genetic disruption of IL-17A signalling each increases epithelial damage or the risk of systemic infection (Godinez et al., 2011; Mayuzumi et al., 2010; Raffatellu et al., 2008). In humans, patients with IL-12 or IL-23 deficiencies have increased susceptibility to NTS infection and systemic bacteraemia, suggesting an important role for both Th1 and Th17 cells in controlling infection in humans (Sanal et al., 2006; van de Vosse and Ottenhoff, 2006). Taken together, these studies suggest that an effective immune response to STM incorporates a dynamic CD4 T cell response including an early Th17/IL17A response and a Th1 response including TRM cells. How the response of these different Th subsets and cell types is controlled and balanced is unclear.

1.4.5 Tracking *Salmonella*-specific T cells

The capability to track antigen-specific CD4 T cells following infection is a valuable tool for understanding the development and control of the T cell response to infection. Several tools for tracking STM-specific T cells have been developed, including transfer of transgenic T cells with TCRs specific for ovalbumin (OVA) expressed by STM-OVA, or naturally occurring STM flagellin peptides (Bumann, 2003; Chen and Jenkins, 1999; McSorley et al., 2002; Salazar-Gonzalez et al., 2006). More recently, peptide:MHCII tetramers have been developed to label endogenous CD4 T cells expressing STM-specific TCRs without requiring transfer of transgenic T cells (Moon et al., 2007). STM strains have been generated that express 2W1S, a peptide for which a relatively high

frequency of naïve CD4 T cells are specific. STM-2W1S strains integrate a peptide tag downstream from the 3' portion of the *OmpC* gene, and have been used to successfully track STM-specific T cells for many months *in vivo* (Benoun et al., 2016; Moon and McSorley, 2009; Nelson et al., 2013). These constructs have been engineered with virulent SL1344 and attenuated BRD509, an auxotrophic *aroA* mutant (Benoun et al., 2018; Mooney et al., 2015). The use of STM-2W1S as part of an *in vivo* infection model is depicted in Fig 1.7.

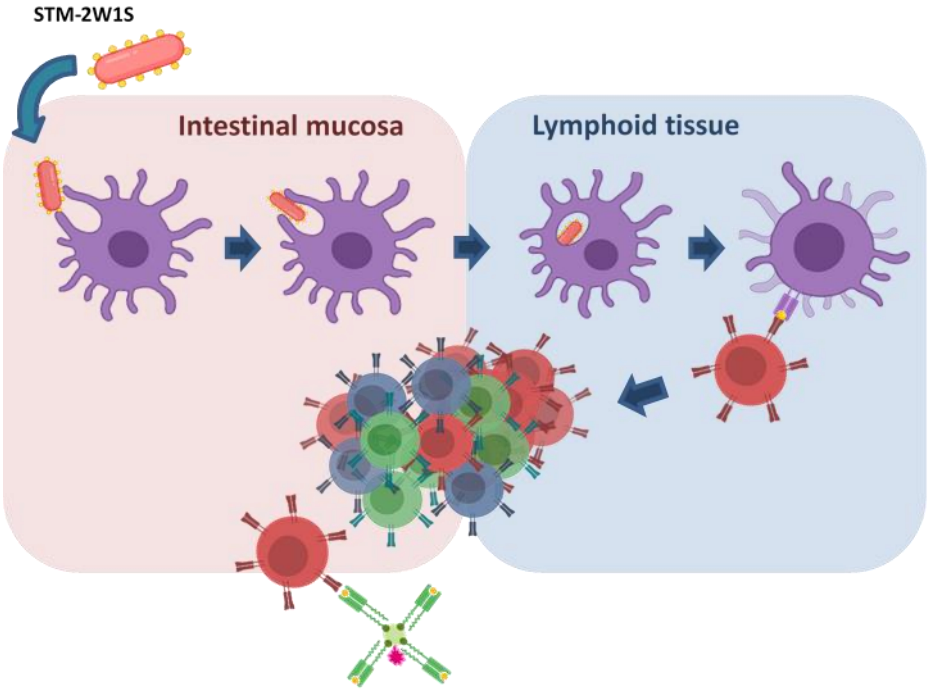

Figure 1.7 Identification of *Salmonella*-specific CD4 T cells using STM-2W1S and IA^b:2W1S tetramers.

Cartoon depiction of STM expressing 2W1S peptide, represented as yellow circles. Following oral infection, DCs phagocytose STM-2W1S and migrate to lymphoid tissue where they present 2W1S:MHC II complexes to 2W1S-specific naïve T cells. These cells proliferate, differentiate into Tconvs and migrate to the intestinal LP. Following digest, intestines are processed into single cell suspension, and 2W1S-specific T cells are labelled with IA^b:2W1S tetramers and identified by flow cytometry.

1.4.6 The role of Tregs in *Salmonella* infection

While the CD4 T cell response has not been well characterised in the STM colitis model, the role of Tregs has been poorly studied in *Salmonella* infection generally. It has been suggested that Tregs constrain the Tconv response to STM, which leads to reduced bacterial clearance, increased bacterial proliferation and a worse outcome for the host. This view is supported by Johanns et al. (2010), who show that Treg depletion or anti-

CTLA-4 treatment 5 days p.i. led to increased Tconv activation and decreased bacterial burden 6 days later. The authors also report decreased CTLA-4 expression and suppressive potency in Tregs at 37 days p.i., when the Tconv response is more robust and the infection is naturally cleared. These data support the hypothesis that Treg suppression during STM infection is deleterious for the host. However, this research utilised an infection model where resistant *Slc11a1*$^{+/+}$ mice were infected i.v. with a virulent STM strain. As such, this model is not physiologically relevant to natural infection in terms of host strain or route of infection. This raises questions about whether similar results would be found in susceptible mouse strains with intestinal disease. More generally, this raises questions about the Treg response to STM infection: including whether responding Tregs have a thymic or peripheral ontogeny, if they are STM-specific, and whether they exert their suppressive function in lymphoid tissue, in the intestinal mucosa or both sites.

1.4.7 Conclusions

STM can be used as a versatile tool to study systemic and intestinal infection. There are many bacterial strains available and a wide range of pathology and outcomes can be induced depending on STM strain, route of infection, host strain and host microbial colonisation. While this versatility is an advantage, it presents a challenge when assessing previous research using known and unknown adaptations to these models.

The focus of this research is the CD4 T cell response to intestinal infection and inflammation; as such, the STM colitis model is an appropriate tool to study site-specific T cell responses to be tracked over time. Previous STM research leaves many unanswered questions about the response to STM in the gut and associated lymphoid tissue. The CD4 T cell response to STM colitis has not been well characterised and it is unclear how Th1 and Th17 responses develop in the intestinal mucosa and draining lymph nodes. The role of Tregs during STM infection is also unclear and the Treg response itself is poorly characterised, especially in the intestines. Research characterising the Tconv and Treg response to STM intestines has potential to elucidate how the CD4 T cell response to intestinal pathogens is controlled.

1.5 Hypothesis and Aims

In this introduction, questions have been highlighted about how the CD4 T cell response is controlled in the intestines. These include what directs CD4 T cell differentiation and to one Th subset over another, and where the response develops over time. Unanswered questions remain about Treg ontogeny, differentiation, antigen-specificity, migration, and the selective suppression of Th subsets during infection. The STM-colitis model will be used to address these questions and achieve the primary aim of this work: **Investigate the role of Tregs in shaping the CD4 T cell response to *Salmonella*.**

Previous research highlights that Tregs comprise diverse and highly plastic cells that can modulate inflammation in a more nuanced way than previously appreciated. Recent advances from researchers including Levine et al. (2017), Tosiek et al. (2016) and Britton et al. (2019) have contributed to the key hypothesis: **Regulatory T cells can actively shape the CD4 T cell response in a temporal and site-specific manner.**

To test this hypothesis, experiments were carried out to achieve three major objectives:

1) Develop a STM model to induce non-lethal colitis and track STM-specific CD4 T cells. This will allow analysis of temporal and site-specific dynamics of antigen-specific and polyclonal T cells during intestinal infection.

2) Characterise the CD4 T cell response to a colitis model of STM infection. There has been surprisingly little research characterising the CD4 T cell response to STM-induced colitis. This objective includes analysis of Th subsets and Tregs expressing Th 'master' TFs in lymphoid and mucosal sites.

3.) Investigate the potential for Tregs to shape the CD4 T cell response. To address the third objective, Tregs will be manipulated to determine if they are necessary and sufficient for the bias of the Tconv response in the intestines.

Together, these objectives address important questions about the site-specific CD4 T cell response to STM, and the role of Tregs in controlling this response. Beyond the scope of *Salmonella* infection, this work has potential to highlight the role of Tregs in shaping the CD4 T cell response during intestinal infection and inflammation in general.

Chapter 2 Materials and methods

2.1 Mouse strains

Male C57BL/6J mice were purchased from Envigo (Huntingdon, UK) at 5-6 weeks of age and housed in individually ventilated cages (IVCs) prior to procedures, when they were transferred to conventional cages. FoxP3^{GFP} mice were kindly provided by Prof. Rick Maizels (University of Glasgow, UK) and bred and maintained in conventional cages. FoxP3^{RFP} RORγT^{GFP} (FoxROR) mice were a kind gift from by Dr David Withers (University of Birmingham, UK) and bred and maintained in IVCs. FoxP3$^{DTR/eGFP}$ depletion of regulatory T cell (DEREG) mice were a kindly provided by Prof. Mark Travis (University of Manchester, UK) with permission from Prof. Tim Sparwasser (Medizinische Hochschule Hannover, Germany). DEREG mice were maintained and bred in IVCs. Genotyping of DEREG and FoxROR mice was carried out on ear clip samples by Transnetyx (Cordova, TN, USA).

All mice were maintained under specific pathogen-free (SPF) conditions at the University of Glasgow Central Research Facility or Veterinary Research Facility (Glasgow, UK). All procedures were conducted under licenses issued by the UK Home Office under the Animals (Scientific Procedures) Act of 1986 and approved by the University of Glasgow Ethical Review Committee.

2.2 *Salmonella* infections

2.2.1 *Salmonella* strains

Salmonella enterica serotype Typhimurium (STM) strains SL1344-2W1S and BRD509-2W1S were kindly provided by Prof. Stephen McSorley (University of California, Davis, USA). The 2W1S strains expresses the 2W1S (EAWGALANWAVDSA) epitope in frame with OmpC (Mooney et al., 2015; Nelson et al., 2013). BRD509 was generated as an *aroA aroD* mutant strain, although more recent genotyping of BRD509-2W1S revealed this strain had lost the *aroD* mutation (Benoun et al., 2018). STM strains SL1344, BRD509

and pGFP were kindly provided by Dr Dónal Wall (University of Glasgow). STM strains JH3008 and JH3016 were kindly provided by Prof. Jay Hinton (University of Liverpool, UK).

2.2.2 Bacterial culture

STM cultures were streaked out on Luria-Bertani (LB) agar plates before culturing in LB broth for 5 hrs at 37°C in an incubator shaking at 180 rpm. Cultures were then back-diluted 1:10 in LB broth before static culture at 37°C overnight (O/N). Cultures were then adjusted to an OD_{600} of 1.00, centrifuged at 5,000G for 10 min, and resuspended in sterile phosphate buffered saline (PBS) at an estimated concentration of 1.0-1.5 x 10^9 CFU/ml or as stated in the results. Following infections, actual bacterial dosage was confirmed by plating serial dilutions of STM inocula onto LB agar plates.

2.2.3 *In vivo* infections

6-10 week old mice were pre-treated with 20 mg streptomycin (Sigma-Aldrich, USA) suspended in 100 µl sterile PBS by oral gavage 24 hrs before STM infection. Mice were infected by administration of 100 µl of STM inoculum by oral gavage.

2.2.4 Enrofloxacin treatment

Antibiotic treatment of STM-infected mice was carried out by adding enrofloxacin (Bayer, Germany) to drinking water at 2 mg/ml. Enrofloxacin treatment was provided from day 10-21 post infection (p.i.) and water was replaced every 72 hrs.

2.2.5 Bacterial recovery

Single cell suspensions from tissues were pelleted by centrifuging at 400 G for 5 mins and resuspended in 0.1% Triton X-100 (Sigma-Aldrich) in PBS and incubated at room temperature (RT) for 10 mins. Samples were then washed and pelleted by centrifugation at 5,000 G for 10 mins, before being resuspended in PBS, serially diluted and plated on MacConkey agar No. 2 (ThermoFisher Scientific, UK) containing 5 µg/ml streptomycin (Sigma-Aldrich) and incubated O/N at 37°C before CFUs were calculated. Bacteria were

recovered from faeces and caecal contents, which were collected, aliquoted into 100 µg samples, homogenised and suspended in 1.0 ml PBS. These solutions were then serially diluted and plated on MacConkey agar plates as described above.

2.2.6 *In vitro* infections

STM was prepared as above and used to infect RAW 264.7 cells and intraperitoneal (IP) macrophages. IP macrophages were harvested by injecting 8 ml of PBS into the peritoneal cavity of humanely sacrificed mice, recovering the wash fluid, and resuspending cells in RPMI 1640 media with 2 mM L-Glutamine, 100 µg/ml streptomycin, 100 units/ml penicillin and 10% FCS (All Gibco, UK). Cells were then cultured for 24 hrs at 37°C in 24 well plates before non-adherent cells were washed off with RPMI. RAW 264.7 cells and IP macrophages were cultured in 24 well plates in RPMI media with 10% Foetal calf serum (FCS) and 1% L-glutamine at 37°C until confluent. Lipopolysaccharide (LPS) was added to cultures at 1.0 µl/ml for 4-6 hrs before infection. STM was cultured as described above, and following static incubation, OD_{600} was adjusted to 0.5 before being diluted 1:5 in RPMI with 5% FCS. This inoculum was then adding to macrophage cultures in 24 well plates. Cells were left at 37°C for 1 hr before washing with RPMI containing 5% FCS and 50 µg/ml gentamycin. The infection was then left to progress for 6 hrs at 37°C before collection.

2.3 Tissue harvest and processing

All murine tissues were collected into Hanks' Balanced Salt Solution (HBSS) with 2% foetal calf serum (FCS) (Gibco) and stored on ice before processing.

2.3.1 Intestines

Intestines were emptied of luminal contents, washed in HBSS and stored on ice until further processing. External fat, Peyer' patches (PP) and caecal patches (CP) were removed and the remaining tissue was chopped with scissors into ~5 mm pieces. Next, samples were washed in HBSS with 2 mM Ethylenediaminetetraacetic acid (EDTA) (Gibco) at 37°C in an incubator shaking at 205 rpm for 10 mins. Following incubation,

samples were washed with HBSS. EDTA incubations and HBSS washes were repeated three times before tissues were digested. Digest enzyme cocktails were prepared in complete RPMI media (RPMI 1640 with 100 µg/ml streptomycin, 100 U/m penicillin, 2 mM L-Glutamine and 50 µm 2-Mercaptoethanol) with 10% FCS (all Gibco). Colon and caecal tissue were digested in an enzyme cocktail of 0.45 mg/ml collagenase V (Sigma-Aldrich), 0.65 mg/ml collagenase D (Roche, Switzerland), 1.0 mg/ml dispase (Gibco) and 30 µg/ml DNAse (Roche) in complete RPMI. Small intestines were digested with 0.5 mg/ml collagenase V (Sigma-Aldrich) in complete RPMI. Tissues were added to respective digest cocktails, shaken vigorously by hand and then incubated at 37°C in an incubator shaking at 205 rpm. Digests were carried out for 15-20 mins, with manual shaking continued every 5-6 mins. Following digests, samples were returned to ice, filtered through 100 µm filters, washed twice with fluorescence activated cell sorting (FACS) buffer (PBS with 2% FCS and 2 mm EDTA) and filtered through a 40 µm filter before further processing.

2.3.2 Lymph nodes, Peyer's patches and caecal patches

Lymph nodes, Peyer's patches (PPs) and caecal patches (CPs) were washed in HBSS and maintained on ice. Fat, luminal contents or non-lymphoid tissue was carefully removed. Tissues were chopped into ~1 mm pieces, passed through a 40 µm filter and suspended in FACS buffer before further processing.

2.3.3 Spleens

Spleens were cleaned and fat was removed before being chopped into several pieces and passing through a 40 µm filter with FACS buffer. Samples were suspended in Ammonium-Chloride-Potassium (ACK) lysing buffer (ThermoFisher) for 3-5 mins at RT, before washing and resuspending in FACS buffer.

If lymphoid tissues were being processed to analyse or isolate lymphocytes, tissues were processed without digestion. If mononuclear phagocytes (MNPs) were being analysed or isolated, tissues were digested in complete RPMI with 10% FCS, 0.75 mg/ml DNAse I

(Roche) and 0.40 mg/ml collagenase-dispase (Roche). Digestion was 20 mins at 37°C and shaking at 205 rpm. Following digest, samples were washed with FACS buffer and passed through 40µm filters before further processing.

2.4 Staining for flow cytometry

Following preparation of single cell suspensions, samples can be stained for flow cytometry. Staining for extracellular surface markers, including peptide:IA^b tetramer staining can be carried out immediately. But staining for intracellular markers including transcription factors or cytokines, requires a fixation and permeabilization step.

2.4.1 Tetramer staining

2W1S:I-A^b tetramer was kindly provided by the NIH tetramer core facility (USA). Following infection with STM-2W1S strains, tissues were harvested and processed as described above. Samples were transferred into 96 well round bottom plates, centrifuged for 5 mins at 400G, and resuspended in 25µl of tetramer mix containing complete RPMI with 10% FCS, 7 µg/ml 2W1S:IA^b tetramer, 20 µl/ml mouse serum and 10 µl/ml Fc block (CD16/32) (Biolegend, USA). Once cells were resuspended in the tetramer mix, plates were incubated for 2 hrs at 37°C, with plates briefly vortexed every 30 mins. Following tetramer staining, antibodies for extracellular surface markers were added directly into tetramer-stained wells.

2.4.2 Surface staining

Following tissue processing or tetramer staining, samples were stained with fixable viability dye at a 1 µl/ml in PBS. Next, antibodies for extracellular markers were prepared at 1:100 or 1:200 dilutions in FACS buffer, as specified in the list of antibodies used (Table 2.1). Surface staining was performed at 4°C for 30 mins before diluting with FACS buffer, centrifuging at 400 G for 5 mins, and resuspended pellets in FACS buffer. After surface staining, cells can be analysed, sorted or fixed and stained for intracellular markers.

2.4.3 Transcription factor staining

Transcription factor (TF) staining was carried out after cells were fixed using one of three methods. If cytokine staining was not planned and there were no fluorescent reporters, the eBioscience FoxP3 transcription factor staining kit (ThermoFisher) was used according to manufacturer's instruction. If cytokine staining was to be carried out, BD Cytofix (BD Biosciences, Belgium) was used to manufacturers instructions. If fluorescent reporters were being used, cells were fixed with 4% paraformaldehyde (PFA) in PBS. In all cases, cells were fixed for 1 hr at room temperature (RT) in the dark before washing and resuspending in eBioscience FoxP3 permeabilization buffer (PB) (ThermoFisher). Following fixation, TF antibodies were diluted in PB at concentrations listed in Table 2.1, added to samples and incubated O/N at 4°C. The next morning, cells were washed in PB and resuspended in FACS buffer for analysis or further staining.

2.4.4 Cytokine staining

For cytokine staining, cells are initially stimulated by suspending them in complete RPMI with 10% FCS and a 2 µl/ml of eBioscience cell stimulation cocktail (ThermoFisher) containing phorbol 12-myristate 13-acetate (PMA), ionomycin, brefeldin A and monensin. Cells were suspended at 1 x 10^6 cells/100µl of stimulation buffer and incubated for 4 hrs at 37°C before washing with FACS buffer and staining. Following surface staining, samples were fixed with BD Cytofix (BD Biosciences) according to manufacturer's instructions and stained with cytokine antibodies diluted in PB and incubated for 2 hrs at RT. Following cytokine staining, cells were washed and resuspended in FACS buffer.

2.4.5 Flow cytometry

Samples were analysed using the BD LSR Fortessa analyser or sorted using the BD FACSAria IIu or III (BD Biosciences) at the Institute of Infection, Immunity and Inflammation Flow Core Facility (University of Glasgow). For cell sorting experiments, 5 µl of 7AAD viability dye (Biolegend) was added to samples 10 mins before sorting, and cells were collected in complete RPMI with 10% FCS.

Table 2.1 Antibodies used for flow cytometry

Marker	Fluorochrome	Clone	Conc.	Manufacturer
Mouse samples:				
7AAD	N/A	N/A	5µl/sample	Biolegend
B220	BV510	RA3-6B2	1:200	Biolegend
B220	PerCP/Cy5.5	RA3-6B2	1:200	Biolegend
CCR6	BV605	29-2L17	1:100	Biolegend
CD25	PE/Cy7	PC61	1:200	Biolegend
CD3	BV605	17A2	1:100	Biolegend
CD3ε	AF700	eBio500A2	1:100	eBioscience
CD3ε	BUV395	145-2C11	1:100	BD Biosciences
CD4	BUV805	GK1.5	1:200	BD Biosciences
CD4	AF647	GK1.5	1:200	Biolegend
CD4	AF647	RM4-5	1:200	Biolegend
CD4	PE/Cy7	GK1.5	1:200	Biolegend
CD4	AF700	GK1.5	1:200	Biolegend
CD44	PerCP/Cy5.5	IM7	1:200	Biolegend
CD44	BV510	IM7	1:100	Biolegend
CD44	BV605	IM7	1:100	Biolegend
CD44	BV785	IM7	1:100	Biolegend
CD44	BUV395	IM7	1:200	BD Biosciences
CD45	BUV395	30-F11	1:200	BD Biosciences
CD45	BV785	30-F11	1:200	Biolegend
CD45	AF700	30-F11	1:200	Biolegend
CD64	PercP/Cy5.5	X54-5/7.1	1:200	Biolegend
CD8α	BV510	53-6.7	1:200	Biolegend
CD8α	PerCP/Cy5.5	53-6.7	1:200	Biolegend
CXCR3	PE	CXCR3-173	1:100	Biolegend
CXCR3	BV421	CXCR3-173	1:100	Biolegend
CXCR3	BV605	CXCR3-173	1:100	Biolegend
F4/80	PercP/Cy5.5	BM8	1:200	Biolegend
F4/80	BV510	BM8	1:200	Biolegend
Fixable viability	eFluor 780	N/A	1:1000	Invitrogen
FoxP3	APC	FJK-16s	1:100	eBioscience
FoxP3	PE	FJK-16s	1:100	eBioscience
FoxP3	AF700	FJK-16s	1:100	Invitrogen
FoxP3	BV421	MF-14	1:100	Biolegend
FoxP3	AF488	MF-14	1:100	Biolegend
GATA3	eFluor660	TWAJ	1:100	eBiosciene
GATA3	PerCP/Cy5.5	TWAJ	1:100	eBioscience
Helios	AF488	22F6	1:100	BD Biosciences
Helios	PerCP/Cy5.5	22F6	1:100	Biolegend
I-A/I-E	BV510	M5/114.15.2	1:200	Biolegend
I-A/I-E	PerCP/Cy5.5	M5/114.15.2	1:200	Biolegend
IFNγ	PE	3E4	1:100	eBioscience
IFNγ	PerCP/Cy5.5	XMG1.2	1:100	Biolegend
IL-10	PerCP/Cy5.5	JES5-16ES	1:100	Biolegend
IL-17A	BV605	TC11-18H10.1	1:100	Biolegend
RORγT	PE	AFKJS-9	1:100	eBioscience

RORγT	APC	B2D	1:100	Invitrogen
T-bet	BV421	4B10	1:100	Biolegend
T-bet	PE/Cy7	eBio4B10	1:100	eBioscience
Human samples:				
CCR6	PE/Cy7	G034E3	5µl/sample	Biolegend
CD127	BV421	A019D5	5µl/sample	Biolegend
CD25	PE	BC96	5µl/sample	Biolegend
CD25	APC	BC96	5µl/sample	Biolegend
CD3	AF700	HIT3a	5µl/sample	Biolegend
CD3	PE/Cy7	OKT3	5µl/sample	Biolegend
CD3	PerCP/Cy5.5	HIT3a	5µl/sample	Biolegend
CD4	BV785	OKT4	5µl/sample	Biolegend
CD4	BUV395	RPA-T4	5µl/sample	BD Biosciences
CD4	PerCP/Cy5.5	RPA-T4	5µl/sample	Biolegend
CD45	BV510	HI30	5µl/sample	Biolegend
CD45	BUV805	HI30	5µl/sample	BD Biosciences
CD8α	BUV395	RPA-T8	5µl/sample	BD Biosciences
CD8α	BV605	RPA-T8	5µl/sample	Biolegend
CD8α	PE/C7	RPA-T8	5µl/sample	Biolegend
CXCR3	PerCP/Cy5.5	G025H7	5µl/sample	Biolegend
CXCR3	G025H7	BV510	5µl/sample	Biolegend
CXCR3	AF647	G025H7	5µl/sample	Biolegend
Fixable viability dye	eFluor 780	N/A	1:000	eBioscience
FoxP3	AF488	PCH101	5µl/sample	eBioscience
FoxP3	APC	PCH101	5µl/sample	eBioscience
RORγT	PE	AFKJS-9	5µl/sample	eBioscience
T-bet	PE/Cy7	eBio4B10	5µl/sample	eBioscience

2.5 Regulatory T cell depletion

Diphtheria toxin (DT) (Sigma-Aldrich) was suspended in sterile PBS at a concentration of 10.0 µg/ml. DT was administered intraperitoneally (IP) twice and 24 hrs apart, at a volume of 50-100 µl, equivalent to of 30 ng/g mouse weight. DT was administered to DTR^{+} DEREG mice and DT^{-}littermates as wild type (WT) controls.

2.6 Regulatory T cell transfer

Regulatory T cells (Tregs) were isolated from peripheral lymph nodes including brachial, axillary, cervical, inguinal, lumbar, inguinal and mesenteric lymph nodes (MLNs). Following processing as described above, CD4 T cells were pooled and isolated using EasySep CD4 negative selection kits (STEMCELL, Canada) according to manufacturer

instructions. Cells were then washed and stained for surface markers and subsequently sorted as live, single, RFP^+ $CD4^+$ T cells. Following sorting, cells were washed twice in PBS, counted, and resuspended in PBS at concentrations of 3-6 x 10^6 cells/ml. Cell suspensions were kept on ice and 100 µl volumes were transferred into recipients by intravenous (IV) injection into a lateral tail vein.

2.7 Treg suppression assay

Suppression assay experiments were adapted from methods previously described (Collison and Vignali, 2011). Tregs were isolated from lymph nodes of STM-infected or uninfected donors, as described above for Treg transfers. Conventional T cell responder cells (Tresps) were sorted as RFP^- $CD4^+$ T cells and were stained with a CellTrace Violet (CTV) cell proliferation kit (ThermoFisher) according to manufacturer instructions. Dendritic cells (DCs) were isolated from digested spleens of uninfected C57BL/6 mice using CD11c UltraPure micro beads (Miltenyi Biotec, Germany) according to manufacturer instructions.

Briefly, assays were carried out in 96 well round bottom plates (ThermoFisher) by combining 1.0 x 10^5 Tresps, 5.0 x 10^4 DCs and 1:2 serial dilutions of Tregs from 5.0 x10^4 cells to 6.3 x 10^3 cells/well. The number of Tregs corresponded to Tresp:Treg ratios of 1:2, 1:4, 1:8 and 1:16. Cells were suspended in 200 µl complete RPMI with 10% FCS and 5 µl/ml αCD3ε antibody, to provide T cell receptor (TCR) stimulation. All conditions were repeated in triplicate and incubated at 37°C for 84 hrs before harvest. Following incubations, plates were washed with FACS buffer and each well was divided into two samples to be stained with surface antibodies only, or fixed with 4% PFA and stained for TF expression, as described above.

2.8 Human colon biopsies

Colon biopsies were kindly provided by Dr Daniel Gaya at the Glasgow Royal Infirmary (United Kingdom), who received patient consent before colonoscopies were performed. Samples were managed by the National Health Service Greater Glasgow and Clyde

(NHSGGC) Research Tissue Bank under ethics granted by the West of Scotland Research Ethics committee (REC 14/WS/1035).

Ulcerative colitis (UC) patients were classified as having active inflammation or being in remission by the attending gastroenterologist at the time of colonoscopy. Following collection, samples were stored in sterile PBS on ice and delivered to the laboratory for analysis. Biopsies were incubated in HBSS with 2 mM EDTA for 10 minutes, shaking at 220 rpm at 37°C. This incubation was repeated three times with fresh EDTA HBSS buffer each time. Biopsies wee then digested in complete RPMI with 10% FCS containing 0.5 mg collagenase VIII (Sigma-Aldrich), 0.6 mg collagenase D (Roche), 1mg/ml dispase (Gibco) and 0.015 mg/ml DNAse (Roche). The digest was carried out for 10 mins at 37°C, shaking at 220 rpm, with vigorous manual shaking every 2-3 mins. Following digest, samples were added to FACS buffer on ice and filtered through 100 µm then 40 µm strainers, centrifuged at 400 G for 10 mins at 4°C, then resuspended in FACS buffer for staining with antibodies listed in Table 2.1.

2.9 Immunofluorescent imaging

Immunofluorescence (IF) images were produced from colonic sections and RAW 264.7 cells infected with STM strain JH3016, which expresses green fluorescent protein (GFP). Colonic tissues were harvested from C57BL/6 mice, as described above. Tissues were washed with PBS and 5 cm ‘donut’ sections were frozen in optimal cutting temperature (OCT) compound (Sakura Finetek, Netherlands) using dry ice and isopentane. Samples were then stored at -80°C O/N before sectioning with a Cryotome cryostat (ThermoFisher). Sections were then mounted on Superfrost Plus slides (ThermoFisher) for further processing. RAW 264.7 were infected *in vitro* as described above, and round coverslips (ThermoFisher) were placed into wells before culturing. These were subsequently stained and mounted for imaging.

Colon sections or infected RAW 264.7 cells were processed for IF imaging using the same method. Briefly, samples were washed three times with PBS containing 0.1% Tween

(PBST) (Sigma-Aldrich) and fixed with 4% PFA in PBS for 20 mins at RT. Samples were washed again and blocked with PBS containing 10% goat serum (ThermoFisher), 1% bovine serum albumin (BSA) (Sigma-Aldrich) and 0.1% Triton X-100 (Sigma-Aldrich) for 20 mins at RT. Samples were washed and stained with 5 units/ml of Phalloidin-AF647 (ThermoFisher) in PBS. Samples were washed and cover slips were mounted onto slides using Vectashield mounting medium with DAPI (Vector Labs, USA). Images were acquired with a Zeiss LSM510 confocal microscope (Carl Zeiss, Germany) at the University of Glasgow.

2.10 Statistical analysis and software

Statistical analysis was performed using Prism Graphpad (USA). Statistical difference between two groups were calculated using a two-tailed Student's t test or a Mann Whitney test. One way ANOVA was used to calculate statistical difference between three or more groups. A Holm-Šídák test was applied if specific groups or pairs were compared, and a Tukey's test was applied if all groups were compared. Two way ANOVA was used to determine significance between groups when multiple parameters were measured. Analysis of flow cytometry data including proliferation analysis was performed with Flowjo version 10 (FlowJo LLC, USA). IF images were processed and analysed using ImageJ (NIH, USA). Finally, figures were created using Powerpoint (Microsoft, USA) and Biorender (Canada).

Chapter 3 Optimisation of *Salmonella* Models to Track Bacteria and CD4 T Cells

3.1 Introduction

CD4 T cells play an essential role in clearing *Salmonella enterica* serotype Typhimurium (STM) infection but there are unanswered questions about how the T cell response develops and is controlled. Two important factors that underlie the outcome of infection are the dissemination of bacteria within the host and the development of an STM-specific CD4 T cell response. An early aim of this work was to optimise infection models that allow these dynamics to be studied. As previously discussed, STM-2W1S strains allow STM-specific CD4 T cells to be tracked using 2W1S: IA^b tetramers. To track bacteria *in vivo*, STM strains have been developed that express fluorescent reporters including green fluorescent protein (GFP).

The *in vivo* dissemination of STM has been studied for 50 years and continues to reveal important aspects of infection dynamics (Goldberg et al., 2018; Jones, 1994; Takeuchi, 1967). STM-GFP strains can be used to track bacteria by fluorescence microscopy and flow cytometry. Recent work from our lab characterised the dissemination of STM from the intestines to the MLNs in lymph (Bravo-Blas et al., 2018). Other recent research has identified sites of persistent infection including the MLNs (Goldberg et al., 2018; Griffin et al., 2011). As previously discussed, different STM models can induce systemic disease or localised infection within the intestines. Unanswered questions remain about which tissues are infected, for how long they remain colonised and how bacterial persistence influences the CD4 T cell response. An early objective of this project was to develop a model of infection with an STM-GFP strain to address these questions.

The potential to identify STM-specific CD4 T cells is a valuable tool for studying how the CD4 T cell response develops and is controlled. Where and when the STM-specific T cells response develops during STM colitis is not fully understood and questions remain about how the response is controlled over time.

The following experiments were conducted to achieve two aims. First, protocols were developed to optimise a non-lethal STM colitis model using strains expressing GFP or 2W1S. Second, an STM-specific CD4 T cell response was characterised in multiple tissues following infection. These experiments help elucidate where and when the STM-specific CD4 T cell response develops and lays the groundwork for later research into how this response is controlled.

3.2 Selection and optimisation of *Salmonella* strains for *in vivo* infection

The first step to studying the immune response to STM is developing an appropriate *in vivo* infection model. Two groups of STM strains were considered for use. The first are GFP reporter strains developed to track STM *in vivo*. These include two chromosomal constructs engineered from a virulent SL1344 parent: JH3016 is a constitutive GFP reporter and JH3008 is a conditional reporter that expresses GFP upon activation of SPI1 proteins within phagolysosomes. A plasmid GFP (pGFP) construct was also considered because these have been shown to express higher levels of GFP than chromosomal constructs at early timepoints (Wendland and Bumann, 2002). The second group of STM strains tested are 2W1S-expressing constructs. Infection with these strains induce a population of 2W1S-specific CD4 T cells trackable using 2W1S-MHCII tetramers. Two 2W1S strains evaluated are unattenuated SL1344-2W1S and attenuated BRD509-2W1S, a construct engineered from an aroA mutant strain. Besides expression of GFP or 2W1S, any strain used for *in vivo* infections must establish consistent and non-lethal infection.

3.2.1 *In vitro* culture of virulent and attenuated *Salmonella* strains expressing GFP or 2W1S reveals similar growth dynamics

Initially, STM strains were cultured *in vitro* to assess growth dynamics under the same conditions used for preparation of *in vivo* infections. GFP reporters, 2W1S strains, and their parent strains were cultured in lysogeny broth (LB) in a 37°C shaking incubator for 5 hrs before 1:10 back dilution and static incubation. During static incubation, optical density (OD) was measured and a sample was plated in LB agar plates to identify colony forming

units (CFU). Growth curves for GFP reporters (Fig 3.1A) show similar OD dynamics between the four strains, with an early lag phases preceding exponential growth from 1-2 hrs following back-dilution. When CFUs from each time point were counted however, fewer CFUs were recovered from the pGFP construct during the exponential phase. After 3-6 hrs of static culture, pGFP cultures contained >20% fewer CFU than the SL1344 parent strain or chromosomal GFP constructs. Growth curves of 2W1S strains show similar dynamics. The BRD509 cultures had marginally lower OD than the SL1344 strains, with BRD509-2W1S having a slightly lower OD than the parent strain. Similar numbers of CFUs were recovered from the 2W1S strains, with the SL1344 parent strain yielding slightly more CFUs than the 2W1S expressing strains during the exponential phase.

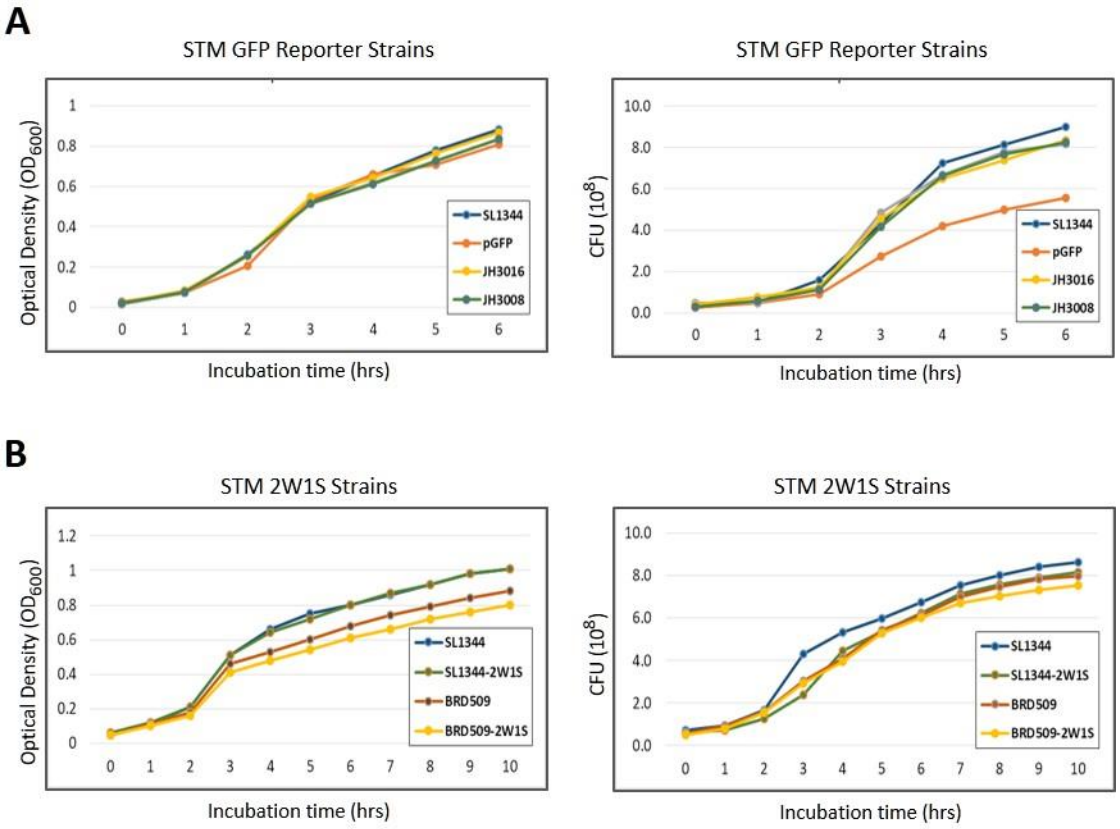

Figure 3.1 Growth curves for *Salmonella* strains expressing GFP or 2W1S.

(A) STM strains JH3008 and JH3016, incorporating chromosomally integrated GFP genes, show similar growth dynamics as parent strain SL1344. STM strain pGFP, with a plasmid GFP construct, shows similar growth to SL1344 when measured by OD (left) but reduced growth of viable bacteria measured by CFU(right). **(B)** STM strains expressing 2W1S show similar growth dynamics as their virulent (SL1344) or attenuated (BRD509) parent strains. Growth curves are representative plots of two independent experiments.

These experiments indicate that despite the differences noted, all strains have similar dynamics, reaching logarithmic growth by 3 hrs. In terms of inter-strain differences, pGFP

has a lower CFU:OD ratio, requiring higher OD values to attain the same CFUs as other strains (Fig 3.1A). Following the characterisation of these growth dynamics, experiments were carried out to detect and image GFP reporter strains.

3.2.2 Detection of GFP$^+$ Salmonella *in vitro* and *in vivo*

To assess GFP expression, STM strain JH3016 was selected to begin flow cytometry experiments and immunofluorescence (IF) imaging of infected cells. JH3016 was selected because of its constitutive GFP expression and more robust *in vitro* growth dynamics than STM pGFP (Fig 3.1A). *In vitro* infections were initially carried out with RAW 264.7 macrophage-like cells (Fig 3.2A) and then with peritoneal macrophages harvested from C57BL/6 mice (Fig 3.2B). Following 1 hr infections, cells were washed with gentamycin media before flow cytometry analysis. Following infection with JH3016, 15.1% of RAW 264.7 cells were in the GFP$^+$ gate, compared to 0.3% following infection with non-GFP expressing SL1344 (Fig 3.2A). In peritoneal macrophages, 43.3% of JH3016-infected cells were in the GFP$^+$ gate compared to 4.3% of STM SL1344-infected controls (Fig 3.2B). JH3016-infected RAW 264.7 cells were also stained with phalloidin and DAPI and imaged using fluorescence confocal microscopy (Fig 3.2C). Images show intracellular STM bacteria in green, including clusters of bacteria and dividing bacteria.

Next, JH3016 was used to orally infect C57BL/6 mice that were sacrificed 24 hrs later. Colonic and SI LP were sectioned and stained with phalloidin and DAPI before imaging by fluorescence confocal microscopy (Fig 3.2D and E). Imaging ten sections of colonic mucosa identified just one green area that resembles a GFP$^+$ bacterium (Fig 3.2D, enlarged in Fig 3.2E).

While JH3016 was validated as a useful tool to detect STM bacteria by flow cytometry and fluorescence microscopy, imaging of infected tissue, even 24 hrs p.i., made it apparent that tracking bacteria *in vivo* would be challenging. While this could be a potentially valuable direction for ongoing research, interest in characterising the adaptive immune response and the successful importation of 2W1S strains shifted the project

towards optimising 2W1S-expressing STM strains to detect and characterisation antigen-specific CD4 T cells.

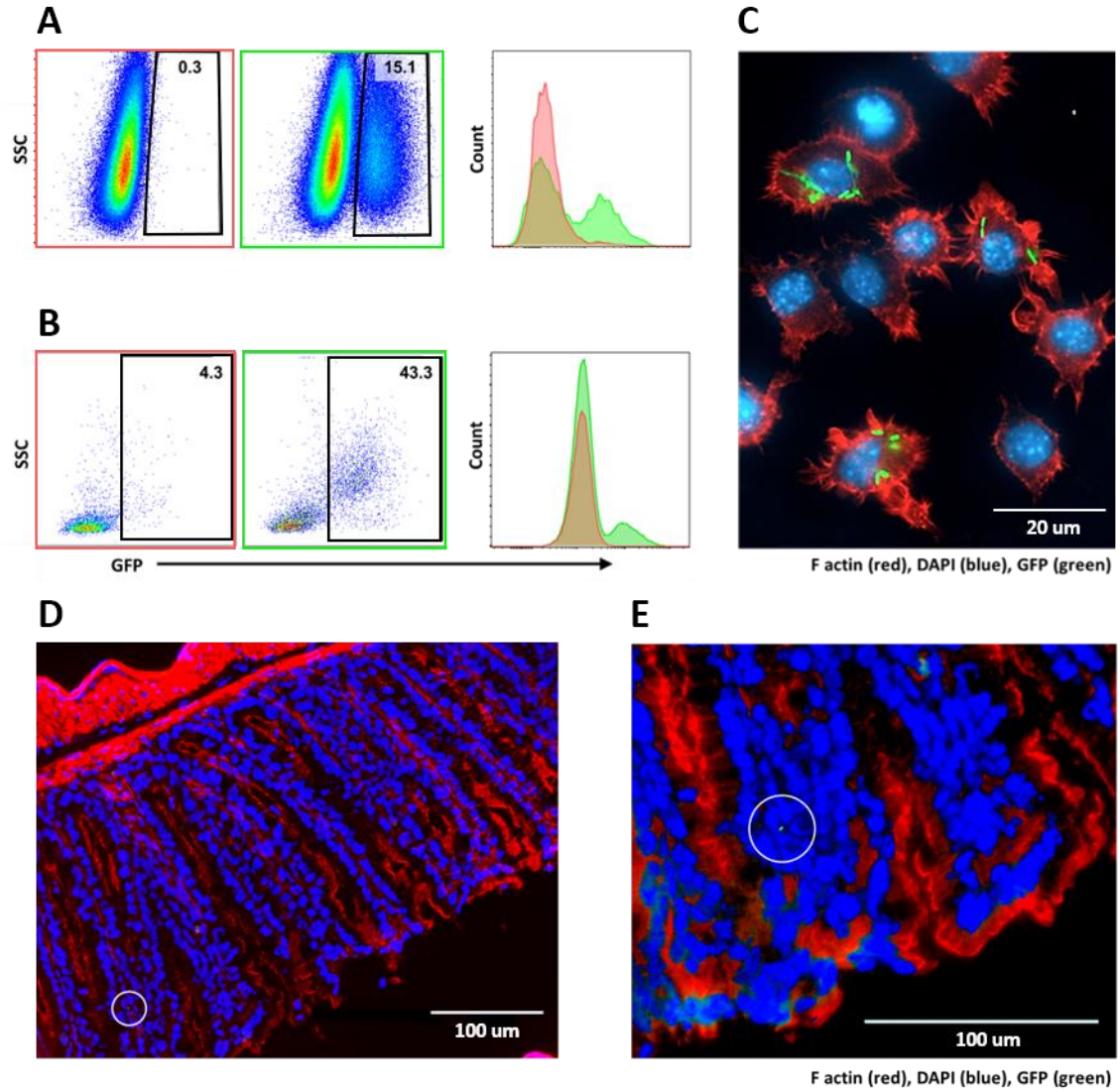

Figure 3.2 Detection of GFP⁺ STM strain JH3016 by FACS and fluorescence confocal microscopy.
STM strains JH3016 or SL1344 were used to infect cells *in vitro* and C57BL/6 mice *in vivo*. **(A)** RAW 264.7 macrophage-like cells or **(B)** peritoneal macrophages were cultured and infected with STM SL1344 (left) or GFP expressing STM JH3016 (centre) before FACS analysis. Histograms show JH3016-infected cells (in green) overlaid by non-GFP STM infected cells (in red) **(C)** RAW 264.7 macrophage-like cells were infected with STM JH3016, stained with phalloidin and DAPI, and imaged using fluorescence confocal microscopy. **(D, E)** STM JH3016 was used to infect mice *in vivo*, colons were harvested 24 hrs p.i. and stained as in **(C)**.

3.2.3 In vivo pathology induced by 2W1S *Salmonella* strains

To track T cell responses to STM infection, a model was sought that caused consistent infection but low mortality. To assess the pathology caused by infection with 2W1S-expressing strains, a series of experiments were conducted to assess the severity of infection induced in C57BL/6 mice. The objective of these experiments was to select an

appropriate strain, dosage and streptomycin pre-treatment schedule to induce infection with low mortality. To assess pathology, mice were infected with different strains and dosages, and weight change was monitored daily for 2 weeks p.i.

These are adaptations to the well-established STM colitis model, where mice are orally infected 24 hrs after treatment with streptomycin (Barthel et al., 2003)(Fig 3.3A). When mice are infected with $5x10^7$ CFU of virulent SL1344-2W1S, weight loss was severe and all mice reached the terminal endpoint of 20% weight loss by day 11 p.i. (Fig 3.3B). Another group was infected with the same dose of SL1344-2W1S but without streptomycin pre-treatment (Fig 3.3C). In this group, 50% of infected mice survived.

Next, the dosage of SL1344-2W1S was serially diluted and mice were infected with doses from $1x10^5$-$5x10^7$ CFU (Fig 3.3D). In this group, 33% survived to day 14 p.i. and lower doses did not correlate with higher survival rates. Unexpectedly, the two mice that received the lowest doses did not survive. The last group received $1x10^8$ CFU of BRD509-2W1S, a dose that has been used previously (Nelson et al., 2013) (Fig 3.3E). In this group all mice survived, with only one losing more than 5% of its initial body weight. In Fig 3.3F, the survival rates of mice from these four groups are shown, based on data from three experiments. 100% of uninfected mice, 33% of mice infected with SL1344-2W1S, 50% of infected with SL1344-2W1S without streptomycin and 83% of mice infected with BRD509-2W1S survived. In Fig 3.3G, representative caeca and colons are shown from mice that were mock-infected with PBS (top), infected with BRD509-2W1S (middle) or SL1344-2W1S (bottom). Signs of colitis increase from top to bottom and include emptied and shrivelled caeca, shortened colons and thickened intestinal walls indicating oedema.

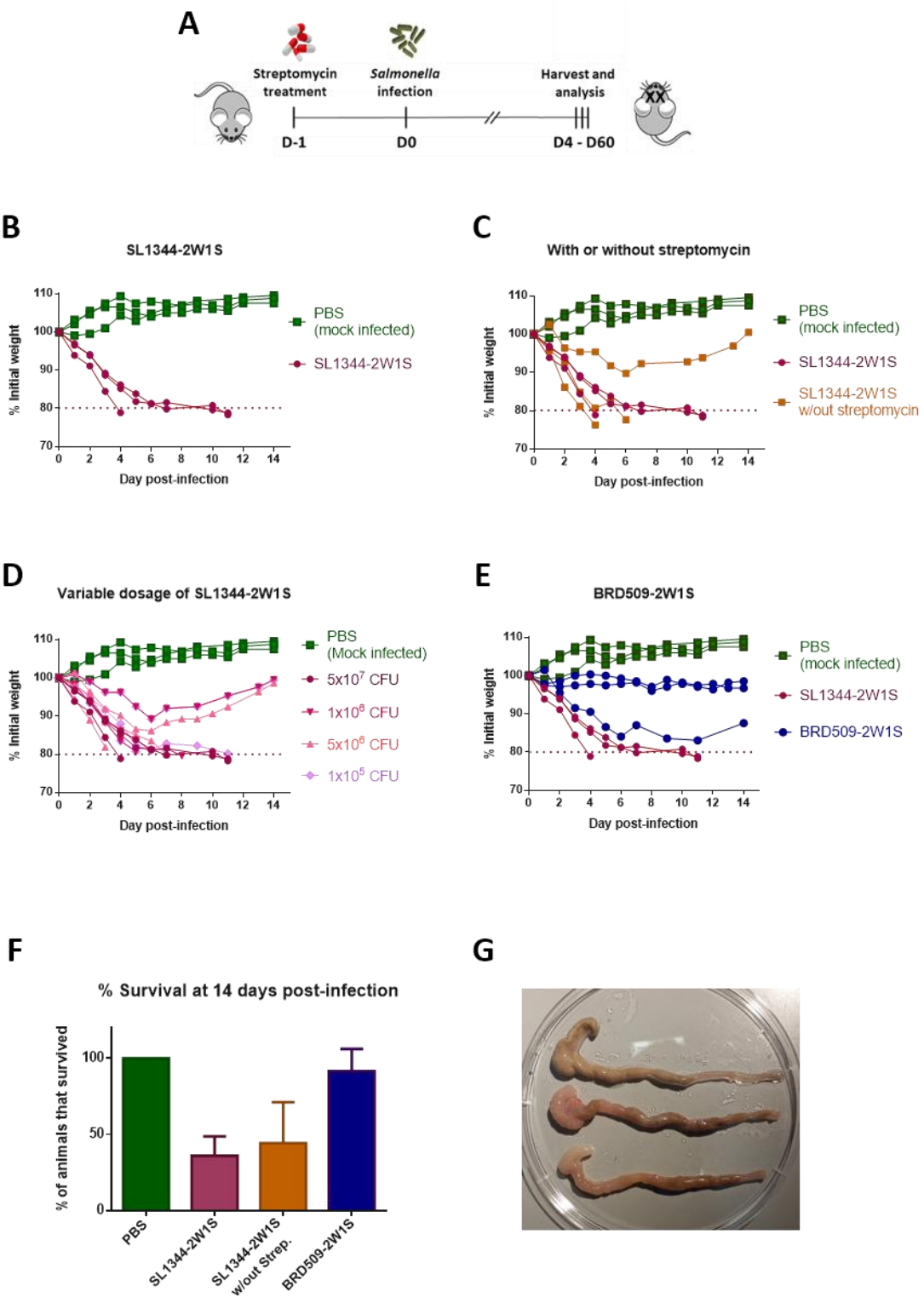

Figure 3.3 Weight loss, colitis and mortality following infection with 2W1S expressing STM strains.

Mice were orally infected with variable doses of attenuated and virulent STM-2W1S strains, with and without streptomycin pre-treatment. **(A)**. Weight loss is plotted for 14 days post-infection (p.i.) in mice infected with virulent SL1344-2W1S or mock infected with PBS **(B)**, without streptomycin pre-treatment **(C)**, with serial dilutions of STM doses **(D)**, or with attenuated strain BRD509-2W1S **(E)**. Dashed lines represent the humane endpoint of 80% weight loss. **(F)** The percent survival of groups mock-infected, SL1344-2W1S infected with and without streptomycin, or BRD509-2W1S infected. **(G)** Representative image are shown of colons and caeca from mock-infected (top) BRD509-2W1S (centre) or SL1344-2W1S (bottom) mice. Each line **(B-E)** represents a single animal and survival graphs represent data pooled from three independent experiments (n=3-4). Mean ± standard error of the mean (SEM) are plotted.

Based on these results, BRD509-2W1S was selected for further study because it induces colitis but only moderate weight loss and mortality. Further experiments characterised gross pathology, infection and cellular changes to infection (Fig 3.4). C57BL/6 mice infected with $1x10^8$ CFU BRD509-2W1S lost <5% of initial weight, which recovered to levels of mock-infected controls by 14 days p.i. (Fig 3.4A). At 6 days p.i., intestinal and lymphoid tissues were processed into single cell suspensions, permeabilised with Triton X-100 and plated on MacConkey agar, which is selective for Gram-negative intestinal bacilli, with streptomycin, to which STM is naturally resistant (Fig 3.4B). STM CFUs were recovered from the colon and small intestine (SI), although significantly more were recovered from the colon than the SI. STM CFU were also recovered from the MLN and Peyer's patches but not from the spleen. Representative images of caeca, colons (Fig 3.4C) and MLN chains (Fig 3.4C) are shown from infected (top) and uninfected (bottom) animals. As shown in Fig 3.3G, infected colons show signs of colitis including colonic shortening, oedema, and an enlarged caecal patch (Fig 3.4C, inset). In Fig 3.4D, specific colon- and caecum-draining lymph nodes (cMLN1, far left and cMLN2, far right) are also enlarged in infected animals.

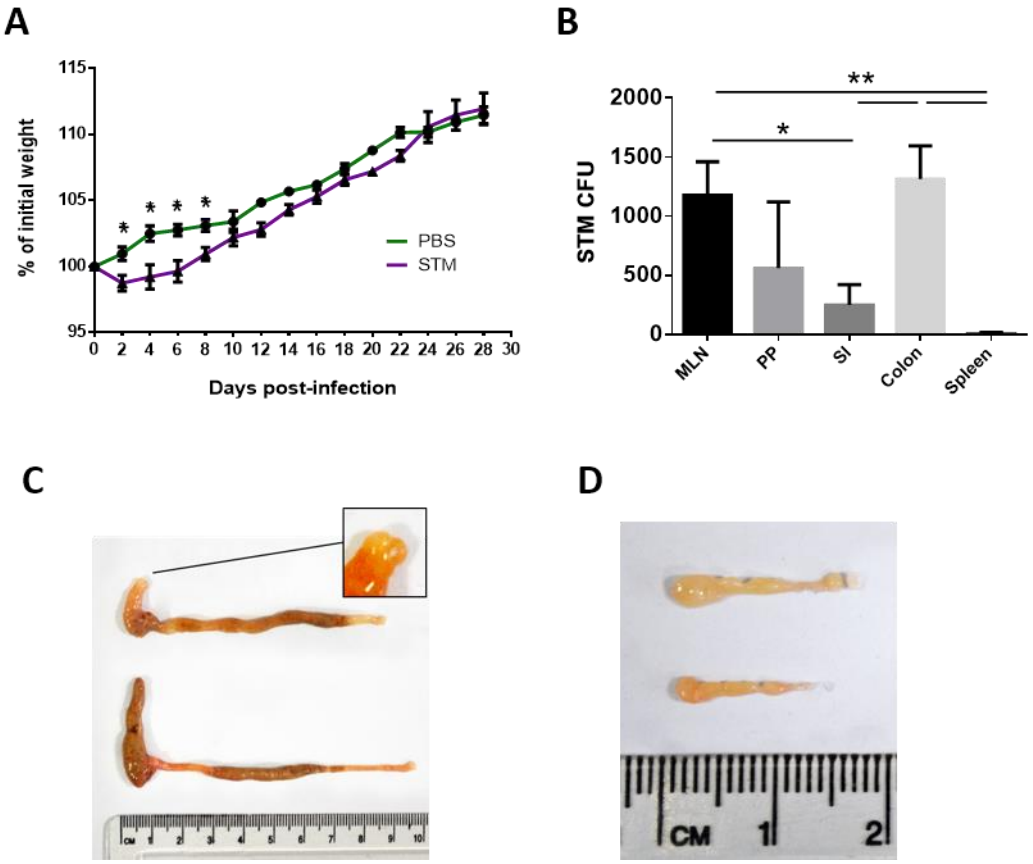

Figure 3.4 BRD509-2W1S induces intestinal infection and colitis but only moderate weight loss.
(A) Weight loss for 30 days following infection with BRD509-2W1S or mock infection with PBS. **(B)** STM CFUs recovered from five tissues 6 days post-infection. **(C)** Representative image of colons and caeca from infected (top) and uninfected (bottom) mice. Inset shows the tip of a BRD509-2W1S infected caecum with enlarged caecal patch. **(D)** Representative images of MLN chains from BRD509-2W1S infected (top) and mock infected (bottom) mice. cMLN1 is shown far left. **(A)** Weight charts show data from two independent experiments (n=3-5) and CFU data **(B)** is from one experiment (n=3). Mean ± SEM are plotted. Statistical significance between weights at specific time points and CFUs between tisssues are calculated by one-way ANOVA with Tukey's test. *p<.05; **p<.01. MLN, mesenteric lymph nodes; PP, Peyer's patches; SI, small intestine.

Having a clearer understanding of gross physiological changes during infection, experiments were next conducted to assess organ-specific changes in cell numbers following infection. A major aim of this project is understanding the control of the CD4 T cell response to STM, so changes in cell numbers, CD4 T cells and FoxP3^{+} regulatory T cells (Tregs) were enumerated. Cell numbers were calculated at 6, 30 and 60 days p.i. in the colon, caecal patch (CP), MLNs and the spleen (Fig 3.5). In the colon there was a significant increase in the number of total cells, CD4 T cells and Tregs at day 6 p.i. Total cell numbers remained elevated at 60 days p.i., although the number of colonic CD4 T cells and Tregs returned to normal levels by 30 days p.i. The number of total MLN cells also increased 6 days p.i., but this increase was resolved by day 30 p.i. Unlike in the colon,

there was no significant increase in the number of MLN CD4 T cells or Tregs. Changes in splenic cells showed an inverse dynamic to that seen in the colon, with decreased numbers of total cells and CD4 T cells at day 6 and day 30 p.i., which resolved to normal numbers by day 60 p.i. In the CP, the trend was similar to that seen in the colon, with increased CD4 T cells at day 6 p.i., resolving to normal levels by day 30 p.i. The increase in total CP cells is not significant however, potentially because harvest of the tissue is less precise, and samples include variable quantities of surrounding non-lymphoid tissue.

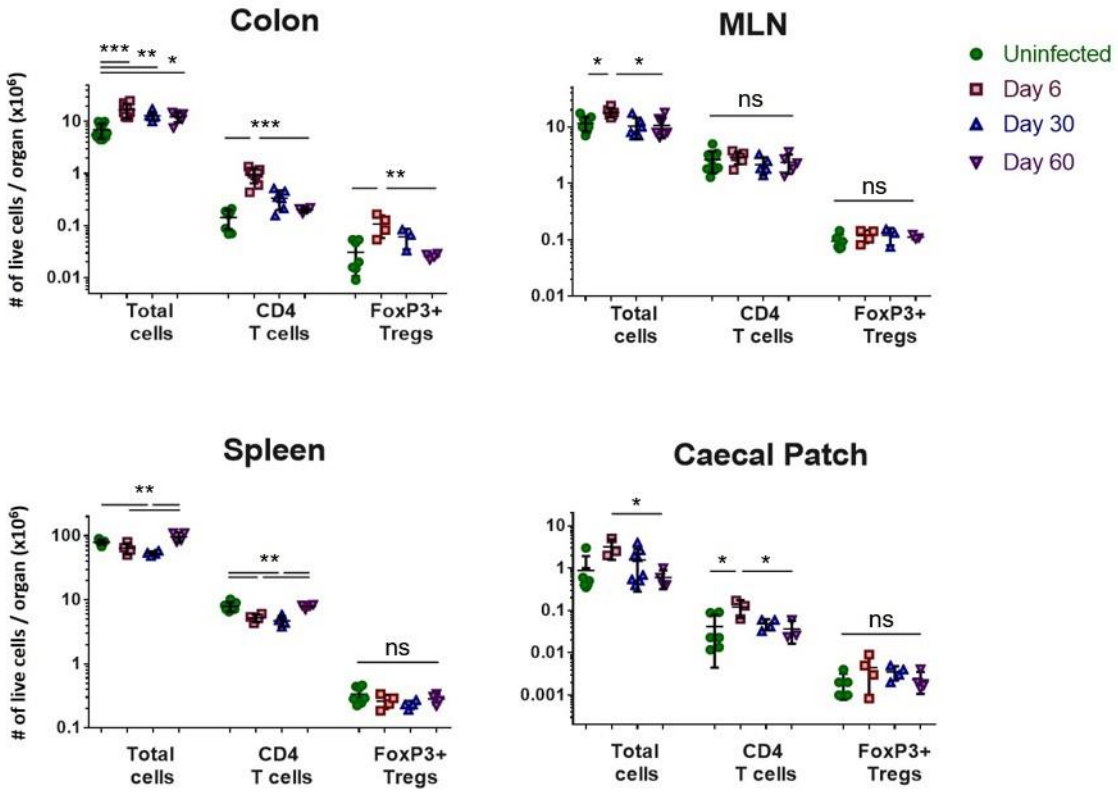

Figure 3.5 Change in the number of total cells, CD4 T cells and Tregs following BRD509-2W1S infection.

Total cells were enumerated from single cell suspension by haemocytometer, CD4 T cells were identified by flow cytometry as live, single $CD45^+$, $CD3^+$, $Dump^-$ (MHCII, B220, CD8, CD64) $CD4^+$ cells. FoxP3 Tregs were identified by FACS as $FoxP3^+$ cells that are CD4 T cells. Uninfected cells are from mice mock-infected with PBS. Data points represent individual animals from two independent experiments (n=4-8). Mean ± SEM are plotted. Statistical significance calculated by a one-way ANOVA with Tukey's test. ns, not significant; *p<.05; **p<.01; ***p<.001; ****p<.0001.

In summary, BRD509-2W1S infection induces an increase in total cells, CD4 T cells and Tregs in the colon that at least partially resolves by day 60 p.i. There is a short-term increase in total MLN cells but not CD4 T cells. In the spleen there is a decrease in the number of total cells and CD4 T cells that resolves by day 60 p.i. (Fig 3.5). These cellular

changes, with weight loss and STM plating data reflect an STM infection model that induces consistent non-lethal infection with limited bacterial dissemination but clear signs of colitis. This fulfils the requirement for a model of non-lethal infection, so the next experiments use this model to optimise detection of STM-specific CD4 T cells.

3.3 Tracking *Salmonella*-specific CD4 T cells

To identify antigen-specific CD4 T cells following BRD509-2W1S infection, samples are stained with 2W1S:1-A^b tetramers. These tetramers bind 2W1S-specific T cell receptors (TCR) and are conjugated to Phycoerythrin (PE) fluorophores, allowing tetramer$^+$ (2W1S-specific) cells to be identified by flow cytometry. Since 2W1S is not an endogenous peptide, activated tetramer$^+$ cells can be characterised as an STM-2W1S-specific T cell population.

3.3.1 Optimisation of BRD509-2W1S infection and MHCII tetramer staining to detect *Salmonella*-specific CD4 T cells

2W1S:1-A^b tetramer$^+$ CD4 T cells are identified by flow cytometry with the gating strategies shown in Fig 3.6. Following MHC II tetramer and surface staining, CD4 T cells are identified as live, single, CD45$^+$, CD3$^+$, MHCII$^-$, B220$^-$, CD8$^-$, CD64$^-$, CD4$^+$ cells. Tetramer$^+$ CD4 T cells are then identified as CD44hi Tetramer$^+$ cells. This strategy can identify 2W1S-specific CD4 T cells in mucosal tissue, such as colon (Fig 3.6A) or lymphoid tissue, including MLNs (Fig 3.6B).

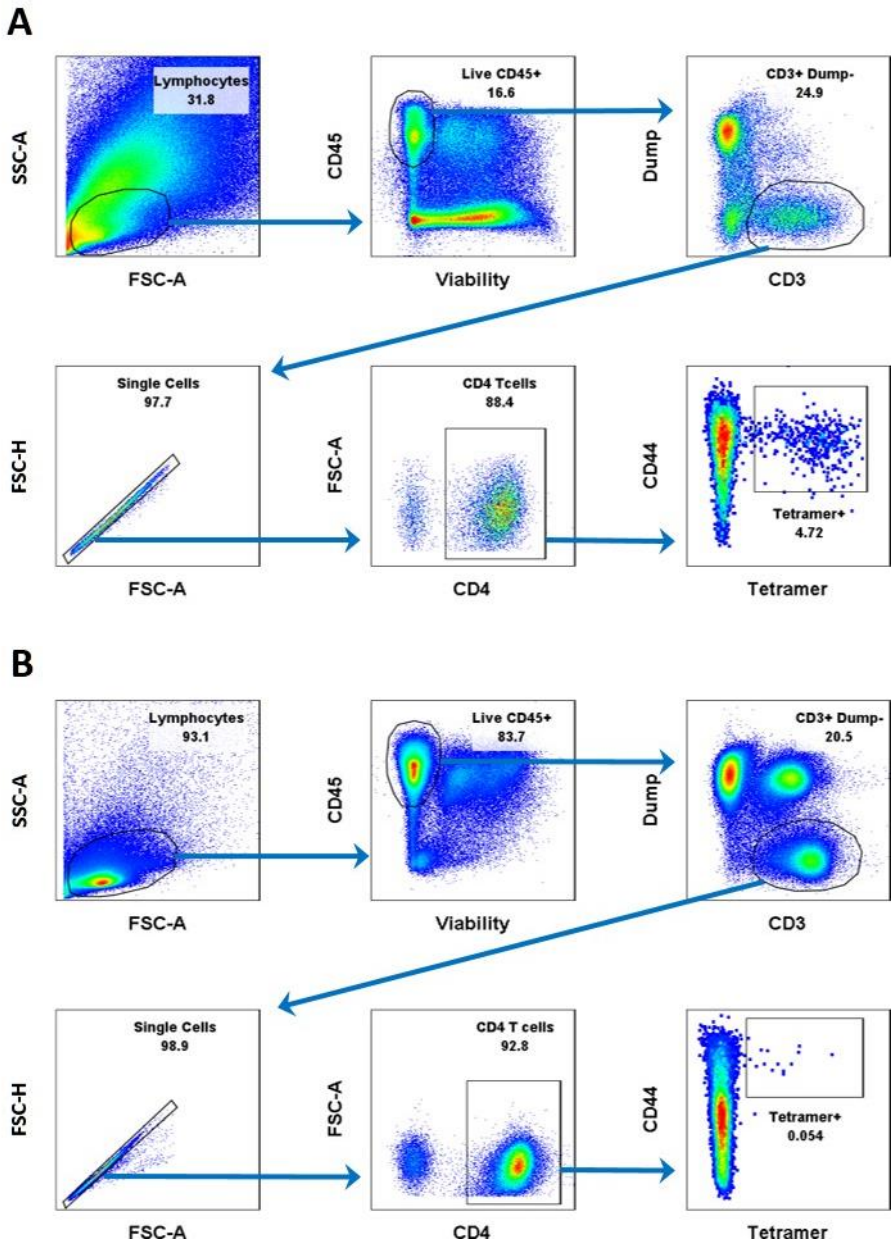

Figure 3.6 Gating strategy for tetramer$^+$ CD4 T cells in the colon and MLN.

Representative plots of cells from BRD509-2W1S infected mice 6 days p.i. Tetramer$^+$ CD4 T cells are identified from single cell suspension of colonic cells **(A)** and MLN cells **(B)**. Cells are identified as live, single CD45$^+$, CD3$^+$, Dump$^-$ (MHCII, B220, CD8, CD64), CD4$^+$, CD44^{hi} and tetramer$^+$ cells.

The tetramer staining protocol was optimised by staining splenocytes from BRD509-2W1S infected mice with serial dilutions of 2W1S:1-A^b tetramers (Fig 3.7). An increased proportion of tetramer$^+$ cells was observed in the 2W1S exposed mice but not in non-2W1S infected mice. Based on these results, 7.0µg/ml was the concentration selected for future experiments as a balance between a high proportion of tetramer$^+$ cells labelled and conserving tetramer stocks.

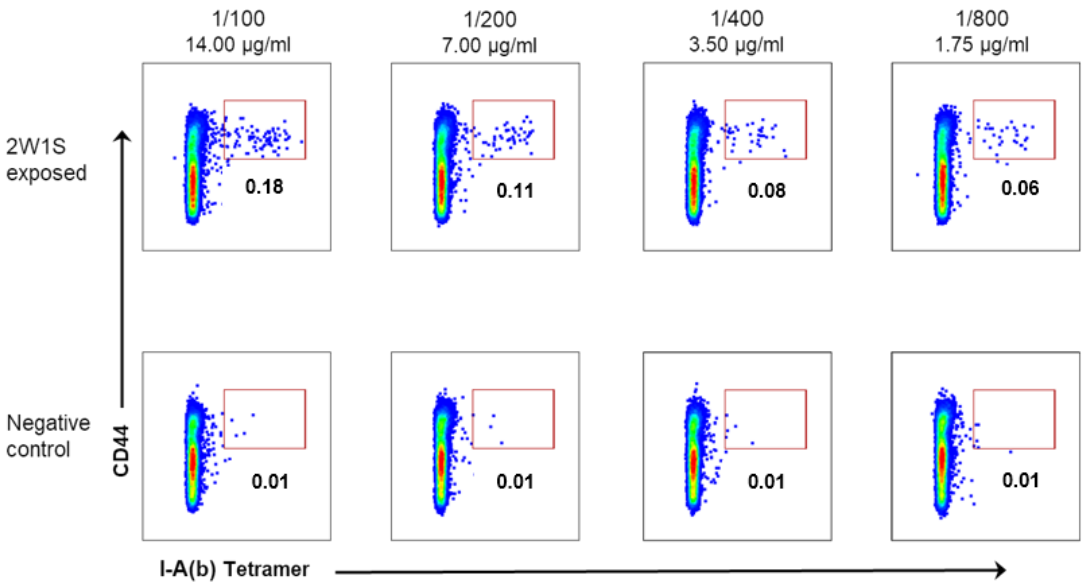

Figure 3.7 Detection of 2W1S- specific CD4 T cells using titrated tetramer.

Representative plots of splenic CD4 T cells from BRD509-2W1S infected (top) and non-2W1S BRD509-infected mice (bottom), stained with serial dilutions of 2W1S:IA^b tetramer. Spleens were harvested 6 days p.i. and were stained with tetramer for 2 hrs at 37C, before surface staining and analysis by flow cytometry.

After developing a gating strategy and optimising tetramer staining, the next objective was to track tetramer$^+$ cells across tissues at multiple time points. Initially, MLN and spleens were harvested at day 6 and day 30 p.i. (Fig 3.8). Representative plots showing tetramer$^+$ CD4 T cells in both tissues from BRD509-2W1S-infected mice but not mock infected controls are shown in Fig 3.8A. Charts showing the proportion of CD4 T cells that are tetramer$^+$ are shown for the MLN (Fig 3.8B) and spleen (Fig 3.8C). These data confirm specific tetramer staining in both tissues. At day 6 p.i., 0.20% and 0.27% of CD4 T cells are tetramer$^+$ in the MLN and spleen respectively. Unexpectedly, the mean proportion of CD4 T cells that are tetramer$^+$ in the spleen increased to over 1.5% at day 30, while the proportion of tetramer$^+$ cells in the MLN was unchanged (Fig 3.8B and C).

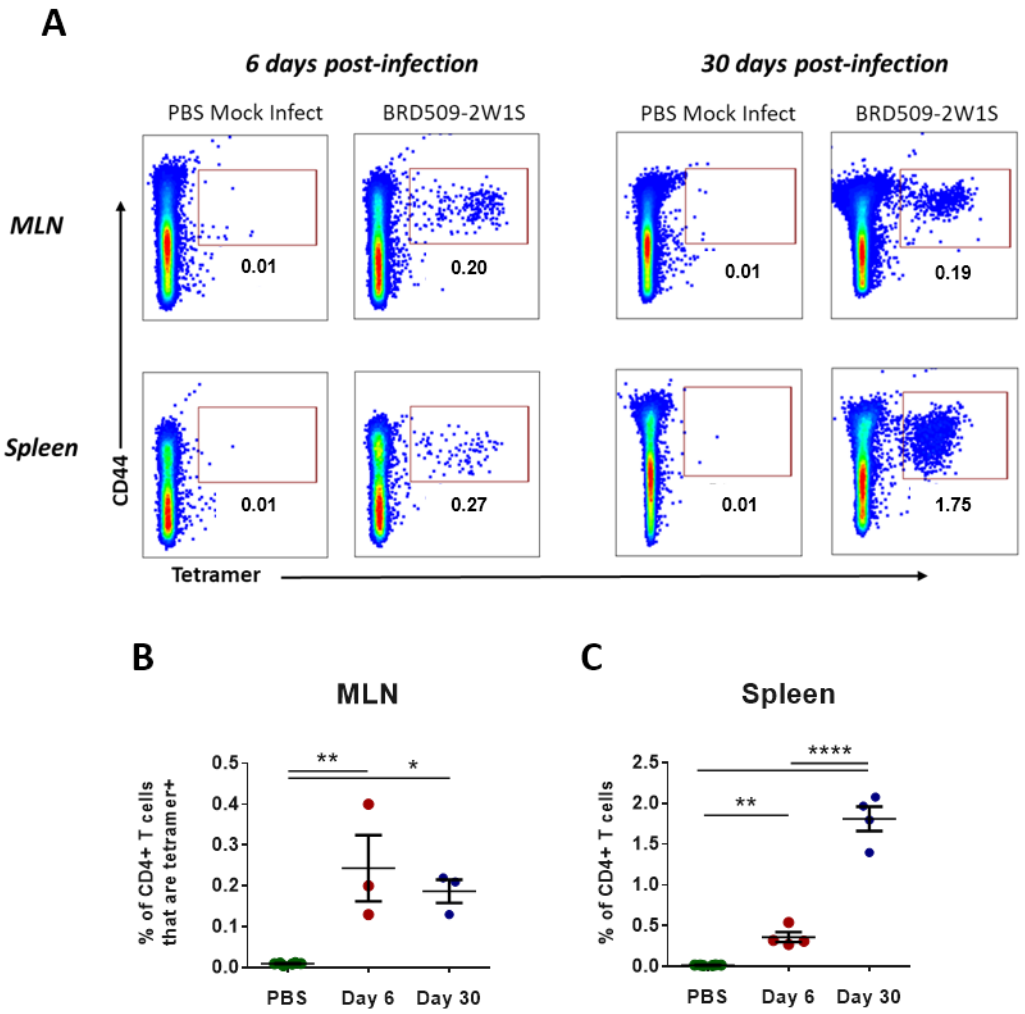

Figure 3.8 Detection of 2W1S-specific tetramer$^+$ CD4 T cells 6 days and 30 days p.i.

(A) Representative plots of tetramer$^+$ CD4 T cells (as gated in Fig 3.6) from MLN (top) and spleen (bottom) at 6 days and 30 days p.i. with BRD509-2W1S or mock-infected with PBS. The proportion of CD4 T cells that are tetramer$^+$ in the MLN **(B)** and spleen **(C)** are plotted at day 6 and 30 p.i. Data points represent individual animals from two independent experiments (n=3-8). Mean ± SEM are plotted. Statistical significance calculated by a one-way ANOVA with Tukey's test. *p<.05; **p<.01; ***p<.001; ****p<.0001.

The high proportion of 2W1S-specific splenocytes at 30 days p.i., prompted analysis of tetramer$^+$ cells in multiple intestinal and lymphoid tissues at day 6 and day 30 p.i. Representative plots from the colon, caecum, CP, spleen, MLN, SI and PP at day 30 p.i. are shown in Fig 3.9. CD4 T cells in the colon and caecum are 7.33% and 8.95% tetramer$^+$, respectively. These figures dwarf the proportion of CD4 T cells that are tetramer$^+$ in the SI and PPs, which are only 0.05% and 0.02% tetramer$^+$ respectively (Fig 3.9). This paucity of CD4 T cells in the SI informed the decision to focus subsequent analyses of intestinal LP to colonic and caecal tissue.

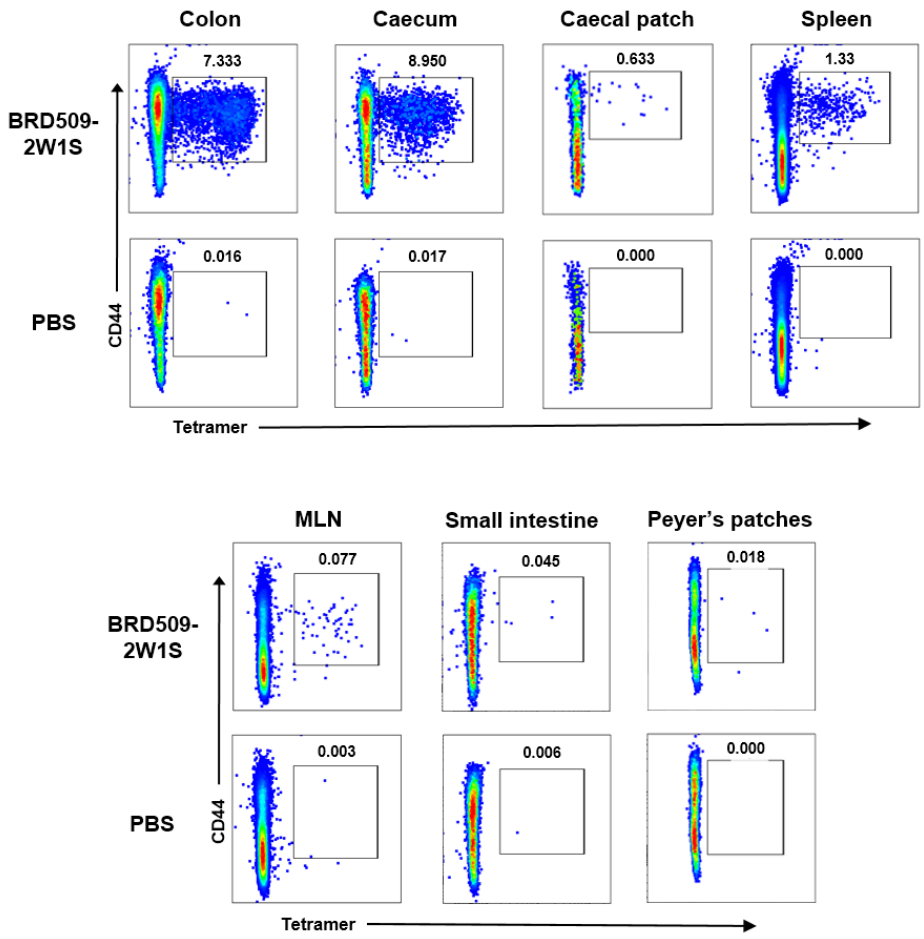

Figure 3.9 Tetramer$^+$ CD4 T cells are detected in multiple intestinal and lymphoid sites 30 days p.i., with the highest proportion in the colon and caecum.

Representative plots of tetramer$^+$ CD4 T cells from 7 tissues at day 30 post-infection with BRD509-2W1S (top) or mock-infected with PBS (bottom).

The high proportion of tetramer$^+$ cells at day 30 p.i. in colonic and caecal LP raises questions about what drives this response. Further infections with larger groups were carried out to assess the tetramer$^+$ response across tissues and to investigate the possibility that persistent infection is increasing the tetramer$^+$ CD4 T cell response.

3.3.2 BRD509-2W1S infection drives a sustained tetramer$^+$ CD4 T cell response that is reduced following antibiotic treatment

To assess whether persistent infection is driving the tetramer$^+$ T cell response, mice were infected with BRD509-2W1S or mock-infected, as described above. One group of each cohort was harvested 6 days p.i. and half of the remaining animals were treated with enrofloxacin in drinking water from day 7 until day 28 p.i., as previously described to treat persistent STM infection (Griffin et al., 2009). Enrofloxacin-treated and untreated groups

were harvested at day 30 p.i. for analysis (Fig 3.10A and B). Additionally, tissue and intestinal contents from both groups, and an untreated group infected for 60 days, were plated to identify the presence of STM CFUs (Fig 3.10C).

From day 6 to 30 days p.i., the proportion of tetramer$^+$ CD4 T cells increased 5-10 fold in all tissues analysed except the MLN (Fig 3.10A). These increased proportions correspond to increased absolute numbers of tetramer$^+$ cells in the spleen, colon and caecum (Fig 3.10B). At 30 days p.i., enrofloxacin-treated mice had lower proportions of tetramer$^+$ cells in all tissues except the MLN and a lower number of colonic tetramer$^+$ cells than untreated mice. Although enrofloxacin treatment reduces the proportion of tetramer$^+$ cells in most tissues, these levels remain higher than values observed at day 6 p.i. in in the spleen, colon and caecum (Fig 3.10A).

When tissues and intestinal content were plated at day 6 p.i., STM CFUs were recovered from caecal content (~$1x10^6$ CFU/mg), faeces (~$1x10^5$ CFU/mg), colon and caecal LP, CP and MLN (~$1x10^3$-$1x10^4$/organ) (Fig 3.10C). At day 30 p.i., <$1x10^2$ CFU/mg were recovered from caecal contents and <$5x10^2$ CFU were recovered from the CP and spleen. Following enrofloxacin-treatment, no bacteria were recovered from intestinal contents or tissues. STM bacteria was also not recovered from untreated mice that were harvested 60 days p.i. (Fig 3.10C). These data indicate that the STM-specific response at day 30 p.i. is at least partially driven by persistent infection in lymphoid tissues such as the spleen or CP.

Considering the potential for persistent, low-level infection, tetramer$^+$ cells were tracked across intestinal and lymphoid tissues up to 90 days p.i. At 60 days p.i., the proportion (Fig 3.11A) and absolute number (Fig 3.11B) of tetramer$^+$ cells were not significantly reduced in any tissues. This stability of 2W1S-specific CD4 T cells at 60 days p.i. occurs despite a paucity of detectable STM CFUs (Fig 3.10C) and a concurrent reduction in the number of CD4 T cells at this time point in the colon, caecum and CP (Fig 3.5).

Finally, 2W1S-specific T cell were tracked at 90 days p.i. to try to identify a time point where tetramer$^+$ CD4 T cells are reduced (Fig 3.11). Even after 90 days, the proportion of CD4 T cells that are tetramer$^+$ remains near peak levels in the colon and caecum (Fig 3.11A). There is a trend towards reduced proportions of tetramer$^+$ cells in the CP, and MLN, but the spleen is the only organ showing a significant reduction in the proportion of tetramer$^+$ cells from levels observed at 30 days p.i. There is a consistent trend of decreased numbers of tetramer$^+$ cells at day 90 compared to day 60 and day 30 p.i. This trend is observed in all tissues analysed (Fig 3.11B).

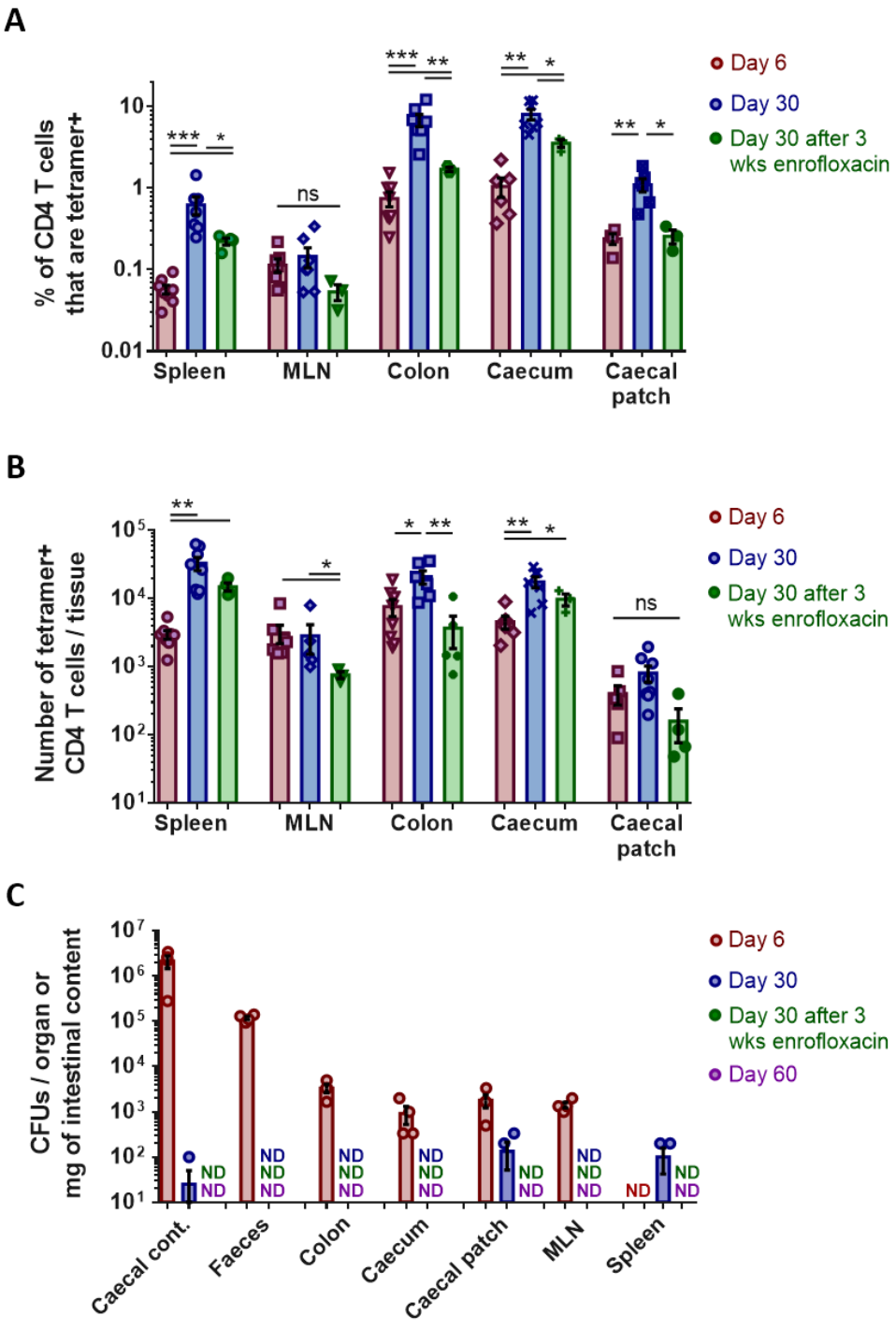

Figure 3.10 Enrofloxacin treatment reduces the number of tetramer⁺ CD4 T cells and STM CFUs recovered 30 days p.i.

The proportion **(A)** and absolute number **(B)** of CD4 T cells that are tetramer⁺ at day 6, 30 or 60 p.i. is shown following 3 weeks of treatment with enrofloxacin in drinking water from 6 days p.i. **(C)** Samples of caecal content, faeces and tissues were plated following harvest and the number of STM CFUs recovered / organ or mg of intestinal content was plotted. Data points represent individual animals from two independent experiments **(A, B)** or one experiment **(C)** (n=3-8). Mean ± SEM are plotted. Statistical significance calculated for each tissue by a one-way ANOVA with Tukey's test. ns, not significant; *p<.05; **p<.01; ***p<.001; ****p<.0001; ND, not detected).

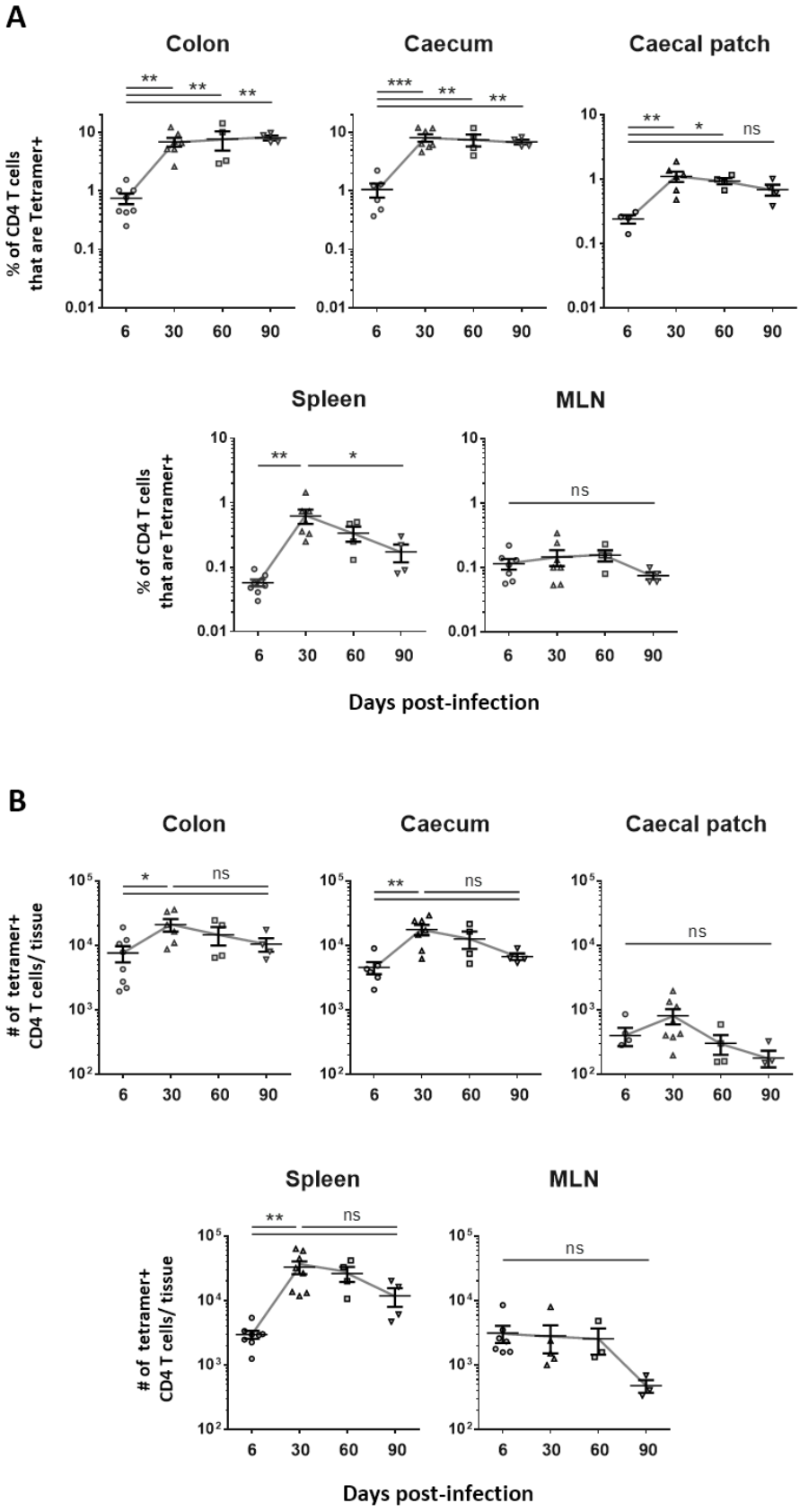

Figure 3.11 The proportion of tetramer⁺ CD4 T cells remains elevated in the large intestine 90 days p.i.

The proportion **(A)** and absolute number **(B)** of CD4 T cells that are tetramer⁺ 6 days, 30 days, 60 days or 90 days p.i. Data points represent individual animals from three independent experiments (n=3-8). Mean ± SEM are plotted. Statistical significance calculated for each tissue by a one-way ANOVA with Tukey's test. ns, not significant; *p<.05; **p<.01; ***p<.001; ****p<.0001.

In vivo infections with STM BRD509-2W1S allows tracking of 2W1S-specific CD4 T cells in multiple sites over months following infection. These data show that a long lasting STM-specific T cell response occurs in the large intestine and MLNs, and peaks between day 6 and day 60 p.i., after weight loss and other signs of pathology have resolved. The colon and caecum are the sites with the highest proportion and number of tetramer$^+$ cells in the intestines, with a 100-200 fold higher proportion of tetramer$^+$ CD4 T cells than in the SI at 30 days p.i. (Fig 3.9).

The greater STM bacterial burden and CD4 T cell response in the large intestine than the SI, the muted changes in MLN cell numbers following infection (Fig 3.5) and the selective enlargement of infected cMLNs (Fig 3.4D) led to the hypothesis that STM-specific T cells are primarily induced in the cMLN instead of the sMLNs. This hypothesis is consistent with previous work from our lab showing different intestinal sites drain to specific MLNs (Houston et al., 2015; Mayer et al., 2017). If the STM-specific T cells are primarily present in the cMLNs. analysis of the entire MLN chain may dilute the previously observed MLN T cell response, measured in pooled MLNs in the experiments above. With the aim of improving sensitivity of detecting STM responses in the MLNs, a comparison of CD4 T cells in the cMLN and sMLN was conducted following STM infection.

3.3.3 The CD4 T cell response to *Salmonella* is constrained to colon draining mesenteric lymph nodes

BRD509-2W1S or mock-infected mice were harvested 6 days p.i. and CD4 T cells were compared between cMLNs (cMLN1 and cMLN2) and the sMLN chain (Fig 3.3A). The number and proportion of total cells, CD4 T cells and CD4 T cells expressing CXCR3 and 2W1S-specific TCRs (representative plots shown Fig 3.12B) are charted in Fig 3.12C. The increase in total cells is constrained to the cMLN (Fig 3.12C, top left). Following infection, the number of sMLN cells is unchanged but the number of cMLN cells increases by >300%, skewing the ratio of sMLN to cMLN cells from 1:1 to 1:3. The number of CD4 T cells significantly increases in the cMLN but not the sMLN (Fig 3.13C, top right), indicating that the unchanged number of CD4 T cells observed in total MLN cells (Fig 3.5)

masks a cMLN-specific CD4 T cell increase. Most cells entering the cMLN following STM infection are not CD4 T cells however, as the proportion of total cells that are CD4 T cells decreases in the cMLN (Fig 3.13C, top right). Other cells known to migrate into MLNs during infection include CD8 T cells and B cells. When characterising CD4 T cells by expression of CXCR3 expression, a chemokine receptor used to identify Th1 cells, there is a significant increase in the proportion and number of $CXCR3^+$ cells only in the cMLN (Fig 3.13, bottom left). Finally, when analysing 2W1S-specific CD4 T cells, $2W1S:IA^b$ $tetramer^+$ cells are only found in the cMLNs, indicating that at this timepoint the STM-specific response in the MLNs are confined to colon and caecum draining LNs (Fig 3.5C, bottom right).

Together, these data show that in this model, the STM-specific CD4 T cell response in the MLN is restricted to the cMLN, which reflects the colon and caecal-specific pathology and T cell responses observed in the intestinal LP. This helps characterise how the CD4 T cell response develops and guides our approach to upcoming experiments. In following experiments, only cMLN will be harvested and future reference to ‘MLN’ will specifically refer to cMLN.

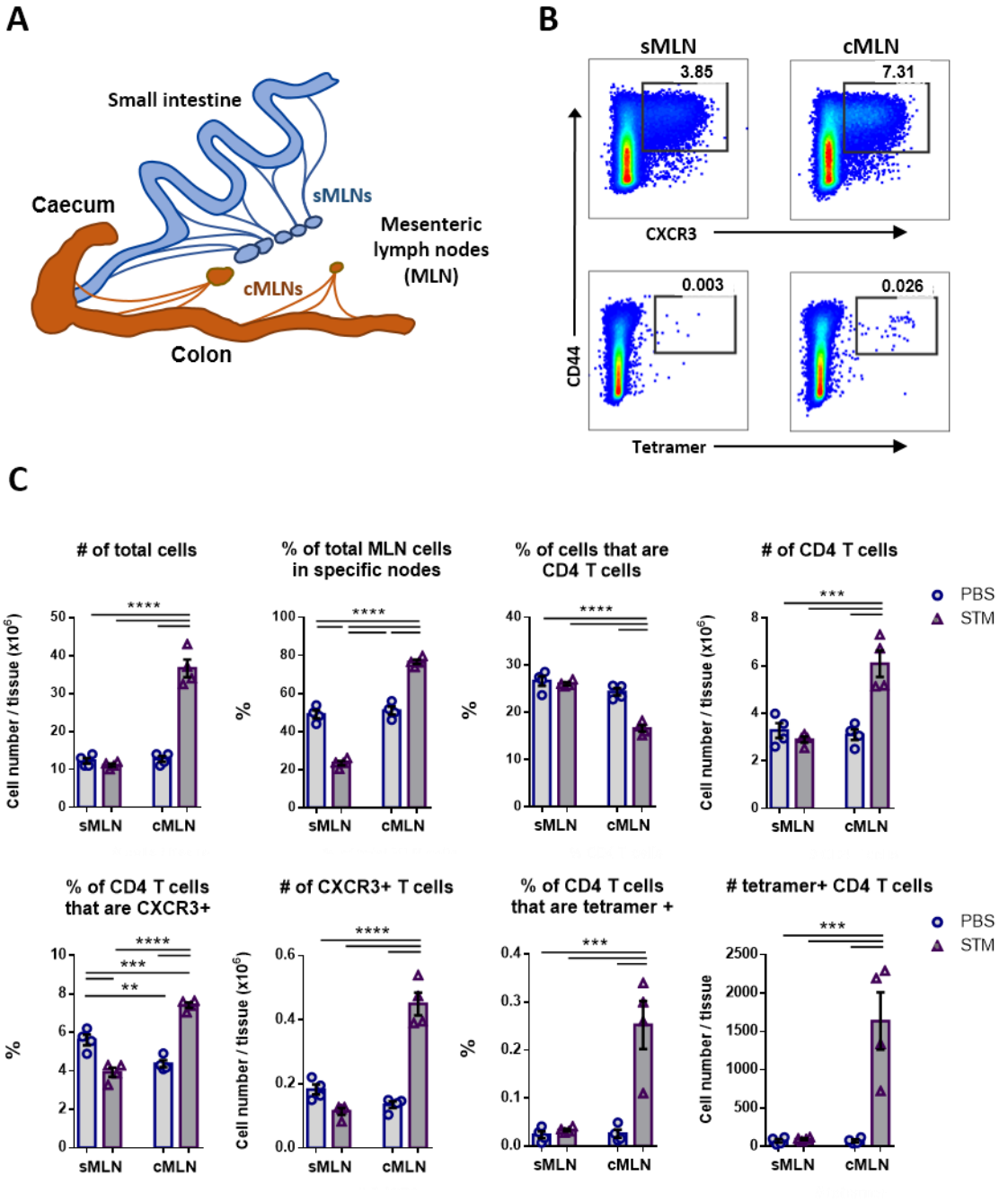

Figure 3.12 The T cell response to STM in the MLN is confined to colon and caecum draining nodes.

(A) Schematic representation of intestines and MLNs, including small intestine draining MLNs (sMLN), and colonic draining MLNs (cMLN). **(B)** Representative plots of CD4 T cells from sMLN (left) and cMLN (right) that are CXCR3$^+$ (top) and tetramer$^+$ (bottom), 6 days p.i. **(C)** Graphs showing the number and proportion of total cells, CD4 T cells, and of CD4 T cells that are CXCR3$^+$ or tetramer$^+$ at day 6 p.i. Data points represent individual animals (n=4). Mean ± SEM are plotted. Statistical significance calculated by a one-way ANOVA with Tukey's test. *p<.05; **p<.01; ***p<.001; ****p<.0001.

3.4 Discussion

The initial aim of this project was to optimise *in vivo* models of STM infection and to characterise antigen-specific CD4 T cells following infection. This is an important step to investigate how the T cell response to STM is controlled. The STM infections described here are based on a streptomycin pre-treatment model developed as a model of non-typhoid intestinal infection (Barthel et al., 2003). Streptomycin treatment removes >90% of the intestinal microbiota and reduces colonisation resistance, allowing consistent infection by STM, which is naturally streptomycin-resistant (Hapfelmeier and Hardt, 2005; Kaiser et al., 2012). The first step to optimise an *in vivo* infection model for this project was selecting STM strains that could be easily cultured and establish consistent, non-lethal infections. The next step was to test strains for expression of GFP or 2W1S, to track bacteria or responding T cells respectively.

Growth dynamics were plotted to identify differences between strains or inconsistency in the ratio between OD and CFUs in culture. This was important because cultures are prepared for infection by OD, before CFU can be confirmed by overnight (o/n) growth on plates. These experiments are also useful to identify the time required for cultures to move from static to exponential growth, the target phase for initiating infections. Data show that all strains exhibit similar growth dynamics and enter an exponential phase within three hours of culture and extend for over six hours (Fig 3.1B). These results were consistent with other strains used in our lab, so infection experiments were conducted following established protocols for o/n static incubation.

GFP reporter strain JH3016 was selected for initial imaging experiments because it incorporates a chromosomal GFP insert. Previous work in our lab (Bravo-Blas et al., 2018) revealed plasmid constructs such as STM-pGFP quickly lose GFP expression *in vivo*, so chromosomal constructs were preferable for durable GFP expression. The *in vitro* detection of macrophages infected by JH3016 was successful by both FACS (Fig 3.2A,B) and fluorescence microscopy (Fig 3.2C), but *in vivo* imaging was more difficult (Fig 3.2D,E). Colon and SI sections were processed from JH3016 and SL1344 (non-GFP

control) 24 hrs p.i. to attempt identification of GFP^+ bacteria by fluorescence microscopy. This time point was selected because intestinal LP penetration has been documented within 12 hrs p.i. and this is before severe pathology and weight loss is detected in mice infected by virulent STM (Barthel et al., 2003; Coburn et al., 2005). GFP^+ rod-shaped bacteria were detectable in the luminal contents of JH3016 infected mice by immunofluorescence microscopy, but not SL1344 infected controls. However, no GFP^+ bacteria were identified in the SI LP and only one GFP^+ bacterium was detected in 10 sections of JH3016-infected colon (Fig 3.2D,E). This highlighted the challenge of tracking bacterial dissemination *in vivo*. Following these initial experiments to track GFP^+ STM, focus shifted to examining the immune response against STM, using 2W1S strains to track STM-specific CD4 T cells.

3.4.1 Tracking 2W1S-specific T cells

2W1S-expressing STM strains integrate a peptide tag downstream from the 3' portion of the OmpC gene (Nelson et al., 2013). These constructs have been engineered with virulent SL1344 and attenuated BRD509, an auxotrophic *aroA* mutant (Mooney et al., 2015). The choice of STM strain to use must consider the host strain to be infected. $Nramp1^{-/-}$ mice, including C57BL/6-derived strains, are highly susceptible to infection with virulent STM and succumb to infection within 1-2 weeks. Conversely, $Nramp1^{+/+}$ mice, including 129SvJ, are resistant to virulent STM and survive infection (Brown et al., 2013; Fritsche et al., 2012). Therefore, most STM infection models use either attenuated STM with Nramp1-deficient mice or virulent STM with $Nramp1^{+/+}$ mice. Because of the wide range of C57BL/6-derived strains available, an attenuated STM strain was sought for this work. Since the 2W1S insert itself may attenuate bacteria *in vivo*, SL1344-2W1S and BRD509-2W1S were both included in experiments to assess pathology induced in C57BL/6 mice. Weight loss and colitis were severe in SL1344-2W1S infected mice, with high mortality rates, even when dosage was decreased or streptomycin pre-treatment was omitted (Fig 3.3B-F). BRD509-2W1S was less virulent however, causing signs of colitis with less weight loss and higher survival rates (Fig 3.3E-G). As such, BRD509-2W1S was selected for future infections.

To assess bacterial dissemination, intestinal tissue was plated at 6 days p.i. The colon contained significantly higher bacterial loads than the SI, consistent with the specific enlargement of colon and caecal draining MLNs (Fig 3.4B,D). The colon and caecum were also the intestinal site with the highest number of 2W1S-specific T cells. These tissues contain >150-fold higher proportion of 2W1S-specific CD4 T cells than the SI LP (Fig 3.9). Consistent with the colon and caecum being the primary effector sites, we showed that colon and caecum-draining MLNs are the nodes with expanded total cells, CD4 T cells and 2W1S-specific T cells 6 days p.i. (Fig 3.13).

The finding that the colon and caecum are primary sites of STM infection is consistent with previous characterisation of the streptomycin pre-treatment model, which was developed as a model of colitis (Barthel et al., 2003; Kaiser et al., 2012). Change in cell numbers following infection, including increased total cells in the MLN, colon and CP, are consistent with observed physical pathology in these tissues (Fig 3.4C). The decreased number of cells in the spleen was unexpected, especially considering the moderate splenomegaly often observed following infection. One explanation for this is that splenic lymphocytes migrate from the spleen to effector sites like the colon following infection. This hypothesis is supported by findings that STM infection induces a large increase in the number of splenic red blood cells (RBC) and RBC pre-cursors, but a decrease in lymphocytes (Rosche et al., 2015). Together, these data form a coherent picture of organ-specific pathology caused by a non-lethal model of STM infection and colitis.

3.4.2 Tracking 2W1S-Specific CD4 T Cells

After selecting of BRD509-2W1S for future experiments, the next objective was to use this model to characterise the 2W1S-specific T cell response to infection. Identifying and eventually characterising STM-specific CD4 T cells helps elucidate the immune response to infection in several ways. First, it allows an easy confirmation of infection. Second, it allows analysis of a STM-specific T cells and not T cells specific for other microbial or host peptides. Third, it allows STM-specific T cells to be tracked through time and across tissues. Tetramer staining of 2W1S-specific CD4 T cells was validated by comparing

splenocytes from mice infected with BRD509-2W1S to mice infected with the parent BRD509 strain. Tetramer^{+} cells were only detected from BRD509-2W1S infected mice, validating tetramer staining specificity. Once initially validated, infections were carried out using 'mock-infected' mice as controls. Mock infected mice are administered PBS by gavage 24 hrs after streptomycin treatment. This controls for any changes induced by streptomycin pre-treatment and allows analysis of differences between infected and uninfected mice.

Following validation of tetramer staining (Fig 3.7), the next objective was to track 2W1S-specific CD4 T cells through time and in multiple sites. Tissues were harvested 6 days and 30 days p.i. as examples of early and late time points. Day 6 p.i. corresponds to time points near to peak levels of CD4 T cell responses to viral infections like influenza (Román et al., 2002) and intracellular bacteria such as *Listeria monocytogenes* (Kursar et al., 2002). In our model, day 6 p.i. corresponds to a period of weight loss and increased cell numbers in intestinal tissue, while at day 30 p.i. mice have recovered to normal weight and increased cell numbers have at least partially recovered to baseline levels. Initial analysis of MLNs and spleens revealed a significant increase in the proportion of CD4 T cells that were tetramer^{+} between 6 and 30 days p.i. in the spleen, while numbers of tetramer^{+} cells in the MLN remained stable (Fig 3.8). Subsequent tetramer staining of seven tissues showed a stable or increased number of tetramer^{+} cells in all tissues from 6 days to 30 days p.i.

The stable population of 2W1S-specific T cells is consistent with previous research using virulent STM with Nramp$^{+/+}$ mice showing that a stable population of 2W1S-specific cells were detected in lymphoid tissue for >500 days (Nelson et al., 2013). As reported here, the colon and caecum were the tissues with the highest proportion of tetramer^{+} cells, while the SI and PP were the tissues with lowest proportion. This highlighted that the caecum and colon are important intestinal effector sites for STM-specific CD4 T cells. Following these tetramer staining experiments, the colon and caecum were selected as the intestinal sites to analyse in future experiments.

Infection experiments revealed a significant increase in the number of 2W1S-specific T cells in the colon, caecum and spleen between 6 days and 30 days p.i. One explanation for this delayed response is that BRD509-2W1S, although attenuated, can survive *in vivo* and cause persistent infection, as reported with virulent strains (Nelson et al., 2013). To test the hypothesis that persistent infection was driving the sustained 2W1S-specific T cell response, infected mice were either left untreated or treated with enrofloxacin in drinking water for 3 weeks prior to harvest at day 30 p.i. (Fig 3.10). Enrofloxacin treatment reduced the proportion and number of tetramer^{+} CD4 t cells and removed the small number of STM CFUs recoverable from untreated animals. This suggests that bacteria persist *in vivo* longer than 10 days p.i. and this persistence at least partially drives the 2W1S-specific T cell response at 30 days p.i.

These data are consistent with previous studies showing that enrofloxacin treatment can reduce bacterial burden, but that this clearance reduces compromised protective immunity (Griffin et al., 2009, 2011). This prolonged T cell response might not be a detriment to the host however, since protective CD4 T cell responses often require prolonged antigen presentation (Obst et al., 2005; Rabenstein et al., 2014). Recent research has shown that early antibiotic treatment of *Salmonella* infection reduces protective immunity (Benoun et al., 2016; Griffin et al., 2009). As such, the persistent, low level infection we detect, without physical signs of pathology, may be an important aspect of the development of a robust protective immune response. Even without enrofloxacin treatment, by 60 days p.i., STM bacteria are not recoverable from any tissue analysed (Fig 3.10C). A lack of detectable bacteria does not preclude low level infection or infection in sites not sampled here, but these data indicate that any ongoing infection is diminished by 60 days p.i.

3.4.3 Conclusion

In summary, these experiments show infection with BRD509-2W1S causes short-term colitis with mild weight loss that resolves within 2 weeks. This strain allows tracking of a long-lasting STM-specific effector CD4 T cell response that is at least partially primed in the cMLN and detected in largest numbers in the colonic and caecal LP. This infection

model has many advantages: BRD509-2W1S is easy to culture and use for oral infection, it allows infection of various mouse strains on a C57BL/6 background, it causes consistent infection and colitis with low mortality, and it allows sensitive and specific identification of STM-specific T cells. Disadvantages include only being able to detect one TCR clone to an STM-exogenous peptide, and persistent infection may complicate the characterisation of an antigen-specific memory T cell response. Despite these limitations, this model is a valuable tool that I will use to characterise the CD4 T cell response to infection. This will include analysis of antigen-specific and overall T cell responses, and the dynamics between conventional T and regulatory T cells that shape the overall response.

Chapter 4 Characterisation of the CD4 T Cell Response Following *Salmonella* infection

4.1 Introduction

Previous experiments using STM strain BRD509-2W1S allowed us to track antigen-specific CD4 T cells in multiple tissues following infection, elucidating when and where these cells are present. To better understand how the CD4 T cell response develops and is controlled, experiments were carried out to characterise changes to the CD4 T cell pool following STM infection. CD4 T cells were stained for transcription factors (TFs), cytokines and chemokine receptors to identify populations of conventional T cells (Tconvs), including subsets of T helper (Th) cells, and FoxP3$^+$ regulatory T cells (Tregs). Results from these experiments highlight the dynamic nature of the response to STM and identify potential interactions between subpopulations of Tconvs and Tregs that may control the overall response.

Here we describe a dynamic and multi-phase CD4 T cell response following STM infection, which raises questions about what drives Th differentiation and polarisation. Previous work has identified a wide range of factors that influence Th differentiation, including the mode of infection, the cognate antigen recognised by TCRs, the site of infection and the cytokine milieu (Constant, 1995; Lee et al., 2012b; Pepper et al., 2010). The potential for FoxP3$^+$ Tregs to shape Th differentiation has also been demonstrated (Campbell et al., 2018; Chaudhry et al., 2009; Koch et al., 2009; Levine et al., 2017; Sefik et al., 2015).

The Treg response to STM infection has been less studied than the Tconv response. There is an increased number of Tregs in colonic lamina propria following infection but their impact on the overall CD4 T cell response is unclear. Previous research has shown that Tregs play an important role in constraining the Tconv response to STM and depletion facilitates a more rapid bacterial clearance (Johanns et al., 2010). Tregs in the intestine are a heterogenous population and it is unclear which sub-populations play a role in

regulating the Tconv response, how they change following infection, and if they actively shape Th differentiation.

The following experiments were conducted to characterise both Tconv and Treg responses following STM infection in the colon and MLN. TF, cytokine and chemokine receptor expression were assessed to elucidate site-specific and temporal aspects of the CD4 T cell response and address questions about how this response is controlled.

4.2 Reciprocal dynamics between regulatory and conventional T cells

4.2.1 TF expression by Tconvs following *Salmonella* infection

The initial aim of characterising the CD4 T cell response to STM infection was to identify Th subsets and Tregs. CD4 T cells were stained for T-bet, RORγT and FoxP3; master TFs used to identify Th1 cells, Th17 cells and Tregs respectively (Ivanov et al., 2006; Szabo et al., 2000; Zheng and Flavell, 1997). Following infection with STM strain BRD509-2W1S, CD4 T cells from colons and draining MLNs were stained for surface markers, TFs, and 2W1S:I-A^b tetramers to identify 2W1S-specific T cells. As such, a 2W1S-specific, tetramer$^+$ population could be assessed independently of the tetramer$^-$ population, containing a presumably polyclonal pool of cells recognising diverse antigen (Fig 4.1).

In Figure 4.1A, representative plots from colonic CD4 T cells 6 days p.i. show expression of T-bet, RORγT and FoxP3 by tetramer$^+$ or tetramer$^-$ populations. While there are distinct populations of tetramer$^-$ cells that are either positive or negative for T-bet, RORγT and FoxP3, the tetramer$^+$ cells are almost exclusively T-bet$^+$. The Th1 phenotype of tetramer$^+$ cells is sustained at 30 and 60 days p.i., in both tissues (Fig 4.1B). These data suggest that while the heterogenous CD4 T cell pool contains a mixed population of Th1 cells, Th17 cells, and Tregs, 2W1S-specific T cells are almost exclusively Th1 cells.

To assess changes in Th subsets and Tregs following infection, the bulk CD4 T cell pool was also characterised by TF expression (Fig 4.2). Tconvs and Tregs were identified as

FoxP3$^-$ and FoxP3$^+$ CD4 T cells, respectively. Representative plots show gating of colonic Tconvs as CD44^{hi} FoxP3$^-$ cells, which are further characterised by T-bet and RORγT expression (Fig 4.2A). The proportion and number of Tconvs expressing T-bet, RORγT, T-bet and RORγT, or GATA3 were plotted (Fig 4.2B). Samples are from PBS (mock)-infected mice or STM-infected mice harvested at 6, 30 or 60 days p.i.

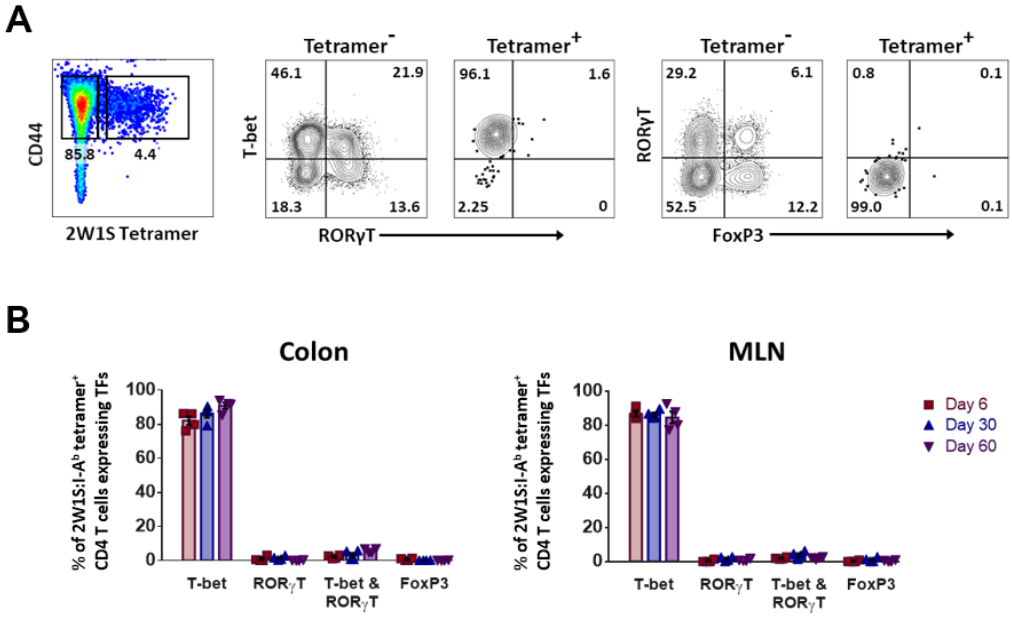

Figure 4.1 2W1S-specific CD4 T cells express T-bet but not RORγT or FoxP3.

CD4 T cells (live, single, CD45$^+$, dump (MHCII, B220, CD64, CD8)$^-$, CD3$^+$, CD4$^+$ cells) were identified as 2W1S:I-A^b tetramer$^-$ or tetramer$^+$ and characterised by expression of T-bet, RORγT or FoxP3. **(A)** Representative plots are shown of colonic CD4 T cells that are tetramer$^-$ or tetramer$^+$ stained for T-bet, RORγT and FoxP3. **(B)** TF expression by tetramer$^+$ cells in the colon or MLN at day 6, day 30 and day 60 p.i. Data points represent individual animals (n=4) from a representative example of three independent experiments. Means ± SEM are plotted.

Consistent with the increased number of colonic CD4 T cells following STM infection (Fig 3.5), there is an increased number of Tconvs expressing T-bet (Th1) cells, RORγT (Th17) cells or T-bet and RORγT 6 days p.i. While both Th1 and Th17 cells increase in number, the increase in Th17 cells is greater; this underlies an increased proportion of Th17 cells and a decreased proportion of both Th1 cells and GATA3$^+$ Th2 cells (Fig 4.2B). The reduced proportion of Th1 cells and the increased proportion of Th17 cells is indicative of a shift towards a Th17 bias 6 days p.i. This increased Th17 bias is transient however, and by day 30 p.i. there is a strong Th1 bias. The increased proportion and number of T-bet$^+$RORγT$^+$ cells remain elevated and the proportion of Th2 cells remains reduced at day

30 p.i. (Fig 4.2B). The change in the proportions of colonic Tconvs that are T-bet$^+$ Th1 cells or RORγT$^+$ Th17 cells are shown in line charts (Fig 4.2C).

The proportion and number of Tconvs expressing TFs in the MLN are shown in bar charts (Fig 4.2D) and line charts (Fig 4.2E). In the MLN, there are increased proportions and numbers of Tconvs that are Th1 cells, Th17 cells and T-bet$^+$RORγT$^+$ cells 6 days p.i. These increases resolve by day 30 p.i. for all subsets except Th1 cells, which remain elevated until 60 days p.i. In summary, despite the increase in Th1 and Th17 cells in the MLN, there is no shift in Th bias as observed in the colon.

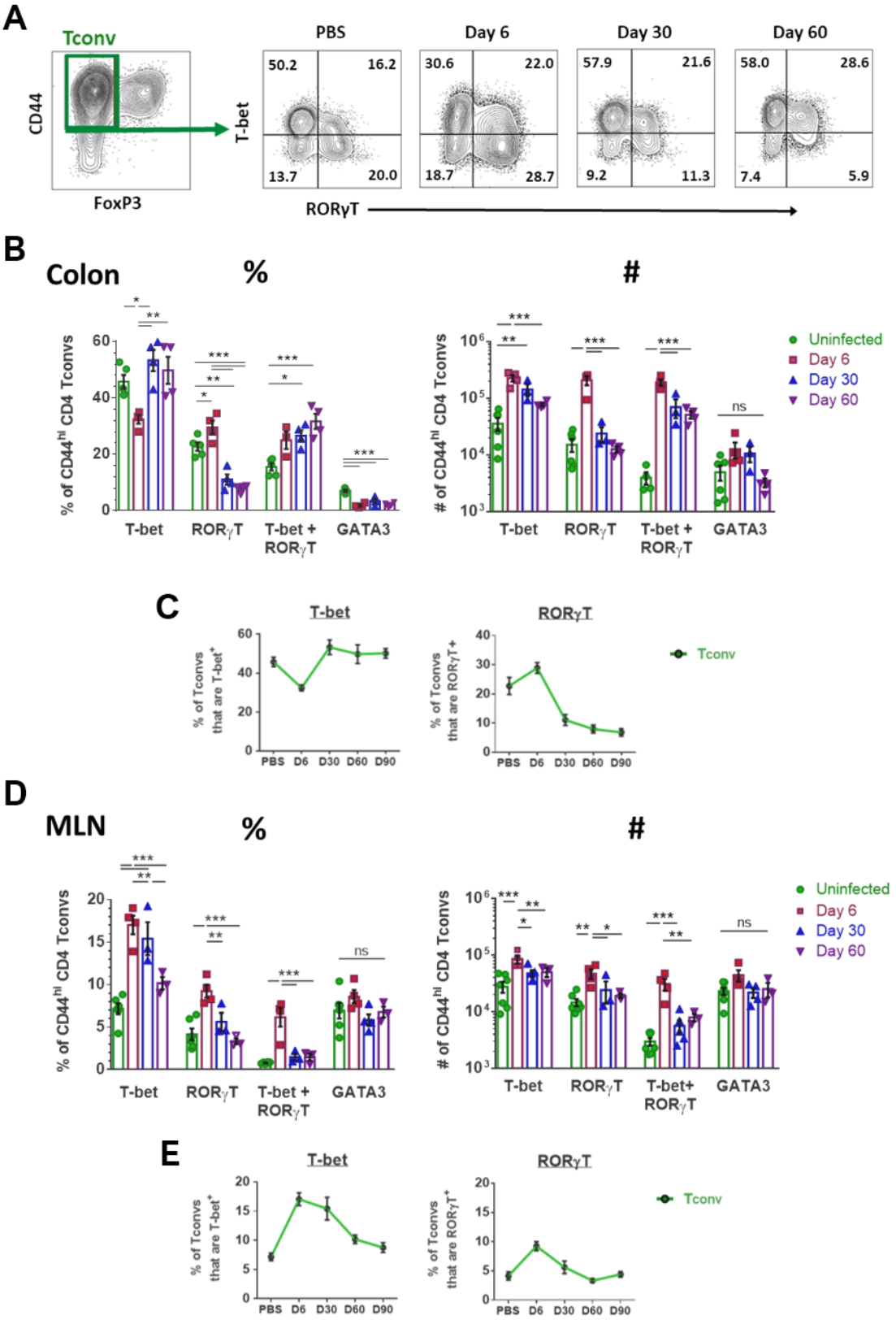

Figure 4.2 Transcription factor expression by CD4 Tconvs.

(A) Representative plots of colonic Tconvs (CD44^{hi} FoxP3^{-} CD4 T cells, gated left) stained for T-bet and RORγT following STM or mock (PBS) infection. **(B)** Expression of TFs by colonic CD44^{hi} Tconvs, shown as proportions or absolute number of Tconvs following infection. **(C)** Line charts show changes in in the proportion of colon Tconvs expressing T-bet or RORγT. **(D)** TF expression by MLN Tconvs following infection and **(E)** line charts show changes in the proportion of MLN Tconvs expressing T-bet or RORγT following STM infection. Data points represent individual animals (n=3-6) from a representative example of at least two independent experiments. Means ± SEM are plotted. Statistical significance calculated for each TF by one-way ANOVA with Tukey's test. ns, not significant; *p<.05; **p<.01; ***p<.001.

4.2.2 TF expression by Tregs following *Salmonella* infection

Next, FoxP3$^+$ Tregs were assessed for co-expression of the Th 'master' TFs used to identify Th subsets. Tregs were gated as FoxP3$^+$ CD44^{hi} CD4 T cells and representative plots showing T-bet and RORγT are shown in Fig 4.3A. The proportion and absolute number of Tregs expressing T-bet, RORγT, T-bet and RORγT, or GATA3 were graphed (Fig 4.3B). Groups include samples from PBS (mock)-infected mice and mice harvested at 6 days, 30 days and 60 days p.i.

There is an increased number of Tregs that are T-bet$^+$ and T-bet$^+$RORγT$^+$ at 6 days p.i., but no significant increase in the number of RORγT$^+$ or GATA3$^+$ Tregs (Fig 4.3B, right). These numerical changes correspond with an increased proportion of T-bet$^+$Tregs and a reduced proportion of RORγT$^+$ Tregs (Fig 4.3B, left). While these proportional changes are partially resolved by day 60 p.i., the percentage of Tregs that are T-bet$^+$ remain higher and the proportion of RORγT$^+$ Tregs remain lower than in mock-infected controls. The proportion and number of Tregs that are GATA3$^+$ remained unchanged following infection (Fig 4.3B, left). In Fig 4.3C the change in the proportion of colonic Tregs that are T-bet$^+$ or RORγT$^+$ are shown (red lines) with green lines representing the proportion of Tconvs that express the same TFs (as shown in Fig 4.2C). These charts show that the transient decrease in the proportion of colonic Th1 cells occurs concurrently with a transient increase in the proportion of T-bet$^+$ Tregs (Fig 4.3C, left). When assessing RORγT expression, the transient increase in the proportion Th17 cells corresponds with transient decrease in the proportion of Tregs that are RORγT$^+$ (Fig 4.3, right).

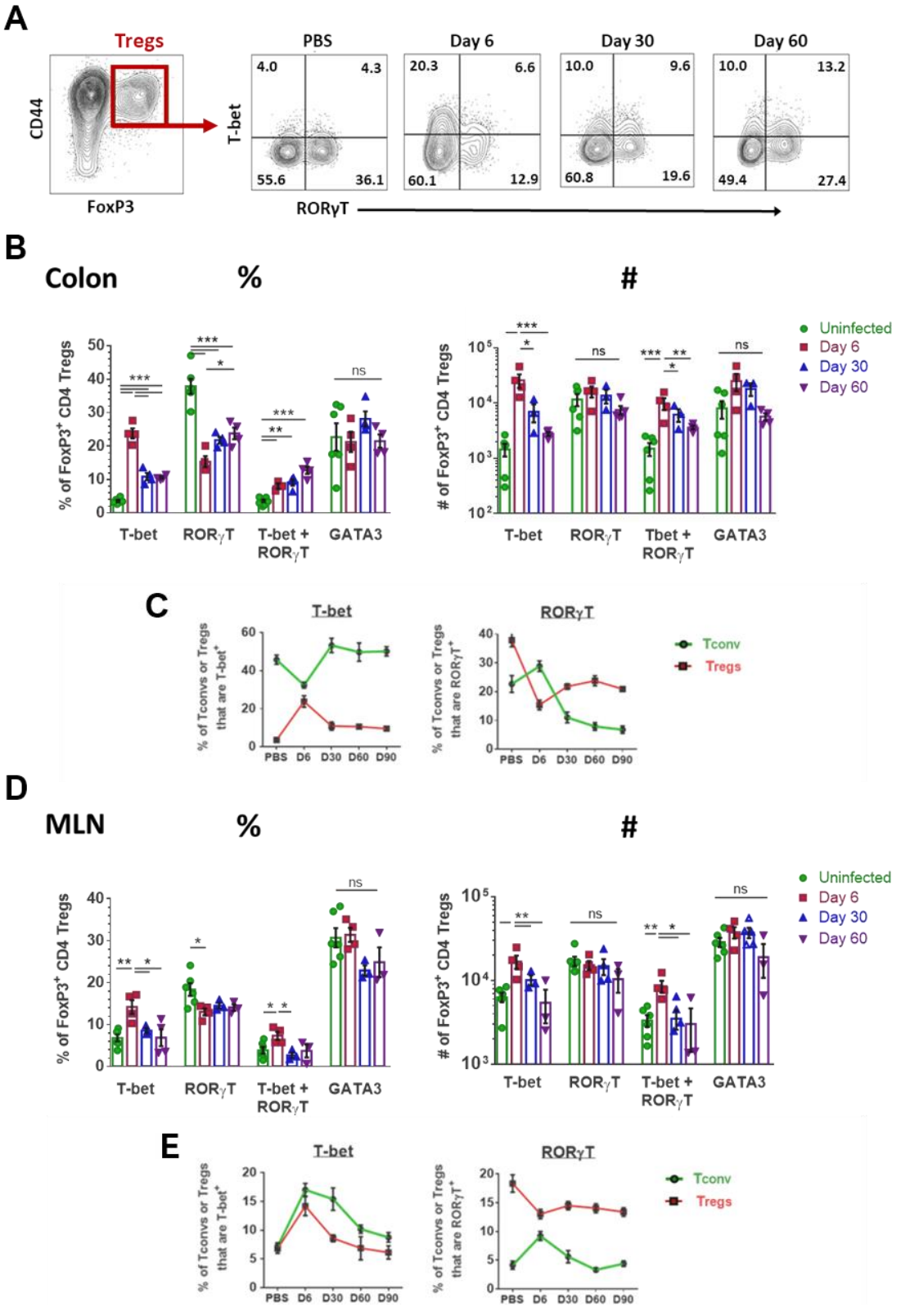

Figure 4.3 Transcription factor expression in FoxP3⁺ Tregs.

(A) Representative plots of colon Tregs (FoxP3⁺ CD4 T cells, gated left) stained for T-bet and RORγT following mock (PBS) or STM infection. **(B)** Expression of TFs by colonic Tregs are shown as absolute numbers and proportions of total Tregs. **(C)** Line charts show changes in in the proportion of Tregs expressing T-bet or RORγT (red) plotted with line charts showing the proportion of Tconvs expressing the same TFs (green). **(D)** TF expression by MLN Tregs following infection and **(E)** charts showing changes in the proportion of MLN Tregs expressing T-bet or RORγT (red) plotted with the proportions of Tconvs expressing the same TFs (green). Data points represent individual animals (n=3-6) from a representative example of at least two independent experiments. Means ± SEM are plotted. Statistical significance calculated for each TF by one-way ANOVA with Tukey's test. ns, not significant; *p<.05; **p<.01; ***p<.001.

The proportion and number of Tregs expressing TFs in the MLN are shown in bar charts (Fig 4.3D) and line charts (Fig 4.3E). In the MLN, as in the colon, there is an increased number of Tregs that are T-bet$^+$ or T-bet$^+$RORγT$^+$ following infection, but no increase in the number of RORγT$^+$ or GATA3$^+$ Tregs (Fig 4.3D, right). These numerical changes correspond with an increased proportion of Tregs that are T-bet$^+$ and reduced proportion that are RORγT$^+$ (Fig 4.3D, left). In Fig 4.3E the change in the proportion of MLN Tregs that are T-bet$^+$ or RORγT$^+$ are shown (red lines) with green lines representing the proportion of Tconvs that express the same TFs (as shown in Fig 4.2E). These charts show that the increase in the proportion of MLN Th1 cells occurs concurrently with an increase in the proportion of T-bet$^+$ Tregs (Fig 4.3E, left). The transient increase in the proportion of Th17 cells corresponds with transient decrease in the proportion of Tregs that are RORγT$^+$ (Fig 4.3, right). These data highlight a reciprocal dynamic between Tconvs and Tregs expressing T-bet or RORγT in the colon. This tissue-specific reciprocity is most evident in the first 30 days p.i., which prompted a closer investigation of these dynamics with a tighter time-course.

4.2.3 Reciprocal dynamics between colonic Tconvs and Tregs expressing the same TFs

An infection time-course with 7-8 harvest timepoints in the first 30 days p.i. was carried out to validate the reciprocal dynamics highlighted in Fig 4.3 and outlined in Fig 4.4A. These data reveal a more convincing and detailed picture of reciprocity between colonic Tconvs and Tregs expressing the same TF (4.4B). These experiments indicate that day 6 p.i. is the peak of the early Th17 response and a Th1 bias is established by day 11 p.i. On the other hand, these data suggest there is no clear reciprocity between MLN Tconvs and Tregs (Fig 4.4C). In summary, the early Th17 response in the colon coincides with an increased proportion of T-bet$^+$ Tregs, and the later Th1 bias coincides with an increased proportion of RORγT$^+$ Tregs. These results are consistent with the hypothesis that Th1 cells are being selectively suppressed by T-bet$^+$ Tregs early after infection and Th17 cells are being selectively suppressed by RORγT$^+$ Tregs later. If validated, this could elucidate a mechanism for Tregs to shape the Tconv response in a nuanced and fine-tuned way.

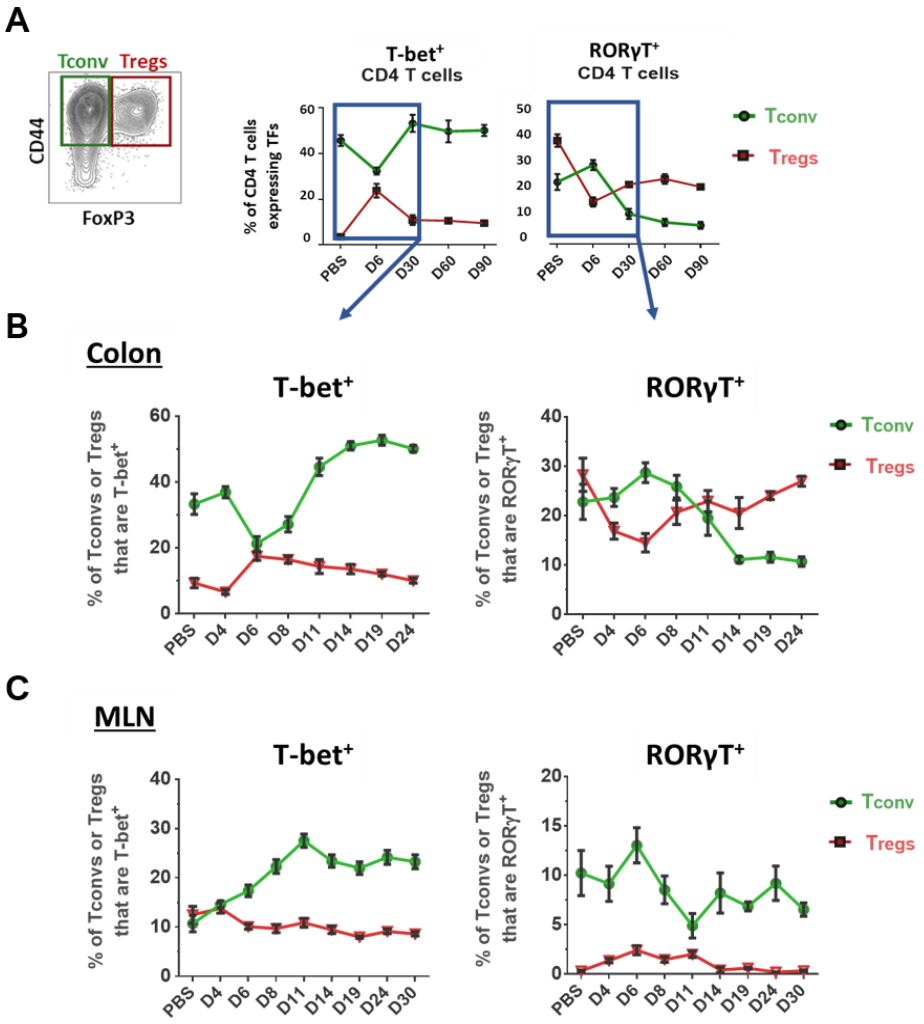

Figure 4.4 Reciprocal dynamic between Tconvs and Tregs expressing T-bet or RORγT occur in the colon but not the MLN.

CD4 T cells were identified as Tregs and Tconvs as described in Fig 4.1-4.3. **(A)** The expression of T-bet or RORγT by colonic Tconvs and Tregs described previously, was measured during a time course in the first 30 days p.i. in the colon **(B)** and in the MLN **(C)**. Data points represent groups of mice (n=4-6). Means ± SEM are plotted.

4.3 Cytokine expression by CD4 T cells following *Salmonella* infection

TF expression can be used to identify Th subsets and Tregs, but cytokine expression reveals functional characteristics that can be used with TF staining to validate the phenotype of Th populations. In the following experiments, we sought to characterise the cytokine expression by CD4 T cells following STM infection. Tregs and Tconvs were stained for TFs and IFNγ and IL-17A, cytokines expressed by Th1 and Th17 cells, respectively. The aim of these experiments was to characterise cytokine production following STM infection and to validate the classification of Th subset by TFs.

4.3.1 Cytokine expression by Tconvs

Tconvs were assessed for expression of T-bet, RORγT, IFNγ and IL-17A following PMA Ionomycin stimulation (Fig 4.5). There were increased proportions of T-bet$^+$ and T-bet$^+$RORγT$^+$ Tconvs 11 days p.i., which is consistent with previous experiments (Fig 4.5B). A smaller proportion of colonic Tconvs express cytokines compared to TFs, but there was an increased proportion IFNγ$^+$, IL-17A$^+$ and IFNγ$^+$IL-17A$^+$ Tconvs 11 days p.i. (Fig 4.5C). As in the colon, there was an increased proportion of MLN Tconvs that expressed T-bet$^+$ or T-bet$^+$RORγT$^+$ 11 days p.i., and there was an increased proportion of IL-17A$^+$ and IFNγ$^+$ Tconvs (Fig 4.5D, E). Few MLN Tconvs expressed IFNγ or IL-17A following mock-infection, but ~50% were IFNγ$^+$ and ~10% were IL17-A$^+$ 11 days p.i. (Fig 4.5E). These data show that following infection, an increased proportion of Tconvs expressed TFs and cytokines, with a bias towards T-bet and IFNγ expression. To determine if Th1 cells were producing IFNγ, and Th17 cells were producing IL-17A, as would be expected, further analysis was carried out.

Representative plots of T-bet and IFNγ expression (Fig 4.6 A, left) show that 11 days p.i., >80% of IFNγ$^+$ cells are T-bet$^+$ cells and >75% of T-bet$^+$ Tconvs are IFNγ$^+$. Plots of RORγT and IL-17A expression (Fig 4.6A, right) show that 11 days p.i., >90% of IL-17A$^+$ Tconvs are RORγT$^+$ and >50% of RORγT$^+$ Tconvs are IL-17A$^+$. When IFNγ$^+$ and IL-17A$^+$ Tconvs are overlaid onto plots of T-bet and RORγT expression, the IFNγ$^+$ cells are clearly focused over T-bet$^+$ cells and the IL-17A$^+$ cells are centred over the RORγT$^+$ cells (Fig 4.6B). Finally, donut charts are shown that represent the proportional expression of IFNγ, IL-17a or IFNγ by T-bet$^+$, RORγT$^+$, or T-bet$^+$RORγT$^+$ Tconvs (Fig 4.6C). These charts demonstrate that >90% of T-bet$^+$ Tconvs expressing cytokines in the colon and MLN are IFNγ$^+$, as would be expected for Th1 cells. Cytokine producing RORγT$^+$ Tconvs in the colon and MLN are >85% IL-17A$^+$, consistent with a Th17 phenotype. Cytokine production by T-bet$^+$RORγT$^+$ Tconvs are heterogenous and include IFNγ$^+$, IL-17A$^+$ and IFN$^+$IL-17A$^+$ cells. These T-bet$^+$RORγT$^+$ Tconvs likely include a combination of Th1, Th17 cells and IFNγ$^+$IL-17A$^+$ Tconvs. Based on these analyses, T-bet$^+$ Tconvs are validated as bona fide Th1 cells and RORγT$^+$ Tconvs can be be considered Th17 cells.

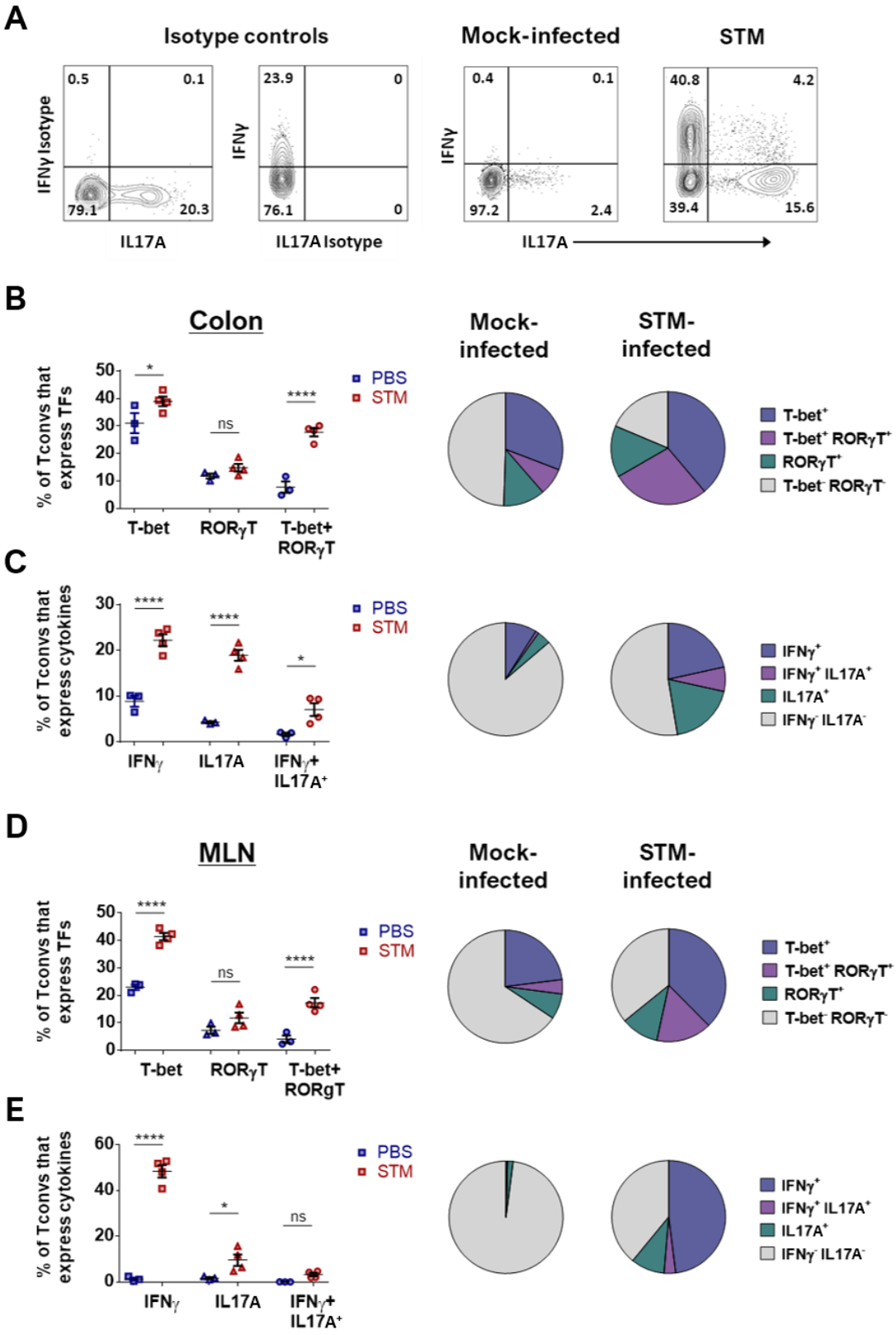

Figure 4.5 Transcription factor and cytokine expression by Tconvs.

(A) Isotype controls and representative plots of IFNγ and IL-17A expression in mock (PBS)- or STM-infected MLN Tconvs are shown at 11 days p.i. **(B)** T-bet and RORγT expression by mock- or STM-infected colonic Tconvs 30 days p.i. are graphed (left) and shown as pie charts (right). **(C)** IFNy and IL-17A expression by colonic Tconvs are graphed (left) or shown as pie charts (right). MLN Tconv TF **(D)** and cytokine expression **(E)** are also depicted. Means ± SEM are plotted. Data points represent individual animals (n=4) from a representative example of two independent experiments. Statistical significance calculated by one-way ANOVA with Holm-Šídák test. ns, not significant; *p<.05; **p<.01; ***p<.001; ****p<.0001.

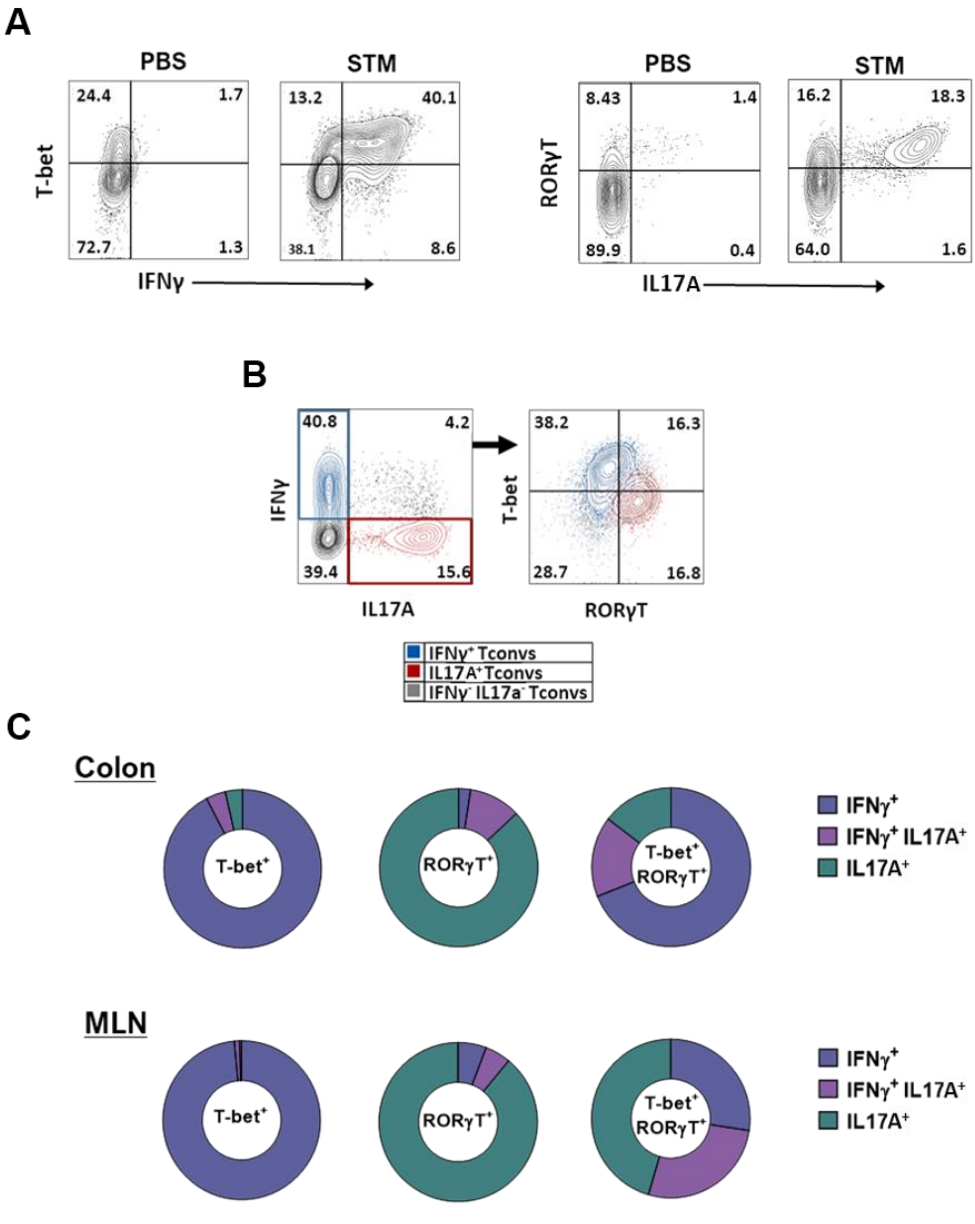

Figure 4.6 Cytokine expression by Tconvs expressing T-bet or RORγT.

(A) IFNγ expression is plotted against T-bet expression and IL-17A expression is plotted against RORγT expression by MLN Tconvs from mock (PBS)- infected or STM-infected mice 11 days p.i. **(B)** IFNγ$^+$ Tconvs (blue) and IL-17A$^+$ Tconvs (red) are overlaid onto a FACS plot of total Tconvs showing T-bet and RORγT expression. **(C)** Expression of IFNγ and/or IL-17A by Tconvs that are T-bet$^+$, RORγT$^+$ or T-bet$^+$RORγT$^+$ are depicted in donut charts.

4.3.2 Cytokine expression by 2W1S-specific T cells

After characterising TF and cytokine expression in the heterogenous CD4 T cell pool, we sought to confirm if 2W1S-specific cells, shown to be consistently T-bet$^+$, are also IFNγ$^+$ as expected of Th1 cells (Fig 4.7). Representative plots of IFNγ and IL-17A expression by 2W1S-specific T cells 11 days p.i. indicates that in both tissues, most of these cells are IFNγ$^+$IL-17A$^-$. The proportion and number of colonic tetramer$^+$ cells that express T-bet and/or RORγT and IFNγ and/or IL-17A are graphed (Fig 4.7B). The proportion of 2W1S-

specific cells that express TFs and cytokines are also represented in pie charts (4.7C). As previously shown, most 2W1S-specific cells are T-bet$^+$ in both the colon and MLN (Fig 4.7B). Approximately 55% of colonic tetramer$^+$ T cells express cytokines, and >90% of these are IFNγ$^+$ (Fig 4.7C, right). In the MLN, 2W1S-specific T cells are also mostly T-bet$^+$ and are >85% IFNγ$^+$ (Fig 4.7E, right). As such, 2W1S-specific CD4 T cells in both the colon and MLN have a Th1 phenotype, like the other T-bet$^+$ Tconvs analysed.

4.3.3 Cytokine expression by FoxP3$^+$ Tregs

The last group of T cells analysed for cytokine expression were FoxP3$^+$ Tregs. Having previously shown that increased numbers and proportions of Tregs express 'master' Th TFs following infection, we aimed to determine whether Tregs expressed the same cytokines as their Th counterparts. Treg expression of T-bet, RORγT, IFNγ and IL-17A was analysed (Fig 4.8). The proportion and number of colonic Tregs expressing TFs and cytokines were graphed (Fig 4.8A) and the proportions of Tregs expressing TFs and cytokines were represented in pie charts (Fig 4.8B). Following infection an increased proportion of Tregs in both tissues were IFNγ$^+$ and an increased proportion of MLN Tregs were IL-17A$^+$, but the proportion of Tregs expressing these cytokines in either tissue remained small. Although the proportion of colonic Tregs expressing T-bet and/or RORγT 11 days p.i. was almost 50%, the proportion of Tregs expressing IFNγ and/or IL-17A remained <5%. In the MLN, the proportion of Tregs expressing T-bet and/or RORγT at 11 days p.i. was >30% but the proportion expressing IFNγ or IL-17A was <9% (Fig 4.8C,D).

In summary, analysis of IFNγ and IL-17A expression reveals that STM infection induces a large increase in the number and proportion of Tconvs expressing cytokines in both the colon and MLN. In both tissues, IFNγ expression was predominantly by T-bet$^+$ Th1 cells and IL-17A expression was by RORγT$^+$ Th17 cells. This was the case for all Tconvs and for 2W1S-specific cells, which were mostly T-bet$^+$IFNγ$^+$ Th1 cells. On the other hand, only a small number of Tregs expressed IFNγ or IL-17A, despite increased expression of T-bet or RORγT following infection. As such, T-bet, RORγT and FoxP3 are validated as markers of functional Th1, Th17 and Treg cells.

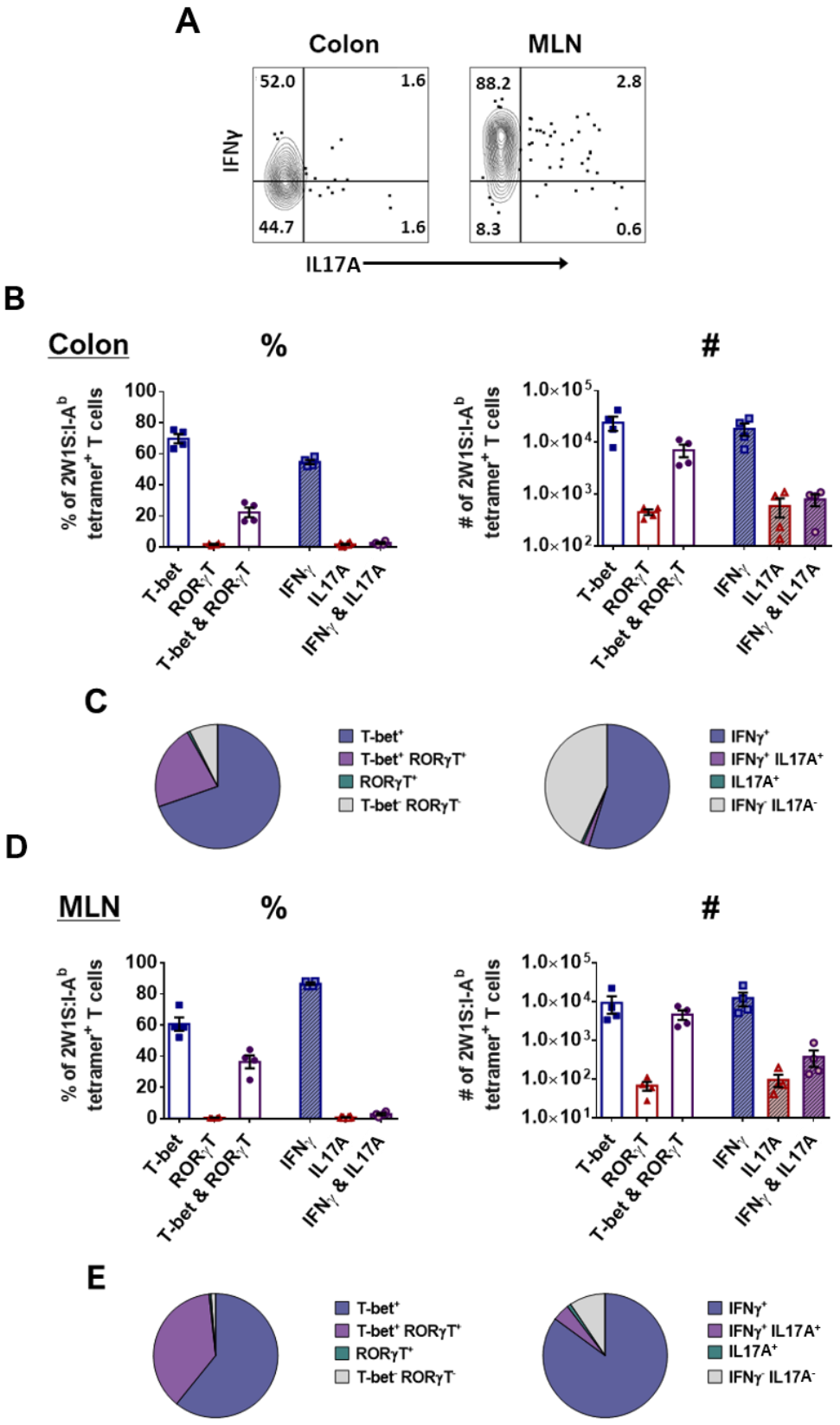

Figure 4.7 Transcription factor and cytokine expression by 2W1S:I-A^b tetramer+ CD4 T cells.

(A) Representative plots of IFNγ and IL-17a expression by 2W1S-specific CD4 T cells from the MLNs and colon at 11 days p.i. **(B)** The proportion (left) and absolute number (right) of colonic tetramer$^+$ CD4 T cells expressing TFs and cytokines are graphed. **(C)** The proportion of tetramer$^+$ CD4 T cells expressing TFs and cytokines is depicted in pie charts. TF and cytokine profiles in the MLN are also shown in graphs **(D)** and pie charts **(E)**. Means ± SEM are plotted.

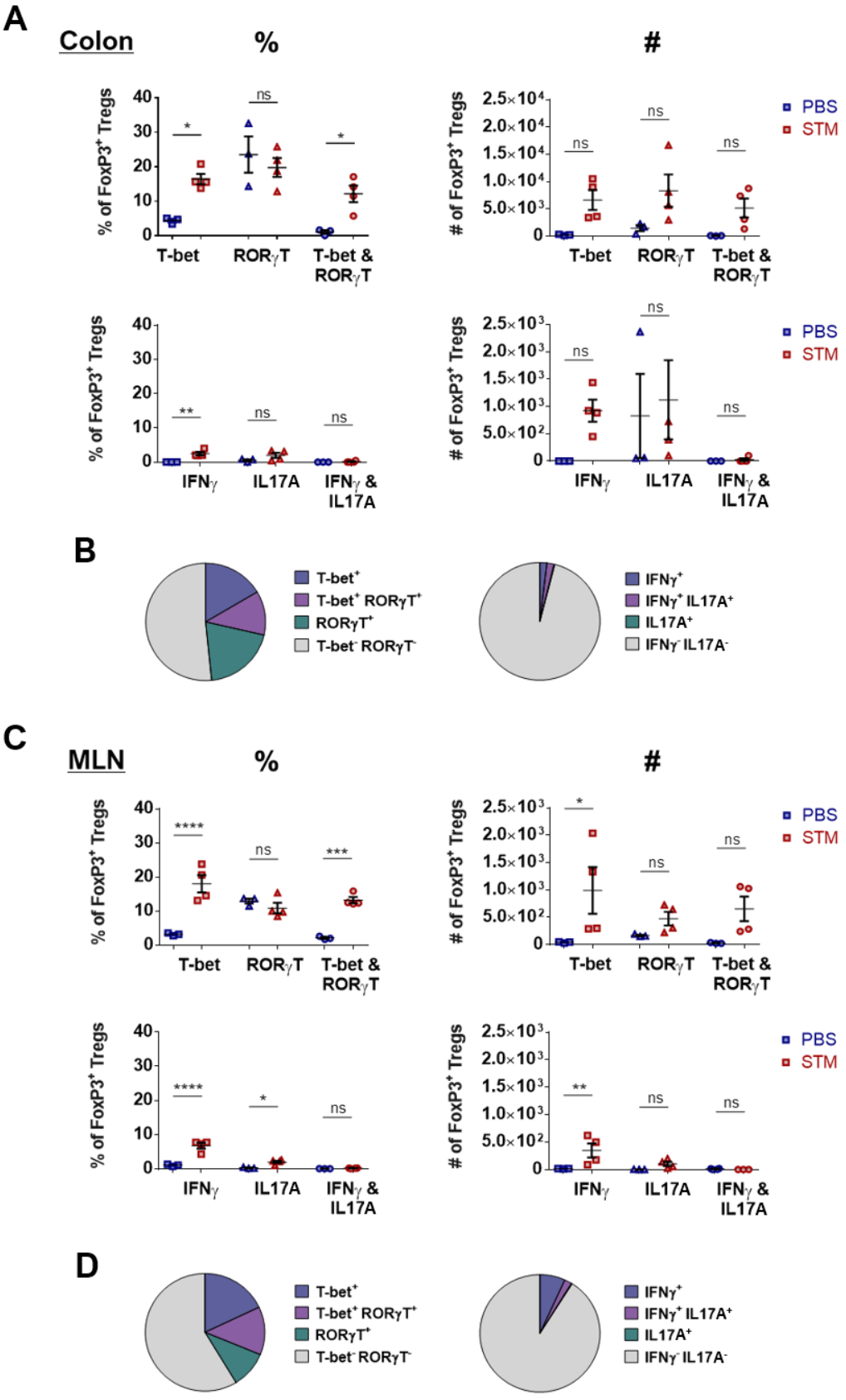

Figure 4.8 Transcription factor and cytokine expression by FoxP3⁺ Tregs.

(A) The proportion and absolute number of colonic FoxP3⁺ Tregs expressing TFs (top) and cytokines are shown from mock (PBS)- and STM–infected mice 11 days p.i. **(B)** The proportion of colon Tregs expressing TFs or cytokines 11 days p.i. is depicted in pie charts. **(C)** TF (top) and cytokine (bottom) expression by Tregs is also shown in the MLN and represented in pie charts **(D)**. Data points represent individual animals (n=4) from a representative example of two independent experiments. Means ± SEM are plotted. Statistical significance for each cytokine or TF calculated by a one-way ANOVA with Holm-Šídák test. ns, not significant; *p<.05; **p<.01; ***p<.001; ****p<.0001.

4.4 Expression of chemokine receptors by CD4 T cells

In addition to TFs and cytokines, expression of chemokine receptors can be used to characterise CD4 T cells and provide information about their potential migration and localisation (Kim et al., 2001; Lim et al., 2008; O'Garra et al., 1998). Chemokine receptors CXCR3 and CCR6, often used as surrogate markers for Th1 and Th17 cells, were examined on Tconvs and Tregs following STM infection to achieve three objectives: First, to validate whether these receptors identify Th or Treg subsets during STM infection; second, to identify changes in the proportion of Tconvs or Tregs expressing them; and third, to determine if changes in their expression might elucidate the potential for co-localisation of Tconvs by Tregs expressing the same receptors.

Representative plots of CXCR3 and CCR6 expression from mock- and STM-infected MLNs 11 days p.i. show $CXCR3^+$ cells can be identified in Tconvs and Tregs, but CCR6 staining has weaker separation (Fig 4.9A). Representative plots of CXCR3 and T-bet expression shows most $CXCR3^+$ Tconvs from STM-infected mice are T-bet^+, but this is not the case with Tregs or Tconvs from mock-infected mice (Fig 4.9B). The proportion of Tconvs or Tregs expressing CXCR3 or CCR6 are graphed in bar charts (Fig 4.9C) and the proportion of Tconvs and Tregs expressing each receptor is overlaid in line graphs (Fig 4.9D). At 6 days p.i., there is a decreased proportion of Tconvs that are $CXCR3^+$ in the colon, a trend that is also seen in $CXCR3^+$ Tregs and both Tconvs and Tregs expressing CCR6. Expression of either receptor by colonic Tconvs are <5%, a small proportion of the colon Tconvs that are T-bet^+ following STM infection (Fig 4.4B).

In the MLN, a higher proportion of Tconvs and Tregs express CXCR3 than in the colon, but <3% of either group are $CCR6^+$ (Fig 4.9E, F). Following infection, an increased proportion of MLN Tconvs and Tregs express CXCR3, and this increase occurs at different timepoints. At 6 days p.i., the proportion of Tregs that are $CXCR3^+$ increases >100% but the proportion of Tconvs that are $CXCR3^+$ remains stable until 8 days p.i. (Fig 4.9 E). Despite low expression levels in the MLN, the proportion of $CCR6^+$ Tregs

decreases following infection and remains suppressed until 14 days p.i. This same trend is also seen in MLN Tconvs, although the changes are not significant (Fig 4.9E, F).

In summary, few $CXCR3^+$ or $CCR6^+$ Tconvs are detected in the colon. In the MLN there is an increased proportion of Tregs that are $CXCR3^+$ 6 days p.i., and this increase is followed by Tconvs 8 days p.i. The early decrease in the proportion of colonic Tconvs and Tregs expressing CXCR3 or CCR6 does not fit with the proportional changes of Th1 and Th17 cells. Low expression levels of colonic Tconvs and poor separation in CCR6 staining make these chemokine receptor data inadequate for identification of Th subsets. While changes in receptor expression following infection can be detected, their interpretation is difficult.

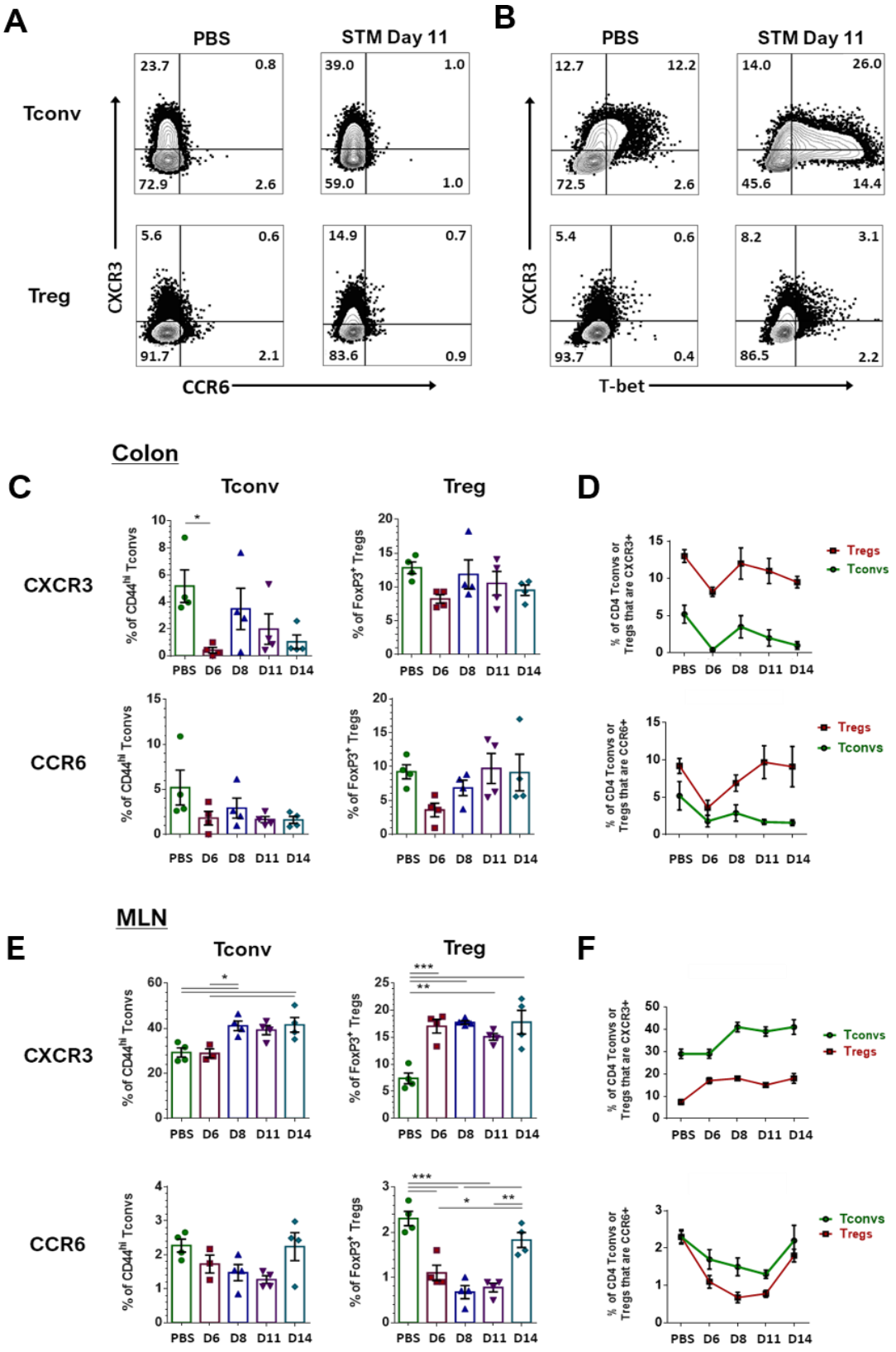

Figure 4.9 CXCR3 and CCR6 expression by Tconvs and FoxP3⁺ Tregs.

(A) Representative plots of CXCR3 and CCR6 expression by Tconvs (top) and Tregs (bottom) from mock (PBS)- and STM-infected MLNs, 11 days p.i. **(B)** CXCR3 expression from the same samples are plotted against T-bet. **(C)** The proportion of colon Tconvs and Tregs expressing CXCR3 and CCR6 are graphed following infection and **(D)** overlaid as line charts. The same charts for MLN Tregs are shown in **(E)** and **(F)** respectively. Data points represent individual animals (n=4) from two experiments. Means ± SEM are plotted. Statistical significance calculated by a one-way ANOVA with Tukey's test. ns, not significant; *p<.05; **p<.01; ***p<.001.

4.5 Characterisation of Tregs by Helios

The observation of reciprocal dynamics between Tregs and Tconvs that express T-bet or RORγT raises questions both about the function and ontogeny of these Treg sub-populations. To address questions about the origins of T-bet$^+$ or RORgT$^+$ Tregs, we assessed their expression of Helios, a Treg-specific TF which has been used both as a marker of thymic ontogeny and Treg activation and stability (Akimova et al., 2011; Elkord et al., 2015; Sebastian et al., 2016).

Tregs from mock- and STM-infected mice were stained for Helios and RORγT (Fig 4.10), molecules proposed as markers for tTregs and pTregs respectively, although this is controversial (Akimova et al., 2011; Elkord et al., 2015; Szurek et al., 2015; Thornton et al., 2019). The proportion of Tregs from mock-infected or STM-infected mice that are Helios$^-$ or Helios$^+$ are graphed in Fig 4.10B. In both the colon and MLN, infection induces an increased proportion of Helios$^+$ Tregs and a decrease in the proportion of Helios$^-$ Tregs at day 6 p.i. These changes are sustained at day 11 p.i. Next, Helios$^-$ and Helios$^+$ populations were segregated by RORγT expression, distinguishing four populations including a Helios$^+$RORγT$^+$ population (Fig 4.10C). This characterisation demonstrates that in both tissues, the decreased proportion of Helios$^-$ Tregs is confined to Helios$^-$ RORγT$^+$ cells. On the other hand, the increased proportion of Helios$^+$ Tregs in the colon 6 days p.i. is confined to the Helios$^+$RORγT$^-$ population. The apparent stability in the proportion of Helios$^+$ Tregs from day 6 to day 11 p.i. conceals a significant decrease in the proportion of Helios$^+$RORγT$^+$ Tregs and a trend towards increased proportions of Helios$^+$RORγT$^-$ Tregs (Fig 4.10C). The changes in these four populations following STM infection are represented in pie charts (Fig 4.10D).

The changes in the proportion of Tregs expressing Helios and/or RORγT, including the increase in Helios$^+$ Tregs following infection highlights unanswered questions about whether Helios is a reliable marker of ontogeny, activation or both.

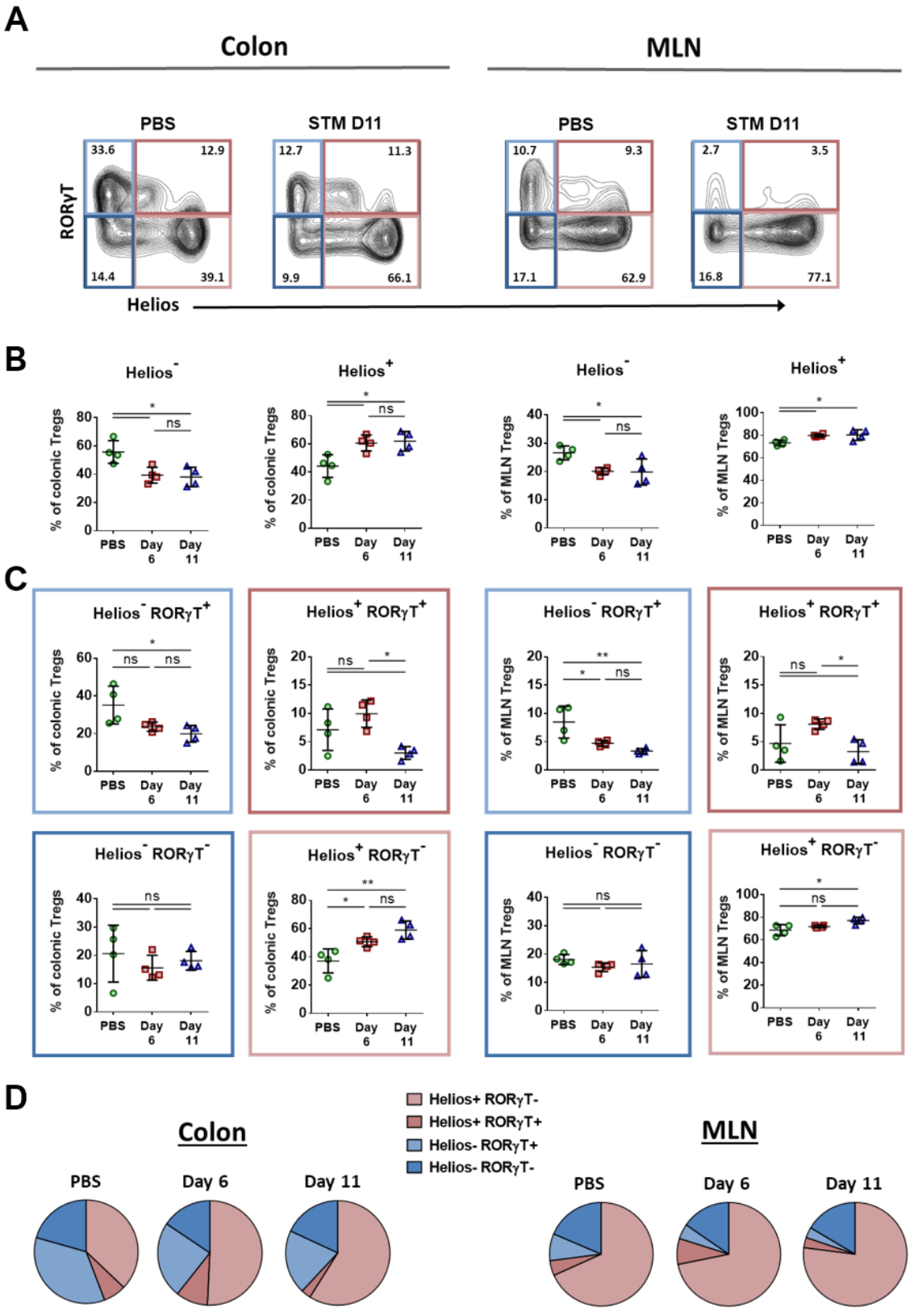

Figure 4.10 Characterisation of FoxP3⁺ Tregs by expression of Helios and RORγT.

(A) Representative plots of Helios and RORγT expression in colon and MLN Tregs from mock- and STM-infected mice 11 days p.i. Quadrants separate populations that are Helios⁺RORγT⁻ (light red), Helios⁺RORγT⁺ (dark red), Helios⁻RORγT⁺ (dark blue) and Helios⁻RORγT⁻ (light blue) **(B)** The proportion of colonic and MLN Tregs that are Helios⁻ or Helios⁺ are plotted from mock- or STM-infected samples **(C)** Helios⁻ and Helios⁺ Tregs are further divided by RORγT expression and **D)** the means of these proportions are represented in pie charts. Data points represent individual animals (n=4) from a representative example from two independent experiments.. Means ± SEM are plotted. Statistical significance calculated by a one-way ANOVA with Tukey's test. ns, not significant; *p<.05; **p<.01; ***p<.001.

To assess the co-expression of Helios and other markers by Tregs, t-SNE (t-Distributed Stochastic Neighbour Embedding) plots were generated (Fig 4.11). Parameters used to generate these plots include CD44, FoxP3, T-bet, RORγT, GATA3, Helios, CXCR3 and CCR6. Selected gates from representative plots are colour-coded and labelled (Fig 4.11A) to allow interpretation in t-SNE plots from mock-infected (4.11B) and STM-infected colons (Fig 4.11C). In the left column, $CD44^{hi}FoxP3^{-}$ Tconvs (blue), $CD44^{lo}FoxP3^{-}$ naïve CD4 T cells (green) and $FoxP3^{+}$ Tregs (red) are plotted. These populations form distinct clusters, with a reduced naïve CD4 T cell population apparent in infected samples. In the centre column, Tregs are gated as $Helios^{hi}$ (dark purple), $Helios^{int}$ (pink) and $Helios^{lo}$ (lilac) populations. Tregs are split across two clusters, with $Helios^{+}$ Tregs forming one lobe and $Helios^{int}$ and $Helios^{lo}$ Tregs forming another. In the right column, CD4 T cells are identified as $T\text{-}bet^{+}$ (light blue), $ROR\gamma T^{+}$ (raspberry), $T\text{-}bet^{+}ROR\gamma T^{+}$ (dark blue) or $GATA3^{+}$ (orange). Cells expressing these TFs overlay t-SNE clusters occupied by Tconvs and Tregs, but not naïve CD4 T cells. In the mock-infected Tconv cluster (Fig 4.11B, right) there are populations of $T\text{-}bet^{+}$, $ROR\gamma T^{+}$ and a smaller population of $GATA3^{+}$ cells, identifying Th1, Th17 and Th2 cells respectively. In the STM-infected Tconv cluster (Fig 4.11C, right), the Th1 and $T\text{-}bet^{+}ROR\gamma T^{+}$ population is larger and the Th2 population is almost absent. In the uninfected Treg cluster (Fig 4.11B, right), there is a large $ROR\gamma T^{+}$ Treg population overlaying the $Helios^{lo/int}$ cluster, $GATA3^{+}$ Tregs overlay the $Helios^{hi}$ cluster and the few $T\text{-}bet^{+}$ cells are present in both Treg clusters. In the STM-infected Treg cluster, $T\text{-}bet^{+}$ Tregs are increased in size and overlay the $Helios^{hi}$ cluster and the $Helios^{int/lo}$ cluster. As with the mock-infected sample, $GATA3^{+}$ Tregs mostly overlay the $Helios^{+}$ cluster.

These t-SNE plots, while limited in terms of inputs, supports the idea that $Helios^{hi}$ Tregs comprise a distinct population from $Helios^{lo/int}$ Tregs. While $T\text{-}bet^{+}$ Tregs overlay both $Helios^{hi}$ and $Helios^{int/lo}$ Treg clusters, $ROR\gamma T^{+}$ Tregs primarily overlay $Helios^{lo/int}$ Tregs and $GATA3^{+}$ Tregs primarily overlay $Helios^{hi}$ Tregs. This adds to the characterisation of the Treg populations by T-bet and RORγT (Fig 4.3) and by Helios (Fig 4.10). However, unanswered questions remain about the role that these populations and their role in regulating the T cell response to STM.

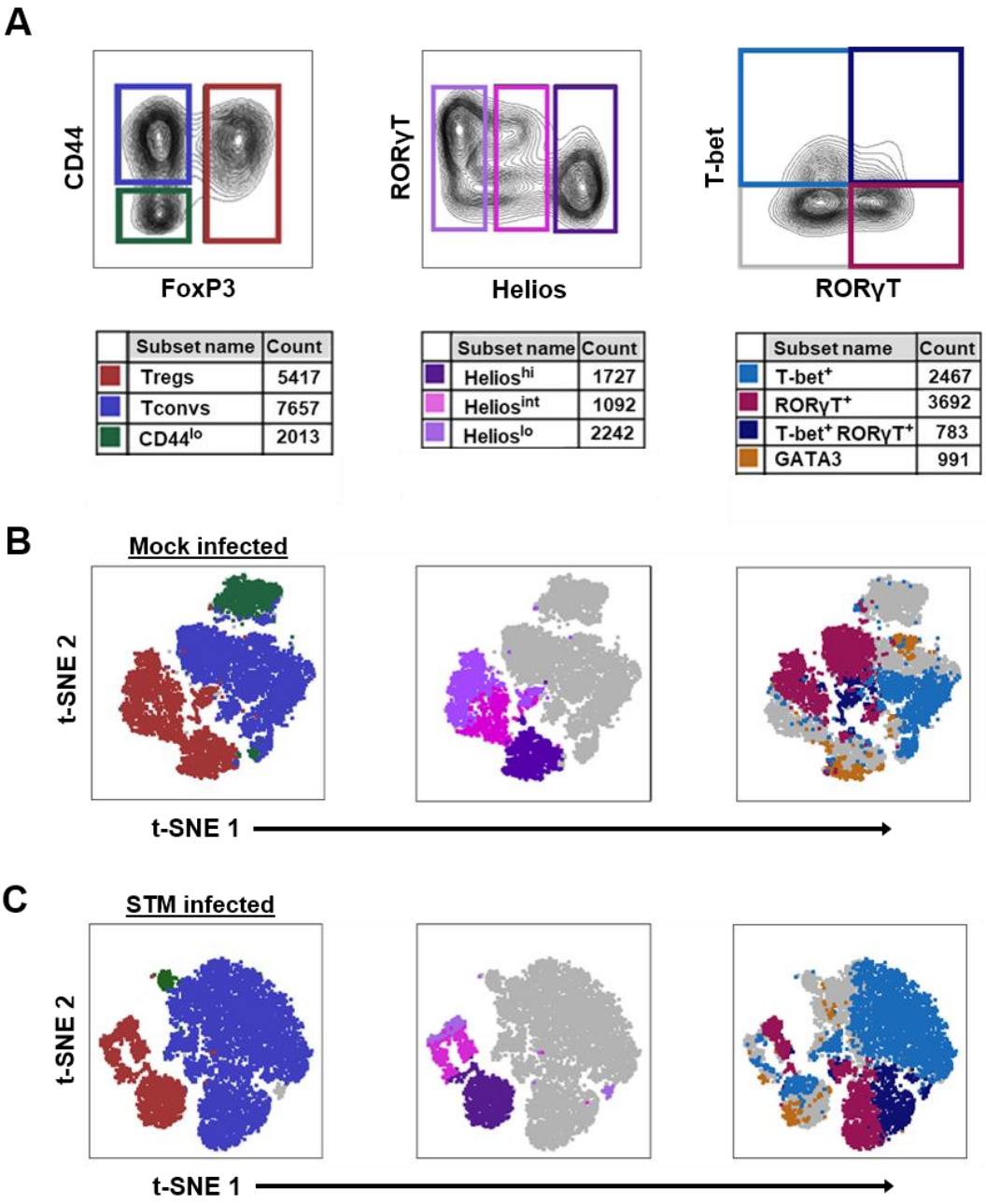

Figure 4.11 t-SNE plots of colonic CD4 T cells from STM- and mock-infected mice.

(A) Representative plots of CD4 T cells from STM-infected colons 11 days p.i. show gating and colour labelling of: $CD44^{hi}$ $FoxP3^{-}$ Tconvs, $FoxP3^{+}$ Tregs and $CD44^{lo}$ $FoxP3^{-}$ CD4 T cells (left); $Helios^{hi}$, $Helios^{int}$ and $Helios^{lo}$ Tregs (centre); and T-bet^{+}, RORγT^{+} and T-bet^{+}RORγT^{+} CD4 T cells (right). **(B)** These populations (with $GATA3^{+}$ cells in orange, right) are overlaid onto t-SNE plots of mock (PBS)-infected colons, generated using parameters of CD45, CD3, CD4, CD44, FoxP3, T-bet, RORγT,Helios, GATA3, CCR6 and CXCR3 expression. Grey areas are negative for all markers represented in plots above. **(C)** Populations of CD4 T cells are overlaid onto t-SNE plots of STM-infected colons at day 11 p.i., as described above.

4.6 Transcription factor expression by Tconvs and Tregs in ulcerative colitis

We have identified a reciprocal dynamic between Tconvs and Tregs that may play a role in shaping the CD4 T cell response in STM-induced colitis in mice. To understand whether

this dynamic might also be observed in humans, we sought to determine whether a similar dynamic could also be observed during inflammation in ulcerative colitis (UC). Colonic biopsies were acquired from UC patients with active disease or in remission. The gating strategy for analysing human colonic CD4 T cells identified live $CD45^+$ $CD3^+$ $CD4^+$ single cells that are $FoxP3^+CD127^{lo}$ Tregs or $FoxP3^-$ Tconvs (Fig 4.12A). Tconvs and Tregs were then analysed for expression of T-bet and RORγT (Fig 4.12B).

The proportion of Tconvs (Fig 4.12C) and Tregs (Fig 4.12C) that are $T\text{-bet}^+$, $ROR\gamma T^+$ or $T\text{-bet}^+ROR\gamma T^+$ were compared between samples from active and remission UC biopsies. Surprisingly, a lower proportion of Tconvs from patients with active UC are $T\text{-bet}^+$ or $T\text{-bet}^+ROR\gamma T^+$ compared to patients in remission, and there was no significant difference in the proportion $ROR\gamma T^+$ Tconvs. A lower proportion of Tregs from patients with active UC are $ROR\gamma T^+$ compared to those in remission. While not significant, there is a trend towards an increased proportion of Tregs that are $T\text{-bet}^+$. Therefore, active UC is associated with a decreased proportion of $T\text{-bet}^+$ Tconvs, decreased proportion of $ROR\gamma T^+$ Tregs and a trend towards an increased proportion of $T\text{-bet}^+$ Tregs. These data show that changes in T-bet expression almost fit a model of reciprocity between Tconvs and Tregs, but the same reciprocity does not apply to RORγT expression.

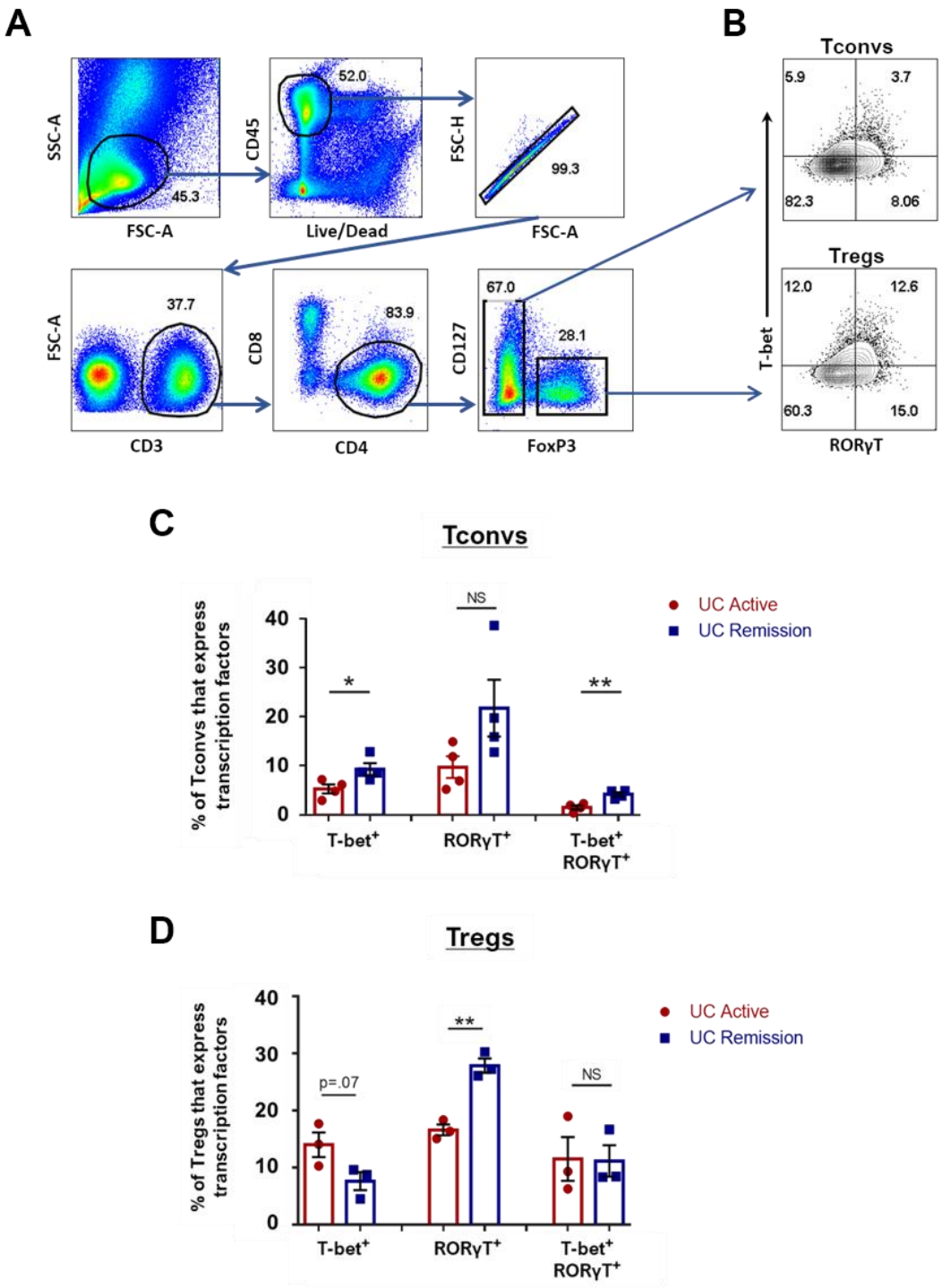

Figure 4.12 T-bet and RORγT expression by Tconvs and Tregs in active or remitted UC.

(A) Gating strategy used to identify Tconvs (live, single CD45$^+$ CD3$^+$ CD4$^+$ FoxP3$^-$) cells and Tregs (live, single CD45$^+$ CD3$^+$ CD4$^+$ CD127^{lo} FoxP3$^+$) cells. **(B)** Representative plots of T-bet and RORγT expression by colonic Tconvs (top) and Tregs (bottom). **(C)** The proportion of Tconvs expressing T-bet and/or RORγT in active UC (red) and remitted UC biopsies (blue) are shown, as well as **(D)** the proportion of Tregs expressing these transcription figures from the same samples. Data points represent individual samples (n=3-4) from 6 independent experiments. Means ± SEM are plotted. Statistical significance between active and remitted samples calculated by a one-way ANOVA with Holm-Šídák test. ns, not significant; *p<.05; **p<.01.

4.7 Summary of results

In this chapter, the CD4 T cell response to STM infection was characterised by populations of Th cells and Tregs expressing 'master' TFs that control gene expression programmes of Th subsets. These sub-populations were further characterised by cytokine, chemokine receptor and Helios expression. We identified a transient colonic Th17 response early after infection, which is followed by sustained Th1 response in both the colon and MLN. In the colon, the shift from an increased Th17 response to Th1 bias is concurrent with a shift from an increased T-bet$^+$ Treg response to an increased RORγT$^+$ Treg bias. This reciprocal dynamic is consistent with a targeted or selective suppression of Th subsets by Tregs expressing the same TFs. Following infection, there is an increased proportion of Helios$^+$RORγT$^-$ Tregs, and T-bet$^+$ is co-expressed by both Helios$^+$ and Helios$^-$ Tregs. Finally, Tconvs and Tregs were characterised in active and remitted UC biopsies and a reciprocal dynamic was observed between cells expressing T-bet but not RORγT. Together, these results highlight the heterogeneity of Tconvs and Tregs, including tissue-specific features and the complex dynamics between inflammatory and regulatory cells underlying the response to infection.

4.8 Discussion

4.8.1 Characterising the Tconv response to *Salmonella*

In the previous chapter, 2W1S-specific T cells were tracked following infection and we initially sought to characterise this population. 2W1S-specific cells that consistently exhibit a T-bet$^+$IFNγ$^+$ Th1 phenotype, independent of tissue or time after infection (Fig 4.1). Conversely, the bulk CD4 T cell pool is phenotypically heterogenous and dynamic following STM infection. 2W1S:1A^b tetramer$^-$ Tconvs likely contain both STM-specific and non-specific cells, and changes in these mixed populations have the potential to reveal important dynamics that shape the T cell response to STM.

Characterisation by TF and cytokine expression shows that underlying an increase in all Th subsets, there is a short-lived proportional shift towards a Th17 bias in the colon after

STM infection (Fig 4.2B). This comprises an increased proportion of Th17 cells and T-bet$^+$RORγT$^+$ cells and decreased proportions of Th1 and Th2 cells compared to uninfected animals. While the proportion of Th2 cells remains suppressed for >90 days p.i., a Th1 bias is established by day 11 p.i. when the number of colonic Th17 cells returns to baseline levels. This Th1 bias is sustained for >90 days p.i. in the colon but in the MLN, the number and proportion of each Th subset return to baseline levels by 60 days p.i. (fig 4.2D).

The T-bet$^+$RORγT$^+$ cells that expand following infection include cells that are IFNγ$^+$, IL-17A$^+$ or IFNγ$^+$IL-17A$^+$ (Fig 4.6D). As such, this is a heterogenous population containing Th1- and Th17-like cells, in addition to IFNγ-IL-17A double-producers, sometimes referred to as Th17.1 cells. The heterogeneity of T-bet$^+$RORγT$^+$ cells may be a technical artefact of gating populations with reduced separation following PMA ionomycin stimulation (Fig 4.6B). On the other hand, this heterogeneity could result from gating cells transdifferentiating from Th17 to Th1-like cells with intermediate stages included. Bona fide IFNγ$^+$IL-17A$^+$ Th17.1 cells have been reported as highly inflammatory, driving pathology in several mouse models including experimental autoimmune encephalomyelitis (EAE), transfer colitis and ocular surface autoimmunity (Chen et al., 2017; Duhen et al., 2013; Harbour et al., 2015). There is evidence that these Th17.1 cells differentiate from Th17 cells that upregulate T-bet in the presence of IFNγ (Wang et al., 2014; Zielinski et al., 2012). This may be an important pathway in the differentiation of Th17.1 cells in response to STM infection, but delineating the differentiation and function of the small population of Th17.1 cells out of the total T-bet$^+$RORγT$^+$ cells would require further experiments, potentially using lineage tracking techniques.

The Th1 response to STM infection has been well documented and both bacterial clearance and protection from re-infection are dependent on an IFNγ-Th1 response (Hess et al., 1996; Kupz et al., 2012; Pie et al., 1997; Ravindran and McSorley, 2005). An early Th17 response to *Salmonella* in the intestinal mucosa has also been reported, and disruption of Th17 cells by genetic mutation, HIV infection, or genetic targeting of IL-17A

signalling have all been shown to increase epithelial damage or risk of systemic infection (Godinez et al., 2011; Lee et al., 2012b; Mayuzumi et al., 2010; Raffatellu et al., 2008). Th17 cells are not the only intestinal cells producing IL-17A following infection however, and innate cells including γδ T cells and ILCs produce IL-17A during infection in the intestinal mucosa (Keestra et al., 2011; Schulz et al., 2008; Xu et al., 2012). As such, an effective immune response to STM in the intestines incorporates a dynamic Tconv response with both an early Th17/IL-17A response and a sustained Th1/IFNγ response.

The factors that drive the early Th17 and later Th1 response are a fundamental aspect of how the CD4 T cell response to STM is controlled. Factors shown to influence Th differentiation and include the route and site of infection, the antigen and antigenic dose, and the cytokine milieu (Constant, 1995; Lee et al., 2012b; Pepper et al., 2010). Using a Listeria-2W1S model, Pepper et al. (2010) demonstrated that intranasal infection induced a short lived mucosal Th17 response, while i.v. infection induced a long-lasting Th1 response. The cognate antigen that T cells respond to has also been reported to influence Th differentiation. STM flagellin has been shown to drive a mixed Th17 and Th1 response in the intestinal mucosa while T3SS-specific CD4 T cells are primarily Th1 cells. T3SS-specific cells are detected at later stages of infection and are more prevalent in systemic tissue (Lee et al., 2012b). These findings raise the possibility that the dynamic Th response to STM may be an adaptation to target different stages of the *Salmonella* infectious cycle- from extracellular targets in the intestinal lumen to antigen upregulated as an intracellular pathogen. It has been reported that Th17 cells respond to extracellular bacteria and Th1 cells respond to intracellular pathogens (Harrington et al., 2006; Weaver et al., 2006), but it is unlikely that antigen alone is capable of driving divergent differentiation pathways between these Th subsets; other context-dependent cues are likely to be required.

Tregs are another regulator of the Tconv response and have been shown to play a crucial role in controlling the CD4 T cell response to infection (Belkaid, 2007; Boer et al., 2015; Maizels and Smith, 2011). To analyse the role of Tregs in controlling the Tconv response

to STM, our first objective was to characterise the development of the Treg response following infection.

4.8.2 Reciprocal dynamics between Tregs and Tconvs

The regulation and control of T cells by Tregs has been widely reported in the contexts of homeostasis, infection, inflammatory diseases and cancer (Baecher-Allan and Hafler, 2004; Belkaid et al., 2002; Mougiakakos et al., 2010; Sakaguchi, 2004). More recently, Tregs co-expressing conventional Th 'master TFs' have been identified in both humans and mice, in multiple tissues and in contexts of inflammation and homeostasis (Duhen et al., 2012; Halim et al., 2017; Levine et al., 2017; Sefik et al., 2015; Wing and Sakaguchi, 2012). There is evidence that these Treg populations differentiate in response to similar environmental cues as Th subsets and have been described as 'effector' Tregs or 'Thx' Tregs (Chaudhry et al., 2009; Wing and Sakaguchi, 2012). Questions remain about the ontogeny and function of these populations, and their role in immune regulation is unclear. Characterising changes in these Treg populations following STM infection has potential to address these questions in the context of a T cell response incorporating Th17 and Th1 biased phases. Our description of a reciprocal dynamic between colonic Tconvs and Tregs is intriguing but is only correlative. This dynamic may be explained by multiple hypotheses, including plasticity between inflammatory Th cells and Th-like Tregs, or selective suppression of Th subsets by Tregs expressing the same TF.

Plasticity between regulatory and conventional CD4 T cells has been demonstrated in several reports. RORγT^{+} Tregs have been shown to downregulate FoxP3 in the absence of IL15 and become 'ex-Tregs' that drive TH17 mediated colitis (Tosiek et al., 2016). It has also been shown that Th1 cells have the potential to upregulate FoxP3 to become T-bet^{+} Tregs (Amarnath et al., 2011; Stathopoulou et al., 2018). On the other hand, evidence from lineage tracking models, transfers and *in vitro* experiments suggest that T-bet^{+} Tregs are highly stable and retain FoxP3^{+} expression independent of environmental conditions (Daniel et al., 2015; Levine et al., 2017).

Using this concept of plasticity to explain the reciprocal dynamics described here (Fig 4.4), it could be argued that the initial decrease in the proportion of Th1 cells and increased proportion of T-bet$^+$ Tregs could be the result of Th1 cells upregulating FoxP3 expression. Furthermore, the early Th17 response and decreased proportion of RORγT$^+$ Tregs could be caused by RORγT$^+$ Tregs downregulating FoxP3. On the other hand, for plasticity to explain these dynamics, the later increase in Th1 cells would result from T-bet$^+$ Tregs losing FoxP3 expression and expressing IFNγ. Because of the demonstrated stability of T-bet$^+$ Tregs, this explanation of reciprocal dynamics is less convincing for the later phases of infection. As such, this appears to be at best a partial explanation.

The concept that Tregs selectively suppress Th subsets expressing the same TFs is consistent with the idea that Th-like Tregs can differentiate in the same setting as Tconvs and therefore respond to context-dependent inflammation in a targeted and fine-tuned manner (Wing and Sakaguchi, 2012). Increasing evidence demonstrates that this targeted suppression occurs *in vivo* with Th1 and Th17 cells. Tregs have been shown to upregulate T-bet in response to type 1 inflammation and T-bet$^+$ Tregs are required to control Th1-mediated inflammation (Koch et al., 2009). In the context of infection, it has been shown that Tregs upregulate T-bet expression during *Listeria* infection, selectively suppress Th1 cells and comprise a stable population that proliferates rapidly during reinfection (Levine et al., 2017). It has been demonstrated that specific intestinal bacteria induce RORγT$^+$ Tregs which limits Th17-mediated colitis and ablation of Treg-specific STAT3 induces Th17 inflammation (Chaudhry et al., 2009; Sefik et al., 2015).

The model of selective suppression does not appear to apply to all Th subsets however, and it has been reported that GATA3$^+$ Tregs do not selectively target Th2 cells (Ohnmacht et al., 2015; Wang et al., 2014). Instead, it has been suggested that GATA3 expression by Tregs plays an important role in maintaining FoxP3 expression and retaining a suppressive phenotype in the context of inflammation (Wang et al., 2011; Wohlfert et al., 2011). Here we have shown that despite an early and sustained suppression of Th2 cells

in the colon, the proportion of colonic GATA3$^+$ Tregs in the colon remains unchanged (Fig 4.2B, 4.3B).

Selective suppression of Th1 cells by T-bet$^+$ Tregs and Th17 cells by RORγT$^+$ Tregs could explain the reciprocal dynamics in the colon following STM infection. If the model of selective suppression were true, the early increased proportion of T-bet$^+$ Tregs selectively targets Th1 cells, while the decreased proportion of RORγT$^+$ Tregs contributes to an increased proportion of Th17 cells. During the later stages of infection, a decreased proportion of T-bet$^+$ Tregs reduces the suppression of Th1 cells, allowing a Th1 expansion; and an increased proportion of RORγT$^+$ Tregs selectively suppresses the Th17 response. While this model of selective suppression is compatible with the reciprocal dynamics we demonstrate, further experiments are required to determine whether subpopulations of Tregs are actively shaping the T cell response to STM.

The selective suppression model raises the question of how targeted suppression of Th subsets is mediated. Each 'effector' Treg subset have been shown to be suppressive in *ex vivo* suppression assays, and express IL10, TGFβ, CTLA4 (Duhen et al., 2012; Levine et al., 2017). However, Tregs expressing T-bet or RORγT have been shown to express CXCR3 and CCR6 respectively, which are signature chemokines for Th1 and Th17 cells. It is well established that Tregs, like Tconvs, are recruited to target tissues via chemokine receptors, and receptor-mediated migration is important for Treg modulation of inflammation (Erhardt et al., 2011; Koch et al., 2009; Lim et al., 2006; Villares et al., 2009; Yamazaki et al., 2008). This suggests that chemokine receptor-mediated colocalization may be an important mechanism that facilitates selective suppression.

In contrast to previous research describing selective suppression (Koch et al., 2009; Levine et al., 2017), chemokine receptor data presented here does not reflect reciprocity between Tconvs and Tregs (Fig 4.9). This could be the result of analysing chemokine receptors at an effector site, where receptors are rapidly internalised following ligand-receptor interactions (Moser et al., 2004; Thelen, 2001). Internalisation of receptors would explain the low levels of CXCR3 and CCR6 by colonic Tconvs (Fig 4.9C). There might

also be technical issues limiting detection of CCR6, which has poor signal separation in FACS plots and low levels of expression in the MLN (Fig 4.9A). Staining of CXCR3 in the MLN is the most convincing receptor data presented, and this shows that the proportion of Tregs expressing CXCR3 increases at least two days before that of Tconvs (Fig 4.9E). While not conclusive, this could be interpreted as suggesting that Tregs, upregulating CXCR3 before Tconvs in the MLN, may be migrating to the inflamed colon before Tconvs and potentially establishing early Th1-targetted suppression. Further work using immunofluorescence imaging of STM-infected colonic tissue would help establish whether co-localisation is occurring and potentially driving a targeted suppression.

In summary, a reciprocal dynamic between Tconvs and Tregs during a multi-phase CD4 T cell response is consistent with the concept that Tregs are selectively suppressing Th subsets and shaping Tconv bias. Such a fine-tuned and dynamic control of T cell responses by Tregs would be intriguing. But this prospect raises questions about potential mechanisms of selective suppression and the ontogeny of these Treg subpopulations.

4.8.3 Characterisation of Tregs by Helios expression

It is well established that FoxP3$^+$ Tregs can differentiate in the thymus or be induced extra-thymically, and I set out to assess whether the populations of Tregs identified following STM infection were tTregs or pTregs. Helios has been proposed as a marker of tTregs and it is expressed by Tregs in the thymus (Thornton et al., 2010). It has also been demonstrated that pTregs can upregulate Helios during activation and in these cells it is a marker of increased suppression and stability (Gottschalk et al., 2012; Kim et al., 2015). Although Helios is an imperfect marker of tTregs, recent research has shown that Helios expression delineates two distinct populations with phenotypic and functional differences, including non-overlapping TCR repertoires (Thornton et al., 2019). Furthermore, Helios$^+$ and Helios$^-$ Tregs have been shown to provide non-redundant immunomodulation, with selective depletion of either subset inducing immunopathology (Akimova et al., 2011; Elkord et al., 2015; Kim et al., 2015; Sebastian et al., 2016). On the other hand, RORγT expression by Tregs has been used as a marker of pTregs, as the differentiation of

RORγT^{+} Tregs is dependent on the presence of microbiota (Ohnmacht et al., 2015; Sefik et al., 2015). While Helios and RORγT are imperfect markers of Treg lineage, they can be used to compliment other techniques to help decipher the ontogeny and function of Treg populations.

Data presented here show that Tregs can be identified as Helios^{+}RORγT^{-}, Helios^{-}RORγT^{+}, Helios^{-}RORγT^{-} or Helios^{+}RORγT^{+} cells (Fig 4.10A). In the colon, the Helios^{+}RORγT^{-} and Helios^{-}RORγT^{+} cells are the largest populations. In the MLN, the majority of Tregs are Helios^{+}RORγT^{-}, followed by Helios^{-}RORγT^{-} cells. Following STM infection, the increased proportion of Helios^{+} Tregs could be interpreted as an increased proportion of tTregs, an increase in Treg activation or of both explanations being correct.

Beyond a binary interpretation of Helios expression, Helios^{int} populations can be detected, and these are gated as separate population in Fig 4.11A. It could be hypothesised that Helios^{int} cells are an activated subpopulation of pTregs that upregulate Helios in response to environmental stimuli, as previously reported (Kim et al., Gottschalk et al., 2015). This population is gated within the Helios^{+}RORγT^{+} population (Fig 4.10A), which trends towards an increased proportion 6 days p.i., before decreased proportions are observed at day 11 p.i (Fig 4.10C). If these are activated Tregs, these data suggest that their increase after infection is transient. Further experiments comparing Tregs with differential Helios expression could help characterise functional differences if combined with analysis of other markers of activation and suppressive potential, like CD25, CTLA4 or PD1. *Ex vivo* assays could also be used to identify differences in suppressive function. Finally. lineage tracking tools could be used to ascertain information about differentiation pathways of these cells. Together, these experiments could help elucidate the role of Helios in Tregs and how its expression contributes to the control of the Tconv response.

To further assess our data shown here, t-SNE plots were generated to identify CD4 T cell populations by multiple parameters and to analyse co-expression of T-bet, RORγT and GATA3 with Helios (Fig 4.11). While t-SNEs of FACS data are limited in scope compared to those generated from data sets with higher dimensionality, these plots give simple

visual representations of multiple overlays. The t-SNE plots demonstrate that in both mock- and STM-infected colons: RORγT^{+} Tregs are mostly Helios$^{lo/int}$ cells, T-bet^{+} Tregs are distributed between Helios$^{lo/int}$ and Helios^{hi} populations, and GATA3 expression is mostly confined to Helios^{hi} Tregs (Fig 4.11B, C). While t-SNEs from STM-infected colons have larger T-bet^{+} Treg and Tconv clusters, the distribution of T-bet^{+} Tregs maintains its distribution pattern between Tregs expressing different levels of Helios expression. These data show that RORγT^{+} Tregs are mostly Helios$^{lo/int}$, while T-bet^{+} Tregs can be Helios$^{lo/int}$ or Helios^{hi}. If Helios^{hi} Tregs are largely tTregs, this analysis suggests that RORγT^{+} Tregs are largely pTregs while T-bet^{+} Tregs appear to include both pTregs and tTregs. This is consistent with previous reports of T-bet expression being expressed in both Helios^{+} and Helios^{-} Tregs in mice and humans (Daniel et al., 2015; Sebastian et al., 2016). This analysis does not provide definitive evidence about Treg lineage but contributes to our characterisation of the diversity and heterogeneity of the Treg compartment in the colon following STM infection.

4.8.4 Reciprocal dynamics between Tconvs and Tregs in UC

After characterising a reciprocal dynamic between Tconvs and Tregs during infection, the next objective was to determine if a similar reciprocity played a role in UC. Oral infection with BRD509-2W1S induces colitis with long-lasting alterations in the Tconvs and Tregs in the colon, with similar pathology as UC, which is thought to be driven by altered populations of Tconvs and Tregs and a dysregulated balance between them. Like mouse Tregs, human Tregs are heterogenous and include effector-like Tregs expressing the same TFs and chemokine receptors as Th subsets (Duhen et al., 2012; Miragaia et al., 2019). Recent research highlighted a connection between mouse models of colitis and human disease, by showing that transfer of microbiota from IBD patients into germ-free mice induces increased colitis compared to mice that received microbiota from healthy donors (Britton et al., 2019). Interestingly, IBD microbiota lead to increased numbers of Th17 cells and reduced numbers of RORγT^{+} Tregs. This is important because it highlights another model with reciprocal dynamics between Tconvs and Tregs expressing the same ‘master’ TF.

In Fig 4.12, we assess the proportion of Tconvs or Tregs expressing T-bet and/or RORγT in colonic biopsies from patients with active UC or UC in remission. We show that in samples from active UC, there is a decrease in the proportion of Tconvs that are T-bet$^+$ (Th1), RORγT$^+$ (Th17) or T-bet$^+$RORγT$^+$ (Fig 4.12C). In active UC biopsies the proportion of Tregs expressing RORγT is decreased but the proportion of T-bet$^+$ Tregs trends towards an increase (Fig 4.13D). These results do not obviously fit with the pattern of reciprocal dynamics shown previously in STM-infected mouse colons. While there may be a trend towards reciprocity between Tconvs and Tregs expressing T-bet, the decrease in Th17 cells is in parallel with the decrease in RORγT$^+$ Tregs.

The decreased proportion of Th1 and Th17 cells is surprising because active UC pathology has been shown to be dependent on CD4 T cells and a commonly held view is that disease is at least partially Th17-mediated. (Caprioli et al., 2008; Kobayashi et al., 2008; Sarra et al., 2010; Zenewicz et al., 2009). The view that Th17 cell drive UC pathology is not universal however, and there is a data demonstrating that there is an increase of Th2 cells or Th2-associated cytokines in the mucosa during active disease (Fuss et al., 1996; Heller et al., 2005; Li et al., 2016; Strober and Fuss, 2011). Indeed, for many years, UC was often considered a Th2-mediated disease while Crohn's disease was considered a Th1-mediated. There are data supporting a role of Th17 cells in UC, but multiple reports of Th17 cells are based on analysis of PBMCs, while many reports of increased Th17-associated cytokines do not identify their cellular sources (Eastaff-Leung et al., 2010; Olsen et al., 2011; Sun et al., 2017). Research focus on PBMCs is understandable in human disease, where biopsies are difficult to obtain. Focus on cytokines instead of T cell phenotype is also understandable since cytokines are tractable therapeutic targets. However, a failure to appreciate tissue-dependent variables and cell-specific dynamics can lead to poor understanding of pathogenesis, which can compromise the development of therapeutic targets.

Our finding that Tconvs in active UC samples have lower proportions of Th1 and Th17 cells might be explained by an increased proportion of Tconvs expressing GATA3, which

we did not assess, or by a decrease in all CD4 Tconvs expressing 'master' TFs. A previous study analysing active UC biopsies reported a reduction in IL-17A, IFNγ and IL4, but an increase in IL-8 (Pearl et al., 2011). Interestingly, the decreased expression of Th1, Th2 and Th17 cytokines was specific to biopsies of active lesions compared to healthy tissue; no change was detected between non-lesioned tissue from active UC patients and healthy controls. This raises questions about which cells are driving pathology within UC lesions, if there are distinct sources of pathology outwith lesions, and if either is directly Th-mediated or driven by other cells, such as neutrophils.

Continued research into the dynamics between colonic Tconvs and Tregs in UC is warranted because it has the potential to elucidate the dysregulation reported in IBD. Future experiments could be expanded to analyse GATA3 expression to evaluate Th2 cells, and intracellular cytokine staining could be incorporated to assess the functional role of Tconv and Treg subsets. Finally, analysis of more biopsies, including lesioned and non-lesioned mucosa from active UC could be compared to biopsies from both UC in remission and healthy controls, to elucidate differences between all four groups. This would provide a more complete picture of the changes in CD4 T cell populations during remission, active disease and in inflamed and uninflamed sites.

4.8.5 Conclusion

In this chapter, we have reported a dynamic and site-specific CD4 T cell response to STM infection, with complex interplay between heterogenous Treg and Tconv populations. We report a reciprocal dynamic between Tconvs and Tregs expressing the same TFs, which raises the possibility that this is driven by selective suppression of Th1 cells by T-bet$^+$ Tregs and Th17 cells by RORγT$^+$ Tregs. Analysis of cytokine, chemokine receptors and Helios added to the characterisation of the Th subsets and Tregs expressing shared TFs. Analysis of active and remitted UC biopsies did not fit the same pattern of reciprocity but highlighted important questions about the CD4 T cells driving pathology, which could inform future work investigating the balance between colonic Tconvs and Tregs during inflammation.

The reciprocal dynamics following STM infection, although only correlative, could be driven by Treg mediated selective suppression. This prospect is intriguing because it highlights the potential for Tregs to not only inhibit Tconvs, but to shape the CD4 T cell response in a fine-tuned way. To investigate whether Tregs are shaping the dynamic Tconv response to STM infection, we designed experiments to manipulate Tregs *in vivo* and assess the impact this has on the overall CD4 T cell response to infection.

Chapter 5 Investigating the Potential for Tregs to Shape Th Bias

5.1 Introduction

The reciprocal dynamics between Tregs and Tconvs during STM infection are consistent with the hypothesis that Tregs expressing 'effector' TFs selectively target Th subsets to skew Th bias. The aim of the following experiments is to determine if manipulating Treg populations affects Th bias following infection. Treg depletion and transfer experiments were carried out to determine whether Tregs are necessary and sufficient to control the dynamic Th bias following STM infection. While Tregs have been shown to selectively target Th subsets (Koch et al., 2009; Levine et al., 2017), the potential for Tregs to shape a multi-stage and dynamic CD4 T cell response has not been reported.

To test the hypothesis that Tregs are necessary for the Th bias following STM infection, we carried out Treg depletion experiments using FoxP3^{DTR} 'DEpletion of REGulatory T cell' (DEREG) mice. DEREG mice express a diphtheria toxin receptor (DTR) protein under control of a FoxP3 promoter in a BAC (bacterial artificial chromosome) construct, allowing selective ablation of FoxP3^{+} Tregs following treatment with diphtheria toxin (DT) (Kim et al., 2007; Lahl et al., 2007). If T-bet^{+} Tregs are actively suppressing Th1 cells and driving the early Th17 response, we would expect Treg depletion early after STM infection to increase the Th1 response. On the other hand, if RORγT^{+} Tregs selectively suppress Th17 cells at later time points, we would expect later Treg depletion to increase the Th17 response and reduce the Th1 bias.

To test the hypothesis that Tregs are sufficient to drive Th bias, transfer experiments were designed where Tregs expressing 'effector' TFs would be isolated from infected donors and transferred into STM-infected DEREG recipients. If subpopulations of Tregs are sufficient to shape Th bias, we would expect transfer of T-bet^{+} Tregs to drive an increased Th17 bias. Similarly, we would expect transferred RORγT^{+} Tregs to drive an increased Th1 bias. Following unexpected results from initial transfer experiments, we conducted *in*

vitro suppression assays to compare the suppressive capacity of Tregs isolated from STM-infected and uninfected donors. Together, these experiments highlight the important role for Tregs in actively shaping the dynamic Th response to infection. They also raise further questions about the function and plasticity of heterogenous Treg populations, their differentiation, and their impact on the overall CD4 T cell response to STM.

5.2 Treg depletion following *Salmonella* infection

Treg depletion in DEREG mice is a useful strategy to assess the temporal modulation of immune responses by Tregs without inducing systemic autoimmunity or high mortality. An advantage of using DEREG mice is an effective and highly specific Treg ablation. A disadvantage is DT toxicity, which has been shown to cause pathology independent of Treg depletion (Lahl and Sparwasser, 2011; Mayer et al., 2014a). As such, DT treatment must be optimised to minimise pathological effects while efficiently ablating Tregs *in vivo*.

5.2.1 Optimisation of Treg depletion in DEREG mice

DT was administered intraperitoneally (IP) on two consecutive days, at a dose of 30ng/g mouse weight. This is a lower dose than reported by other groups (Johanns et al., 2010; Lahl and Sparwasser, 2011; Mayer et al., 2014a) but did not compromise the depletion of Tregs (Fig 5.1). Because of potential DT-mediated effects independent of Treg depletion, WT littermates treated with DT were used as controls for these experiments. We planned to assess the effect of Treg depletion 4 days post-treatment, so the effect of DT treatment on FoxP3$^+$ Tregs was monitored for up to 5 days. Tregs were not detectable in peripheral blood mononuclear cells (PBMCs) 24 hrs following treatment, but 5 days post-treatment, Tregs had re-emerged and were detected at ~33% of the proportion observed in littermate controls (Fig 5.1A). In the colon, 5 days post-treatment, Treg depleted mice had <10% of the Tregs as littermate controls (Fig 5.1B). While Tregs repopulate following depletion, the depletion is effective and sustained enough that a clear impact is expected.

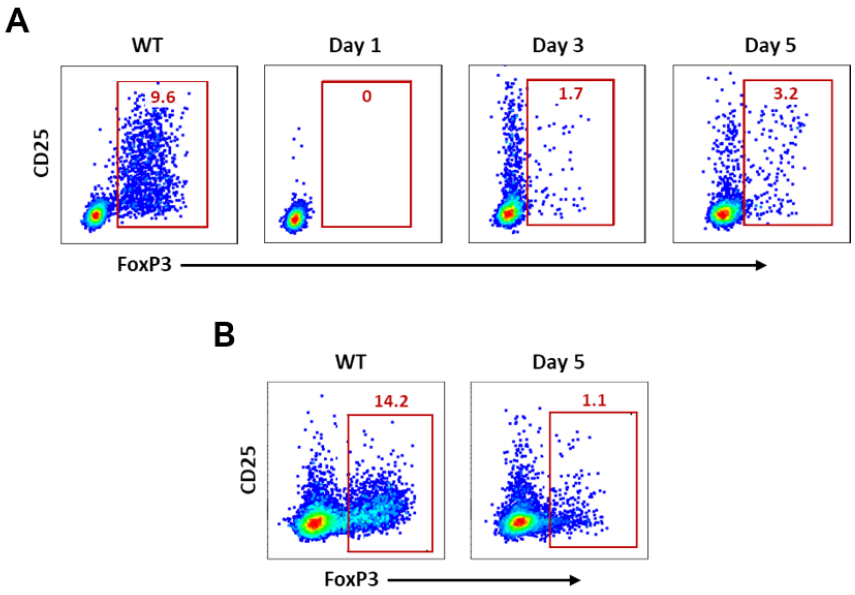

Figure 5.1 DT-mediated Treg depletion in DEREG mice.

CD4 T cells were identified as live, single, $CD3^+$, Dump (MHCII, B220, $CD8)^-$ $CD4^+$ cells. **(A)** Representative plots of CD4 T cells from PBMCs are shown from a WT littermate (left) and DEREG mouse at 1, 3 or 5 days following two daily DT treatments. Numbers represent the proportion of cells that are $FoxP3^+$ **(B)** Plots represent the proportion of colon CD4 T cells that are $FoxP3^+$ 5 days after DT treatment.

5.2.2 Treg depletion 1-2 days p.i. prevents colonic Th17 bias 6 days p.i.

The first depletion experiment was designed to determine if Tregs were necessary to enable the early colonic Th17 response at 6 days p.i. (Fig 5.2A). Tregs were depleted in DEREG mice by DT treatment at day 1 and 2 p.i. and were culled at day 6 p.i. (Fig 5.2B). Both DEREG mice and littermate controls lost ~5% of their initial body weight at day 4 p.i. and mean weights in both groups were stabilised by day 6 p.i. (Fig 5.2C). Treg depletion had no significant impact on STM CFUs recovered in faeces 6 days p.i., although there may be a trend towards decreased bacterial load in DEREG mice compared to littermate controls (Fig 5.2D). Treg depletion did not significantly increase the absolute number of total colon cells 6 days p.i. (Fig 5.2E), although there was an increased number of colonic CD4 T cells (Fig 5.2F) and $CD44^{hi}$ Tconvs (Fig 5.2G).

Assessing the proportion of colonic Th1 and Th17 cells, DEREG mice have a clear increase in the proportion of T-bet^+ Th1 cells and a decreased proportion of RORγT^+ Th17 cells 6 days p.i. (Fig 5.3A). This increased Th1 bias correlates with a specific increase in the absolute number of colonic Th1 cells, while the number of Th17 cells remains

unchanged compared to littermate controls (Fig. 5.3B). These data demonstrate that the increased proportion of Th17 cells 6 days p.i. (Fig. 4.2B) is dependent on the presence of Tregs, which include a higher proportion of T-bet^{+} cells at this time point (Fig 4.3B). These data support the hypothesis that Tregs are necessary to suppress the early Th1 response and shift the Tconv response towards a Th17 bias.

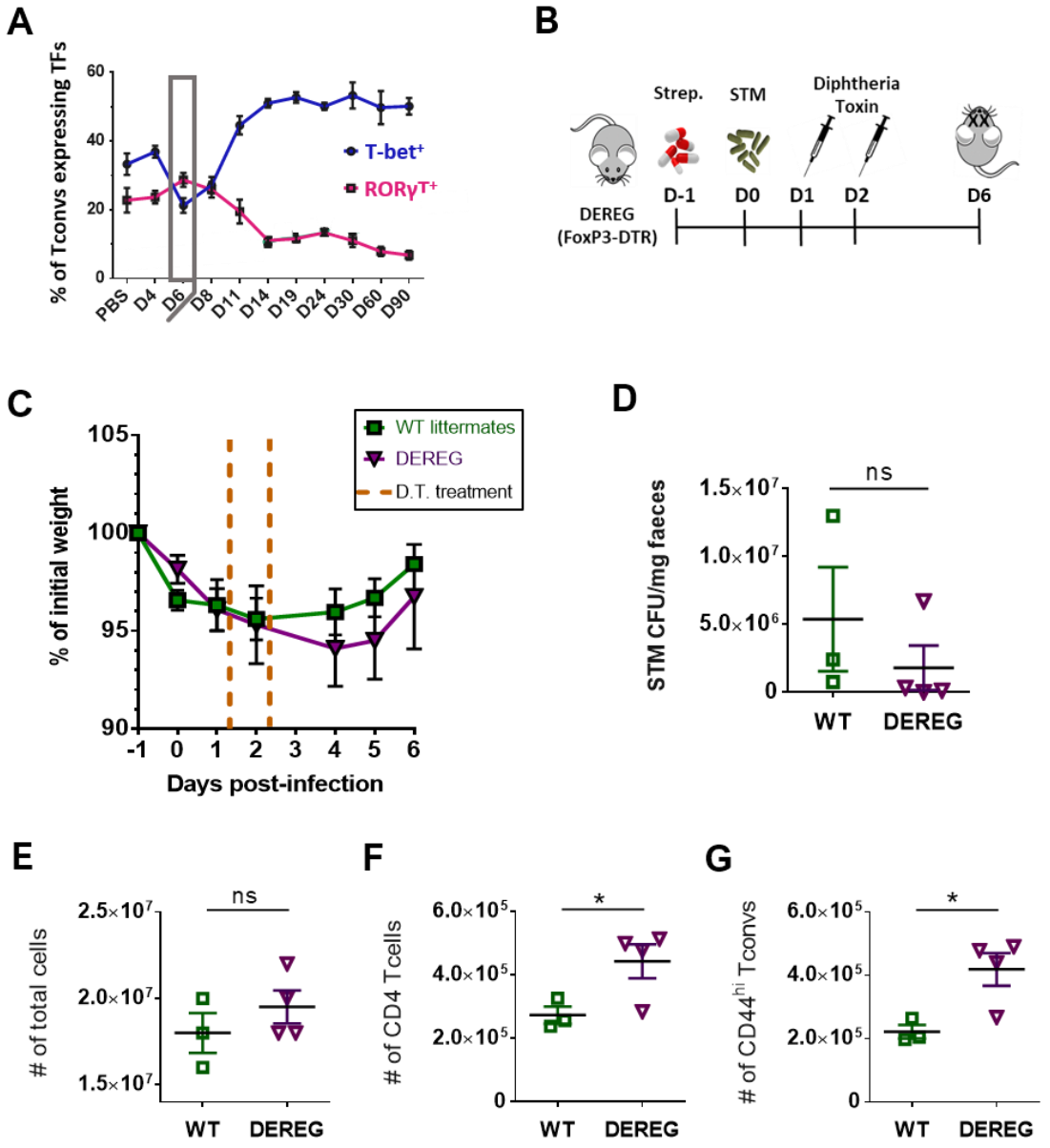

Figure 5.2 Treg ablation at day 1-2 p.i. increases the number of colonic CD4 T cells.

(A) Time course showing the proportion of colon Tconvs expressing T-bet (blue) or RORγT (pink), with the early increased proportion of Th17 cells highlighted at day 6 p.i. **(B)** Experimental design of Treg depletion with an endpoint 6 days p.i. **(C)** Weight loss in DEREG mice and WT littermates following STM infection DT treatments (represented by mustard dashed lines). **(D)** STM CFU recovered from faeces at day 6 p.i. **(E)** The absolute number of colon cells in DEREG mice and WT littermates are shown, in addition to the number of CD4 T cells **(F)** and CD44^{hi} Tconvs **(G)**. Data points represent individual animals (n=3-4) from one example of three independent experiments. Means ± SEM are plotted. Statistical significance calculated by Mann-Whitney test. ns, not significant; *p<.05.

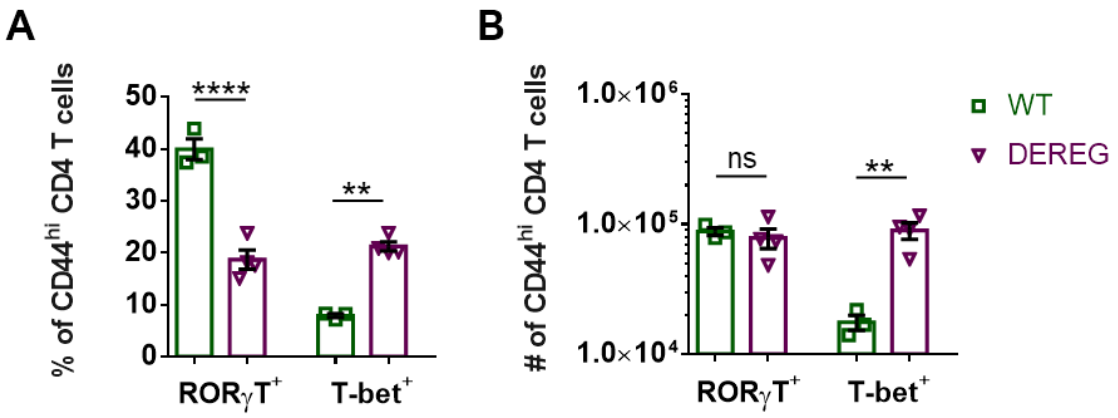

Figure 5.3 Treg ablation day 1-2 p.i. increases the colonic Th1 bias at day 6 p.i.

The proportion **(A)** and absolute number **(B)** of colon Tconvs that are RORγT$^+$ or T-bet$^+$ are shown. Data points represent individual animals (n=3-4) from a representative example of three independent experiments. Means ± SEM are plotted. Statistical significance calculated by two-way ANOVA with Holm-Šídák test. ns, not significant; *p<.05; **p<.01; ***p<.001; ****p<.0001.

5.2.3 Treg depletion at days 6-7 p.i. increases the Th17 response 11 days p.i.

The second depletion experiment was conducted to determine if Tregs were necessary to enable the Th1 response that becomes more prominent by day 11 p.i. (Fig 5.4A). DT was administered at day 6-7 p.i. and mice were culled at day 11 p.i. (Fig 5.4B). As such, mice were culled 4 days after completing DT treatment, consistent with the previous experiment. Following infection, both DEREG mice and littermate controls lost ~5% of their initial body weight in the first 4 days p.i., with mean weights in both groups stabilising by day 6 p.i. Following DT treatment, both groups lost weight again, although the amount of weight loss was variable (Fig 5.4C). Like the previous experiment, Treg depletion had no significant impact on faecal STM CFUs recovered (Fig 5.4D) and did not increase the absolute number of total colon cells (Fig 5.4E). There is a trend towards increased numbers of colonic CD4 T cells (Fig 5.4F) and CD44^{hi} Tconvs (fig 5.4G), but these are not significant.

Assessing the proportion of Th1 and Th17 cells in the colon 11 days p.i., DEREG mice have an increased proportion of RORγT$^+$ Th17 cells while the proportion of T-bet$^+$ Th1 cells remains unchanged (Fig 5.5A). The increased Th17 bias correlates with an increase in the absolute number of both colonic Th1 and Th17 cells compared to littermate controls (Fig. 5.5B). These data show that, like the Th17 bias at day 6 p.i., the Th1 bias at day 11

days p.i. is dependent on Tregs, which include a higher proportion of RORγT^{+} cells at this time point (Fig 4.3B). This supports the hypothesis that Tregs to suppress colon Th17 cells and shift the CD4 T cell response towards a Th1 bias. Together, these results show that Tregs are required for the early Th17 response, contribute to the later Th1 response, and balance the multi-stage and dynamic CD4 T cells to STM infection. Next, we aimed to determine whether Tregs expressing specific TFs were sufficient to drive Th bias following infection.

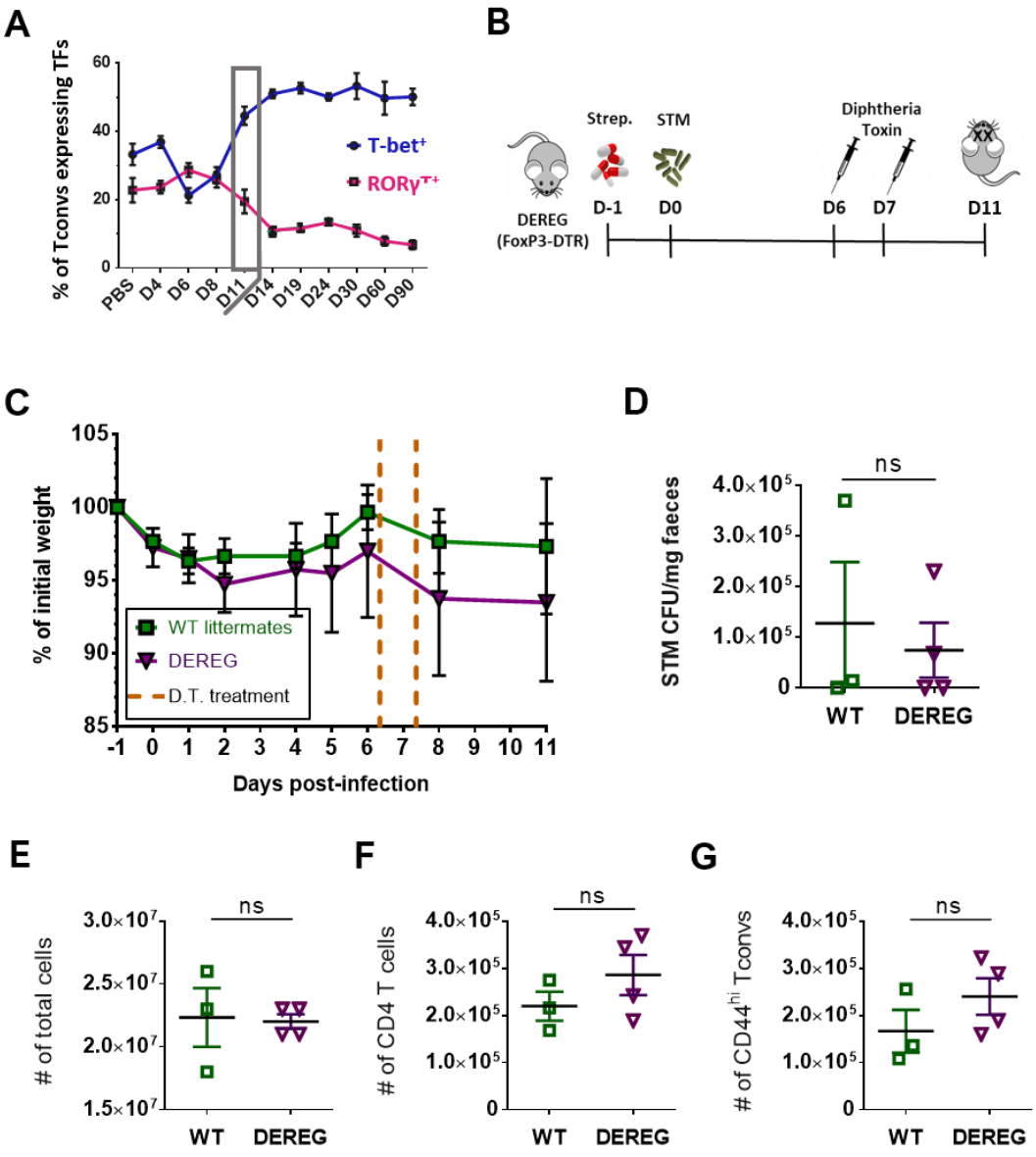

Figure 5.4 Treg ablation 6-7 days p.i. has less impact on CD4 T cell numbers than at 1-2 day 6 p.i.

(A) The proportion of colon Tconvs expressing T-bet (blue) or RORγT (pink) are shown, with the initiation of a Th1 bias highlighted at 11 days p.i. **(B)** Experimental design of Treg depletion at 6-7 days p.i., with an endpoint 11 days p.i. is shown **(C)** Weight loss in DEREG mice and WT littermates following STM infection and two daily DT treatments (orange dashed lines) are indicated. **(D)** STM bacteria were recovered from faeces at day 11 p.i. **(E)** The absolute number of colon cells in DEREG mice and WT littermates are shown, in addition to the number of CD4 T cells **(F)** and CD44^{hi} Tconvs **(G)**. Data points represent individual animals (n=3-4) from a representative example of three independent experiments. Means ± SEM are plotted. Statistical significance calculated by Mann-Whitney test. ns, not significant.

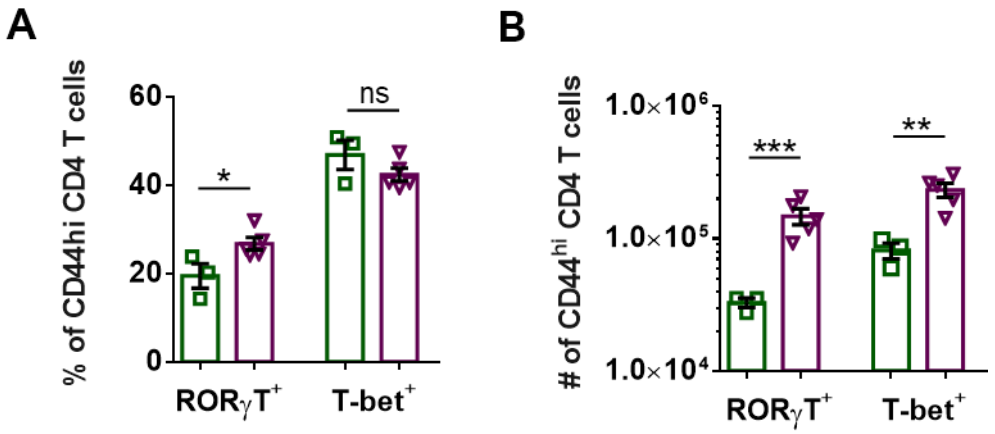

Figure 5.5 Treg ablation 6-7 days p.i. increases the colonic Th17 bias at day 11 p.i.

The proportion **(A)** and absolute number **(B)** of colon Tconvs that are RORγT$^+$ or T-bet$^+$ are shown. Data points represent individual animals (n=3-4) from one example of three independent experiments. Means ± SEM are plotted. Statistical significance calculated by two-way ANOVA with Holm-Šídák test. ns, not significant; *p<.05; **p<.01.

5.3 Transfer of Tregs into *Salmonella*-infected DEREG recipients

To assess the potential for specific Tregs to control the Tconv response to STM we designed transfer experiments into DEREG recipients. Tregs from FoxP3^{RFP}xRORgT^{GFP} (FoxROR) donors were isolated from peripheral lymph nodes using CD4 negative-selection beads and FACS. Tregs were then transferred into DEREG recipients following DT treatment at day 1-2 p.i. (Fig 5.6). DEREG recipients were used to allow assessment of specific Treg populations after ablation of endogenous Tregs. If the hypothesis is correct that Tregs expressing specific TFs are sufficient to enable Th bias, we would expect transfer of T-bet$^+$ Tregs to selectively suppress Th1 cells and increase the Th17 bias. On the other hand, we would expect RORγT$^+$ Tregs to selectively suppress Th17 cells and increase Th1 bias.

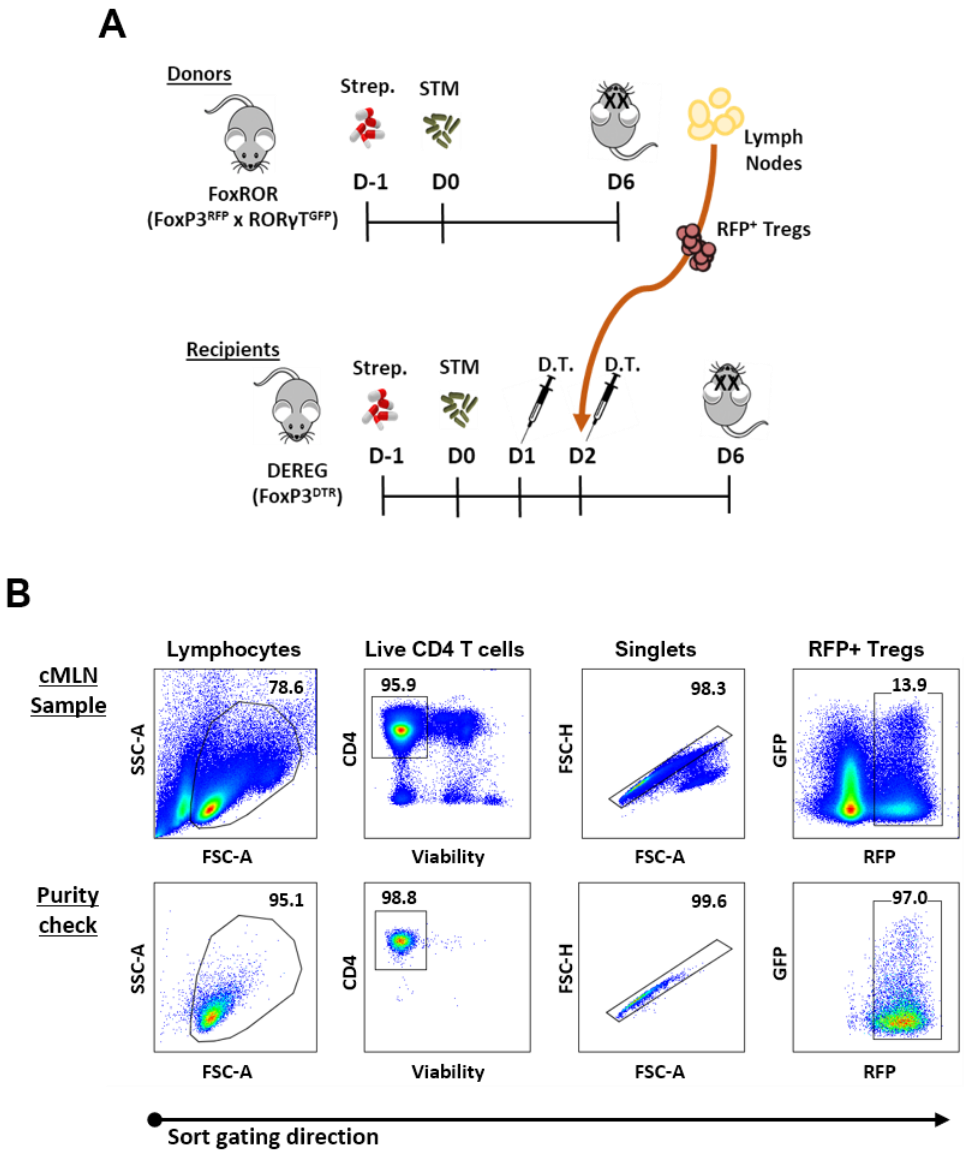

Figure 5.6 Experimental design and cell sorting for Treg transfers into DEREG recipients.

(A) Timelines outlining transfer of lymph node Tregs from STM-infected FoxROR donors into STM-infected DEREG recipients. **(B)** FACS plots show gating of RFP$^+$ Tregs from CD4-enriched lymphocytes (top) and purity analysis of sorted cells using the same gates (below). Gating order is left to right, as indicated.

5.3.1 Transfer of total Tregs from STM-infected donors

Before sorting T-bet$^+$ or RORγT$^+$ Tregs, the first transfer experiment included transfer of total RFP$^+$ Tregs. The aim of this initial transfer was to confirm that the dysregulated response following Treg depletion (Fig 5.3A,B) would be reduced by replacing ablated Tregs with transferred cells. In addition to confirming Treg-mediated regulation, a total Treg transfer was intended as a control for transfers of T-bet$^+$ or RORγT$^+$ Tregs. The gating strategy for total Tregs, sorted from CD4-enriched lymph node cells are shown with analysis of a sorted sample, confirming the purity of transferred cells (Fig 5.6B). Following

FACS sorting, $6x10^5$ RFP^+ Tregs or PBS only was injected i.v. into Treg-depleted DEREG recipients. The number of transferred cells corresponded to the mean number of Tregs harvested from each donor's lymph nodes. Following infection, DT treatment and Treg or mock-transfer, recipients were culled at day 6 p.i. and colons and cMLNs were analysed.

Mice exhibited moderate weight loss following infection and DT treatment, but there was no significant difference between mice receiving Tregs or PBS (Fig 5.5A). There was also no significant difference in the number of STM CFUs recovered from faeces at day 6 p.i. (Fig 5.5B). Differences were clear however, in the number of total cells and $CD44^{hi}$ Tconvs between groups. Representative plots of MLN CD4 T cells demonstrate that Treg recipients had a higher proportion of $CD44^{hi}$ Tconvs than mock-transfer recipients (Fig 5.7C). In the colon and cMLN, the number of total cells (Fig 5.7D,F) and $CD44^{hi}$ CD4 T cells (Fig 5.7E,G) were increased in Treg recipients. This was a surprising result because it indicated that Tregs not only failed to reduce inflammation but increased signs of inflammation including higher cell numbers and CD44 expression. In addition to increased cell numbers, Treg recipients had an increased number of Th1 cells and increased Th1 bias cells in the colon (Fig 5.8A). Treg recipients had a decreased proportion of Th17 cells in both the colon and cMLN (Fig 5.8A,B). Since Treg depletion was shown to increase the colonic Th1 bias at day 6 p.i. (Fig 5.3A,B), Treg transfer in this experiment exacerbated the dysregulated Th1 response instead of ameliorating it, as expected.

This surprising result raised questions about what aspect of the Treg transfer increased dysregulation following Treg depletion. One possible explanation is that there is something about the Tregs themselves that exacerbated inflammation in DEREG recipients. Since the donors were STM infected, it was hypothesised that Tregs from infected animals might become inflammatory in a DEREG recipient. Another potential factor, although unlikely, is inflammation caused by a graft-versus-host disease (GvHD) reaction, independent of the type of cells transferred.

To determine if Tregs from infected donors were more inflammatory than Tregs from uninfected donors, two experiments were planned. The first was another transfer using

uninfected donors. In this transfer, CD44^{lo} naïve CD4 T cells were transferred as a non-Treg control instead of PBS, to rule out potential effects of a GvHD-like response. The second experiment was an *in vitro* suppression assay comparing the suppressive potential of Tregs from STM-infected and uninfected donors.

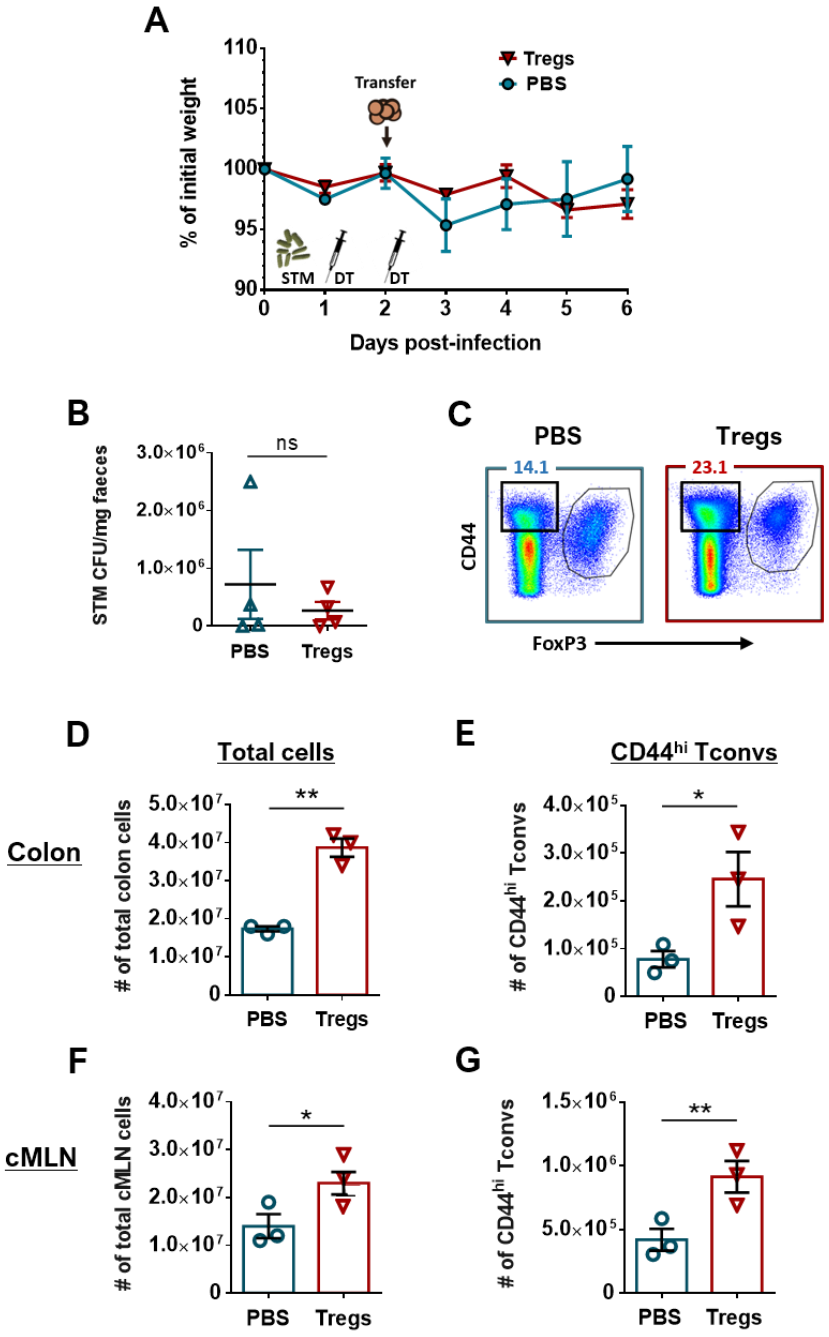

Figure 5.7 Treg transfer increases the numbers and activation of Tconvs 6 days p.i.

(A) Weight loss following STM infection, DT treatment, and Treg or mock transfer. **(B)** STM bacteria recovered from faeces from Treg or PBS recipients **(C)** Representative plots of cMLN CD4 T cells that are CD44^{hi} Tconvs from PBS (left) and Treg recipients (right). The number of total colonic cells **(D)** and CD44^{hi} Tconvs **(E)** are shown for PBS and Treg recipients. The number of total cMLN cells **(F)** and CD44^{hi} Tconvs **(G)** are also shown. Data points represent mean weights/group (A) or individual animals (D-G) (n=3). Means ± SEM are plotted. Statistical significance calculated by Mann-Whitney test (B) and Student's t test (D-G). ns, not significant; *p<.05; **p<.01.

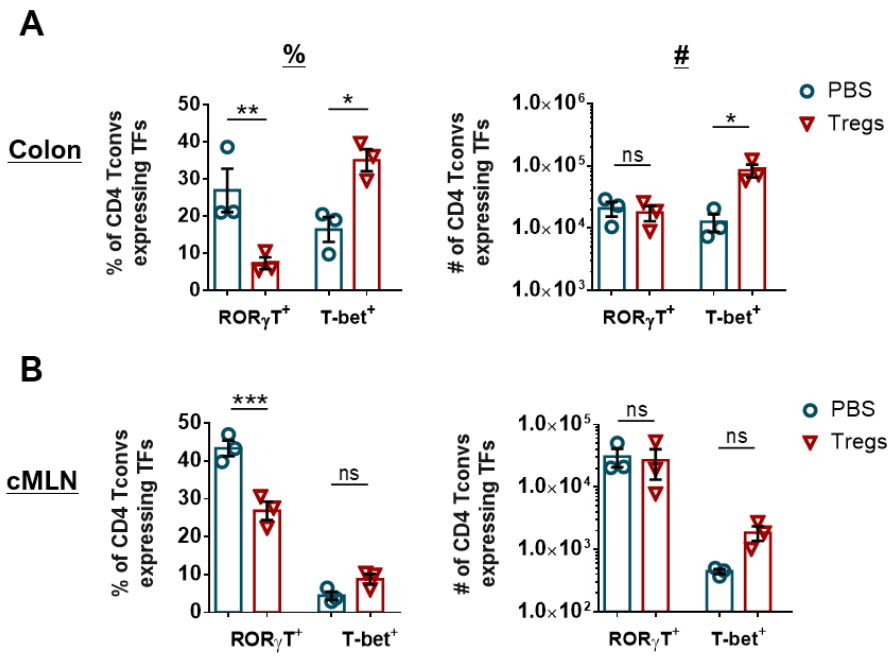

Figure 5.8 Treg transfer into DEREG recipients increases the Th1 response 6 days p.i.

(A) Plots show the proportion (left) and absolute number (right) of colon CD4 T cells that are RORγT$^+$ or T-bet$^+$, in Treg or PBS recipients at 6 days p.i. **(B)** The proportion and absolute number of cMLN CD4 T cells expressing RORγT or T-bet are also shown. Data points represent individual animals (n=3). Means ± SEM are plotted. Statistical significance for each TF calculated by two-way ANOVA with Holm-Šídák test. ns, not significant; *p<.05; **p<.01; ***p<.001.

5.3.2 Transfer of total Tregs from uninfected donors

Gating of Tregs and Tconvs isolated from uninfected FoxROR donors are shown, with analysis of sorted RFP$^+$ Tregs and CD44^{lo} Tconvs displayed to confirm sort purity (Fig 5.9A). Following FACS sorting, 3x10^5 RFP$^+$ Tregs or CD44^{lo} Tconvs were transferred into DEREG recipients. This number corresponds to the mean number of Tregs harvested from each donor's lymph nodes. Following infection, DT treatment and cell transfer, recipients were culled 6 days p.i. and colons and cMLN were analysed.

In Fig 5.9B, weight change is shown for Treg or Tconv recipients in this experiment (hereby referred to as transfer B) and are overlaid with recipients of PBS or Tregs from STM-infected donors. Like recipients in the first transfer (hereby referred to as transfer A). Tconv recipients lost ~5% of initial weight. On the other hand, recipients of Tregs from uninfected donors recovered more weight than other groups and were significantly heavier than recipients of Tregs from infected animals or Tconv 6 days p.i., (Fig 5.9B). In contrast

to the increased number of total cells and CD44^{hi} Tconvs in STM Treg recipients observed in transfer A, Treg recipients in transfer B had similar cell numbers to Tconv recipients (Fig 5.9D-F), with a reduced number of CD44^{hi} Tconvs in the cMLN (Fig 5.9G). In transfer B, there was little change in the proportion of Tconvs expressing T-bet or RORγT (Fig 5.10A,B). Treg recipients had a lower number of RORgT^{+} Tconvs in the cMLN than Tconv recipients, but no other changes were significant (Fig 5.10). As such, transfer of Tregs from uninfected donors did not skew the Th bias compared to Tconv recipients.

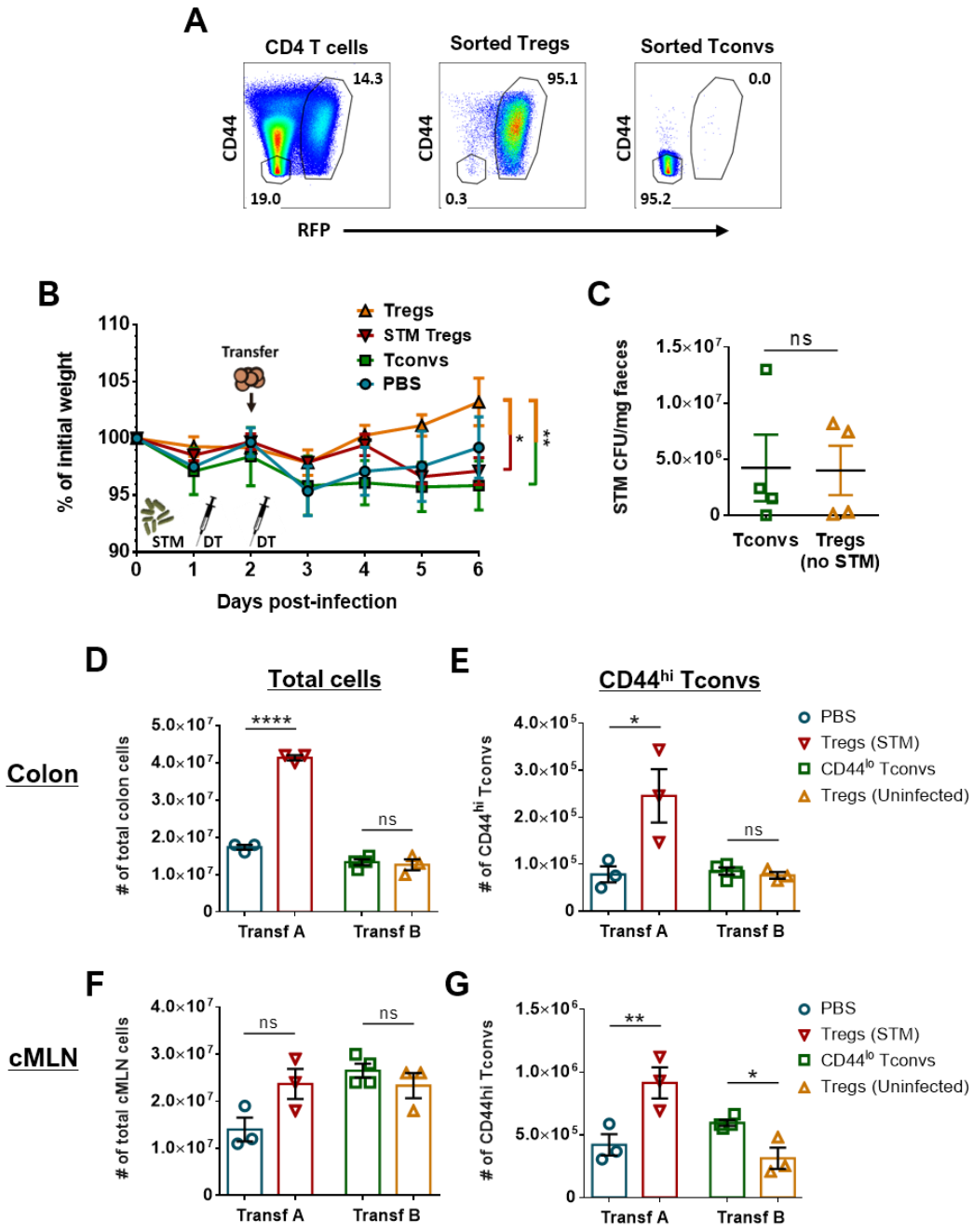

Figure 5.9 Recipients of Tregs from uninfected donors show signs associated with reduced inflammation compared to Tconv recipients.

(A) FACS plots show gates used to sort Tregs and CD44^{lo} Tconvs from lymph nodes of uninfected donors (left). Plots show purity of sorted CD44^{lo} Tconvs (centre) and Tregs (right). **(B)** Weight change following STM infection, DT treatment, and cell transfer. **(C)** STM bacteria recovered from faeces from recipients of Tconvs (green) or Tregs (orange). The number of total colonic cells **(D)** and CD44^{hi} Tconvs **(E)** are shown for recipients of Tconvs (green), Tregs (orange), and PBS (blue) and Tregs from infected donors (red), as shown previously (Fig 5.5). The number of total cMLN cells **(F)** and CD44^{hi} Tconvs **(G)** are also shown. Data points represent mean weights/group (A) or individual animals (D-G) (n=3-4). Means ± SEM are plotted. Statistical significance calculated by Mann-Whitney (B) and Student's t test (D-G) pairwise, within experiments. ns, not significant; *p<.05; **p<.01; ****p<.0001.

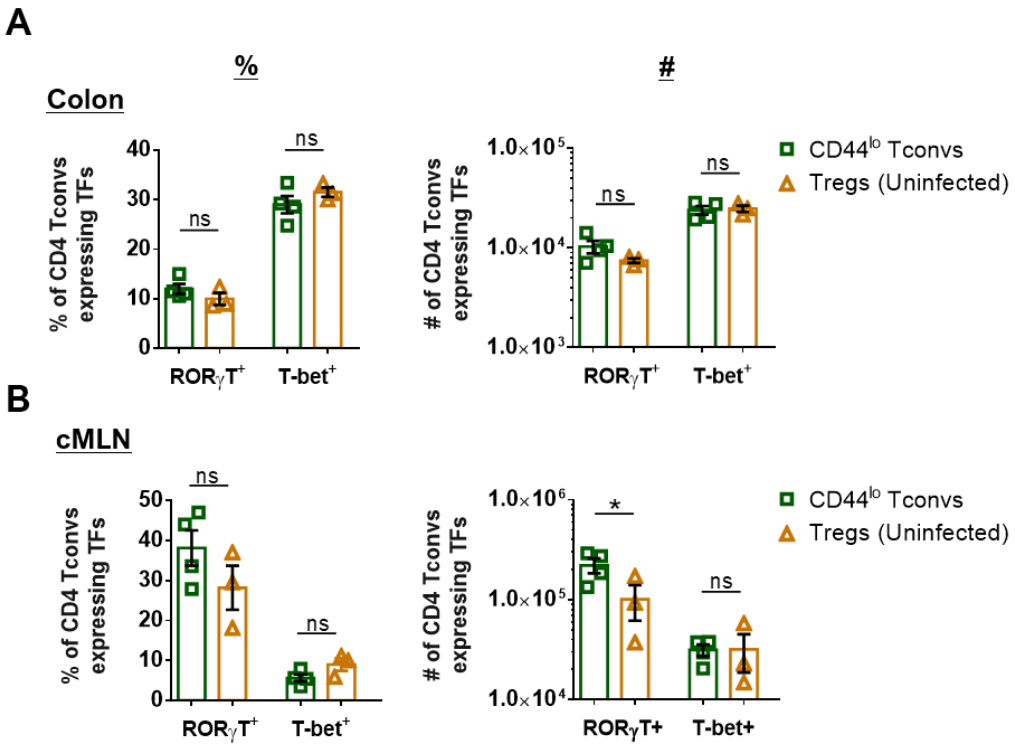

Figure 5.10 Treg transfer does not alter the colonic Th bias compared to recipients of Tconvs.

(A) Plots show the proportion (left) and absolute number (right) of colon CD4 T cells that are RORγT$^+$ or T-bet$^+$, in recipients of Tconvs (green) or Tregs (orange) at 6 days p.i. **(B)** The proportion and absolute number of cMLN CD4 T cells expressing RORγT or T-bet are also shown. Data points represent individual animals (n=3-4). Means ± SEM are plotted. Statistical significance for each TF calculated by two-way ANOVA with Holm-Šídák test. ns, not significant; *p<.05.

The subdued modulation of the Tconv response in transfer B, and indeed the increased signs of inflammation observed in transfer A, raises questions about the fate of transferred cells. In both transfers, no RFP$^+$ cells could be detected in recipients (Fig 5.11). Possible explanations for a lack of detectable RFP$^+$ cells include transferred cells being retained in unassessed tissues like the spleen, a failure of transferred cells to survive, or downregulation of RFP post-transfer. This highlights that viability and plasticity of Tregs post-transfer are potentially important factors.

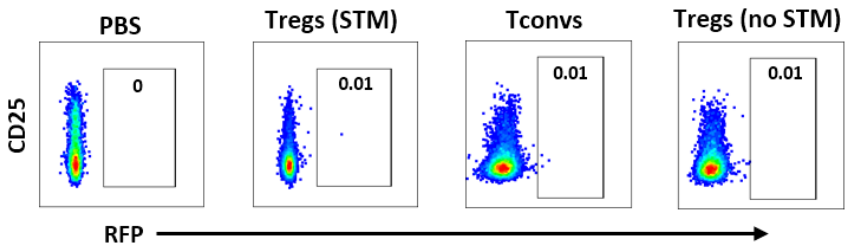

Figure 5.11 RFP$^+$ CD4 T cells are not detected following transfer.
Representative plots of unfixed colonic CD4 T cells from two transfer experiments including recipients of PBS, Tregs from infected donors, Tconvs from uninfected donors and Tregs from uninfected donors (left to right).

Although these Treg transfer experiments failed to regulate Treg depletion-mediated dysregulation, they identify a potentially important distinction between the phenotype and function of Tregs from uninfected or STM-infected donors. Potential mechanisms that could underlie a disparity include differences in suppressive function or commitment to a regulatory phenotype. To investigate the difference between Tregs in these transfers, suppression assays were carried out to compare the suppressive potential of Tregs from STM-infected and uninfected mice.

5.4 Suppression assay with Tregs from infected and uninfected animals

Following adoptive transfers, *in vitro* assays were conducted to compare the suppressive potential of Tregs from infected and uninfected animals. Briefly, Tconvs from STM-infected mice were FACS sorted and stained with cell trace violet (CTV) proliferation dye. These cells were used as responder T cells (Tresp) and were cultured with FACS sorted RFP$^+$ Tregs from STM-infected or uninfected mice. Different Treg:Tresp ratios were co-cultured, including 1:2, 1:4 and 1:8. Purified splenic DCs and αCD3ε antibodies were added to provide co-stimulation and TCR stimulation, respectively. After 84 hrs, cells were harvested and Tresp proliferation was determined by CTV signal, as a readout for Treg-mediated suppression.

CTV signal in Tresps after culture is shown as a representative pseudocolour dot plot and histogram (Fig 5.12A). Histogram peaks identify decreasing CTV levels (from right to left), corresponding to successive generations of Tresp proliferation (Fig 5.12A, left, centre left).

A sample cultured without Tregs is shown as a positive control and appears as a single CTV^{lo} peak, demonstrating most Tresps have proliferated through at least 7 generations (Fig 5.12A, centre right). A sample cultured without CD3ε shows cells appearing as a single CTV^{hi} peak, demonstrating cells have not proliferated, as expected without TCR stimulation (Fig 5.12A, right).

Representative histograms from cultures with Tregs from infected and uninfected mice are shown in Fig 5.12B. In these plots, $CD44^{hi}$ Tconvs (green), $CD44^{lo}$ Tconvs (blue) and $FoxP3^{+}$ Tregs (red) are overlaid. In plots from cultures with a 1:2 Treg:Tresp ratio, a peak of CTV^{hi} unproliferated cells are mostly $CD44^{lo}$, and a peak of CTV^{-} cells contains both Tregs and $CD44^{hi}$ Tconvs. Between these peaks, 7 peaks of proliferated CTV^{+} cells can be identified as distinct generations and are mostly $CD44^{hi}$ Tconvs (Fig 5.12, top). At lower Treg:Tconv ratios, the effect of Tregs is reduced and successive generations are no longer distinguishable. Assays with 1:8 ratios are indistinguishable from 1:0 negative controls (Fig 5.12B, bottom; Fig 5.12A, centre right).

Comparison of Tresp proliferation indicators such as proportions of unproliferated cells, CTV^{-} cells or subgroups of different Tresp generations, showed no difference between assays with Tregs from infected or uninfected mice (Fig 5.13A). A detailed comparison was then made between assays using five indicators generated by formulae based on CTV proliferation data (Fig 5.13B). Values were plotted and there was no significant difference between groups using any of these statistics applied to 1:2 and 1:4 ratios.

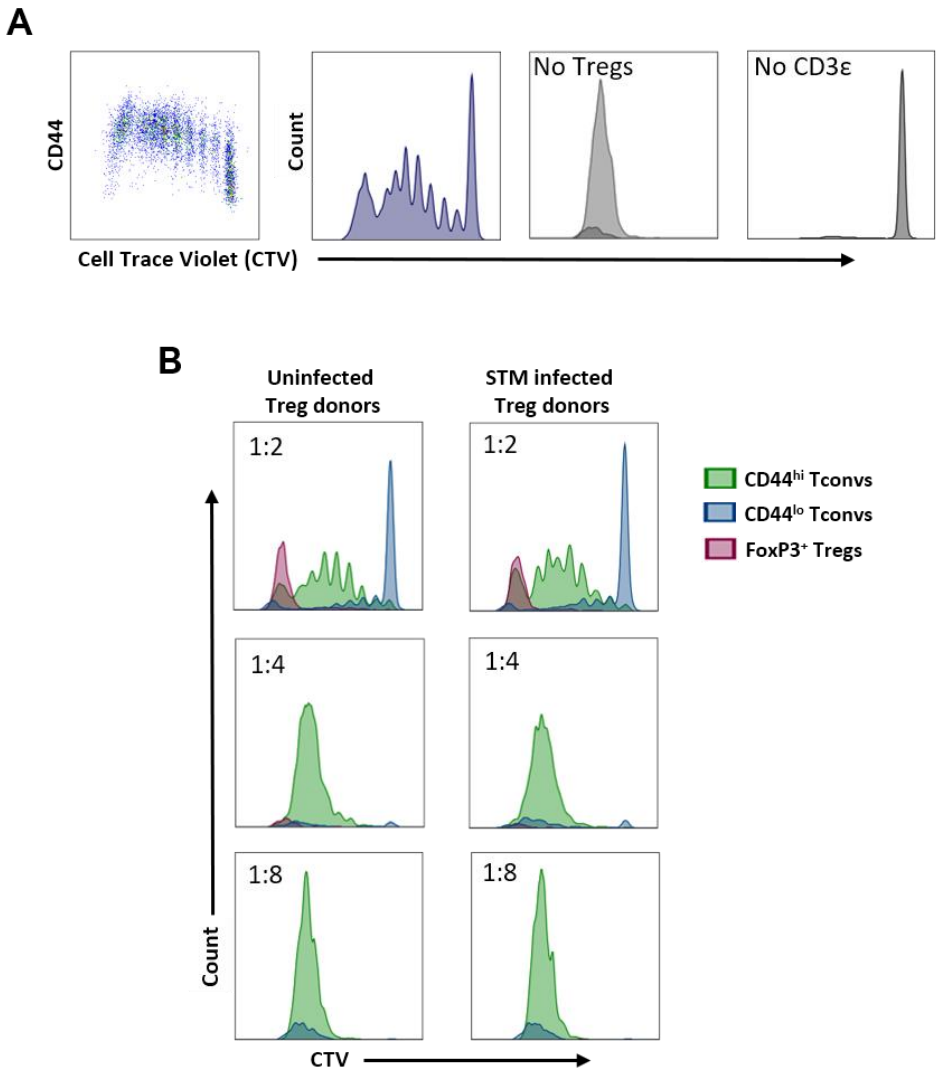

Figure 5.12 Tregs from infected and uninfected donors suppress responder T cells *in vitro*.

(A) Representative plots of cell trace violet (CTV) staining of CD4 T cells are displayed as a pseudocolour plot or histogram following an 84 hr suppression assay. Plots on the right show proliferation in cultures without Tregs or without CD3ε. **(B)** Representative histograms depict CTV staining in $CD44^{hi}$ Tconvs (green), $CD44^{lo}$ Tconvs (blue) and $FoxP3^{+}$ Tregs (red) following culture of responder T cells (Tresps) with serial dilutions of Tregs from donors that were uninfected or STM-infected. Treg:Tresp ratios depicted are 1:2, 1:4 and 1:8.

Although Tregs from infected and uninfected donors have undistinguishable suppressive potential in these assays, samples were further analysed to assess potential differences between groups. Tconv and Treg expression of T-bet and RORγT were compared between groups to determine if Tregs expressed different TFs following culture and whether these Tregs skew the Th bias of Tconvs *in vitro*. Following culture however, both $FoxP3^{-}$ Tconvs and $FoxP3^{+}$ Tregs were predominantly $T\text{-}bet^{+}ROR\gamma T^{+}$, with no detectable difference between assay conditions (Fig 5.13C).

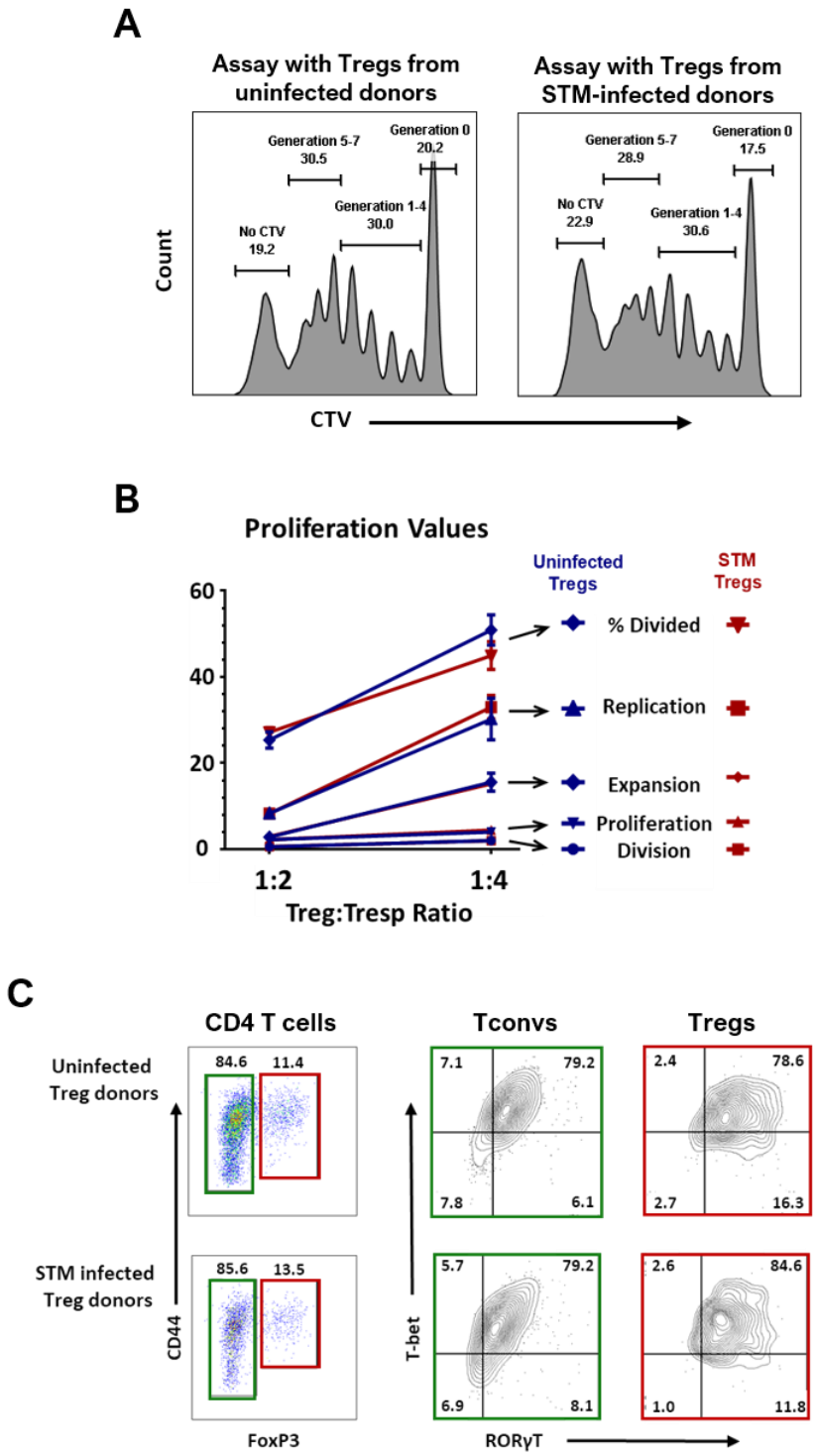

Figure 5.13 Tregs from STM-infected and uninfected mice are similarly suppressive and do not alter T-bet or RORγT expression in Tconvs *in vitro*.

(A) Representative histograms of CD4 T cells show gates applied between peaks and identifying un-proliferated (generation 0) cells, two groups of proliferated cells, and CTV$^-$ cells. **(B)** Five formulae were used to calculate proliferation values for cultures with two proportions of Tregs from uninfected (blue) and STM-infected donors (red). **(C)** Representative plots show CD4 T cells following suppression assays with 1:2 Treg:Tresp ratio with Tregs from uninfected (top) and STM-infected donors (bottom). Tconvs (green) and Tregs (red) are stained for T-bet and RORγT.

The final comparison between assays addressed the hypothesis that Tregs from STM-infected donors are more prone to become pro-inflammatory following transfer. Since

Tregs were not CTV stained, any Tregs would be present in the CTV$^-$ population. The proportion of CTV$^-$cells expressing RFP or FoxP3 were therefore compared to determine if Tregs from infected mice might be more likely to downregulate FoxP3 (Fig 5.14). Representative CTV histograms with RFP$^-$ cells (blue) and RFP$^+$ cells (red) show that cultures with Tregs from infected mice have a lower proportion of CTV$^-$cells that are RFP$^+$ (Fig 5.14A). When graphed, CTV$^-$cells from cultures with Tregs from STM-infected mice have a lower proportion of RFP+ cells at 1:2 and 1:4 ratios (Fig 5.14B, left). These cultures also have a lower proportion of FoxP3$^+$ cells at 1:4 ratios and trend towards lower proportions of FoxP3+ cells at 1:2 and 1:8 ratios (Fig 5.14B, right).

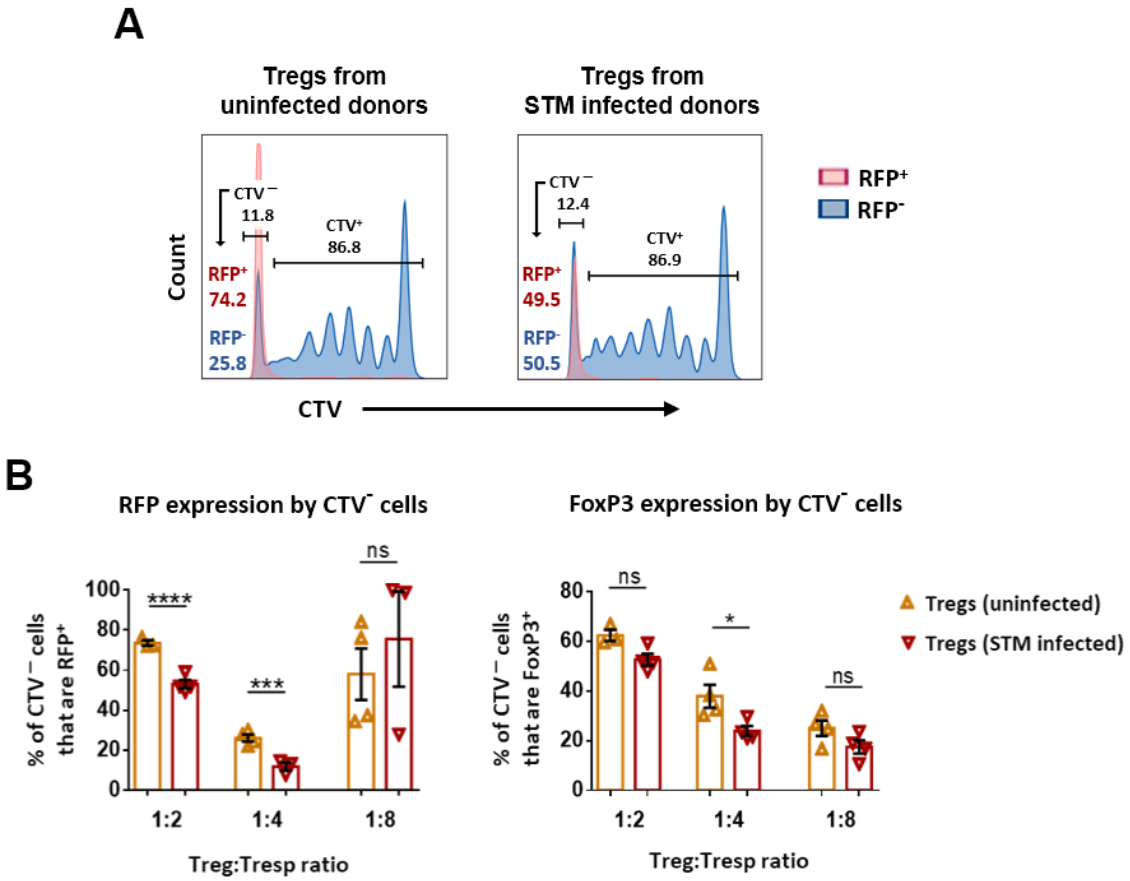

Figure 5.14 A higher proportion of CTV$^-$cells are RFP$^-$ in assays with Tregs from infected donors.

(A) Representative histograms show CTV$^+$ and CTV$^-$ CD4 T cells, with RFP$^+$ (red) and RFP$^-$ (blue) populations overlaid. The proportion of CTV$^-$cells that are RFP$^+$ or RFP$^-$are indicated in red and blue text, respectively. **(B)** The proportion of CTV$^-$cells that express FoxP3 (left) and RFP (right) are plotted from cultures with Tregs from STM-infected (red) and uninfected donors (orange). Data points represent individual animals (n=4) Means ± SEM are plotted. Statistical significance calculated for each group by two-way ANOVA with Holm-Šídák test ns, not significant; *p<.05; **p<.01; ***p<.001; ****p<.0001.

These results are consistent with the hypothesis that Tregs from infected mice are more prone to downregulate RFP and FoxP3 expression, which suggests that they have a less stable regulatory phenotype. Although this difference did not result in a detectable difference in Tresp proliferation *in vitro*, increased instability in Tregs from infected mice might plausibly contribute to increased inflammation observed in recipients of Tregs from infected donors.

Together, experiments in this chapter demonstrate that Tregs play an important role in shaping the CD4 T cell response and further highlight complexities in their heterogeneity, ontogeny, function and plasticity. Treg depletion experiments show that Tregs are required for the early colonic Th17 and contribute to the later Th1 responses to STM. Treg transfer experiments, designed to determine if subpopulations of Treg are sufficient to drive Th bias, were side-tracked when initial experiments revealed that Tregs from infected donors increased inflammation in DEREG recipients. Another transfer experiment showed that Tregs transferred from uninfected donors did not increase inflammation, and *in vitro* suppression assays demonstrated that Tregs from infected donors are potentially less stable and more likely to downregulate RFP and FoxP3. In summary, these results show that Tregs not only inhibit Tconvs, but play an important role in shaping Th bias, and in some situations can increase inflammation. This raises further questions about the complex role of Tregs in controlling the Tconv response to infection.

5.5 Discussion

In the previous chapter, a dynamic and multi-stage CD4 T cell response to STM was characterised and a reciprocity between Tconvs and Tregs was identified. Here we sought to determine if the dynamic Th response was controlled by Tregs expressing the same TFs, which would explain their reciprocity and support the hypothesis that Tregs expressing effector TFs are selectively suppressing Th subsets.

5.5.1 Treg depletion

The aim of these Treg depletion experiments was to determine if Tregs were necessary to shape the Tconv bias following STM infection. The use of DEREG mice has advantages and disadvantages compared to other depletion techniques. Treg depletion using *in vivo* αCD25 treatment depletes a lower proportion of Tregs and is less specific because it also depletes a population of $CD25^{hi}$ Tconvs (Seddiki et al., 2006). αCD25 treatment depletes ~70% of $FoxP3^{+}$ Tregs but leaves a population of $FoxP3^{+}CD25^{lo}$ Tregs intact (Setiady et al., 2010). On the other hand, DT treatment of DEREG mice targets all $FoxP3^{+}$ cells with >95% FoxP3+ Tregs depleted 24 hrs post-treatment (Lahl et al., 2007; Mayer et al., 2014a). This depletion is transient however, with Tregs re-emerging within days of DT treatment (Berod et al., 2014; Lahl and Sparwasser, 2011; Nyström et al., 2014). While depletion is transient, this model allows time-sensitive characterisation of Treg effects without causing systemic autoimmunity seen in sustained Treg ablation.

In the previous chapter, day 6 p.i. was identified as a peak of the early Th17 response and day 11 p.i. was identified as a timepoint where a Th1 bias was re-established (Fig 4.4B,C). Treg depletion experiments were designed to assess whether Tregs are required to control Th bias at these timepoints. Treg depletion in DEREG mice is most complete 24 hrs after DT treatment but the proportion of colon CD4 T cells that are $FoxP3^{+}$ remains ~90% below levels seen in littermate controls 5 days post-treatment (Fig 5.1). In the first DEREG experiment, DT was administered at days 1 and 2 p.i. and mice were culled at day 6 p.i. This time course meant that Tregs were at least partially depleted from day 1 p.i. until the terminal endpoint, with the greatest depletion at day 2-4 p.i. As such, day 6 p.i. was not the timepoint with highest rate of Treg depletion but these experiments were designed to maximise the effect of depletion on the Tconv response at 6 days p.i.

In the second Treg depletion experiment, DT was administered at day 6 and 7 p.i., and mice were culled at 11 days p.i. These timings were selected because they maintained a 5 day period between the first DT treatment and experimental endpoint, as used with the first DEREG experiment. It also allowed a focused assessment of the effect of Tregs on

the Tconv response from day 6 to 11 p.i., without effecting the Tconv response before day 6 p.i.

Treg depletion at day 1 and 2 p.i. caused increased numbers and activation of colonic CD4 T cells (Fig 5.2F,G), consistent with previous reports (Boehm et al., 2012; Kim et al., 2009, 2007; Lahl and Sparwasser, 2011; Nyström et al., 2014). Treg depletion did not significantly reduce the number of STM CFUs recovered from faeces however (Fig 5.2D), in contrast to a previous report of reduced bacterial load in STM-infected DEREG animals (Johanns et al., 2010). This previous report is consistent with the hypothesis that Tregs are restraining Tconvs and inhibiting bacterial clearance. This experiment measured bacterial load in systemic tissues with a systemic model of infection however, so this cannot be considered a direct comparison. Further DEREG experiments measuring STM CFUs in intestinal LP or MLNs might elucidate whether Treg depletion reduces bacterial burden in this model.

In the second DEREG experiment, Treg depletion 6-7 days p.i. had no impact on faecal STM recovery and there was no significant increase in the number of CD4 T cells 11 days p.i., although there was a trend towards an increase in total CD4 T cells and $CD44^{hi}$ Tconvs (Fig 5.4D-G). The reduced impact on cell numbers at this later time point suggests that Tregs play a less important role in constraining the number of CD4 T cells at this phase of infection. One explanation is that by 6 days p.i., Tconvs have already reached near-maximum capacity for expansion and activation. Another explanation which is not incompatible with the first, is that Tregs become less suppressive at later stages of infection, as previously reported (Johanns et al., 2010). As stated, this report is based on a different model, but it is consistent with our findings that later Treg depletion has less impact on the number of colonic CD4 T cells. While there are unanswered questions about the effect of Treg depletion on bacterial load and number of CD4 T cells, the main aim of these experiments was to assess the impact of Treg depletion on Th bias in the colon, where the reciprocal dynamic had been demonstrated.

Assessing TF expression by colonic Tconvs shows that early Treg depletion drives a selective expansion of Th1 cells and prevents the Th17 bias normally seen at day 6 p.i. (Fig 5.3). Treg depletion at day 6-7 p.i. drives an increase in the number of Th1 and Th17 cells, but selectively increases the proportion of Th17 cells (Fig 5.5A,B). At both timepoints, Treg depletion disrupts the balance between Th1 and Th17 cells. These results demonstrate that Tregs play an important role in shaping both the early Th17 response and later Th1 following STM infection. This indicates that the reciprocal dynamics described earlier are not just correlative, but that the dynamic Tconv response requires Tregs. These results are consistent with the hypothesis that Th bias is shaped by selective suppression by sub-populations of Tregs. Further experiments are warranted to confirm the hypothesis that Tregs drive Th bias by selective suppression.

One way to address this hypothesis is using *Tbx21*$^{\text{RFP-cre}}$FoxP3$^{\text{fl}}$ mice to selectively deplete T-bet^{+} Tregs, as described by Levine et al. (2017). *Rorc*$^{\text{cre}}$FoxP3$^{\text{fl}}$ could also be generated to assess the role of targeted depletion of RORγT^{+} Tregs. This would allow us to determine the effect of manipulating specific Treg populations instead of depleting all Tregs at timepoints known to have a higher proportion of T-bet^{+} or RORγT^{+} cells. Another approach to assess the role of specific Treg populations is to adoptively transfer purified subpopulations of Tregs into STM-infected recipients.

5.5.2 Treg transfers experiments

Having demonstrated that Tregs are necessary for controlling the dynamic Th response following STM infection, our next aim was to determine if Tregs are sufficient to enable Tconv polarisation. To answer this question, adoptive transfer experiments were designed so that populations of Tregs that are T-bet^{+} or RORγT^{+} could be transferred into DEREG recipients. If the hypothesis is correct that Tregs can drive Th polarisation by selectively suppressing Th subsets, we would expect transfer of T-bet^{+} Tregs to suppress Th1 cells and enable a Th17 bias. On the other hand, we would expect RORγT^{+} Tregs to selectively suppress Th17 cells and enable a Th1 bias.

Treg transfers have been used widely and were an important technique for the early characterisation of Tregs and their potential to modulate inflammation (Maloy et al., 2003; Uhlig et al., 2006). Treg-depleted DEREG recipients are replete of all lymphocytes except FoxP3^{+} Tregs. As such, the effects of transferred cells will not be diluted by an endogenous Treg population and the immune status of recipients is more physiologically relevant than Rag$^{-/-}$ mice, frequently used for Treg transfers. These experiments were designed to correspond with the day 6 Treg-depletion experiment carried out previously. The transfers initially planned involved sorting subpopulations of Tregs from FoxP3^{RFP}RORγT^{GFP} donors: GFP^{+}RFP^{+} cells would identify RORγT^{+} Tregs and CXCR3^{+}GFP^{-}RFP^{+} cells would be used as surrogates for T-bet^{+} Tregs, as described previously (Levine et al., 2017).

Tregs were isolated from donor lymph nodes (LN) instead of colonic mucosa because LN Tregs can be processed without tissue digest, reducing processing time and increasing viability. Even viable colonic Tregs undergo significant stress during digest, which has unknown functional effects. Furthermore, colonic Tregs have been shown to express low levels of CXCR3, so it would be challenging to use this receptor as a surrogate for T-bet in this tissue (Fig 4.9C). Even if T-bet^{+} cells could be sorted, for example from T-bet-FoxP3 reporters, it is not clear colonic Tregs would effectively upregulate CXCR3 following transfer.

Tregs were sorted from infected donors for two reasons: First, because they would be more phenotypically similar to Tregs depleted from infected recipients and potentially more likely to restore a regulation following Treg depletion. TF expression, cytokine production and Helios expression have all been shown to change following infection. Antigen specificity of Tregs that expand following infection might also be altered compared to mock-infected mice. Second, the number of Tregs expressing T-bet and CXCR3 increase following infection and it would require fewer donors to isolate enough T-bet/CXCR3^{+} Tregs to transfer. STM-infected DEREG recipients were DT treated and Tregs were transferred at day 2 p.i., 4 days before recipients were culled (Fig 5.6A).

Transferred Tregs were not susceptible to DT-mediated deletion because they were not from DEREG donors.

The initial transfer of total RFP^+ Tregs was conducted to confirm that transferred Tregs would restore a more regulated Tconv response, as in Treg-replete WT littermates (Fig 5.3). The unexpected increase in the number of CD4 T cells and $CD44^{hi}$ Tconvs, in addition to the increased Th1 response, suggested that Treg transfer was exacerbating inflammation rather than controlling it. While unexpected, Tregs have previously been reported to drive inflammation following transfer.

Duarte et al. (2009) reported that 50% of Tregs transferred into $Rag2^{-/-}$ mice lost FoxP3 expression and could drive pathology in recipients. They also reported that IL-2 could prevent FoxP3 downregulation. Tregs with transient FoxP3 expression have been identified in several models, where they have been reported to become 'ex-Tregs' following transfer, producing inflammatory cytokines and inducing inflammatory disease (Oldenhove et al., 2009; Tosiek et al., 2016; Tsuji et al., 2009; Zhou et al., 2009). Despite this potential for plasticity and a pro-inflammatory phenotype, many Treg transfers have been shown to reduce Tconv-mediated inflammation, including several using DEREG recipients (van der Veeken et al., 2016; Yu et al., 2018). Some reports have shown that the proportion of Tregs that downregulate FoxP3 increase in inflammatory conditions (Yang et al., 2008; Zhou et al., 2009). These studies and results from our initial transfer support the idea that Tregs from STM-infected hosts may have an unstable regulatory phenotype and therefore could drive inflammation following transfer. To test the hypothesis that Tregs from infected donors induce more inflammation in recipients than Tregs from uninfected donors, we carried out transfer B.

Transfer B differed from transfer A in three ways: first, Tregs were purified from uninfected donors; second, the number of Tregs transferred was $3x10^5$, half the number transferred in transfer A; and third, a matched number of $CD44^{lo}$ Tconvs were transferred as a non-Treg control instead of PBS. Tregs from uninfected mice were used to indicate whether the inflammation induced by transfer A was dependent on donors having been infected.

The reduced number of Tregs used in transfer B was a result of a reduced number of Tregs present in uninfected FoxROR donors. As such, the number of Tregs transferred in both experiments was approximately the same number as were harvested from donor LNs. $CD44^{lo}$ Tconvs were used as controls instead of PBS to compensate for any non-Treg specific effects of transferred cells. Although both FoxROR and DEREG strains are engineered on C57BL/6 backgrounds, we wanted to exclude the potential that a GvHD-type response was causing inflammation.

Transfer B demonstrated that recipients of Tregs from uninfected donors lost less weight than recipients of Tconvs (Fig 5.9B) and had a decreased number of $CD44^{hi}$ Tconvs in the cMLNs (Fig 5.9D-G). Despite these signs that Treg recipients may have had less inflammation, there was no significant difference in Th bias between the two groups (Fig 5.10A,B). These results indicate that Tregs from uninfected donors did not increase inflammation compared to Tconvs and may cause a moderate reduction of inflammation as measured by weight change and the number of $CD44^{hi}$ cMLNs. Treg transfer did not recover the Th balance towards the balance characterised in Treg-replete mice (Fig 5.3, Fig 5.10).

Together, results from transfer A and B suggest that Tregs from infected donors induce greater inflammation than Tregs from uninfected donors. These data do not definitively support this hypothesis however, since different controls were used, and the number of cells transferred was inconsistent between experiments. Despite these issues, data show that Tregs from infected donors induce increased inflammation compared to PBS controls and recipients of Tregs from uninfected donors show signs of reduced inflammation compared to Tconv recipients. Experimental repeats with consistent numbers of transferred cells and inclusion of PBS and Tconv controls would help clarify these results.

In light of previous research showing $FoxP3^{+}$ Tregs can become inflammatory 'ex-Tregs' (Bhela et al., 2017; Tosiek et al., 2016), these results raise questions about the fate of transferred RFP^{+} Tregs. It is unknown if transferred cells maintain a FoxP3 expression because no RFP^{+} cells were detectable in Treg recipients from either transfer (Fig 5.11).

Possible explanations for the lack of RFP^+ cells include poor viability, retention of transferred cells in other tissues, or down-regulation of RFP, which is faithfully co-expressed with FoxP3 in donor mice (Wan and Flavell, 2005). Future experiments could utilise methods to facilitate tracking transferred Tregs, such as crossing FoxROR donors with a CD45.1 strain, labelling purified cells with dyes such as cell trace violet (CTV), or using other fate tracking models. These strategies would allow identification of transferred cells independently of FoxP3 expression and would facilitate an assessment of other phenotypic changes in transferred cells, including stability of FoxP3 expression or upregulation of inflammatory markers.

Once the fate of the transferred cells is characterised, transfer experiments could be optimised by adjusting the timing of transfers and depletions, and the number of cells transferred to try to recover a regulated response. After optimisation, other adaptations could be made, including assessing the impact of transfers at different timepoint following infection and with different Treg populations. The use of more specific Treg depletion models could also be employed to allow a more focused assessment of Treg subpopulations and their potential to shape the Tconv response to STM. For example, Tregs expressing T-bet or RORγT could be transferred into *Tbx21*$^{RFP\text{-}cre}$FoxP3^{fl} or *Rorc*^{cre}FoxP3^{fl} recipients that have been selectively depleted of either T-bet$^+$ or RORγT$^+$ Tregs.

While there are many ways to develop Treg transfer models to assess the potential for Tregs to shape the Tconv response, our next aim was to assess why Tregs from uninfected or infected donors appeared to have different effects in recipients. One hypothesis for this difference is that Tregs from infected donors are impaired in their suppressive potential. Another hypothesis is that Tregs from infected animals are less committed to a regulatory phenotype and are more prone to downregulate FoxP3 and become pro-inflammatory. To test these hypotheses, a suppression assay was conducted to compare their suppressive potential and plasticity *in vitro*.

5.5.3 Suppression assays

Suppression assays, that measure the potential for Tregs to suppress proliferation of responder T cells (Tresps), have been used extensively to characterise *in vitro* Treg suppression (Earle et al., 2005; Gerriets et al., 2016; Miyara and Sakaguchi, 2007; Vu et al., 2007). Here we used suppression assays to evaluate the potential for Tregs from infected or uninfected donors to suppress Tresps with some of the variables inherent in adoptive transfer models removed. Assays were carried out as previously reported (Collison and Vignali, 2011), but with two adaptations. First, DCs were added to cultures to provide co-stimulation instead of αCD28 antibody. DCs were used so assays would incorporate effects of co-inhibitory molecules known to interact with DCs, including CTLA-4 and LAG3. This is a potentially important aspect of Treg suppression *in vivo*, since reduced CTLA-4 expression has been associated with reduced Treg suppressive potency following STM infection (Johanns, 2010). Second, CTV was used as a proliferation dye instead of CFSE because it has improved resolution of peaks, allows tracking of more generations, and is less toxic (Quah and Parish, 2012).

These assays successfully identified up to 8 generations of proliferation, although there was no detectable difference in Tresp proliferation between cultures with Tregs from infected or uninfected animals (Fig 5.13). Proliferation profiles were compared between groups based on statistics generated by formulae assessing the fraction of cells divided, the probability that cells have divided, the fold-expansion of cells during culture and the average number of divisions (Fig 5.13B). Besides proliferation, there was no difference in the expression of T-bet or RORγT by Tconvs or Tregs following co-culture: 80% of Tregs and Tconvs were T-bet$^+$RORγT$^+$ (Fig 5.13C). This highlights the profound effect of culture conditions on the TF profile of these cells, since there is a higher proportion of T-bet$^+$ and T-bet$^+$RORγT$^+$ Tregs in STM-infected animals *in vivo* (Fig 4.3B). As such, any difference in TF profile (known) or potential suppression (unknown) between Tregs from infected and uninfected animals is lost during co-culture.

Despite similar Tresp suppression, a lower proportion of CTV$^-$cells were RFP$^+$ or FoxP3$^+$ in cultures with Tregs from infected mice (Fig 5.14). One interpretation of these data is that Tregs from infected mice are more likely to downregulate FoxP3, which is consistent with the hypothesis that Tregs from infected donors are more likely to become pro-inflammatory.

One caveat with this interpretation is it overlooks the possibility that Tresps have proliferated beyond the limit of CTV detection, and could be another source of RFP$^-$ cells in the CTV$^-$ peak. Representative histograms indicate a gap between the 7th-8th generation Tresp peak and the CTV$^-$ peak, although it is impossible to rule out the presence of some highly proliferated Tresps within these cells (Fig 5.13A). In future experiments, verification of the source of CTV$^-$cells could be achieved by using CD45.1 Treg donors or staining Tregs with another dye, such as CFSE or Cell Trace Orange, which can be distinguished from CTV staining. Another improvement to this protocol would be a reduction in CD3ε concentrations or a shorter assay timecourse. Besides reducing the potential contamination of CTV$^-$populations with highly proliferated Tresps, this would reduce the number of proliferative generations and allow comparison of Tregs at lower Treg:Tresp ratios.

Despite these limitations, the differences between CTV$^-$populations indicate that Tregs from infected mice might be more prone to downregulate FoxP3/RFP. Although this increased plasticity could play a role *in vivo*, these differences have not impacted the Tresp proliferation *in vitro*. These assays obfuscate many *in vivo* dynamics however, including differences in TF expression and the potential role of selective suppression by co-localisation. Indeed, the aspect of site-specific regulation is not incorporated in these models. As such, these results may reveal as much about the assay limitations as they do about *in vivo* dynamics.

In summary, this suppression assay shows there is no inherent, context-independent difference in suppressive potential between Tregs from infected and uninfected animals. Cultures with Tregs from infected mice have a lower proportion of CTV$^-$cells that are RFP$^+$

or FoxP3$^+$ however, which is consistent with higher plasticity and less commitment to a regulatory phenotype. Although further repeats are required, these results support the hypothesis that Tregs from infected mice drive inflammation by downregulating FoxP3 and becoming pro-inflammatory 'ex-Tregs'. This could explain the increased inflammation in transfer A that did not occur in transfer B.

5.5.4 Conclusion

The primary aims of experiments in this chapter were to determine if Tregs were necessary and sufficient to shape the dynamic CD4 T cell response to STM. These aims followed from our earlier characterisation of a reciprocal dynamic between Tregs and Tconvs expressing the same TFs. Treg depletion experiments demonstrated that Tregs are required for the early Th17 and later Th1 phases of the Tconv response. Because an increased proportion of Tregs are T-bet$^+$ 6 days p.i. and RORγT$^+$ 11 days p.i. (Fig 4.4), these results are consistent with the hypothesis that selective suppression shapes the Th bias following infection.

Next, adoptive transfers were planned to determine if Tregs expressing T-bet or RORγT were sufficient to skew Th polarisation towards a Th17 or Th1 bias, respectively. Unexpectedly, initial transfers suggested that total Tregs from infected donors may increase inflammation and Tconv dysregulation, while Tregs from uninfected mice did not have this effect (Fig 5.7-5.10). While further experiments are needed to track the fate of transferred cells, Treg transfers and suppression assays support the hypothesis that Tregs from STM-infected animals are highly plastic and could become pro-inflammatory *in vivo*.

In addition to selective suppression, the potential for CD4 T cells to up- or downregulate FoxP3 expression is an alternative explanation for the reciprocity between populations of Tconvs and Tregs expressing the same TFs. This plasticity could be another factor that influences the dynamic CD4 T cell response to STM. Indeed, the ideas of selective suppression and Treg plasticity are not mutually exclusive; both processes could contribute to the T cell response to STM.

In summary, this work reveals an essential role for Tregs to shape the CD4 T cell response to STM. Results presented here highlight a role for Tregs to not only inhibit the Tconv response, but direct Th bias in a site-specific and time-dependent manner. These results also highlight unanswered questions. We have characterised a reciprocity between Tregs and Tconvs and demonstrated that Tregs are required for the dynamic Th bias; but we have not revealed direct evidence of selective suppression or other mechanisms for Treg control of Th bias. Although we have shown data supporting Treg plasticity, we have not demonstrated that Tregs downregulate FoxP3 during the natural course of STM infection.

Further studies are warranted to elucidate the *in vivo* plasticity of Tregs following infection and mechanisms that could underlie selective suppression, including co-localisation. Ongoing work will contribute to a large body of research being undertaken globally to elucidate Treg diversity, ontogeny, activation, plasticity and their mechanisms of suppression in a wide range of settings. Together, this research will improve our understanding of Treg function and inform the next generation of Treg targeted therapeutics.

Chapter 6 General discussion

The aim of this work was to investigate the potential for Tregs to shape the CD4 T cell response to intestinal infection. To test the hypothesis that Tregs can shape the Th bias in a time and site-specific manner, an STM infection model was developed. This model facilitated a detailed characterisation of the CD4 T cell response to infection, including a reciprocal dynamic between Tconvs and Tregs, and an essential role for Tregs to maintain Th bias.

6.1 Summary of key findings

In the STM model we developed, infection with strain BRD509-2W1S in streptomycin pre-treated mice caused consistent, non-lethal infection with clear signs of colitis that resolved within 2 weeks. This allowed both 2W1S-specific and other T cells to be characterised in mucosal and lymphoid sites. A long-lasting 2W1S-specific CD4 T cell response was detected in multiple tissues for over 90 days, with the highest number of these cells in the large intestine. While 2W1S-specific T cells are consistently Th1 cells, analysis of 2W1S tetramer-negative T cells revealed a dynamic and tissue-specific response. In the colon but not draining lymph nodes, there is an early and transient Th17 response and a later, sustained Th1 response. This dynamic Th response is paralleled by a reciprocal dynamic in Tregs; an early proportional increase in T-bet$^+$ Tregs is followed by an increased proportion of RORgT$^+$ Tregs. Finally, Treg depletion experiments showed that Tregs are essential for the early colonic Th17 response and contribute to the later Th1 response. The Treg-dependent Th bias and the Tconv-Treg reciprocity are consistent with the hypothesis that Tregs shape the Tconv response by selective suppression. The proposed influence of Tregs on the colonic Th bias is diagrammed in Fig 6.1.

The Th1 response to STM has been previously reported in multiple models, but the Th17 response has been less well studied, partly because it is transient and occurs only in the intestines. The early Th17 response described here is consistent with previous work identifying an early expansion and contraction of flagellin-specific Th17 cells in the

intestine (Lee et al., 2012b). It is also consistent with research using calves, non-human primates and humans, suggesting that Th17 cells reduce pathology and reduce the risk of systemic infection (Godinez et al., 2011; Keestra et al., 2011; Raffatellu et al., 2008; van de Vosse and Ottenhoff, 2006).

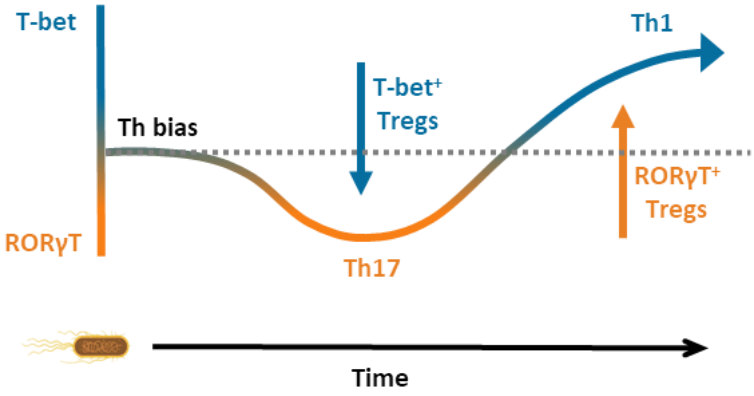

Figure 6.1 The dynamic Th bias in the colon is shaped by Tregs.
Schematic diagram of the dynamic Th bias in colonic Tconvs following STM infection. Early after STM infection, there is a Th17 bias associated with an increased proportion of T-bet$^+$ Tregs. Later, a Th1 bias is established in parallel with an increased proportion of RORγT$^+$ Tregs. The potential for Tregs to shape the Th bias at each stage of the Tconv response is represented by vertical arrows. The baseline Th bias is indicated by a dashed grey line.

The STM colitis model is a convenient platform to study a dynamic, site-specific CD4 T cell response. Initial characterisation of this response revealed a reciprocal dynamic that led to Treg depletion and transfer experiments. Together, these experiments elucidate a nuanced role for Tregs to shape Th bias, instead of just suppressing the overall response. Selective suppression of Th subsets by Tregs would explain both the reciprocal dynamic and the Treg-dependent bias described, although the mechanism of selective suppression is unclear. In addition to selective suppression, this research highlights unanswered questions about antigen specificity, Treg ontogeny, and site-specific control. Each of these topics will be discussed below.

6.2 Antigen specificity of CD4 T cells

STM strain BRD509-2W1S allows tracking of CD4 T cells that express TCR receptors specific for the 2W1S peptide. Despite dynamic shifts in Th bias and Treg populations following infection, 2W1S-speific T cells maintained a consistent Th1 phenotype. This

indicates that specific TCRs may predispose T cells to adopt a specific Th phenotype. Previous research using an oral STM infection model showed that Tconvs specific for TTSS peptides are predominantly Th1 cells, while those specific for flagellin peptides can be Th1 or Th17 cells (Lee et al., 2012b). Why 2W1S-specific T cells are consistently restricted to a Th1 phenotype in this model is unclear.

As the focus of this research shifted to the bulk, presumably polyclonal T cell response, the antigen specificity of cells of interest became less clear. It could be speculated that the non-2W1S-specific Tconvs contain a diverse population of STM- and non-STM-specific TCRs. The role of non-STM specific T cells is difficult to assess with this model, but non-cognate activation of 'bystander' cells may play an important role in the overall response to STM. While the TCR repertoire of different Th subsets at different time points warrants attention, the impact of this repertoire on the dynamic Th bias described here, whether STM-specific or not, remains unknown.

The uncertainty about Tconv antigen-specificity also applies to Tregs. Treg antigen-specificity during infection is poorly understood. During homeostasis, Tregs that are specific for self-antigen are selected in the thymus, and these play an important role in the prevention of autoimmunity (Huter et al., 2008; Sakaguchi et al., 2001). It has also been shown that Tregs specific for microbial and food antigens are important for inhibiting food intolerance or immunopathology induced by the microbiota (Kim et al., 2016; Lathrop et al., 2011). While the role for antigen-specific Tregs during homeostasis is well reported, it is less clear what role pathogen-specific Tregs play during infection or following resolution. Pathogen-specific Tregs have been identified following influenza, LCMV and *S. Typhi* infection (McArthur et al., 2015; Su et al., 2016). It is unclear however, whether pathogen-specific Tregs are necessary to control the immune response to infection, whether they regulate responses to specific epitopes, and what effect Treg pathogen-specificity has on the clearance of infection or immunopathology.

While STM-specific Tregs may play an important role in shaping the T cell response, no 2W1S-specific Tregs were detected in any tissue or at any timepoint. While Tregs may be

specific to other STM antigens, it is unclear whether this specificity is required to modulate the Tconv response to STM. This is because, following activation, Tregs can modulate nearby Tconvs regardless of their antigen-specificity. Treg activation could be achieved by a range of mechanisms including cognate activation by STM antigen, self-antigen, self-mimicking STM antigen, commensal microbial antigen, or cross-reactive STM antigens. Finally, Tregs can be activated by non-cognate activation (Szymczak-Workman et al., 2009; Vignali et al., 2008). Further research is warranted to elucidate the role of antigen specificity of Treg during infection. This will improve our understanding of how Tregs become activated and may reveal therapeutic approaches to target specific Tregs and manipulate the immune response to infections or vaccines with improved precision.

6.3 Ontogeny of Tregs

In addition to questions about antigen-specificity, this research raises questions about the ontogeny of Tregs that respond to STM infection. While Helios is an imperfect marker of tTregs, it could be speculated that Helios^{hi} Tregs, which can co-expresses GATA3 but not RORγT, represents a largely tTreg population. On the other hand, Helios^{lo} Tregs, that can co-express RORγT but not GATA3, could represents a largely pTreg population. If this were true it would indicate that tTregs play a major role in the immune response to STM in the colon. Although tTregs are selected in the thymus for expression of self-reactive TCRs, they have been shown to play a role modulating immune response during infection (Lee et al., 2012a; Pacholczyk et al., 2007; Shevach and Thornton, 2014). Cognate activation of tTregs could occur following presentation of cross-reactive STM peptides or by self-antigen presented by APCs in the vicinity of damaged or infected host cells. Further research is required to determine the individual or synergistic role of tTregs and pTregs in shaping the immune response to STM infection. As with antigen-specificity, delineating the contribution of Tregs with different ontogeny may reveal therapeutic targets or inform the development of tools that employ Tregs in a clinical setting.

6.4 Site-specific control of T cell responses

The dynamic Th bias, the reciprocal dynamic between Tconvs and Tregs, and the Treg dependent control of Th bias occur in the colonic mucosa but not in the cMLN. This raises questions about where and when the CD4 T cell response to STM develops. Understanding the sites where T cells are activated, where they migrate and where they are retained, provides a fundamental insight into how the T cell response develops and how it is controlled. It also reveals insights about how to improve targeting response to reduce immunopathology or enhance responses to infections, tumours or vaccine immunogens.

While the MLNs are important sites of T cell priming in the intestines, the GALT can also be an important induction site. Previous research has shown that STM-specific T cells are activated in PPs <6 hrs p.i., a process dependent on $CCR6^{+}$ DCs (McSorley et al., 2002; Salazar-Gonzalez et al., 2006). While the early T cell response may be primed in the MLNs and GALT, a high number of 2W1S-specific T cells are sustained in the colon. As such, it can be speculated that the CD4 T cells that are primed in the cMLN and CP/PP migrate to the colon where they proliferate and are retained. Because the entire colon, including LP and ILFs were digested together in these experiments, it is difficult to delineate whether cells are situated in lymphoid tissue or dispersed through the LP. While it is difficult to spatially discriminate ILFs and the LP, it can be speculated that Treg suppression occurs in either region, since STM can penetrate both sites.

The site-specific reciprocal dynamics between Tconvs and Tregs, and the Treg-dependent Th bias could be explained by selective suppression of Th subsets. It could be further hypothesised that this selective suppression is driven by co-localisation of Tregs and Th subsets expressing the same ‘master’ TFs, since these TFs can regulate the expression of specific chemokine receptors. If this hypothesis is correct, Tregs that differentiate under the control of these TFs, can be primed to upregulate chemokine receptors, migrate to the same sites as Th subsets and carry out selective suppression by targeting Tconvs and DCs through contact dependent and independent mechanisms.

A cartoon depiction of co-localisation mediated selective suppression is depicted in Fig. 6.2.

The hypothesis that selective suppression is mediated by co-localisation is attractive because it explains the site-specific reciprocal dynamics and the requirement for Tregs to maintain the dynamic Th bias. Although results here do not directly support this hypothesis, other reports have shown that co-localisation of T-bet^{+} Tregs with Th1 cells is essential for optimal selective suppression (Levine et al., 2017). Immunofluorescence microscopy could help elucidate whether Th1 cells colocalise with and T-bet^{+} Tregs or if Th17 cells co-localise with RORγT+ Tregs following STM infection. It would also be interesting to determine if co-localisation occurs in MLNs and/or mucosal tissue. While further research is needed to validate the hypothesis of co-localisation, the concept of selective suppression itself has important implications for understanding the development of T cell responses.

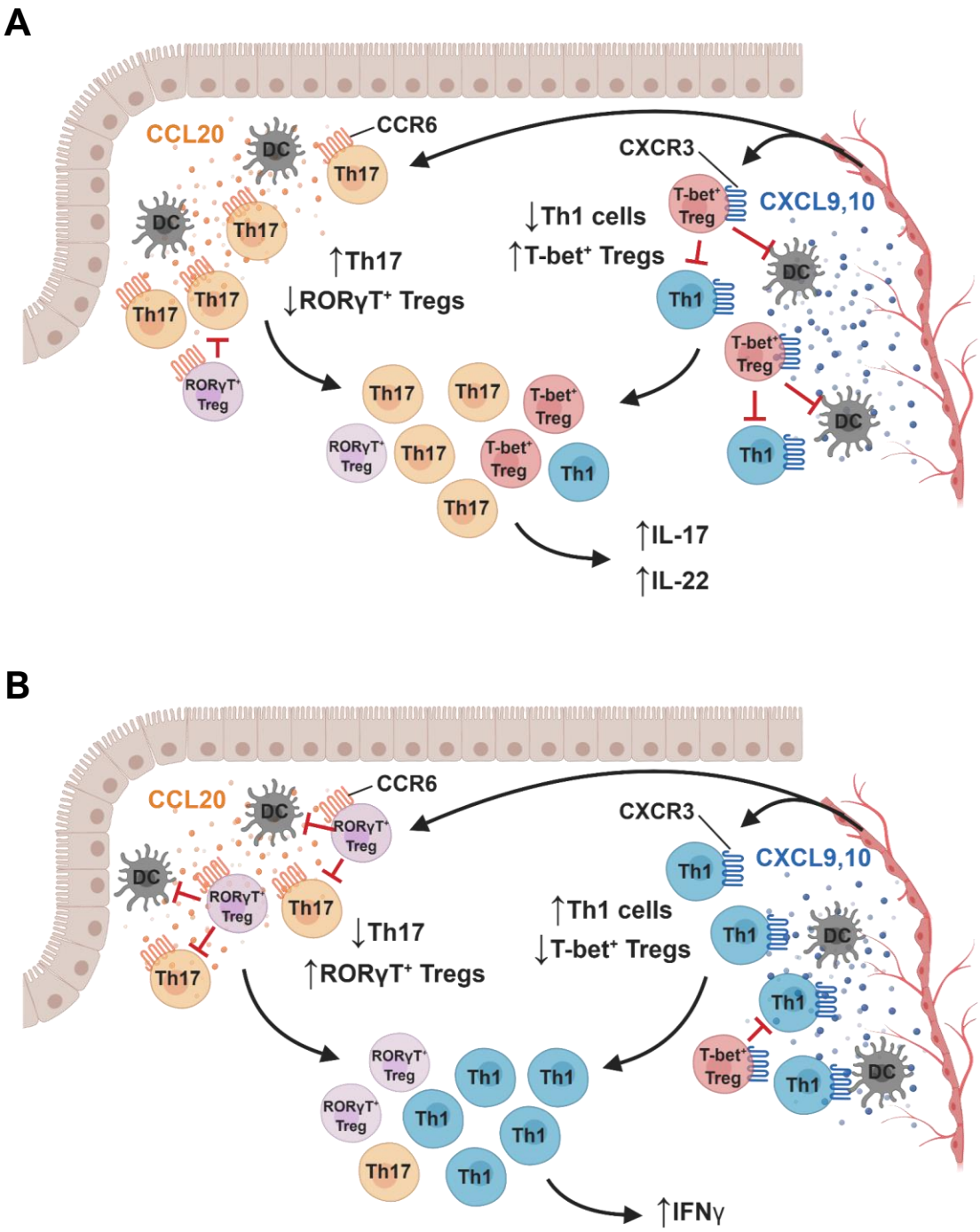

Figure 6.2 Co-localisation as a potential mechanism for selective suppression of Th subsets.

Co-localisation could drive selective suppression of Th subtypes and is consistent with the site-specific reciprocal dynamics reported here. **(A)** During the early colonic Th17 response, T-bet$^+$ Tregs (red), primed in GALT or MLNs upregulate CXCR3, migrate through the peripheral blood and home to CXCL9 or CXCL10 in the colon, e.g. in the proximity of HEV endothelial cells. These T-bet$^+$CXCR3$^+$ Tregs could suppress Th1 cell (blue) expansion in the colon by targeting DCs (grey) and T cells that home to the same regions, allowing Th17 cells (yellow) to expand and produce cytokines such as IL-17 and IL-22. **(B)** According to this model, the later Th1 bias could be driven by RORγT$^+$ Tregs (purple) that upregulate CCR6 in the MLN or GALT before migrating through blood vessels and home to CCL20 rich areas, e.g. near FAE. In these regions, RORγT$^+$CCR6$^+$ Tregs could target DCs and T cells to inhibit the Th17 response and facilitate a Th1 expansion.

6.5 Selective suppression and the equilibrium model of immunity

The idea that Tregs expressing 'master' TFs might selectively suppress Th subsets is not a new concept. This concept has been proposed by immunologists including Shimon Sakaguchi and Daniel Campbell, and supported by research showing that T-bet$^+$ Tregs can suppress Th1 cells and RORγT/STAT3+ Tregs can selectively suppress Th17 cells in some contexts (Chaudhry et al., 2009; Duhen et al., 2012; Koch et al., 2009; Wing and Sakaguchi, 2012). This model has not been universally accepted however and it contradicts the equilibrium model of immunity, proposed by Gerard Eberl and others (Eberl, 2016; Park and Eberl, 2018).

According to the equilibrium model, type 1, type 2, or type 3 responses are defined by T-bet, GATA3/IRF4 or RORγT expression, respectively. In this model, immune responses are biased towards one of these types, incorporating a cohesive response where Tconvs and Tregs expressing the same master TFs expand and contract together. In a type 1 response for example, environmental factors will induce T-bet expression in Tconvs and Tregs, so that T-bet$^+$ Tregs and Th1 cells will expand in parallel. An important aspect of the equilibrium model is that it suggests a balanced immune response is maintained because Tregs that arise in one response type will selectively supress the Th subsets of the other responses. In this way the equilibrium model directly contradicts the selective suppression model, which proposes Tregs selectively suppress Th subsets that express the same TF. Schematic representations of the selective suppression model and the equilibrium model of immunity are shown in Fig 6.3.

In support of the equilibrium model, research has shown that RORγT$^+$ Tregs suppress Th2 responses, and that GF mice with impaired RORγT$^+$ Tregs have a dysregulated Th2 response (Ohnmacht et al., 2015). On the other hand, microbiota depletion or targeting RORγT$^+$ Tregs has also been reported to drive a dysregulated Th17 response (Lochner et al., 2011; Sefik et al., 2015). These conflicting results may be partially dependent on the models used or other variables. While it is logical to assume that lymphocytes that

express the same TFs form a ‘type’ response that suppresses other types; there is growing evidence that Tregs selectively suppress Tconvs of the same type (Britton et al., 2019; Levine et al., 2017).

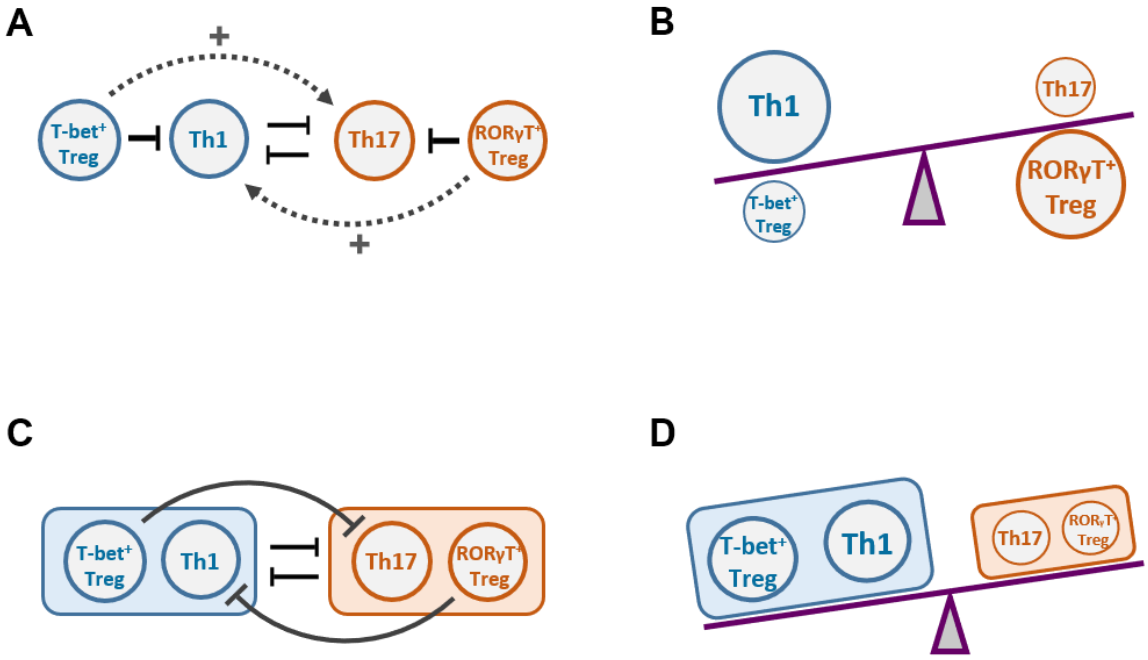

Figure 6.3 Selective suppression and equilibrium models of Th bias.

(A) In the model of selective suppression, supported by data here, Tregs expressing Th ‘master’ TFs selectively suppress Th subsets that express the same TFs, and indirectly facilitate expansion of other Th subsets (represented by ‘+’). **(B)** According to this selective suppression model, an increased proportion of RORγT$^+$ Tregs selectively suppress Th17 cells, which facilitates an expansion of Th1 cells. **(C)** The equilibrium model of immunity proposes that Th subsets and Tregs expressing the same TFs expand and contract in parallel. **(D)** According to this model, Th1 responses incorporate increases in T-bet$^+$ Tregs and Th1 cells, and function synergistically to suppress other (non-Th1) Th subsets.

Results from research described here, including the reciprocal dynamics between Tregs and Th subsets, are consistent with a selective suppression model and not with the equilibrium model. Both models are over-simplified constructs however; *in vivo* dynamics are more complex and could incorporate aspects of both models depending on context. These models and the research described here focus on Treg control of CD4 T cell responses. This focus has overlooked other important cell types, including ILCs. Recent work has highlighted the important role for RORγT$^+$ ILC3s to produce IL-2 and maintain Treg populations in the intestines (Zhou et al., 2019). This has potentially important implications for understanding how Tregs can be sustained in the absence of Tconv-derived IL-2. Because ILCs can express the same ‘master’ TFs and chemokine receptors

as Th subsets and Tregs, ILCs may also support site-specific immune-modulation, dependent on co-localisation of multiple cell types. While the control of CD4 T cell responses is likely more complex and nuanced than these results or other models convey, this research can provide important insights into the dynamics that underlie the dynamic and site-specific T cell response.

6.6 Final conclusions

This research has shown that there is a dynamic Th response in the colon and a reciprocal dynamic between Tconvs and Tregs expressing the same TFs. Treg depletion experiments indicate that the early Th17 response and the later Th1 bias are shaped by Tregs. These results reveal an important role for Tregs to influence the CD4 T cell response in a fine-tuned manner. This raises further questions about the development of site-specific T cell responses, the phenotype and function of Treg populations that respond to infection, the potential for selective suppression, and the impact this has on the overall immune response. These results not only have implications for understanding how the T cell response to STM colitis is controlled, but also for how T cell responses are balanced during infection or inflammation in general. By investigating the potential for Tregs to shape or skew Th bias, there will be opportunities to improve and fine-tune therapeutic options for cancer, infectious disease vaccines, autoimmunity, inflammatory diseases and transplant rejection. Further work is therefore clearly warranted to improve our basic understanding of how Tregs shape immune responses.

References

Adamczyk, A., Gageik, D., Frede, A., Pastille, E., Hansen, W., Rueffer, A., Buer, J., Büning, J., Langhorst, J., and Westendorf, A.M. (2017). Differential expression of GPR15 on T cells during ulcerative colitis. JCI Insight *2*, e90585.

Agace, W. (2010). Generation of gut-homing T cells and their localization to the small intestinal mucosa. Immunology Letters *128*, 21–23.

Agace, W.W., and McCoy, K.D. (2017). Regionalized Development and Maintenance of the Intestinal Adaptive Immune Landscape. Immunity *46*, 532–548.

Akimova, T., Beier, U.H., Wang, L., Levine, M.H., and Hancock, W.W. (2011). Helios Expression Is a Marker of T Cell Activation and Proliferation. PLoS ONE *6*, e24226.

Allen, F., Tong, A.A., and Huang, A.Y. (2016). Unique Transcompartmental Bridge: Antigen-Presenting Cells Sampling across Endothelial and Mucosal Barriers. Frontiers in Immunology *7*.

Amarnath, S., Mangus, C.W., Wang, J.C.M., Wei, F., He, A., Kapoor, V., Foley, J.E., Massey, P.R., Felizardo, T.C., Riley, J.L., et al. (2011). The PDL1-PD1 Axis Converts Human TH1 Cells into Regulatory T Cells. Science Translational Medicine *3*, 111ra120-111ra120.

Annacker, O., Asseman, C., Read, S., and Powrie, F. (2003). Interleukin-10 in the regulation of T cell-induced colitis. J. Autoimmun. *20*, 277–279.

Arpaia, N., Godec, J., Lau, L., Sivick, K.E., McLaughlin, L.M., Jones, M.B., Dracheva, T., Peterson, S.N., Monack, D.M., and Barton, G.M. (2011). TLR Signaling Is Required for Salmonella typhimurium Virulence. Cell *144*, 675–688.

Asseman, C., Mauze, S., Leach, M.W., Coffman, R.L., and Powrie, F. (1999). An essential role for interleukin 10 in the function of regulatory T cells that inhibit intestinal inflammation. J. Exp. Med. *190*, 995–1004.

Baatar, D., Olkhanud, P., Sumitomo, K., Taub, D., Gress, R., and Biragyn, A. (2007). Human Peripheral Blood T Regulatory Cells (Tregs), Functionally Primed CCR4+ Tregs and Unprimed CCR4- Tregs, Regulate Effector T Cells Using FasL. The Journal of Immunology *178*, 4891–4900.

Baecher-Allan, C., and Hafler, D.A. (2004). Suppressor T cells in human diseases. J. Exp. Med. *200*, 273–276.

Bain, C.C., and Mowat, A.McI. (2014). Macrophages in intestinal homeostasis and inflammation. Immunological Reviews *260*, 102–117.

Ballesteros-Tato, A., Randall, T.D., Lund, F.E., Spolski, R., Leonard, W.J., and León, B. (2016). T Follicular Helper Cell Plasticity Shapes Pathogenic T Helper 2 Cell-Mediated Immunity to Inhaled House Dust Mite. Immunity *44*, 259–273.

Barker, N., van de Wetering, M., and Clevers, H. (2008). The intestinal stem cell. Genes & Development *22*, 1856–1864.

Barthel, M., Hapfelmeier, S., Quintanilla-Martínez, L., Kremer, M., Rohde, M., Hogardt, M., Pfeffer, K., Rüssmann, H., and Hardt, W.-D. (2003). Pretreatment of mice with streptomycin provides a Salmonella enterica serovar Typhimurium colitis model that allows analysis of both pathogen and host. Infect. Immun. *71*, 2839–2858.

Barton, G.M. (2003). Toll-Like Receptor Signaling Pathways. Science *300*, 1524–1525.

Barzaghi, F., Passerini, L., and Bacchetta, R. (2012). Immune dysregulation, polyendocrinopathy, enteropathy, x-linked syndrome: a paradigm of immunodeficiency with autoimmunity. Front Immunol *3*, 211.

Belkaid, Y. (2007). Regulatory T cells and infection: a dangerous necessity. Nature Reviews Immunology *7*, 875–888.

Belkaid, Y., Piccirillo, C.A., Mendez, S., Shevach, E.M., and Sacks, D.L. (2002). CD4+CD25+ regulatory T cells control Leishmania major persistence and immunity. Nature *420*, 502–507.

Bennett, C.L., Christie, J., Ramsdell, F., Brunkow, M.E., Ferguson, P.J., Whitesell, L., Kelly, T.E., Saulsbury, F.T., Chance, P.F., and Ochs, H.D. (2001). The immune dysregulation, polyendocrinopathy, enteropathy, X-linked syndrome (IPEX) is caused by mutations of FOXP3. Nature Genetics *27*, 20–21.

Benoun, J.M., Labuda, J.C., and McSorley, S.J. (2016). Collateral Damage: Detrimental Effect of Antibiotics on the Development of Protective Immune Memory. MBio *7*.

Benoun, J.M., Peres, N.G., Wang, N., Pham, O.H., Rudisill, V.L., Fogassy, Z.N., Whitney, P.G., Fernandez-Ruiz, D., Gebhardt, T., Pham, Q.-M., et al. (2018). Optimal protection against *Salmonella* infection requires noncirculating memory. Proceedings of the National Academy of Sciences 201808339.

Berlin, C., Berg, E.L., Briskin, M.J., Andrew, D.P., Kilshaw, P.J., Holzmann, B., Weissman, I.L., Hamann, A., and Butcher, E.C. (1993). α4β7 integrin mediates lymphocyte binding to the mucosal vascular addressin MAdCAM-1. Cell *74*, 185–195.

Berod, L., Stüve, P., Varela, F., Behrends, J., Swallow, M., Kruse, F., Krull, F., Ghorbani, P., Mayer, C.T., Hölscher, C., et al. (2014). Rapid Rebound of the Treg Compartment in DEREG Mice Limits the Impact of Treg Depletion on Mycobacterial Burden, but Prevents Autoimmunity. PLoS ONE *9*, e102804.

Bettelli, E., Carrier, Y., Gao, W., Korn, T., Strom, T.B., Oukka, M., Weiner, H.L., and Kuchroo, V.K. (2006). Reciprocal developmental pathways for the generation of pathogenic effector TH17 and regulatory T cells. Nature *441*, 235–238.

Bhela, S., Varanasi, S.K., Jaggi, U., Sloan, S.S., Rajasagi, N.K., and Rouse, B.T. (2017). The Plasticity and Stability of Regulatory T Cells during Viral-Induced Inflammatory Lesions. The Journal of Immunology *199*, 1342–1352.

Bjerknes, M., and Cheng, H. (1999). Clonal analysis of mouse intestinal epithelial progenitors. Gastroenterology *116*, 7–14.

Bluestone, J.A., and Abbas, A.K. (2003). Natural versus adaptive regulatory T cells. Nature Reviews Immunology *3*, 253–257.

Boehm, F., Martin, M., Kesselring, R., Schiechl, G., Geissler, E.K., Schlitt, H.-J., and Fichtner-Feigl, S. (2012). Deletion of Foxp3+ regulatory T cells in genetically targeted mice supports development of intestinal inflammation. BMC Gastroenterology *12*.

Boer, M.C., Joosten, S.A., and Ottenhoff, T.H.M. (2015). Regulatory T-Cells at the Interface between Human Host and Pathogens in Infectious Diseases and Vaccination. Frontiers in Immunology *6*.

Bohnhoff, M., Drake, B.L., and Miller, C.P. (1954). Effect of Streptomycin on Susceptibility of Intestinal Tract to Experimental Salmonella Infection. Experimental Biology and Medicine *86*, 132–137.

Bopp, T., Becker, C., Klein, M., Klein-Heßling, S., Palmetshofer, A., Serfling, E., Heib, V., Becker, M., Kubach, J., Schmitt, S., et al. (2007). Cyclic adenosine monophosphate is a key component of regulatory T cell–mediated suppression. The Journal of Experimental Medicine *204*, 1303–1310.

Borsellino, G., Kleinewietfeld, M., Di Mitri, D., Sternjak, A., Diamantini, A., Giometto, R., Hopner, S., Centonze, D., Bernardi, G., Dell'Acqua, M.L., et al. (2007). Expression of ectonucleotidase CD39 by Foxp3+ Treg cells: hydrolysis of extracellular ATP and immune suppression. Blood *110*, 1225–1232.

Bouskra, D., Brézillon, C., Bérard, M., Werts, C., Varona, R., Boneca, I.G., and Eberl, G. (2008). Lymphoid tissue genesis induced by commensals through NOD1 regulates intestinal homeostasis. Nature *456*, 507–510.

Bravo-Blas, A., Utriainen, L., Clay, S.L., Kästele, V., Cerovic, V., Cunningham, A.F., Henderson, I.R., Wall, D.M., and Milling, S.W.F. (2018). Salmonella enterica Serovar Typhimurium Travels to Mesenteric Lymph Nodes Both with Host Cells and Autonomously. J. Immunol.

Brewer, J.M., Conacher, M., Hunter, C.A., Mohrs, M., Brombacher, F., and Alexander, J. (1999). Aluminium hydroxide adjuvant initiates strong antigen-specific Th2 responses in the absence of IL-4- or IL-13-mediated signaling. J. Immunol. *163*, 6448–6454.

Brincks, E.L., Roberts, A.D., Cookenham, T., Sell, S., Kohlmeier, J.E., Blackman, M.A., and Woodland, D.L. (2013). Antigen-Specific Memory Regulatory CD4+Foxp3+ T Cells Control Memory Responses to Influenza Virus Infection. The Journal of Immunology *190*, 3438–3446.

Briskin, M., Winsor-Hines, D., Shyjan, A., Cochran, N., Bloom, S., Wilson, J., McEvoy, L.M., Butcher, E.C., Kassam, N., Mackay, C.R., et al. (1997). Human mucosal addressin cell adhesion molecule-1 is preferentially expressed in intestinal tract and associated lymphoid tissue. Am. J. Pathol. *151*, 97–110.

Britton, G.J., Contijoch, E.J., Mogno, I., Vennaro, O.H., Llewellyn, S.R., Ng, R., Li, Z., Mortha, A., Merad, M., Das, A., et al. (2019). Microbiotas from Humans with Inflammatory Bowel Disease Alter the Balance of Gut Th17 and RORγt+ Regulatory T Cells and Exacerbate Colitis in Mice. Immunity *50*, 212-224.e4.

Brown, D.E., Libby, S.J., Moreland, S.M., McCoy, M.W., Brabb, T., Stepanek, A., Fang, F.C., and Detweiler, C.S. (2013). Salmonella enterica Causes More Severe Inflammatory Disease in C57/BL6 Nramp1 G169Mice Than Sv129S6 Mice. Veterinary Pathology *50*, 867–876.

Broz, P., Newton, K., Lamkanfi, M., Mariathasan, S., Dixit, V.M., and Monack, D.M. (2010). Redundant roles for inflammasome receptors NLRP3 and NLRC4 in host defense against *Salmonella*. The Journal of Experimental Medicine *207*, 1745–1755.

Bueno, S.M., González, P.A., Carreño, L.J., Tobar, J.A., Mora, G.C., Pereda, C.J., Salazar-Onfray, F., and Kalergis, A.M. (2008). The capacity of *Salmonella* to survive inside dendritic cells and prevent antigen presentation to T cells is host specific. Immunology *124*, 522–533.

Buettner, M., and Lochner, M. (2016). Development and Function of Secondary and Tertiary Lymphoid Organs in the Small Intestine and the Colon. Frontiers in Immunology *7*.

Bumann, D. (2003). T cell receptor-transgenic mouse models for studying cellular immune responses to *Salmonella* in vivo. FEMS Immunology & Medical Microbiology *37*, 105–109.

Campbell, D.J. (2015). Control of Regulatory T Cell Migration, Function, and Homeostasis. The Journal of Immunology *195*, 2507–2513.

Campbell, C., Dikiy, S., Bhattarai, S.K., Chinen, T., Matheis, F., Calafiore, M., Hoyos, B., Hanash, A., Mucida, D., Bucci, V., et al. (2018). Extrathymically Generated Regulatory T Cells Establish a Niche for Intestinal Border-Dwelling Bacteria and Affect Physiologic Metabolite Balance. Immunity *48*, 1245-1257.e9.

Campbell, D.J., Kim, C.H., and Butcher, E.C. (2001). Separable effector T cell populations specialized for B cell help or tissue inflammation. Nature Immunology *2*, 876–881.

Cao, X., Cai, S.F., Fehniger, T.A., Song, J., Collins, L.I., Piwnica-Worms, D.R., and Ley, T.J. (2007). Granzyme B and Perforin Are Important for Regulatory T Cell-Mediated Suppression of Tumor Clearance. Immunity *27*, 635–646.

Caprioli, F., Pallone, F., and Monteleone, G. (2008). Th17 immune response in IBD: A new pathogenic mechanism. Journal of Crohn's and Colitis *2*, 291–295.

Caron, J., Loredo-Osti, J.C., Laroche, L., Skamene, E., Morgan, K., and Malo, D. (2002). Identification of genetic loci controlling bacterial clearance in experimental Salmonella enteritidis infection: an unexpected role of Nramp1 (Slc11a1) in the persistence of infection in mice. Genes Immun. *3*, 196–204.

Cassani, B., Villablanca, E.J., Quintana, F.J., Love, P.E., Lacy–Hulbert, A., Blaner, W.S., Sparwasser, T., Snapper, S.B., Weiner, H.L., and Mora, J.R. (2011). Gut-Tropic T Cells That Express Integrin α4β7 and CCR9 Are Required for Induction of Oral Immune Tolerance in Mice. Gastroenterology *141*, 2109–2118.

Cerovic, V., Bain, C.C., Mowat, A.M., and Milling, S.W.F. (2014). Intestinal macrophages and dendritic cells: what's the difference? Trends in Immunology *35*, 270–277.

Chaudhry, A., Rudra, D., Treuting, P., Samstein, R.M., Liang, Y., Kas, A., and Rudensky, A.Y. (2009). CD4+ Regulatory T Cells Control TH17 Responses in a Stat3-Dependent Manner. Science *326*, 986–991.

Cheminay, C., Mohlenbrink, A., and Hensel, M. (2005). Intracellular Salmonella Inhibit Antigen Presentation by Dendritic Cells. The Journal of Immunology *174*, 2892–2899.

Chen, Z.M., and Jenkins, M.K. (1999). Clonal expansion of antigen-specific CD4 T cells following infection with Salmonella typhimurium is similar in susceptible (Itys) and resistant (Ityr) BALB/c mice. Infect. Immun. *67*, 2025–2029.

Chen, W., Jin, W., Hardegen, N., Lei, K., Li, L., Marinos, N., McGrady, G., and Wahl, S.M. (2003). Conversion of Peripheral $CD4^+CD25^-$ Naive T Cells to $CD4^+CD25^+$ Regulatory T Cells by TGF-β Induction of Transcription Factor *Foxp3*. The Journal of Experimental Medicine *198*, 1875–1886.

Chen, Y., Chauhan, S.K., Shao, C., Omoto, M., Inomata, T., and Dana, R. (2017). IFN-γ–Expressing Th17 Cells Are Required for Development of Severe Ocular Surface Autoimmunity. The Journal of Immunology *199*, 1163–1169.

Cherayil, B.J. (2009). Indoleamine 2,3-dioxygenase in intestinal immunity and inflammation: Inflammatory Bowel Diseases *15*, 1391–1396.

Cho, I., Yamanishi, S., Cox, L., Methé, B.A., Zavadil, J., Li, K., Gao, Z., Mahana, D., Raju, K., Teitler, I., et al. (2012). Antibiotics in early life alter the murine colonic microbiome and adiposity. Nature *488*, 621–626.

Clark, E.A., and Ledbetter, J.A. (1994). How B and T cells talk to each other. Nature *367*, 425–428.

Clark, L.B., Appleby, M.W., Brunkow, M.E., Wilkinson, J.E., Ziegler, S.F., and Ramsdell, F. (1999). Cellular and molecular characterization of the scurfy mouse mutant. J. Immunol. *162*, 2546–2554.

Clevers, H. (2013). The Intestinal Crypt, A Prototype Stem Cell Compartment. Cell *154*, 274–284.

Coburn, B., Li, Y., Owen, D., Vallance, B.A., and Finlay, B.B. (2005). Salmonella enterica Serovar Typhimurium Pathogenicity Island 2 Is Necessary for Complete Virulence in a Mouse Model of Infectious Enterocolitis. Infection and Immunity *73*, 3219–3227.

Collison, L.W., and Vignali, D.A.A. (2011). In vitro Treg suppression assays. Methods Mol. Biol. *707*, 21–37.

Collison, L.W., Workman, C.J., Kuo, T.T., Boyd, K., Wang, Y., Vignali, K.M., Cross, R., Sehy, D., Blumberg, R.S., and Vignali, D.A.A. (2007). The inhibitory cytokine IL-35 contributes to regulatory T-cell function. Nature *450*, 566–569.

Constant, S. (1995). Extent of T cell receptor ligation can determine the functional differentiation of naive CD4+ T cells. Journal of Experimental Medicine *182*, 1591–1596.

Coombes, J.L., Robinson, N.J., Maloy, K.J., Uhlig, H.H., and Powrie, F. (2005). Regulatory T cells and intestinal homeostasis. Immunological Reviews *204*, 184–194.

Coquet, J.M., Schuijs, M.J., Smyth, M.J., Deswarte, K., Beyaert, R., Braun, H., Boon, L., Hedestam, G.B.K., Nutt, S.L., Hammad, H., et al. (2015). Interleukin-21-Producing CD4+ T Cells Promote Type 2 Immunity to House Dust Mites. Immunity *43*, 318–330.

Craig, S.W., and Cebra, J.J. (1971). Peyer's patches: an enriched source of precursors for IgA-producing immunocytes in the rabbit. J. Exp. Med. *134*, 188–200.

Cretney, E., Xin, A., Shi, W., Minnich, M., Masson, F., Miasari, M., Belz, G.T., Smyth, G.K., Busslinger, M., Nutt, S.L., et al. (2011). The transcription factors Blimp-1 and IRF4 jointly control the differentiation and function of effector regulatory T cells. Nat. Immunol. *12*, 304–311.

Damsker, J.M., Hansen, A.M., and Caspi, R.R. (2010). Th1 and Th17 cells: Adversaries and collaborators. Annals of the New York Academy of Sciences *1183*, 211–221.

Daniel, V., Trojan, K., Adamek, M., and Opelz, G. (2015). IFNγ+ Treg in-vivo and in-vitro represent both activated nTreg and peripherally induced aTreg and remain phenotypically stable in-vitro after removal of the stimulus. BMC Immunology *16*.

Deaglio, S., Dwyer, K.M., Gao, W., Friedman, D., Usheva, A., Erat, A., Chen, J.-F., Enjyoji, K., Linden, J., Oukka, M., et al. (2007). Adenosine generation catalyzed by CD39 and CD73 expressed on regulatory T cells mediates immune suppression. The Journal of Experimental Medicine *204*, 1257–1265.

Denning, T.L., Kim, G., and Kronenberg, M. (2005). Cutting Edge: CD4+CD25+ Regulatory T Cells Impaired for Intestinal Homing Can Prevent Colitis. The Journal of Immunology *174*, 7487–7491.

Desai, M.S., Seekatz, A.M., Koropatkin, N.M., Kamada, N., Hickey, C.A., Wolter, M., Pudlo, N.A., Kitamoto, S., Terrapon, N., Muller, A., et al. (2016). A Dietary Fiber-Deprived Gut Microbiota Degrades the Colonic Mucus Barrier and Enhances Pathogen Susceptibility. Cell *167*, 1339-1353.e21.

Di Marco Barros, R., Roberts, N.A., Dart, R.J., Vantourout, P., Jandke, A., Nussbaumer, O., Deban, L., Cipolat, S., Hart, R., Iannitto, M.L., et al. (2016). Epithelia Use Butyrophilin-like Molecules to Shape Organ-Specific γδ T Cell Compartments. Cell *167*, 203-218.e17.

Donaldson, D.S., Bradford, B.M., Artis, D., and Mabbott, N.A. (2015). Reciprocal regulation of lymphoid tissue development in the large intestine by IL-25 and IL-23. Mucosal Immunology *8*, 582–595.

Dong, C., Juedes, A.E., Temann, U.-A., Shresta, S., Allison, J.P., Ruddle, N.H., and Flavell, R.A. (2001). ICOS co-stimulatory receptor is essential for T-cell activation and function. Nature *409*, 97–101.

Dougan, G., Hormaeche, C.E., and Maskell, D.J. (1987). Live oral Salmonella vaccines: potential use of attenuated strains as carriers of heterologous antigens to the immune system. Parasite Immunology *9*, 151–160.

Duarte, J.H., Zelenay, S., Bergman, M.-L., Martins, A.C., and Demengeot, J. (2009). Natural Treg cells spontaneously differentiate into pathogenic helper cells in lymphopenic conditions. European Journal of Immunology *39*, 948–955.

Duhen, R., Glatigny, S., Arbelaez, C.A., Blair, T.C., Oukka, M., and Bettelli, E. (2013). Cutting Edge: The Pathogenicity of IFN- -Producing Th17 Cells Is Independent of T-bet. The Journal of Immunology *190*, 4478–4482.

Duhen, T., Duhen, R., Lanzavecchia, A., Sallusto, F., and Campbell, D.J. (2012). Functionally distinct subsets of human FOXP3+ Treg cells that phenotypically mirror effector Th cells. Blood *119*, 4430–4440.

Duthoit, C.T., Mekala, D.J., Alli, R.S., and Geiger, T.L. (2005). Uncoupling of IL-2 signaling from cell cycle progression in naive CD4+ T cells by regulatory CD4+CD25+ T lymphocytes. J. Immunol. *174*, 155–163.

Earle, K., Tang, Q., Zhou, X., Liu, W., Zhu, S., Bonyhadi, M., and Bluestone, J. (2005). In vitro expanded human CD4+CD25+ regulatory T cells suppress effector T cell proliferation. Clinical Immunology *115*, 3–9.

Eastaff-Leung, N., Mabarrack, N., Barbour, A., Cummins, A., and Barry, S. (2010). Foxp3+ regulatory T cells, Th17 effector cells, and cytokine environment in inflammatory bowel disease. J. Clin. Immunol. *30*, 80–89.

Eberl, G. (2016). Immunity by equilibrium. Nature Reviews Immunology *16*, 524–532.

Elkord, E., Abd Al Samid, M., and Chaudhary, B. (2015). Helios, and not FoxP3, is the marker of activated Tregs expressing GARP/LAP. Oncotarget *6*, 20026–20036.

Elphick, D.A. (2005). Paneth cells: their role in innate immunity and inflammatory disease. Gut *54*, 1802–1809.

Erhardt, A., Wegscheid, C., Claass, B., Carambia, A., Herkel, J., Mittrucker, H.-W., Panzer, U., and Tiegs, G. (2011). CXCR3 Deficiency Exacerbates Liver Disease and Abrogates Tolerance in a Mouse Model of Immune-Mediated Hepatitis. The Journal of Immunology *186*, 5284–5293.

Ermund, A., Schütte, A., Johansson, M.E.V., Gustafsson, J.K., and Hansson, G.C. (2013). Studies of mucus in mouse stomach, small intestine, and colon. I. Gastrointestinal mucus layers have different properties depending on location as well as over the Peyer's patches. American Journal of Physiology-Gastrointestinal and Liver Physiology *305*, G341–G347.

Fahlén, L., Read, S., Gorelik, L., Hurst, S.D., Coffman, R.L., Flavell, R.A., and Powrie, F. (2005). T cells that cannot respond to TGF-β escape control by CD4 $^{+}$ CD25 $^{+}$ regulatory T cells. The Journal of Experimental Medicine *201*, 737–746.

Fallarino, F., Grohmann, U., Hwang, K.W., Orabona, C., Vacca, C., Bianchi, R., Belladonna, M.L., Fioretti, M.C., Alegre, M.-L., and Puccetti, P. (2003). Modulation of tryptophan catabolism by regulatory T cells. Nature Immunology *4*, 1206–1212.

Feasey, N.A., Dougan, G., Kingsley, R.A., Heyderman, R.S., and Gordon, M.A. (2012). Invasive non-typhoidal salmonella disease: an emerging and neglected tropical disease in Africa. The Lancet *379*, 2489–2499.

Fina, D., Sarra, M., Fantini, M.C., Rizzo, A., Caruso, R., Caprioli, F., Stolfi, C., Cardolini, I., Dottori, M., Boirivant, M., et al. (2008). Regulation of Gut Inflammation and Th17 Cell Response by Interleukin-21. Gastroenterology *134*, 1038-1048.e2.

Fischer, A., Zundler, S., Atreya, R., Rath, T., Voskens, C., Hirschmann, S., López-Posadas, R., Watson, A., Becker, C., Schuler, G., et al. (2016). Differential effects of α4β7 and GPR15 on homing of effector and regulatory T cells from patients with UC to the inflamed gut in vivo. Gut *65*, 1642–1664.

Fleming, L.L., and Floch, M.H. (1986). Digestion and absorption of fiber carbohydrate in the colon. Am. J. Gastroenterol. *81*, 507–511.

van der Flier, L.G., and Clevers, H. (2009). Stem Cells, Self-Renewal, and Differentiation in the Intestinal Epithelium. Annual Review of Physiology *71*, 241–260.

Fontenot, J.D., Gavin, M.A., and Rudensky, A.Y. (2003). Foxp3 programs the development and function of CD4+CD25+ regulatory T cells. Nature Immunology *4*, 330–336.

Fontenot, J.D., Rasmussen, J.P., Gavin, M.A., and Rudensky, A.Y. (2005). A function for interleukin 2 in Foxp3-expressing regulatory T cells. Nature Immunology *6*, 1142–1151.

Fritsche, G., Nairz, M., Libby, S.J., Fang, F.C., and Weiss, G. (2012). Slc11a1 (Nramp1) impairs growth of *Salmonella enterica* serovar *typhimurium* in macrophages via stimulation of lipocalin-2 expression. Journal of Leukocyte Biology *92*, 353–359.

Fuss, I.J., Neurath, M., Boirivant, M., Klein, J.S., de la Motte, C., Strong, S.A., Fiocchi, C., and Strober, W. (1996). Disparate CD4+ lamina propria (LP) lymphokine secretion profiles in inflammatory bowel disease. Crohn's disease LP cells manifest increased secretion of IFN-gamma, whereas ulcerative colitis LP cells manifest increased secretion of IL-5. J. Immunol. *157*, 1261–1270.

Garrett, W.S., Gordon, J.I., and Glimcher, L.H. (2010). Homeostasis and Inflammation in the Intestine. Cell *140*, 859–870.

Gavin, M.A., Rasmussen, J.P., Fontenot, J.D., Vasta, V., Manganiello, V.C., Beavo, J.A., and Rudensky, A.Y. (2007). Foxp3-dependent programme of regulatory T-cell differentiation. Nature *445*, 771–775.

Geissmann, F., Manz, M.G., Jung, S., Sieweke, M.H., Merad, M., and Ley, K. (2010). Development of Monocytes, Macrophages, and Dendritic Cells. Science *327*, 656–661.

Gerbe, F., Sidot, E., Smyth, D.J., Ohmoto, M., Matsumoto, I., Dardalhon, V., Cesses, P., Garnier, L., Pouzolles, M., Brulin, B., et al. (2016). Intestinal epithelial tuft cells initiate type 2 mucosal immunity to helminth parasites. Nature *529*, 226–230.

Gerriets, V.A., Kishton, R.J., Johnson, M.O., Cohen, S., Siska, P.J., Nichols, A.G., Warmoes, M.O., de Cubas, A.A., MacIver, N.J., Locasale, J.W., et al. (2016). Foxp3 and Toll-like receptor signaling balance Treg cell anabolic metabolism for suppression. Nature Immunology *17*, 1459–1466.

Gersemann, M., Becker, S., Kübler, I., Koslowski, M., Wang, G., Herrlinger, K.R., Griger, J., Fritz, P., Fellermann, K., Schwab, M., et al. (2009). Differences in goblet cell differentiation between Crohn's disease and ulcerative colitis. Differentiation *77*, 84–94.

Gimmi, C.D., Freeman, G.J., Gribben, J.G., Gray, G., and Nadler, L.M. (1993). Human T-cell clonal anergy is induced by antigen presentation in the absence of B7 costimulation. Proceedings of the National Academy of Sciences *90*, 6586–6590.

Girard, J.-P., Moussion, C., and Förster, R. (2012). HEVs, lymphatics and homeostatic immune cell trafficking in lymph nodes. Nature Reviews Immunology *12*, 762–773.

Godinez, I., Keestra, A.M., Spees, A., and Bäumler, A.J. (2011). The IL-23 axis in Salmonella gastroenteritis: The IL-23 axis in Salmonella gastroenteritis. Cellular Microbiology *13*, 1639–1647.

Goldberg, M.F., Roeske, E.K., Ward, L.N., Pengo, T., Dileepan, T., Kotov, D.I., and Jenkins, M.K. (2018). Salmonella Persist in Activated Macrophages in T Cell-Sparse

Granulomas but Are Contained by Surrounding CXCR3 Ligand-Positioned Th1 Cells. Immunity.

Gottschalk, R.A., Corse, E., and Allison, J.P. (2012). Expression of Helios in Peripherally Induced Foxp3+ Regulatory T Cells. The Journal of Immunology *188*, 976–980.

Grakoui, A. (1999). The Immunological Synapse: A Molecular Machine Controlling T Cell Activation. Science *285*, 221–227.

Grassl, G.A., Valdez, Y., Bergstrom, K.S.B., Vallance, B.A., and Finlay, B.B. (2008). Chronic Enteric Salmonella Infection in Mice Leads to Severe and Persistent Intestinal Fibrosis. Gastroenterology *134*, 768-780.e2.

Green, E.A., Gorelik, L., McGregor, C.M., Tran, E.H., and Flavell, R.A. (2003). CD4+CD25+ T regulatory cells control anti-islet CD8+ T cells through TGF- -TGF- receptor interactions in type 1 diabetes. Proceedings of the National Academy of Sciences *100*, 10878–10883.

Griffin, A.J., and McSorley, S.J. (2011). Development of protective immunity to Salmonella, a mucosal pathogen with a systemic agenda. Mucosal Immunology *4*, 371–382.

Griffin, A., Baraho-Hassan, D., and McSorley, S.J. (2009). Successful Treatment of Bacterial Infection Hinders Development of Acquired Immunity. The Journal of Immunology *183*, 1263–1270.

Griffin, A.J., Li, L.-X., Voedisch, S., Pabst, O., and McSorley, S.J. (2011). Dissemination of Persistent Intestinal Bacteria via the Mesenteric Lymph Nodes Causes Typhoid Relapse. Infection and Immunity *79*, 1479–1488.

Grossman, W.J., Verbsky, J.W., Barchet, W., Colonna, M., Atkinson, J.P., and Ley, T.J. (2004). Human T Regulatory Cells Can Use the Perforin Pathway to Cause Autologous Target Cell Death. Immunity *21*, 589–601.

Gu, S., Chen, D., Zhang, J.-N., Lv, X., Wang, K., Duan, L.-P., Nie, Y., and Wu, X.-L. (2013). Bacterial Community Mapping of the Mouse Gastrointestinal Tract. PLoS ONE *8*, e74957.

Gustafson, C.E., Higbee, D., Yeckes, A.R., Wilson, C.C., De Zoeten, E.F., Jedlicka, P., and Janoff, E.N. (2014). Limited expression of APRIL and its receptors prior to intestinal IgA plasma cell development during human infancy. Mucosal Immunology *7*, 467–477.

Guzman, C.A., Borsutzky, S., Griot-Wenk, M., Metcalfe, I.C., Pearman, J., Collioud, A., Favre, D., and Dietrich, G. (2006). Vaccines against typhoid fever. Vaccine *24*, 3804–3811.

Halim, L., Romano, M., McGregor, R., Correa, I., Pavlidis, P., Grageda, N., Hoong, S.-J., Yuksel, M., Jassem, W., Hannen, R.F., et al. (2017). An Atlas of Human Regulatory T

Helper-like Cells Reveals Features of Th2-like Tregs that Support a Tumorigenic Environment. Cell Reports *20*, 757–770.

Halle, S., Bumann, D., Herbrand, H., Willer, Y., Dahne, S., Forster, R., and Pabst, O. (2007). Solitary Intestinal Lymphoid Tissue Provides a Productive Port of Entry for Salmonella enterica Serovar Typhimurium. Infection and Immunity *75*, 1577–1585.

Hamada, H., Hiroi, T., Nishiyama, Y., Takahashi, H., Masunaga, Y., Hachimura, S., Kaminogawa, S., Takahashi-Iwanaga, H., Iwanaga, T., Kiyono, H., et al. (2002). Identification of Multiple Isolated Lymphoid Follicles on the Antimesenteric Wall of the Mouse Small Intestine. The Journal of Immunology *168*, 57–64.

Hansson, G.C. (2012). Role of mucus layers in gut infection and inflammation. Current Opinion in Microbiology *15*, 57–62.

Hapfelmeier, S., and Hardt, W.-D. (2005). A mouse model for S. typhimurium-induced enterocolitis. Trends Microbiol. *13*, 497–503.

Harbour, S.N., Maynard, C.L., Zindl, C.L., Schoeb, T.R., and Weaver, C.T. (2015). Th17 cells give rise to Th1 cells that are required for the pathogenesis of colitis. Proceedings of the National Academy of Sciences *112*, 7061–7066.

Hardison, J.L., Wrightsman, R.A., Carpenter, P.M., Lane, T.E., and Manning, J.E. (2006). The Chemokines CXCL9 and CXCL10 Promote a Protective Immune Response but Do Not Contribute to Cardiac Inflammation following Infection with Trypanosoma cruzi. Infection and Immunity *74*, 125–134.

Harrington, L.E., Hatton, R.D., Mangan, P.R., Turner, H., Murphy, T.L., Murphy, K.M., and Weaver, C.T. (2005). Interleukin 17-producing CD4+ effector T cells develop via a lineage distinct from the T helper type 1 and 2 lineages. Nat. Immunol. *6*, 1123–1132.

Harrington, L.E., Mangan, P.R., and Weaver, C.T. (2006). Expanding the effector CD4 T-cell repertoire: the Th17 lineage. Current Opinion in Immunology *18*, 349–356.

Harris, N. (2016). The enigmatic tuft cell in immunity. Science *351*, 1264–1265.

Hawrylowicz, C.M., and O'Garra, A. (2005). Potential role of interleukin-10-secreting regulatory T cells in allergy and asthma. Nature Reviews Immunology *5*, 271–283.

Hayatsu, N., Miyao, T., Tachibana, M., Murakami, R., Kimura, A., Kato, T., Kawakami, E., Endo, T.A., Setoguchi, R., Watarai, H., et al. (2017). Analyses of a Mutant Foxp3 Allele Reveal BATF as a Critical Transcription Factor in the Differentiation and Accumulation of Tissue Regulatory T Cells. Immunity *47*, 268-283.e9.

Hedrick, S.M., Cohen, D.I., Nielsen, E.A., and Davis, M.M. (1984). Isolation of cDNA clones encoding T cell-specific membrane-associated proteins. Nature *308*, 149–153.

Heller, F., Florian, P., Bojarski, C., Richter, J., Christ, M., Hillenbrand, B., Mankertz, J., Gitter, A., Burgel, N., and Fromm, M. (2005). Interleukin-13 Is the Key Effector Th2

Cytokine in Ulcerative Colitis That Affects Epithelial Tight Junctions, Apoptosis, and Cell Restitution. Gastroenterology *129*, 550–564.

Hepworth, M.R., Monticelli, L.A., Fung, T.C., Ziegler, C.G.K., Grunberg, S., Sinha, R., Mantegazza, A.R., Ma, H.-L., Crawford, A., Angelosanto, J.M., et al. (2013). Innate lymphoid cells regulate CD4+ T-cell responses to intestinal commensal bacteria. Nature *498*, 113–117.

Herbrand, H., Bernhardt, G., Forster, R., and Pabst, O. (2008). Dynamics and Function of Solitary Intestinal Lymphoid Tissue. Critical Reviews™ in Immunology *28*, 1–13.

Herman, A.E., Freeman, G.J., Mathis, D., and Benoist, C. (2004). CD4+CD25+ T regulatory cells dependent on ICOS promote regulation of effector cells in the prediabetic lesion. J. Exp. Med. *199*, 1479–1489.

Hess, J., Ladel, C., Miko, D., and Kaufmann, S.H. (1996). Salmonella typhimurium aroA- infection in gene-targeted immunodeficient mice: major role of CD4+ TCR-alpha beta cells and IFN-gamma in bacterial clearance independent of intracellular location. J. Immunol. *156*, 3321–3326.

Hoiseth, S.K., and Stocker, B.A.D. (1981). Aromatic-dependent Salmonella typhimurium are non-virulent and effective as live vaccines. Nature *291*, 238–239.

Holtmeier, W., and Kabelitz, D. (2005). gammadelta T cells link innate and adaptive immune responses. Chem Immunol Allergy *86*, 151–183.

Houot, R., Perrot, I., Garcia, E., Durand, I., and Lebecque, S. (2006). Human CD4+CD25high regulatory T cells modulate myeloid but not plasmacytoid dendritic cells activation. J. Immunol. *176*, 5293–5298.

Houston, S.A., Cerovic, V., Thomson, C., Brewer, J., Mowat, A.M., and Milling, S. (2015). The lymph nodes draining the small intestine and colon are anatomically separate and immunologically distinct. Mucosal Immunology 9, 468-478.

Howitt, M.R., Lavoie, S., Michaud, M., Blum, A.M., Tran, S.V., Weinstock, J.V., Gallini, C.A., Redding, K., Margolskee, R.F., Osborne, L.C., et al. (2016). Tuft cells, taste-chemosensory cells, orchestrate parasite type 2 immunity in the gut. Science *351*, 1329–1333.

Hsieh, C., Macatonia, S., Tripp, C., Wolf, S., O'Garra, A., and Murphy, K. (1993). Development of TH1 CD4+ T cells through IL-12 produced by Listeria-induced macrophages. Science *260*, 547–549.

Huang, C.-T., Workman, C.J., Flies, D., Pan, X., Marson, A.L., Zhou, G., Hipkiss, E.L., Ravi, S., Kowalski, J., Levitsky, H.I., et al. (2004). Role of LAG-3 in regulatory T cells. Immunity *21*, 503–513.

Huang, F.-P., Platt, N., Wykes, M., Major, J.R., Powell, T.J., Jenkins, C.D., and MacPherson, G.G. (2000). A Discrete Subpopulation of Dendritic Cells Transports

Apoptotic Intestinal Epithelial Cells to T Cell Areas of Mesenteric Lymph Nodes. Journal of Experimental Medicine *191*, 435–444.

Huter, E.N., Stummvoll, G.H., DiPaolo, R.J., Glass, D.D., and Shevach, E.M. (2008). Cutting Edge: Antigen-Specific TGF -Induced Regulatory T Cells Suppress Th17-Mediated Autoimmune Disease. The Journal of Immunology *181*, 8209–8213.

Islam, S.A., Chang, D.S., Colvin, R.A., Byrne, M.H., McCully, M.L., Moser, B., Lira, S.A., Charo, I.F., and Luster, A.D. (2011). Mouse CCL8, a CCR8 agonist, promotes atopic dermatitis by recruiting IL-5+ TH2 cells. Nature Immunology *12*, 167–177.

Ivanov, I.I., McKenzie, B.S., Zhou, L., Tadokoro, C.E., Lepelley, A., Lafaille, J.J., Cua, D.J., and Littman, D.R. (2006). The Orphan Nuclear Receptor RORγt Directs the Differentiation Program of Proinflammatory IL-17+ T Helper Cells. Cell *126*, 1121–1133.

Iwasaki, A., and Kelsall, B.L. (1999). I. Mucosal dendritic cells: their specialized role in initiating T cell responses. American Journal of Physiology-Gastrointestinal and Liver Physiology *276*, G1074–G1078.

Iwasaki, A., and Kelsall, B.L. (2000). Localization of distinct Peyer's patch dendritic cell subsets and their recruitment by chemokines macrophage inflammatory protein (MIP)-3alpha, MIP-3beta, and secondary lymphoid organ chemokine. J. Exp. Med. *191*, 1381–1394.

Jenkins, M.K., Khoruts, A., Ingulli, E., Mueller, D.L., McSorley, S.J., Reinhardt, R.L., Itano, A., and Pape, K.A. (2001). In vivo activation of antigen-specific CD4 T cells. Annu. Rev. Immunol. *19*, 23–45.

Jepson, M.A., and Clark, M.A. (2001). The role of M cells in Salmonella infection. Microbes Infect. *3*, 1183–1190.

Joetham, A., Takeda, K., Takada, K., Taube, C., Miyahara, N., Matsubara, S., Matsubara, S., Koya, T., Rha, Y.-H., Dakhama, A., et al. (2007). Naturally occurring lung CD4(+)CD25(+) T cell regulation of airway allergic responses depends on IL-10 induction of TGF-beta. J. Immunol. *178*, 1433–1442.

Johanns, T.M., Ertelt, J.M., Rowe, J.H., and Way, S.S. (2010). Regulatory T Cell Suppressive Potency Dictates the Balance between Bacterial Proliferation and Clearance during Persistent Salmonella Infection. PLoS Pathogens *6*, e1001043.

Johansson, M.E.V. (2014). Mucus layers in inflammatory bowel disease. Inflamm. Bowel Dis. *20*, 2124–2131.

Johansson, M.E.V., Gustafsson, J.K., Holmén-Larsson, J., Jabbar, K.S., Xia, L., Xu, H., Ghishan, F.K., Carvalho, F.A., Gewirtz, A.T., Sjövall, H., et al. (2014). Bacteria penetrate the normally impenetrable inner colon mucus layer in both murine colitis models and patients with ulcerative colitis. Gut *63*, 281–291.

Jones, B.D. (1994). Salmonella typhimurium initiates murine infection by penetrating and destroying the specialized epithelial M cells of the Peyer's patches. Journal of Experimental Medicine *180*, 15–23.

Jung, C., Hugot, J.-P., and Barreau, F. (2010). Peyer's Patches: The Immune Sensors of the Intestine. International Journal of Inflammation *2010*, 1–12.

Junt, T., Moseman, E.A., Iannacone, M., Massberg, S., Lang, P.A., Boes, M., Fink, K., Henrickson, S.E., Shayakhmetov, D.M., Di Paolo, N.C., et al. (2007). Subcapsular sinus macrophages in lymph nodes clear lymph-borne viruses and present them to antiviral B cells. Nature *450*, 110–114.

Kägi, D., Vignaux, F., Ledermann, B., Bürki, K., Depraetere, V., Nagata, S., Hengartner, H., and Golstein, P. (1994). Fas and perforin pathways as major mechanisms of T cell-mediated cytotoxicity. Science *265*, 528–530.

Kain, M.J.W., and Owens, B.M.J. (2013). Stromal cell regulation of homeostatic and inflammatory lymphoid organogenesis. Immunology *140*, 12–21.

Kaiser, P., Diard, M., Stecher, B., and Hardt, W.-D. (2012). The streptomycin mouse model for Salmonella diarrhea: functional analysis of the microbiota, the pathogen's virulence factors, and the host's mucosal immune response: Streptomycin mouse model. Immunological Reviews *245*, 56–83.

Kaser, A., Ludwiczek, O., Holzmann, S., Moschen, A.R., Weiss, G., Enrich, B., Graziadei, I., Dunzendorfer, S., Wiedermann, C.J., Mürzl, E., et al. (2004). Increased Expression of CCL20 in Human Inflammatory Bowel Disease. Journal of Clinical Immunology *24*, 74–85.

Kearley, J., Barker, J.E., Robinson, D.S., and Lloyd, C.M. (2005). Resolution of airway inflammation and hyperreactivity after in vivo transfer of CD4+CD25+ regulatory T cells is interleukin 10 dependent. J. Exp. Med. *202*, 1539–1547.

Keestra, A.M., Godinez, I., Xavier, M.N., Winter, M.G., Winter, S.E., Tsolis, R.M., and Bäumler, A.J. (2011). Early MyD88-Dependent Induction of Interleukin-17A Expression during Salmonella Colitis. Infection and Immunity *79*, 3131–3140.

Kim, C.H., Rott, L., Kunkel, E.J., Genovese, M.C., Andrew, D.P., Wu, L., and Butcher, E.C. (2001). Rules of chemokine receptor association with T cell polarization in vivo. J. Clin. Invest. *108*, 1331–1339.

Kim, H.-J., Barnitz, R.A., Kreslavsky, T., Brown, F.D., Moffett, H., Lemieux, M.E., Kaygusuz, Y., Meissner, T., Holderried, T.A.W., Chan, S., et al. (2015). Stable inhibitory activity of regulatory T cells requires the transcription factor Helios. Science *350*, 334–339.

Kim, J., Lahl, K., Hori, S., Loddenkemper, C., Chaudhry, A., deRoos, P., Rudensky, A., and Sparwasser, T. (2009). Cutting Edge: Depletion of Foxp3+ Cells Leads to Induction

of Autoimmunity by Specific Ablation of Regulatory T Cells in Genetically Targeted Mice. The Journal of Immunology *183*, 7631–7634.

Kim, J.M., Rasmussen, J.P., and Rudensky, A.Y. (2007). Regulatory T cells prevent catastrophic autoimmunity throughout the lifespan of mice. Nature Immunology *8*, 191–197.

Kim, K.S., Hong, S.-W., Han, D., Yi, J., Jung, J., Yang, B.-G., Lee, J.Y., Lee, M., and Surh, C.D. (2016). Dietary antigens limit mucosal immunity by inducing regulatory T cells in the small intestine. Science *351*, 858–863.

Kim, S.V., Xiang, W.V., Kwak, C., Yang, Y., Lin, X.W., Ota, M., Sarpel, U., Rifkin, D.B., Xu, R., and Littman, D.R. (2013). GPR15-Mediated Homing Controls Immune Homeostasis in the Large Intestine Mucosa. Science *340*, 1456–1459.

Knoop, K.A., and Newberry, R.D. (2012). Isolated Lymphoid Follicles are Dynamic Reservoirs for the Induction of Intestinal IgA. Frontiers in Immunology *3*.

Knoop, K.A., Gustafsson, J.K., McDonald, K.G., Kulkarni, D.H., Kassel, R., and Newberry, R.D. (2017). Antibiotics promote the sampling of luminal antigens and bacteria via colonic goblet cell associated antigen passages. Gut Microbes *8*, 400–411.

Kobayashi, T., Okamoto, S., Hisamatsu, T., Kamada, N., Chinen, H., Saito, R., Kitazume, M.T., Nakazawa, A., Sugita, A., Koganei, K., et al. (2008). IL23 differentially regulates the Th1/Th17 balance in ulcerative colitis and Crohn's disease. Gut *57*, 1682–1689.

Kobie, J.J., Shah, P.R., Yang, L., Rebhahn, J.A., Fowell, D.J., and Mosmann, T.R. (2006). T regulatory and primed uncommitted CD4 T cells express CD73, which suppresses effector CD4 T cells by converting 5'-adenosine monophosphate to adenosine. J. Immunol. *177*, 6780–6786.

Koch, M.A., Tucker-Heard, G., Perdue, N.R., Killebrew, J.R., Urdahl, K.B., and Campbell, D.J. (2009). The transcription factor T-bet controls regulatory T cell homeostasis and function during type 1 inflammation. Nature Immunology *10*, 595–602.

Kraehenbuhl, J.-P., and Neutra, M.R. (2000). Epithelial M Cells: Differentiation and Function. Annual Review of Cell and Developmental Biology *16*, 301–332.

Kuka, M., and Iannacone, M. (2014). The role of lymph node sinus macrophages in host defense: LN macrophages orchestrate antimicrobial immunity. Annals of the New York Academy of Sciences *1319*, 38–46.

Kulkarni, D.H., McDonald, K.G., Knoop, K.A., Gustafsson, J.K., Kozlowski, K.M., Hunstad, D.A., Miller, M.J., and Newberry, R.D. (2018). Goblet cell associated antigen passages are inhibited during Salmonella typhimurium infection to prevent pathogen dissemination and limit responses to dietary antigens. Mucosal Immunology *11*, 1103–1113.

Kunkel, E.J., Campbell, J.J., Haraldsen, G., Pan, J., Boisvert, J., Roberts, A.I., Ebert, E.C., Vierra, M.A., Goodman, S.B., Genovese, M.C., et al. (2000). Lymphocyte Cc Chemokine

Receptor 9 and Epithelial Thymus-Expressed Chemokine (Teck) Expression Distinguish the Small Intestinal Immune Compartment: Epithelial Expression of Tissue-Specific Chemokines as an Organizing Principle in Regional Immunity. The Journal of Experimental Medicine *192*, 761–768.

Kupz, A., Guarda, G., Gebhardt, T., Sander, L.E., Short, K.R., Diavatopoulos, D.A., Wijburg, O.L.C., Cao, H., Waithman, J.C., Chen, W., et al. (2012). NLRC4 inflammasomes in dendritic cells regulate noncognate effector function by memory $CD8^+$ T cells. Nat. Immunol. *13*, 162–169.

Kupz, A., Scott, T.A., Belz, G.T., Andrews, D.M., Greyer, M., Lew, A.M., Brooks, A.G., Smyth, M.J., Curtiss, R., Bedoui, S., et al. (2013). Contribution of Thy1+ NK cells to protective IFN- production during Salmonella Typhimurium infections. Proceedings of the National Academy of Sciences *110*, 2252–2257.

Kupz, A., Bedoui, S., and Strugnell, R.A. (2014). Cellular Requirements for Systemic Control of Salmonella enterica Serovar Typhimurium Infections in Mice. Infection and Immunity *82*, 4997–5004.

Kursar, M., Bonhagen, K., Kohler, A., Kamradt, T., Kaufmann, S.H.E., and Mittrucker, H.-W. (2002). Organ-Specific CD4+ T Cell Response During Listeria monocytogenes Infection. The Journal of Immunology *168*, 6382–6387.

Lahl, K., and Sparwasser, T. (2011). In Vivo Depletion of FoxP3+ Tregs Using the DEREG Mouse Model. In Regulatory T Cells, G. Kassiotis, and A. Liston, eds. (Totowa, NJ: Humana Press), pp. 157–172.

Lahl, K., Loddenkemper, C., Drouin, C., Freyer, J., Arnason, J., Eberl, G., Hamann, A., Wagner, H., Huehn, J., and Sparwasser, T. (2007). Selective depletion of $Foxp3^+$ regulatory T cells induces a scurfy-like disease. The Journal of Experimental Medicine *204*, 57–63.

Lahl, K., Sweere, J., Pan, J., and Butcher, E. (2014). Orphan chemoattractant receptor GPR15 mediates dendritic epidermal T-cell recruitment to the skin: Immunomodulation. European Journal of Immunology *44*, 2577–2581.

Lai, N.Y., Musser, M.A., Pinho-Ribeiro, F.A., Baral, P., Ma, P., Potts, D.E., Chen, Z., Paik, D., Soualhi, S., Shi, H., et al. (2019). Gut-innervating nociceptor neurons protect against enteric infection by modulating the microbiota and Peyer's patch microfold cells. BioRxiv.

Langenkamp, A., Messi, M., Lanzavecchia, A., and Sallusto, F. (2000). Kinetics of dendritic cell activation: impact on priming of TH1, TH2 and nonpolarized T cells. Nature Immunology *1*, 311–316.

Lapaque, N., Hutchinson, J.L., Jones, D.C., Meresse, S., Holden, D.W., Trowsdale, J., and Kelly, A.P. (2009). Salmonella regulates polyubiquitination and surface expression of MHC class II antigens. Proceedings of the National Academy of Sciences *106*, 14052–14057.

Lathrop, S.K., Bloom, S.M., Rao, S.M., Nutsch, K., Lio, C.-W., Santacruz, N., Peterson, D.A., Stappenbeck, T.S., and Hsieh, C.-S. (2011). Peripheral education of the immune system by colonic commensal microbiota. Nature *478*, 250–254.

Lawley, T.D., Bouley, D.M., Hoy, Y.E., Gerke, C., Relman, D.A., and Monack, D.M. (2008). Host Transmission of Salmonella enterica Serovar Typhimurium Is Controlled by Virulence Factors and Indigenous Intestinal Microbiota. Infection and Immunity *76*, 403–416.

Lee, H.-M., Bautista, J.L., Scott-Browne, J., Mohan, J.F., and Hsieh, C.-S. (2012a). A Broad Range of Self-Reactivity Drives Thymic Regulatory T Cell Selection to Limit Responses to Self. Immunity *37*, 475–486.

Lee, S.-J., McLachlan, J.B., Kurtz, J.R., Fan, D., Winter, S.E., Baumler, A.J., Jenkins, M.K., and McSorley, S.J. (2012b). Temporal Expression of Bacterial Proteins Instructs Host CD4 T Cell Expansion and Th17 Development. PLoS Pathogens *8*, e1002499.

Leitner, J., Rieger, A., Pickl, W.F., Zlabinger, G., Grabmeier-Pfistershammer, K., and Steinberger, P. (2013). TIM-3 Does Not Act as a Receptor for Galectin-9. PLoS Pathogens *9*, e1003253.

Lelouard, H., Fallet, M., de Bovis, B., Méresse, S., and Gorvel, J. (2012). Peyer's Patch Dendritic Cells Sample Antigens by Extending Dendrites Through M Cell-Specific Transcellular Pores. Gastroenterology *142*, 592-601.e3.

Levine, A.G., Medoza, A., Hemmers, S., Moltedo, B., Niec, R.E., Schizas, M., Hoyos, B.E., Putintseva, E.V., Chaudhry, A., Dikiy, S., et al. (2017). Stability and function of regulatory T cells expressing the transcription factor T-bet. Nature *546*, 421–425.

Lewkowich, I.P., Herman, N.S., Schleifer, K.W., Dance, M.P., Chen, B.L., Dienger, K.M., Sproles, A.A., Shah, J.S., Köhl, J., Belkaid, Y., et al. (2005). CD4 $^{+}$ CD25 $^{+}$ T cells protect against experimentally induced asthma and alter pulmonary dendritic cell phenotype and function. The Journal of Experimental Medicine *202*, 1549–1561.

Li, J., Ueno, A., Fort Gasia, M., Luider, J., Wang, T., Hirota, C., Jijon, H.B., Deane, M., Tom, M., Chan, R., et al. (2016). Profiles of Lamina Propria T Helper Cell Subsets Discriminate Between Ulcerative Colitis and Crohn's Disease: Inflammatory Bowel Diseases *22*, 1779–1792.

Li, M.O., Wan, Y.Y., Sanjabi, S., Robertson, A.-K.L., and Flavell, R.A. (2006). Transforming growth factor-β regulation of immune responses. Annual Review of Immunology *24*, 99–146.

Liang, S.C., Tan, X.-Y., Luxenberg, D.P., Karim, R., Dunussi-Joannopoulos, K., Collins, M., and Fouser, L.A. (2006). Interleukin (IL)-22 and IL-17 are coexpressed by Th17 cells and cooperatively enhance expression of antimicrobial peptides. The Journal of Experimental Medicine *203*, 2271–2279.

Lievin-Le Moal, V., and Servin, A.L. (2006). The Front Line of Enteric Host Defense against Unwelcome Intrusion of Harmful Microorganisms: Mucins, Antimicrobial Peptides, and Microbiota. Clinical Microbiology Reviews *19*, 315–337.

Lim, H.W., Broxmeyer, H.E., and Kim, C.H. (2006). Regulation of Trafficking Receptor Expression in Human Forkhead Box P3+ Regulatory T Cells. The Journal of Immunology *177*, 840–851.

Lim, H.W., Lee, J., Hillsamer, P., and Kim, C.H. (2008). Human Th17 Cells Share Major Trafficking Receptors with Both Polarized Effector T Cells and FOXP3+ Regulatory T Cells. The Journal of Immunology *180*, 122–129.

Linsley, P.S. (1991). Binding of the B cell activation antigen B7 to CD28 costimulates T cell proliferation and interleukin 2 mRNA accumulation. Journal of Experimental Medicine *173*, 721–730.

Linsley, P.S., Brady, W., Urnes, M., Grosmaire, L.S., Damle, N.K., and Ledbetter, J.A. (1991). CTLA-4 is a second receptor for the B cell activation antigen B7. The Journal of Experimental Medicine *174*, 561–569.

Liu, Z., Gerner, M.Y., Van Panhuys, N., Levine, A.G., Rudensky, A.Y., and Germain, R.N. (2015). Immune homeostasis enforced by co-localized effector and regulatory T cells. Nature *528*, 225–230.

Lochner, M., Berard, M., Sawa, S., Hauer, S., Gaboriau-Routhiau, V., Fernandez, T.D., Snel, J., Bousso, P., Cerf-Bensussan, N., and Eberl, G. (2011). Restricted Microbiota and Absence of Cognate TCR Antigen Leads to an Unbalanced Generation of Th17 Cells. The Journal of Immunology *186*, 1531–1537.

Lorenz, R.G., and Newberry, R.D. (2004). Isolated Lymphoid Follicles Can Function as Sites for Induction of Mucosal Immune Responses. Annals of the New York Academy of Sciences *1029*, 44–57.

Luther, S.A., Tang, H.L., Hyman, P.L., Farr, A.G., and Cyster, J.G. (2000). Coexpression of the chemokines ELC and SLC by T zone stromal cells and deletion of the ELC gene in the plt/plt mouse. Proceedings of the National Academy of Sciences *97*, 12694–12699.

Mabbott, N.A., Donaldson, D.S., Ohno, H., Williams, I.R., and Mahajan, A. (2013). Microfold (M) cells: important immunosurveillance posts in the intestinal epithelium. Mucosal Immunology *6*, 666–677.

Macatonia, S.E., Hosken, N.A., Litton, M., Vieira, P., Hsieh, C.S., Culpepper, J.A., Wysocka, M., Trinchieri, G., Murphy, K.M., and O'Garra, A. (1995). Dendritic cells produce IL-12 and direct the development of Th1 cells from naive CD4+ T cells. J. Immunol. *154*, 5071–5079.

Macpherson, A.J., and Smith, K. (2006). Mesenteric lymph nodes at the center of immune anatomy. The Journal of Experimental Medicine *203*, 497–500.

Maizels, R.M., and Smith, K.A. (2011). Regulatory T Cells in Infection. In Advances in Immunology, (Elsevier), pp. 73–136.

Maloy, K.J., Salaun, L., Cahill, R., Dougan, G., Saunders, N.J., and Powrie, F. (2003). CD4+CD25+ T(R) cells suppress innate immune pathology through cytokine-dependent mechanisms. J. Exp. Med. *197*, 111–119.

Man, S.M., Hopkins, L.J., Nugent, E., Cox, S., Gluck, I.M., Tourlomousis, P., Wright, J.A., Cicuta, P., Monie, T.P., and Bryant, C.E. (2014). Inflammasome activation causes dual recruitment of NLRC4 and NLRP3 to the same macromolecular complex. Proceedings of the National Academy of Sciences *111*, 7403–7408.

Mangan, P.R., Harrington, L.E., O'Quinn, D.B., Helms, W.S., Bullard, D.C., Elson, C.O., Hatton, R.D., Wahl, S.M., Schoeb, T.R., and Weaver, C.T. (2006). Transforming growth factor-beta induces development of the T(H)17 lineage. Nature *441*, 231–234.

Marcobal, A., Southwick, A.M., Earle, K.A., and Sonnenburg, J.L. (2013). A refined palate: Bacterial consumption of host glycans in the gut. Glycobiology *23*, 1038–1046.

Marteau, P., Pochart, P., Dore, J., Bera-Maillet, C., Bernalier, A., and Corthier, G. (2001). Comparative Study of Bacterial Groups within the Human Cecal and Fecal Microbiota. Applied and Environmental Microbiology *67*, 4939–4942.

Martens, E.C., Neumann, M., and Desai, M.S. (2018). Interactions of commensal and pathogenic microorganisms with the intestinal mucosal barrier. Nature Reviews Microbiology *16*, 457–470.

Martinez-Argudo, I., and Jepson, M.A. (2008). Salmonella translocates across an in vitro M cell model independently of SPI-1 and SPI-2. Microbiology *154*, 3887–3894.

Mastroeni, P., Simmons, C., Fowler, R., Hormaeche, C.E., and Dougan, G. (2000). Igh-6(-/-) (B-cell-deficient) mice fail to mount solid acquired resistance to oral challenge with virulent Salmonella enterica serovar typhimurium and show impaired Th1 T-cell responses to Salmonella antigens. Infect. Immun. *68*, 46–53.

Mastroeni, P., Chabalgoity, J.A., Dunstan, S.J., Maskell, D.J., and Dougan, G. (2001). Salmonella: Immune Responses and Vaccines. The Veterinary Journal *161*, 132–164.

Mayassi, T., and Jabri, B. (2018). Human intraepithelial lymphocytes. Mucosal Immunol *11*, 1281–1289.

Mayer, C.T., Lahl, K., Milanez-Almeida, P., Watts, D., Dittmer, U., Fyhrquist, N., Huehn, J., Kopf, M., Kretschmer, K., Rouse, B., et al. (2014a). Advantages of Foxp3 $^{+}$ regulatory T cell depletion using DEREG mice: Advantages of Foxp3 $^{+}$ regulatory T cell depletion. Immunity, Inflammation and Disease *2*, 162–165.

Mayer, J.U., Demiri, M., Agace, W.W., MacDonald, A.S., Svensson-Frej, M., and Milling, S.W. (2017). Different populations of CD11b+ dendritic cells drive Th2 responses in the small intestine and colon. Nature Communications *8*, 15820.

Mayer, L., Sandborn, W.J., Stepanov, Y., Geboes, K., Hardi, R., Yellin, M., Tao, X., Xu, L.A., Salter-Cid, L., Gujrathi, S., et al. (2014b). Anti-IP-10 antibody (BMS-936557) for ulcerative colitis: a phase II randomised study. Gut *63*, 442–450.

Mayuzumi, H., Inagaki-Ohara, K., Uyttenhove, C., Okamoto, Y., and Matsuzaki, G. (2010). Interleukin-17A is required to suppress invasion of Salmonella enterica serovar Typhimurium to enteric mucosa: Importance of IL-17A in innate mucosal responses to Salmonella. Immunology *131*, 377–385.

McArthur, M.A., Fresnay, S., Magder, L.S., Darton, T.C., Jones, C., Waddington, C.S., Blohmke, C.J., Dougan, G., Angus, B., Levine, M.M., et al. (2015). Activation of Salmonella Typhi-Specific Regulatory T Cells in Typhoid Disease in a Wild-Type S. Typhi Challenge Model. PLOS Pathogens *11*, e1004914.

McDole, J.R., Wheeler, L.W., McDonald, K.G., Wang, B., Konjufca, V., Knoop, K.A., Newberry, R.D., and Miller, M.J. (2012). Goblet cells deliver luminal antigen to CD103+ dendritic cells in the small intestine. Nature *483*, 345–349.

McGuckin, M.A., and Hasnain, S.Z. (2017). Goblet cells as mucosal sentinels for immunity. Mucosal Immunology *10*, 1118–1121.

McSorley, S.J. (2014). The Role of Non-Cognate T Cell Stimulation during Intracellular Bacterial Infection. Frontiers in Immunology *5*.

McSorley, S.J., Asch, S., Costalonga, M., Reinhardt, R.L., and Jenkins, M.K. (2002). Tracking salmonella-specific CD4 T cells in vivo reveals a local mucosal response to a disseminated infection. Immunity *16*, 365–377.

Mellor, A.L., and Munn, D.H. (2004). Ido expression by dendritic cells: tolerance and tryptophan catabolism. Nature Reviews Immunology *4*, 762–774.

Meresse, B., Malamut, G., and Cerf-Bensussan, N. (2012). Celiac disease: an immunological jigsaw. Immunity *36*, 907–919.

Miao, E.A., Alpuche-Aranda, C.M., Dors, M., Clark, A.E., Bader, M.W., Miller, S.I., and Aderem, A. (2006). Cytoplasmic flagellin activates caspase-1 and secretion of interleukin 1beta via Ipaf. Nat. Immunol. *7*, 569–575.

Miragaia, R.J., Gomes, T., Chomka, A., Jardine, L., Riedel, A., Hegazy, A.N., Whibley, N., Tucci, A., Chen, X., Lindeman, I., et al. (2019). Single-Cell Transcriptomics of Regulatory T Cells Reveals Trajectories of Tissue Adaptation. Immunity.

Misra, N., Bayry, J., Lacroix-Desmazes, S., Kazatchkine, M.D., and Kaveri, S.V. (2004). Cutting edge: human CD4+CD25+ T cells restrain the maturation and antigen-presenting function of dendritic cells. J. Immunol. *172*, 4676–4680.

Mittrücker, H.W., Raupach, B., Köhler, A., and Kaufmann, S.H. (2000). Cutting edge: role of B lymphocytes in protective immunity against Salmonella typhimurium infection. J. Immunol. *164*, 1648–1652.

Miyara, M., and Sakaguchi, S. (2007). Natural regulatory T cells: mechanisms of suppression. Trends in Molecular Medicine *13*, 108–116.

Mondino, A., Khoruts, A., and Jenkins, M.K. (1996). The anatomy of T-cell activation and tolerance. Proceedings of the National Academy of Sciences *93*, 2245–2252.

Moon, J.J., and McSorley, S.J. (2009). Tracking the Dynamics of Salmonella Specific T Cell Responses. In Visualizing Immunity, M. Dustin, and D. McGavern, eds. (Berlin, Heidelberg: Springer Berlin Heidelberg), pp. 179–198.

Moon, J.J., Chu, H.H., Pepper, M., McSorley, S.J., Jameson, S.C., Kedl, R.M., and Jenkins, M.K. (2007). Naive CD4+ T Cell Frequency Varies for Different Epitopes and Predicts Repertoire Diversity and Response Magnitude. Immunity *27*, 203–213.

Mooney, J.P., Lee, S.-J., Lokken, K.L., Nanton, M.R., Nuccio, S.-P., McSorley, S.J., and Tsolis, R.M. (2015). Transient Loss of Protection Afforded by a Live Attenuated Non-typhoidal Salmonella Vaccine in Mice Co-infected with Malaria. PLOS Neglected Tropical Diseases *9*, e0004027.

Morrison, D.J., and Preston, T. (2016). Formation of short chain fatty acids by the gut microbiota and their impact on human metabolism. Gut Microbes *7*, 189–200.

Moser, B., Wolf, M., Walz, A., and Loetscher, P. (2004). Chemokines: multiple levels of leukocyte migration control☆. Trends in Immunology *25*, 75–84.

Mosmann, T.R., and Sad, S. (1996). The expanding universe of T-cell subsets: Th1, Th2 and more. Immunology Today *17*, 138–146.

Mottet, C., Uhlig, H.H., and Powrie, F. (2003). Cutting Edge: Cure of Colitis by CD4+CD25+ Regulatory T Cells. The Journal of Immunology *170*, 3939–3943.

Mougiakakos, D., Choudhury, A., Lladser, A., Kiessling, R., and Johansson, C.C. (2010). Regulatory T Cells in Cancer. In Advances in Cancer Research, (Elsevier), pp. 57–117.

Mowat, A.M., and Agace, W.W. (2014). Regional specialization within the intestinal immune system. Nature Reviews Immunology *14*, 667–685.

Mueller, D.L., Jenkins, M.K., and Schwartz, R.H. (1989). Clonal Expansion Versus Functional Clonal Inactivation: A Costimulatory Signalling Pathway Determines the Outcome of T Cell Antigen Receptor Occupancy. Annual Review of Immunology *7*, 445–480.

Müller, A.J., Kaiser, P., Dittmar, K.E.J., Weber, T.C., Haueter, S., Endt, K., Songhet, P., Zellweger, C., Kremer, M., Fehling, H.-J., et al. (2012). Salmonella Gut Invasion Involves TTSS-2-Dependent Epithelial Traversal, Basolateral Exit, and Uptake by Epithelium-Sampling Lamina Propria Phagocytes. Cell Host & Microbe *11*, 19–32.

Nakamura, K., Kitani, A., and Strober, W. (2001). Cell contact-dependent immunosuppression by CD4(+)CD25(+) regulatory T cells is mediated by cell surface-bound transforming growth factor beta. J. Exp. Med. *194*, 629–644.

Nanton, M.R., Way, S.S., Shlomchik, M.J., and McSorley, S.J. (2012). Cutting edge: B cells are essential for protective immunity against Salmonella independent of antibody secretion. J. Immunol. *189*, 5503–5507.

Nauciel, C. (1990). Role of CD4+ T cells and T-independent mechanisms in acquired resistance to Salmonella typhimurium infection. J. Immunol. *145*, 1265–1269.

Nelson, R.W., McLachlan, J.B., Kurtz, J.R., and Jenkins, M.K. (2013). CD4+ T cell persistence and function after infection are maintained by low-level peptide:MHC class II presentation. J. Immunol. *190*, 2828–2834.

Nguyen, L.P., Pan, J., Dinh, T.T., Hadeiba, H., O'Hara, E., Ebtikar, A., Hertweck, A., Gökmen, M.R., Lord, G.M., Jenner, R.G., et al. (2015). Role and species-specific expression of colon T cell homing receptor GPR15 in colitis. Nature Immunology *16*, 207–213.

Nguyen, N.T., Kimura, A., Nakahama, T., Chinen, I., Masuda, K., Nohara, K., Fujii-Kuriyama, Y., and Kishimoto, T. (2010). Aryl hydrocarbon receptor negatively regulates dendritic cell immunogenicity via a kynurenine-dependent mechanism. Proceedings of the National Academy of Sciences *107*, 19961–19966.

Niess, J.H. (2005). CX3CR1-Mediated Dendritic Cell Access to the Intestinal Lumen and Bacterial Clearance. Science *307*, 254–258.

Nyström, S.N., Bourges, D., Garry, S., Ross, E.M., van Driel, I.R., and Gleeson, P.A. (2014). Transient Treg-cell depletion in adult mice results in persistent self-reactive CD4 $^{+}$ T-cell responses. European Journal of Immunology *44*, 3621–3631.

Obst, R., van Santen, H.-M., Mathis, D., and Benoist, C. (2005). Antigen persistence is required throughout the expansion phase of a CD4 $^{+}$ T cell response. The Journal of Experimental Medicine *201*, 1555–1565.

O'Garra, A. (1998). Cytokines Induce the Development of Functionally Heterogeneous T Helper Cell Subsets. Immunity *8*, 275–283.

O'Garra, A., McEvoy, L.M., and Zlotnik, A. (1998). T-cell subsets: Chemokine receptors guide the way. Current Biology *8*, R646–R649.

Ohnmacht, C., Park, J.-H., Cording, S., Wing, J.B., Atarashi, K., Obata, Y., Gaboriau-Routhiau, V., Marques, R., Dulauroy, S., Fedoseeva, M., et al. (2015). The microbiota regulates type 2 immunity through RORγt^{+} T cells. Science *349*, 989–993.

Oldenhove, G., Bouladoux, N., Wohlfert, E.A., Hall, J.A., Chou, D., Dos santos, L., O'Brien, S., Blank, R., Lamb, E., Natarajan, S., et al. (2009). Decrease of Foxp3+ Treg

Cell Number and Acquisition of Effector Cell Phenotype during Lethal Infection. Immunity *31*, 772–786.

Olsen, T., Rismo, R., Cui, G., Goll, R., Christiansen, I., and Florholmen, J. (2011). TH1 and TH17 interactions in untreated inflamed mucosa of inflammatory bowel disease, and their potential to mediate the inflammation. Cytokine *56*, 633–640.

Pabst, O., Herbrand, H., Worbs, T., Friedrichsen, M., Yan, S., Hoffmann, M.W., Körner, H., Bernhardt, G., Pabst, R., and Förster, R. (2005). Cryptopatches and isolated lymphoid follicles: dynamic lymphoid tissues dispensable for the generation of intraepithelial lymphocytes. European Journal of Immunology *35*, 98–107.

Pacholczyk, R., Kern, J., Singh, N., Iwashima, M., Kraj, P., and Ignatowicz, L. (2007). Nonself-Antigens Are the Cognate Specificities of Foxp3+ Regulatory T Cells. Immunity *27*, 493–504.

Pan, B., Wang, X., Nishioka, C., Honda, G., Yokoyama, A., Zeng, L., Xu, K., and Ikezoe, T. (2017). G-protein coupled receptor 15 mediates angiogenesis and cytoprotective function of thrombomodulin. Scientific Reports *7*, 692.

Park, J.-H., and Eberl, G. (2018). Type 3 regulatory T cells at the interface of symbiosis. Journal of Microbiology *56*, 163–171.

Park, H., Li, Z., Yang, X.O., Chang, S.H., Nurieva, R., Wang, Y.-H., Wang, Y., Hood, L., Zhu, Z., Tian, Q., et al. (2005). A distinct lineage of CD4 T cells regulates tissue inflammation by producing interleukin 17. Nat. Immunol. *6*, 1133–1141.

Pearce, E.J. (1991). Downregulation of Th1 cytokine production accompanies induction of Th2 responses by a parasitic helminth, Schistosoma mansoni. Journal of Experimental Medicine *173*, 159–166.

Pearl, D.S., Shah, K., Brown, J., Shute, J.K., and Trebble, T.M. (2011). Active ulcerative colitis is associated with downregulation of the TH1, TH2 and TH17 cytokine response and elevated IL-8 levels in mucosal biopsies. Gut *60*, A214–A214.

Pepper, M., Linehan, J.L., Pagán, A.J., Zell, T., Dileepan, T., Cleary, P.P., and Jenkins, M.K. (2010). Different routes of bacterial infection induce long-lived TH1 memory cells and short-lived TH17 cells. Nature Immunology *11*, 83–89.

Pham, O.H., O'Donnell, H., Al-Shamkhani, A., Kerrinnes, T., Tsolis, R.M., and McSorley, S.J. (2017). T cell expression of IL-18R and DR3 is essential for non-cognate stimulation of Th1 cells and optimal clearance of intracellular bacteria. PLOS Pathogens *13*, e1006566.

Picarella, D., Hurlbut, P., Rottman, J., Shi, X., Butcher, E., and Ringler, D.J. (1997). Monoclonal antibodies specific for beta 7 integrin and mucosal addressin cell adhesion molecule-1 (MAdCAM-1) reduce inflammation in the colon of scid mice reconstituted with CD45RBhigh CD4+ T cells. J. Immunol. *158*, 2099–2106.

Pie, S., Truffa-Bachi, P., Pla, M., and Nauciel, C. (1997). Th1 response in Salmonella typhimurium-infected mice with a high or low rate of bacterial clearance. Infect. Immun. *65*, 4509–4514.

Piehler, D., Stenzel, W., Grahnert, A., Held, J., Richter, L., Köhler, G., Richter, T., Eschke, M., Alber, G., and Müller, U. (2011). Eosinophils contribute to IL-4 production and shape the T-helper cytokine profile and inflammatory response in pulmonary cryptococcosis. Am. J. Pathol. *179*, 733–744.

Poirier, T.P. (1988). Protective immunity evoked by oral administration of attenuated aroA Salmonella typhimurium expressing cloned streptococcal M protein. Journal of Experimental Medicine *168*, 25–32.

Prescott, S.L., Macaubas, C., Holt, B.J., Smallacombe, T.B., Loh, R., Sly, P.D., and Holt, P.G. (1998). Transplacental priming of the human immune system to environmental allergens: universal skewing of initial T cell responses toward the Th2 cytokine profile. J. Immunol. *160*, 4730–4737.

Quah, B.J.C., and Parish, C.R. (2012). New and improved methods for measuring lymphocyte proliferation in vitro and in vivo using CFSE-like fluorescent dyes. Journal of Immunological Methods *379*, 1–14.

Quigley, E.M.M. (2013). Gut bacteria in health and disease. Gastroenterol Hepatol (N Y) *9*, 560–569.

Qureshi, O.S., Zheng, Y., Nakamura, K., Attridge, K., Manzotti, C., Schmidt, E.M., Baker, J., Jeffery, L.E., Kaur, S., Briggs, Z., et al. (2011). Trans-Endocytosis of CD80 and CD86: A Molecular Basis for the Cell-Extrinsic Function of CTLA-4. Science *332*, 600–603.

Rabenstein, H., Behrendt, A.C., Ellwart, J.W., Naumann, R., Horsch, M., Beckers, J., and Obst, R. (2014). Differential Kinetics of Antigen Dependency of CD4+ and CD8+ T Cells. The Journal of Immunology *192*, 3507–3517.

Radhakrishnan, A., Als, D., Mintz, E.D., Crump, J.A., Stanaway, J., Breiman, R.F., and Bhutta, Z.A. (2018). Introductory Article on Global Burden and Epidemiology of Typhoid Fever. The American Journal of Tropical Medicine and Hygiene *99*, 4–9.

Raffatellu, M., Santos, R.L., Verhoeven, D.E., George, M.D., Wilson, R.P., Winter, S.E., Godinez, I., Sankaran, S., Paixao, T.A., Gordon, M.A., et al. (2008). Simian immunodeficiency virus–induced mucosal interleukin-17 deficiency promotes Salmonella dissemination from the gut. Nature Medicine *14*, 421–428.

Ravindran, R., and McSorley, S.J. (2005). Tracking the dynamics of T-cell activation in response to Salmonella infection. Immunology *114*, 450–458.

Reboldi, A., and Cyster, J.G. (2016). Peyer's patches: organizing B-cell responses at the intestinal frontier. Immunol. Rev. *271*, 230–245.

Reis e Sousa, C. (2006). Dendritic cells in a mature age. Nature Reviews Immunology *6*, 476–483.

Rodríguez-Piñeiro, A.M., Bergström, J.H., Ermund, A., Gustafsson, J.K., Schütte, A., Johansson, M.E.V., and Hansson, G.C. (2013). Studies of mucus in mouse stomach, small intestine, and colon. II. Gastrointestinal mucus proteome reveals Muc2 and Muc5ac accompanied by a set of core proteins. American Journal of Physiology-Gastrointestinal and Liver Physiology *305*, G348–G356.

Romagnani, S. (1997). The Th1/Th2 paradigm. Immunology Today *18*, 263–266.

Romagnani, P., Lasagni, L., Annunziato, F., Serio, M., and Romagnani, S. (2004). CXC chemokines: the regulatory link between inflammation and angiogenesis. Trends in Immunology *25*, 201–209.

Román, E., Miller, E., Harmsen, A., Wiley, J., von Andrian, U.H., Huston, G., and Swain, S.L. (2002). CD4 Effector T Cell Subsets in the Response to Influenza: Heterogeneity, Migration, and Function. The Journal of Experimental Medicine *196*, 957–968.

de la Rosa, M., Rutz, S., Dorninger, H., and Scheffold, A. (2004). Interleukin-2 is essential for CD4+CD25+ regulatory T cell function. Eur. J. Immunol. *34*, 2480–2488.

Rosche, K.L., Aljasham, A.T., Kipfer, J.N., Piatkowski, B.T., and Konjufca, V. (2015). Infection with Salmonella enterica Serovar Typhimurium Leads to Increased Proportions of F4/80+ Red Pulp Macrophages and Decreased Proportions of B and T Lymphocytes in the Spleen. PLOS ONE *10*, e0130092.

Rouvier, E., Luciani, M.F., and Golstein, P. (1993). Fas involvement in Ca(2+)-independent T cell-mediated cytotoxicity. J. Exp. Med. *177*, 195–200.

Rydstrom, A., and Wick, M.J. (2007). Monocyte Recruitment, Activation, and Function in the Gut-Associated Lymphoid Tissue during Oral Salmonella Infection. The Journal of Immunology *178*, 5789–5801.

Rydstrom, A., and Wick, M.J. (2010). Salmonella inhibits monocyte differentiation into CD11chiMHC-IIhi cells in a MyD88-dependent fashion. Journal of Leukocyte Biology *87*, 823–832.

Safinia, N., Scotta, C., Vaikunthanathan, T., Lechler, R.I., and Lombardi, G. (2015). Regulatory T Cells: Serious Contenders in the Promise for Immunological Tolerance in Transplantation. Frontiers in Immunology *6*.

Sakaguchi, S. (2004). Naturally arising CD4+ regulatory t cells for immunologic self-tolerance and negative control of immune responses. Annual Review of Immunology *22*, 531–562.

Sakaguchi, S., Sakaguchi, N., Asano, M., Itoh, M., and Toda, M. (1995). Immunologic self-tolerance maintained by activated T cells expressing IL-2 receptor alpha-chains (CD25).

Breakdown of a single mechanism of self-tolerance causes various autoimmune diseases. J. Immunol. *155*, 1151–1164.

Sakaguchi, S., Sakaguchi, N., Shimizu, J., Yamazaki, S., Sakihama, T., Itoh, M., Kuniyasu, Y., Nomura, T., Toda, M., and Takahashi, T. (2001). Immunologic tolerance maintained by CD25+ CD4+ regulatory T cells: their common role in controlling autoimmunity, tumor immunity, and transplantation tolerance. Immunological Reviews *182*, 18–32.

Salazar-Gonzalez, R.M., Niess, J.H., Zammit, D.J., Ravindran, R., Srinivasan, A., Maxwell, J.R., Stoklasek, T., Yadav, R., Williams, I.R., Gu, X., et al. (2006). CCR6-Mediated Dendritic Cell Activation of Pathogen-Specific T Cells in Peyer's Patches. Immunity *24*, 623–632.

Sallusto, F., and Lanzavecchia, A. (2000). Understanding dendritic cell and T-lymphocyte traffic through the analysis of chemokine receptor expression. Immunological Reviews *177*, 134–140.

Sallusto, F., Lanzavecchia, A., and Mackay, C.R. (1998). Chemokines and chemokine receptors in T-cell priming and Th1/Th2-mediated responses. Immunology Today *19*, 568–574.

Sallusto, F., Lenig, D., Förster, R., Lipp, M., and Lanzavecchia, A. (1999). Two subsets of memory T lymphocytes with distinct homing potentials and effector functions. Nature *401*, 708–712.

Sanal, O., Turul, T., De Boer, T., Vosse, E.V.D., Yalcin, I., Tezcan, I., Sun, C., Memis, L., Ottenhoff, T.H.M., and Ersoy, F. (2006). Presentation of Interleukin-12/-23 Receptor β1 Deficiency with Various Clinical Symptoms of Salmonella Infections. Journal of Clinical Immunology *26*, 1–6.

Sansonetti, P.J. (2004). War and peace at mucosal surfaces. Nat. Rev. Immunol. *4*, 953–964.

Santos, R.L., Zhang, S., Tsolis, R.M., Kingsley, R.A., Adams, L.G., and Bäumler, A.J. (2001). Animal models of Salmonella infections: enteritis versus typhoid fever. Microbes Infect. *3*, 1335–1344.

Sarra, M., Pallone, F., MacDonald, T.T., and Monteleone, G. (2010). IL-23/IL-17 axis in IBD: Inflammatory Bowel Diseases *16*, 1808–1813.

Sasaki, S., Yoneyama, H., Suzuki, K., Suriki, H., Aiba, T., Watanabe, S., Kawauchi, Y., Kawachi, H., Shimizu, F., Matsushima, K., et al. (2002). Blockade of CXCL10 protects mice from acute colitis and enhances crypt cell survival. Eur. J. Immunol. *32*, 3197–3205.

Schroeder, B.O. (2019). Fight them or feed them: how the intestinal mucus layer manages the gut microbiota. Gastroenterology Report *7*, 3–12.

Schroepf, S., Kappler, R., Brand, S., Prell, C., Lohse, P., Glas, J., Hoster, E., Helmbrecht, J., Ballauff, A., Berger, M., et al. (2010). Strong overexpression of CXCR3 axis components in childhood inflammatory bowel disease: Inflammatory Bowel Diseases *16*, 1882–1890.

Schultsz, C., Van Den Berg, F.M., Ten Kate, F.W., Tytgat, G.N., and Dankert, J. (1999). The intestinal mucus layer from patients with inflammatory bowel disease harbors high numbers of bacteria compared with controls. Gastroenterology *117*, 1089–1097.

Schulz, S.M., Kohler, G., Holscher, C., Iwakura, Y., and Alber, G. (2008). IL-17A is produced by Th17, T cells and other CD4- lymphocytes during infection with Salmonella enterica serovar Enteritidis and has a mild effect in bacterial clearance. International Immunology *20*, 1129–1138.

Schwartz, R. (1990). A cell culture model for T lymphocyte clonal anergy. Science *248*, 1349–1356.

Sebastian, M., Lopez-Ocasio, M., Metidji, A., Rieder, S.A., Shevach, E.M., and Thornton, A.M. (2016). Helios Controls a Limited Subset of Regulatory T Cell Functions. The Journal of Immunology *196*, 144–155.

Seddiki, N., Santner-Nanan, B., Martinson, J., Zaunders, J., Sasson, S., Landay, A., Solomon, M., Selby, W., Alexander, S.I., Nanan, R., et al. (2006). Expression of interleukin (IL)-2 and IL-7 receptors discriminates between human regulatory and activated T cells. The Journal of Experimental Medicine *203*, 1693–1700.

Sefik, E., Geva-Zatorsky, N., Oh, S., Konnikova, L., Zemmour, D., McGuire, A.M., Burzyn, D., Ortiz-Lopez, A., Lobera, M., Yang, J., et al. (2015). Individual intestinal symbionts induce a distinct population of ROR?+ regulatory T cells. Science *349*, 993–997.

Senda, T., Dogra, P., Granot, T., Furuhashi, K., Snyder, M.E., Carpenter, D.J., Szabo, P.A., Thapa, P., Miron, M., and Farber, D.L. (2019). Microanatomical dissection of human intestinal T-cell immunity reveals site-specific changes in gut-associated lymphoid tissues over life. Mucosal Immunology *12*, 378–389.

Setiady, Y.Y., Coccia, J.A., and Park, P.U. (2010). *In vivo* depletion of CD4 $^{+}$ FOXP3 $^{+}$ Treg cells by the PC61 anti-CD25 monoclonal antibody is mediated by FcγRIII $^{+}$ phagocytes. European Journal of Immunology *40*, 780–786.

Sheridan, B.S., and Lefrançois, L. (2010). Intraepithelial lymphocytes: to serve and protect. Curr Gastroenterol Rep *12*, 513–521.

Shevach, E.M. (2018). Foxp3+ T Regulatory Cells: Still Many Unanswered Questions—A Perspective After 20 Years of Study. Frontiers in Immunology *9*.

Shevach, E.M., and Thornton, A.M. (2014). tTregs, pTregs, and iTregs: similarities and differences. Immunological Reviews *259*, 88–102.

Singh, U.P., Singh, N.P., Murphy, E.A., Price, R.L., Fayad, R., Nagarkatti, M., and Nagarkatti, P.S. (2016). Chemokine and cytokine levels in inflammatory bowel disease patients. Cytokine *77*, 44–49.

Smigiel, K.S., Richards, E., Srivastava, S., Thomas, K.R., Dudda, J.C., Klonowski, K.D., and Campbell, D.J. (2014). CCR7 provides localized access to IL-2 and defines homeostatically distinct regulatory T cell subsets. The Journal of Experimental Medicine *211*, 121–136.

Sollid, L.M. (2004). Intraepithelial Lymphocytes in Celiac Disease. Immunity *21*, 303–304.

Sonnenberg, G.F., and Artis, D. (2012). Innate Lymphoid Cell Interactions with Microbiota: Implications for Intestinal Health and Disease. Immunity *37*, 601–610.

Sonnenberg, G.F., Monticelli, L.A., Elloso, M.M., Fouser, L.A., and Artis, D. (2011). CD4+ Lymphoid Tissue-Inducer Cells Promote Innate Immunity in the Gut. Immunity *34*, 122–134.

Sonnenburg, J.L. (2005). Glycan Foraging in Vivo by an Intestine-Adapted Bacterial Symbiont. Science *307*, 1955–1959.

Spees, A.M., Kingsbury, D.D., Wangdi, T., Xavier, M.N., Tsolis, R.M., and Bäumler, A.J. (2014). Neutrophils are a source of gamma interferon during acute Salmonella enterica serovar Typhimurium colitis. Infect. Immun. *82*, 1692–1697.

Spits, H., Artis, D., Colonna, M., Diefenbach, A., Di Santo, J.P., Eberl, G., Koyasu, S., Locksley, R.M., McKenzie, A.N.J., Mebius, R.E., et al. (2013). Innate lymphoid cells — a proposal for uniform nomenclature. Nature Reviews Immunology *13*, 145–149.

Srinivasan, A., Foley, J., Ravindran, R., and McSorley, S.J. (2004). Low-Dose Salmonella Infection Evades Activation of Flagellin-Specific CD4 T Cells. The Journal of Immunology *173*, 4091–4099.

Stanaway, J.D., Reiner, R.C., Blacker, B.F., Goldberg, E.M., Khalil, I.A., Troeger, C.E., Andrews, J.R., Bhutta, Z.A., Crump, J.A., Im, J., et al. (2019). The global burden of typhoid and paratyphoid fevers: a systematic analysis for the Global Burden of Disease Study 2017. The Lancet Infectious Diseases *19*, 369–381.

Stathopoulou, C., Gangaplara, A., Mallett, G., Flomerfelt, F.A., Liniany, L.P., Knight, D., Samsel, L.A., Berlinguer-Palmini, R., Yim, J.J., Felizardo, T.C., et al. (2018). PD-1 Inhibitory Receptor Downregulates Asparaginyl Endopeptidase and Maintains Foxp3 Transcription Factor Stability in Induced Regulatory T Cells. Immunity.

Stecher, B., Paesold, G., Barthel, M., Kremer, M., Jantsch, J., Stallmach, T., Heikenwalder, M., and Hardt, W.-D. (2006). Chronic Salmonella enterica Serovar Typhimurium-Induced Colitis and Cholangitis in Streptomycin-Pretreated Nramp1+/+ Mice. Infection and Immunity *74*, 5047–5057.

Stecher, B., Robbiani, R., Walker, A.W., Westendorf, A.M., Barthel, M., Kremer, M., Chaffron, S., Macpherson, A.J., Buer, J., Parkhill, J., et al. (2007). Salmonella enterica Serovar Typhimurium Exploits Inflammation to Compete with the Intestinal Microbiota. PLoS Biology *5*, e244.

Strober, W., and Fuss, I.J. (2011). Proinflammatory Cytokines in the Pathogenesis of Inflammatory Bowel Diseases. Gastroenterology *140*, 1756-1767.e1.

Strugnell, R., Dougan, G., Chatfield, S., Charles, I., Fairweather, N., Tite, J., Li, J.L., Beesley, J., and Roberts, M. (1992). Characterization of a Salmonella typhimurium aro vaccine strain expressing the P.69 antigen of Bordetella pertussis. Infect. Immun. *60*, 3994–4002.

Su, L.F., del Alcazar, D., Stelekati, E., Wherry, E.J., and Davis, M.M. (2016). Antigen exposure shapes the ratio between antigen-specific Tregs and conventional T cells in human peripheral blood. Proceedings of the National Academy of Sciences *113*, E6192–E6198.

Sun, X., He, S., Lv, C., Sun, X., Wang, J., Zheng, W., and Wang, D. (2017). Analysis of murine and human Treg subsets in inflammatory bowel disease. Molecular Medicine Reports *16*, 2893–2898.

Suply, T., Hannedouche, S., Carte, N., Li, J., Grosshans, B., Schaefer, M., Raad, L., Beck, V., Vidal, S., Hiou-Feige, A., et al. (2017). A natural ligand for the orphan receptor GPR15 modulates lymphocyte recruitment to epithelia. Science Signaling *10*, eaal0180.

Swidsinski, A., Loening-Baucke, V., Theissig, F., Engelhardt, H., Bengmark, S., Koch, S., Lochs, H., and Dorffel, Y. (2007). Comparative study of the intestinal mucus barrier in normal and inflamed colon. Gut *56*, 343–350.

Szabo, S.J., Kim, S.T., Costa, G.L., Zhang, X., Fathman, C.G., and Glimcher, L.H. (2000). A Novel Transcription Factor, T-bet, Directs Th1 Lineage Commitment. Cell *100*, 655–669.

Szurek, E., Cebula, A., Wojciech, L., Pietrzak, M., Rempala, G., Kisielow, P., and Ignatowicz, L. (2015). Differences in Expression Level of Helios and Neuropilin-1 Do Not Distinguish Thymus-Derived from Extrathymically-Induced CD4+Foxp3+ Regulatory T Cells. PLOS ONE *10*, e0141161.

Szymczak-Workman, A.L., Workman, C.J., and Vignali, D.A.A. (2009). Cutting Edge: Regulatory T Cells Do Not Require Stimulation through Their TCR to Suppress. The Journal of Immunology *182*, 5188–5192.

Tadokoro, C.E., Shakhar, G., Shen, S., Ding, Y., Lino, A.C., Maraver, A., Lafaille, J.J., and Dustin, M.L. (2006). Regulatory T cells inhibit stable contacts between CD4 $^{+}$ T cells and dendritic cells in vivo. The Journal of Experimental Medicine *203*, 505–511.

Tahoun, A., Mahajan, S., Paxton, E., Malterer, G., Donaldson, D.S., Wang, D., Tan, A., Gillespie, T.L., O'Shea, M., Roe, A.J., et al. (2012). Salmonella Transforms Follicle-

Associated Epithelial Cells into M Cells to Promote Intestinal Invasion. Cell Host & Microbe *12*, 645–656.

Takatori, H., Kanno, Y., Watford, W.T., Tato, C.M., Weiss, G., Ivanov, I.I., Littman, D.R., and O'Shea, J.J. (2009). Lymphoid tissue inducer–like cells are an innate source of IL-17 and IL-22. The Journal of Experimental Medicine *206*, 35–41.

Takeuchi, A. (1967). Electron microscope studies of experimental Salmonella infection. I. Penetration into the intestinal epithelium by Salmonella typhimurium. Am. J. Pathol. *50*, 109–136.

Tam, M.A., Rydström, A., Sundquist, M., and Wick, M.J. (2008). Early cellular responses to Salmonella infection: dendritic cells, monocytes, and more. Immunol. Rev. *225*, 140–162.

Taylor, M.D., van der Werf, N., Harris, A., Graham, A.L., Bain, O., Allen, J.E., and Maizels, R.M. (2009). Early recruitment of natural CD4+Foxp3+ Treg cells by infective larvae determines the outcome of filarial infection. European Journal of Immunology *39*, 192–206.

Tennant, S.M., MacLennan, C.A., Simon, R., Martin, L.B., and Khan, M.I. (2016). Nontyphoidal salmonella disease: Current status of vaccine research and development. Vaccine *34*, 2907–2910.

Teramoto, K., Miura, S., Tsuzuki, Y., Hokari, R., Watanabe, C., Inamura, T., Ogawa, T., Hosoe, N., Nagata, H., Ishii, H., et al. (2005). Increased lymphocyte trafficking to colonic microvessels is dependent on MAdCAM-1 and C-C chemokine mLARC/CCL20 in DSS-induced mice colitis. Clinical & Experimental Immunology *139*, 421–428.

Thelen, M. (2001). Dancing to the tune of chemokines. Nature Immunology *2*, 129.

Thornton, A.M., Korty, P.E., Tran, D.Q., Wohlfert, E.A., Murray, P.E., Belkaid, Y., and Shevach, E.M. (2010). Expression of Helios, an Ikaros Transcription Factor Family Member, Differentiates Thymic-Derived from Peripherally Induced Foxp3+ T Regulatory Cells. The Journal of Immunology *184*, 3433–3441.

Thornton, A.M., Lu, J., Korty, P.E., Kim, Y.C., Martens, C., Sun, P.D., and Shevach, E.M. (2019). Helios+ and Helios- Treg subpopulations are phenotypically and functionally distinct and express dissimilar TCR repertoires. Eur. J. Immunol. *49*, 398–412.

Tobar, J.A., Carreno, L.J., Bueno, S.M., Gonzalez, P.A., Mora, J.E., Quezada, S.A., and Kalergis, A.M. (2006). Virulent Salmonella enterica Serovar Typhimurium Evades Adaptive Immunity by Preventing Dendritic Cells from Activating T Cells. Infection and Immunity *74*, 6438–6448.

Tosiek, M.J., Fiette, L., El Daker, S., Eberl, G., and Freitas, A.A. (2016). IL-15-dependent balance between Foxp3 and RORγt expression impacts inflammatory bowel disease. Nature Communications *7*, 10888.

Tsolis, R.M., Adams, L.G., Ficht, T.A., and Bäumler, A.J. (1999). Contribution of Salmonella typhimurium virulence factors to diarrheal disease in calves. Infect. Immun. *67*, 4879–4885.

Tsolis, R.M., Xavier, M.N., Santos, R.L., and Bäumler, A.J. (2011). How To Become a Top Model: Impact of Animal Experimentation on Human Salmonella Disease Research. Infection and Immunity *79*, 1806–1814.

Tsuji, M., Komatsu, N., Kawamoto, S., Suzuki, K., Kanagawa, O., Honjo, T., Hori, S., and Fagarasan, S. (2009). Preferential Generation of Follicular B Helper T Cells from Foxp3+ T Cells in Gut Peyer's Patches. Science *323*, 1488–1492.

Uhlig, H.H., Coombes, J., Mottet, C., Izcue, A., Thompson, C., Fanger, A., Tannapfel, A., Fontenot, J.D., Ramsdell, F., and Powrie, F. (2006). Characterization of Foxp3+CD4+CD25+ and IL-10-secreting CD4+CD25+ T cells during cure of colitis. J. Immunol. *177*, 5852–5860.

Vaishnava, S., Behrendt, C.L., Ismail, A.S., Eckmann, L., and Hooper, L.V. (2008). Paneth cells directly sense gut commensals and maintain homeostasis at the intestinal host-microbial interface. Proceedings of the National Academy of Sciences *105*, 20858–20863.

Van Parijs, L., Ibraghimov, A., and Abbas, A.K. (1996). The Roles of Costimulation and Fas in T Cell Apoptosis and Peripheral Tolerance. Immunity *4*, 321–328.

van der Veeken, J., Gonzalez, A.J., Cho, H., Arvey, A., Hemmers, S., Leslie, C.S., and Rudensky, A.Y. (2016). Memory of Inflammation in Regulatory T Cells. Cell *166*, 977–990.

Velazquez, E.M., Nguyen, H., Heasley, K.T., Saechao, C.H., Gil, L.M., Rogers, A.W.L., Miller, B.M., Rolston, M.R., Lopez, C.A., Litvak, Y., et al. (2019). Endogenous Enterobacteriaceae underlie variation in susceptibility to Salmonella infection. Nature Microbiology.

Vidal, S.M., Pinner, E., Lepage, P., Gauthier, S., and Gros, P. (1996). Natural resistance to intracellular infections: Nramp1 encodes a membrane phosphoglycoprotein absent in macrophages from susceptible (Nramp1 D169) mouse strains. J. Immunol. *157*, 3559–3568.

Vignali, D.A.A., Collison, L.W., and Workman, C.J. (2008). How regulatory T cells work. Nature Reviews Immunology *8*, 523–532.

Villares, R., Cadenas, V., Lozano, M., Almonacid, L., Zaballos, A., Martínez-A, C., and Varona, R. (2009). CCR6 regulates EAE pathogenesis by controlling regulatory CD4+ T-cell recruitment to target tissues. Eur. J. Immunol. *39*, 1671–1681.

Vivier, E., Raulet, D.H., Moretta, A., Caligiuri, M.A., Zitvogel, L., Lanier, L.L., Yokoyama, W.M., and Ugolini, S. (2011). Innate or Adaptive Immunity? The Example of Natural Killer Cells. Science *331*, 44–49.

Voedisch, S., Koenecke, C., David, S., Herbrand, H., Forster, R., Rhen, M., and Pabst, O. (2009). Mesenteric Lymph Nodes Confine Dendritic Cell-Mediated Dissemination of Salmonella enterica Serovar Typhimurium and Limit Systemic Disease in Mice. Infection and Immunity *77*, 3170–3180.

van de Vosse, E., and Ottenhoff, T.H.M. (2006). Human host genetic factors in mycobacterial and Salmonella infection: lessons from single gene disorders in IL-12/IL-23-dependent signaling that affect innate and adaptive immunity. Microbes and Infection *8*, 1167–1173.

Vu, M.D., Xiao, X., Gao, W., Degauque, N., Chen, M., Kroemer, A., Killeen, N., Ishii, N., and Chang Li, X. (2007). OX40 costimulation turns off Foxp3+ Tregs. Blood *110*, 2501–2510.

Wan, Y.Y., and Flavell, R.A. (2005). Identifying Foxp3-expressing suppressor T cells with a bicistronic reporter. Proc. Natl. Acad. Sci. U.S.A. *102*, 5126–5131.

Wang, C., Kang, S.G., Lee, J., Sun, Z., and Kim, C.H. (2009a). The roles of CCR6 in migration of Th17 cells and regulation of effector T-cell balance in the gut. Mucosal Immunology *2*, 173–183.

Wang, F., Wan, L., Zhang, C., Zheng, X., Li, J., and Chen, Z.K. (2009b). Tim-3-Galectin-9 pathway involves the suppression induced by CD4+CD25+ regulatory T cells. Immunobiology *214*, 342–349.

Wang, Y., Su, M.A., and Wan, Y.Y. (2011). An Essential Role of the Transcription Factor GATA-3 for the Function of Regulatory T Cells. Immunity *35*, 337–348.

Wang, Y., Godec, J., Ben-Aissa, K., Cui, K., Zhao, K., Pucsek, A.B., Lee, Y.K., Weaver, C.T., Yagi, R., and Lazarevic, V. (2014). The Transcription Factors T-bet and Runx Are Required for the Ontogeny of Pathogenic Interferon-γ-Producing T Helper 17 Cells. Immunity *40*, 355–366.

Wang, Z., Zhang, H., Liu, R., Qian, T., Liu, J., Huang, E., Lu, Z., Zhao, C., Wang, L., and Chu, Y. (2018). Peyer's patches-derived CD11b $^{+}$ B cells recruit regulatory T cells through CXCL9 in dextran sulphate sodium-induced colitis. Immunology *155*, 356–366.

Ward, S.J., Douce, G., Figueiredo, D., Dougan, G., and Wren, B.W. (1999). Immunogenicity of a Salmonella typhimurium aroA aroD vaccine expressing a nontoxic domain of Clostridium difficile toxin A. Infect. Immun. *67*, 2145–2152.

Weaver, C.T., Harrington, L.E., Mangan, P.R., Gavrieli, M., and Murphy, K.M. (2006). Th17: An Effector CD4 T Cell Lineage with Regulatory T Cell Ties. Immunity *24*, 677–688.

Weiss, J.M., Bilate, A.M., Gobert, M., Ding, Y., Curotto de Lafaille, M.A., Parkhurst, C.N., Xiong, H., Dolpady, J., Frey, A.B., Ruocco, M.G., et al. (2012). Neuropilin 1 is expressed on thymus-derived natural regulatory T cells, but not mucosa-generated induced Foxp3 $^{+}$ T reg cells. The Journal of Experimental Medicine *209*, 1723–1742.

Wendland, M., and Bumann, D. (2002). Optimization of GFP levels for analyzing Salmonella gene expression during an infection. FEBS Letters *521*, 105–108.

Wermers, J.D., McNamee, E.N., Wurbel, M., Jedlicka, P., and Rivera–Nieves, J. (2011). The Chemokine Receptor CCR9 Is Required for the T-Cell–Mediated Regulation of Chronic Ileitis in Mice. Gastroenterology *140*, 1526-1535.e3.

Wick, M.J. (2011). Innate Immune Control of Salmonella enterica Serovar Typhimurium: Mechanisms Contributing to Combating Systemic Salmonella Infection. Journal of Innate Immunity *3*, 543–549.

Wilson, C.L. (1999). Regulation of Intestinal -Defensin Activation by the Metalloproteinase Matrilysin in Innate Host Defense. Science *286*, 113–117.

Wing, J.B., and Sakaguchi, S. (2012). Multiple treg suppressive modules and their adaptability. Frontiers in Immunology *3*.

Wing, K., Onishi, Y., Prieto-Martin, P., Yamaguchi, T., Miyara, M., Fehervari, Z., Nomura, T., and Sakaguchi, S. (2008a). CTLA-4 Control over Foxp3+ Regulatory T Cell Function. Science *322*, 271–275.

Wing, K., Onishi, Y., Prieto-Martin, P., Yamaguchi, T., Miyara, M., Fehervari, Z., Nomura, T., and Sakaguchi, S. (2008b). CTLA-4 control over Foxp3+ regulatory T cell function. Science *322*, 271–275.

Wohlfert, E.A., Grainger, J.R., Bouladoux, N., Konkel, J.E., Oldenhove, G., Ribeiro, C.H., Hall, J.A., Yagi, R., Naik, S., Bhairavabhotla, R., et al. (2011). GATA3 controls Foxp3$^+$ regulatory T cell fate during inflammation in mice. J. Clin. Invest. *121*, 4503–4515.

Workman, C.J., and Vignali, D.A.A. (2005). Negative regulation of T cell homeostasis by lymphocyte activation gene-3 (CD223). J. Immunol. *174*, 688–695.

Xu, H., Wang, X., Liu, D.X., Moroney-Rasmussen, T., Lackner, A.A., and Veazey, R.S. (2012). IL-17-producing innate lymphoid cells are restricted to mucosal tissues and are depleted in SIV-infected macaques. Mucosal Immunol *5*, 658–669.

Yadav, M., Louvet, C., Davini, D., Gardner, J.M., Martinez-Llordella, M., Bailey-Bucktrout, S., Anthony, B.A., Sverdrup, F.M., Head, R., Kuster, D.J., et al. (2012). Neuropilin-1 distinguishes natural and inducible regulatory T cells among regulatory T cell subsets in vivo. The Journal of Experimental Medicine *209*, 1713–1722.

Yamashita, M., Ukai-Tadenuma, M., Miyamoto, T., Sugaya, K., Hosokawa, H., Hasegawa, A., Kimura, M., Taniguchi, M., DeGregori, J., and Nakayama, T. (2004). Essential role of GATA3 for the maintenance of type 2 helper T (Th2) cytokine production and chromatin remodeling at the Th2 cytokine gene loci. J. Biol. Chem. *279*, 26983–26990.

Yamazaki, T., Yang, X.O., Chung, Y., Fukunaga, A., Nurieva, R., Pappu, B., Martin-Orozco, N., Kang, H.S., Ma, L., Panopoulos, A.D., et al. (2008). CCR6 Regulates the

Migration of Inflammatory and Regulatory T Cells. The Journal of Immunology *181*, 8391–8401.

Yanagi, Y., Yoshikai, Y., Leggett, K., Clark, S.P., Aleksander, I., and Mak, T.W. (1984). A human T cell-specific cDNA clone encodes a protein having extensive homology to immunoglobulin chains. Nature *308*, 145–149.

Yang, X.O., Nurieva, R., Martinez, G.J., Kang, H.S., Chung, Y., Pappu, B.P., Shah, B., Chang, S.H., Schluns, K.S., Watowich, S.S., et al. (2008). Molecular Antagonism and Plasticity of Regulatory and Inflammatory T Cell Programs. Immunity *29*, 44–56.

Yoon, H., McDermott, J.E., Porwollik, S., McClelland, M., and Heffron, F. (2009). Coordinated Regulation of Virulence during Systemic Infection of Salmonella enterica Serovar Typhimurium. PLoS Pathogens *5*, e1000306.

Yoshie, O., and Matsushima, K. (2015). CCR4 and its ligands: from bench to bedside. International Immunology *27*, 11–20.

Yrlid, U., Svensson, M., Kirby, A., and Wick, M.J. (2001). Antigen-presenting cells and anti-Salmonella immunity. Microbes Infect. *3*, 1239–1248.

Yu, W., Geng, S., Suo, Y., Wei, X., Cai, Q., Wu, B., Zhou, X., Shi, Y., and Wang, B. (2018). Critical Role of Regulatory T Cells in the Latency and Stress-Induced Reactivation of HSV-1. Cell Reports *25*, 2379-2389.e3.

Zenewicz, L.A., Antov, A., and Flavell, R.A. (2009). CD4 T-cell differentiation and inflammatory bowel disease. Trends in Molecular Medicine *15*, 199–207.

Zhao, D.-M. (2006). Activated CD4+CD25+ T cells selectively kill B lymphocytes. Blood *107*, 3925–3932.

Zheng, W., and Flavell, R.A. (1997). The Transcription Factor GATA-3 Is Necessary and Sufficient for Th2 Cytokine Gene Expression in CD4 T Cells. Cell *89*, 587–596.

Zheng, Y., Chaudhry, A., Kas, A., deRoos, P., Kim, J.M., Chu, T.-T., Corcoran, L., Treuting, P., Klein, U., and Rudensky, A.Y. (2009). Regulatory T-cell suppressor program co-opts transcription factor IRF4 to control TH2 responses. Nature *458*, 351–356.

Zhou, L., Chong, M.M.W., and Littman, D.R. (2009). Plasticity of CD4+ T Cell Lineage Differentiation. Immunity *30*, 646–655.

Zhou, L., Chu, C., Teng, F., Bessman, N.J., Goc, J., Santosa, E.K., Putzel, G.G., Kabata, H., Kelsen, J.R., Baldassano, R.N., et al. (2019). Innate lymphoid cells support regulatory T cells in the intestine through interleukin-2. Nature.

Zhu, J., and Paul, W.E. (2008). CD4 T cells: fates, functions, and faults. Blood *112*, 1557–1569.

Zielinski, C.E., Mele, F., Aschenbrenner, D., Jarrossay, D., Ronchi, F., Gattorno, M., Monticelli, S., Lanzavecchia, A., and Sallusto, F. (2012). Pathogen-induced human TH17 cells produce IFN-γ or IL-10 and are regulated by IL-1β. Nature *484*, 514–518.